

Geological and Operational Summary, Kodiak Shelf Stratigraphic Test Wells, Western Gulf of Alaska

OCS Report
MMS 87-0109

by

Ronald F. Turner
Maurice B. Lynch
Teresa A. Conner
Patrick J. Hallin
Peter J. Hoose
Gary C. Martin
Donald L. Olson
John A. Larson
Tabe O. Flett
Kirk W. Sherwood
Allen J. Adams

edited by

Ronald F. Turner

October 1987

United States Department of the Interior
Minerals Management Service
Alaska OCS Region
Anchorage, Alaska

Any use of trade names is for descriptive purposes only and does not constitute endorsement of these products by the Minerals Management Service.

CONTENTS

Introduction	1
1. Regional petroleum exploration history, by Maurice B. Lynch	3
2. Operational summary of the Kodiak shelf stratigraphic drilling program, by Teresa A. Conner and Patrick J. Hallin	7
3. Lithologic summary, by Maurice B. Lynch	45
4. Velocity analysis, by Peter J. Hoose	55
5. Seismic stratigraphy and tectonic evolution of the Kodiak shelf, by Peter J. Hoose	71
6. Well log interpretation, by Gary C. Martin	103
7. Biostratigraphy, by Donald L. Olson, John A. Larson, and Ronald F. Turner	139
8. Organic geochemistry, by Tabe O. Flett	193
9. Geothermal gradient, by Tabe O. Flett	225
10. Abnormal formation pressure, by Kirk W. Sherwood	229
11. Shallow geology and geologic hazards, by Peter J. Hoose	253
12. Environmental Considerations, by Allen J. Adams	269
References	279
Appendices	
1. Core data.	
KSSD No. 1 well, conventional cores: Permeabilities, porosities, and grain densities. X-ray diffraction percentage determinations of selected minerals. Core descriptions. Petrographic thin-section analysis.	301

KSSD No. 2 well, conventional cores: Permeabilities, porosities, and grain densities. X-ray diffraction percentage determinations of selected minerals. Core descriptions. Petrographic thin-section analysis.	314
KSSD No. 3 well, conventional and sidewall cores: Permeabilities, porosities, and grain densities. X-ray diffraction percentage determinations of selected minerals. Core descriptions. Petrographic thin-section analysis.	320
KSST No. 1 well, sidewall cores: Permeabilities, porosities, and grain densities.	330
KSST No. 2 well, sidewall cores: Permeabilities, porosities, and grain densities.	331
2. Kerogen types, TAI, and R_0 values from the KSSD No. 1 well.	333
3. Kerogen types, TAI, and R_0 values from the KSSD No. 2 well.	335
4. Kerogen types, TAI, and R_0 values from the KSSD No. 3 well.	337
5. Correlative thermal alteration index (TAI) and random mean vitrinite reflectance (R_0) values.	339
6. Kerogen types and TAI values for the KSST No. 1, KSST No. 2, and KSST No. 4A wells.	341

Figures

1. Map showing proposed Lease Sale 46, Western Gulf of Alaska, Kodiak Shelf.	xii
2. Map showing locations of Kodiak Shelf COST wells and nearby petroleum districts.	4
3. Map showing original intermediate core hole program proposed by Exploration Services Co., Inc., 1975.	8
4. Final location plat showing the position of the KSST No. 1 well.	10
5. Graph showing daily drilling progress for the KSST No. 1 well.	11
6. Schematic diagram showing casing strings, plugging and abandonment program, KSST No. 1 well.	12

7.	Changes of drilling mud properties with depth, KSST No. 1 well.	13
8.	Final location plat showing the position of the KSST No. 2 well.	15
9.	Graph showing daily drilling progress for the KSST No. 2 well.	16
10.	Schematic diagram showing casing strings, plugging and abandonment program, KSST No. 2 well.	18
11.	Changes of drilling mud properties with depth, KSST No. 2 well.	19
12.	Final location plat showing the position of the KSST No. 4A well.	21
13.	Graph showing daily drilling progress for the KSST No. 4A well.	22
14.	Schematic diagram showing casing strings, plugging and abandonment program, KSST No. 4A well.	23
15.	Changes of drilling mud properties with depth, KSST No. 4A well.	24
16.	Final location plat showing the position of the KSSD No. 1 well.	27
17.	Graph showing daily drilling progress for the KSSD No. 1 well.	28
18.	Schematic diagram showing casing strings, plugging and abandonment program, KSSD No. 1 well.	30
19.	Changes of drilling mud properties with depth, KSSD No. 1 well.	31
20.	Final location plat showing the position of the KSSD No. 2 well.	33
21.	Graph showing daily drilling progress for the KSSD No. 2 well.	34
22.	Schematic diagram showing casing strings, plugging and abandonment program, KSSD No. 2 well.	36
23.	Changes of drilling mud properties with depth, KSSD No. 2 well.	37
24.	Final location plat showing the position of the KSSD No. 3 well.	39

25.	Graph showing daily drilling progress for the KSSD No. 3 well.	40
26.	Schematic diagram showing casing strings, plugging and abandonment program, KSSD No. 3 well.	41
27.	Changes of drilling mud properties with depth, KSSD No. 3 well.	43
28.	Lithologic description and core locations of the KSSD No. 1 well.	49
29.	Lithologic description and core locations of the KSSD No. 2 well.	50
30.	Lithologic description and core locations of the KSSD No. 3 well.	51
31.	Lithologic description of the KSST No. 1 well.	52
32.	Lithologic description of the KSST No. 2 well.	53
33.	Lithologic description of the KSST No. 4A well.	54
34.	RMS velocity calculated from the long-spaced sonic log from the KSST No. 1 well.	58
35.	RMS velocity calculated from the long-spaced sonic log from the KSST No. 2 well.	59
36.	RMS velocity calculated from the long-spaced sonic log from the KSST No. 4A well.	60
37.	RMS velocity calculated from the long-spaced sonic log from the KSSD No. 1 well.	61
38.	RMS velocity calculated from the long-spaced sonic log from the KSSD No. 2 well.	62
39.	RMS velocity calculated from the long-spaced sonic log from the KSSD No. 3 well.	63
40.	Interval velocities and a time-depth curve calculated from interval transit time data from the long-spaced sonic log of the KSST No. 1 well.	64
41.	Interval velocities and a time-depth curve calculated from interval transit time data from the long-spaced sonic log of the KSST No. 2 well.	65
42.	Interval velocities and a time-depth curve calculated from interval transit time data from the long-spaced sonic log of the KSST No. 4A well.	66

43.	Interval velocities and a time-depth curve calculated from interval transit time data from the long-spaced sonic log of the KSSD No. 1 well.	67
44.	Interval velocities and a time-depth curve calculated from interval transit time data from the long-spaced sonic log of the KSSD No. 3 well.	68
45.	Interval velocities and a time-depth curve calculated from interval transit time data from the long-spaced sonic log of the KSSD No. 2 well.	69
46.	Map showing trackline coverage of 24-fold seismic reflection profile data across Kodiak shelf.	70
47.	Synthetic seismogram generated from the digitized long-spaced sonic log of the KSST No. 1 well.	73
48.	Synthetic seismogram generated from the digitized long-spaced sonic log of the KSST No. 2 well.	75
49.	Synthetic seismogram generated from the digitized long-spaced sonic log of the KSST No. 4A well.	77
50.	Synthetic seismogram generated from the digitized long-spaced sonic log of the KSSD No. 1 well.	79
51.	Synthetic seismogram generated from the digitized long-spaced sonic log of the KSSD No. 2 well.	81
52.	Synthetic seismogram generated from the digitized long-spaced sonic log of the KSSD No. 3 well.	83
53.	Seismic profile EGAL-75-501.	85
54.	Seismic profile EGAL-75-500.	87
55.	A. The theoretical configuration of the northern Pacific region at 30 Ma and 20 Ma. B. A schematic model showing the uplift and subsidence history of a section of the Aleutian arc summit platform, which overrode the subducting Kula-Pacific spreading center at 30 Ma.	90
56.	Tectonic evolution of the Kodiak shelf, illustrating the development of the more deformed and the less deformed units of the Sitkalidak Formation.	92
57.	Schematic model for the uplift of the Kodiak shelf caused by regional-scale underplating.	94
58.	Structure-contour map of horizon C.	96

59. Tectonostratigraphic terrances underlying southwestern Alaska.	98
60. Lithology and wireline log responses from a progradational sedimentary sequence in the KSST No. 2 well.	106
61. Wireline log responses and formation analysis of sandstone in the KSST No. 2 well.	108
62. Schematic paleogeographic map of the Kodiak shelf area showing texture and genesis of shelf sediments during the Pleistocene.	118
63. Hypothetical vertical cross section across prograding lower and middle-fan system.	120
64. Rose diagrams of dip azimuth frequencies from high-resolution dipmeter log data, 2,835 to 5,060 feet, KSSD No. 3 well.	123
65. Log motifs of submarine-fan sandstones.	125
66. Log of submarine upper- to mid-fan channel deposit, Plio-Pleistocene turbidite sequence, KSSD No. 3 well.	127
67. Log of a submarine lower-fan facies association, Plio-Pleistocene turbidite sequence, KSSD No. 3 well.	128
68. Log of a submarine mid-fan facies association, Plio-Pleistocene turbidite sequence, KSSD No. 3 well.	129
69. Log of a submarine mid-fan facies association, Miocene turbidite sequence, KSSD No. 3 well.	133
70. Biostratigraphy and paleobathymetry of the KSST No. 1 well.	146
71. Biostratigraphy and paleobathymetry of the KSST No. 2 well.	151
72. Biostratigraphy and paleobathymetry of the KSST No. 4A well.	154
73. Biostratigraphy and paleobathymetry of the KSSD No. 1 well.	165
74. Biostratigraphy and paleobathymetry of the KSSD No. 2 well.	175
75. Biostratigraphy and paleobathymetry of the KSSD No. 3 well.	185
76. Biostratigraphic correlation of Kodiak shelf COST wells.	187
77. Organic carbon, kerogen type, and thermal maturity, KSSD No. 1 well.	195
78. Light hydrocarbons from cuttings samples, KSSD No. 1 well.	199

79.	Representative C ₁₅ + gas chromatograms from cuttings samples, KSSD No. 1 well.	201
80.	Organic carbon, kerogen type, and thermal maturity, KSSD No. 2 well.	205
81.	Light hydrocarbons from cuttings samples, KSSD No. 2 well.	207
82.	Representative C ₁₅ + gas chromatograms from cuttings samples, KSSD No. 2 well.	210
83.	Organic carbon, kerogen type, and thermal maturity, KSSD No. 3 well.	213
84.	Light hydrocarbons from cuttings samples, KSSD No. 3 well.	215
85.	Representative C ₁₅ + gas chromatograms from cuttings samples, KSSD No. 3 well.	217
86.	Graph showing the extrapolation of bottom hole temperatures (BHT) to determine static BHT for KSSD No. 1 well.	226
87.	Temperature gradient from KSSD No. 1 well.	227
88.	Index map showing locations of Kodiak Shelf Stratigraphic Test wells.	230
89.	Synopsis of drilling data and wireline log data for shales, KSSD No. 1 well.	232
90.	Synopsis of drilling data and wireline log data for shales, KSSD No. 2 well.	234
91.	Synopsis of pressure data, drilling data, and wireline log data for shales, KSSD No. 3 well.	238
92.	Synopsis of wireline log data for shales, KSST No. 1 well.	242
93.	Synopsis of wireline log data for shales, KSST No. 2 well.	242
94.	Synopsis of wireline log data for shales, KSST No. 4A well.	242
95.	Sketch of seismic panel and map showing locations of near-surface structures in the vicinity of the KSSD No. 2 well.	246
96.	Transverse tectonic boundaries which bound the Kodiak Island block.	248
97.	Schematic cross section illustrating hypothetical model for transfer of level of intense shear and dewatering within accretionary complex at Kodiak-Kenai transverse boundary.	251
98.	Bathymetry of the Kodiak shelf.	254

99. Physiography of the Kodiak shelf.	255
100. Geologic map of the Kodiak shelf showing bedrock outcrops and surficial sedimentary units.	256
101. Shallow folds and faults underlying the Kodiak shelf.	259
102. Major strike-slip faults, historically active volcanoes, and convergence directions between the Pacific and the North American lithospheric plates.	260
103. Locations of sediment slides and sand wave fields.	263
104. Locations of indicators of possible gas.	265

Plates

1. Stratigraphic column and summary chart of geologic data, KSST No. 1 well.	
2. Stratigraphic column and summary chart of geologic data, KSST No. 2 well.	
3. Stratigraphic column and summary chart of geologic data, KSST No. 4A well.	
4. Stratigraphic column and summary chart of geologic data, KSSD No. 1 well.	
5. Stratigraphic column and summary chart of geologic data, KSSD No. 2 well.	
6. Stratigraphic column and summary chart of geologic data, KSSD No. 3 well.	
7. Log and dipmeter patterns of major stratigraphic sequences in the KSSD No. 3 well.	

Tables

1. COST wells drilled on the Kodiak shelf.	5
2. Conventional cores, KSSD No. 1 well.	29
3. Conventional cores, KSSD No. 2 well.	35
4. Conventional cores, KSSD No. 3 well.	42
5. Summary of wireline log interpretations of sandstone reservoir potential in the KSST No. 2 well.	135

6.	Summary of wireline log interpretations of sandstone reservoir potential in the Pleistocene glaciomarine shelf sequence, KSSD No. 3 well.	136
7.	Summary of wireline log interpretations of sandstone reservoir potential of the Plio-Pleistocene turbidite sequence, KSSD No. 3 well.	137
8.	Summary of wireline log interpretations of sandstone reservoir potential of the Miocene turbidite sequence, KSSD No. 3 well.	138
9.	Naphthene/paraffin ratios, paraffin-naphthene/aromatics ratios, and carbon preference indices, KSSD No. 1 well.	198
10.	Naphthene/paraffin ratios, paraffin-naphthene/aromatics ratios, and carbon preference indices, KSSD No. 2 well.	209
11.	Naphthene/paraffin ratios, paraffin-naphthene/aromatics ratios, and carbon preference indices, KSSD No. 3 well.	212
12.	Repeat formation test data, KSSD No. 3 well.	239
13.	Descriptions of surficial sedimentary units, Kodiak shelf.	257
14.	Volcanic activity along the Alaska Peninsula.	266

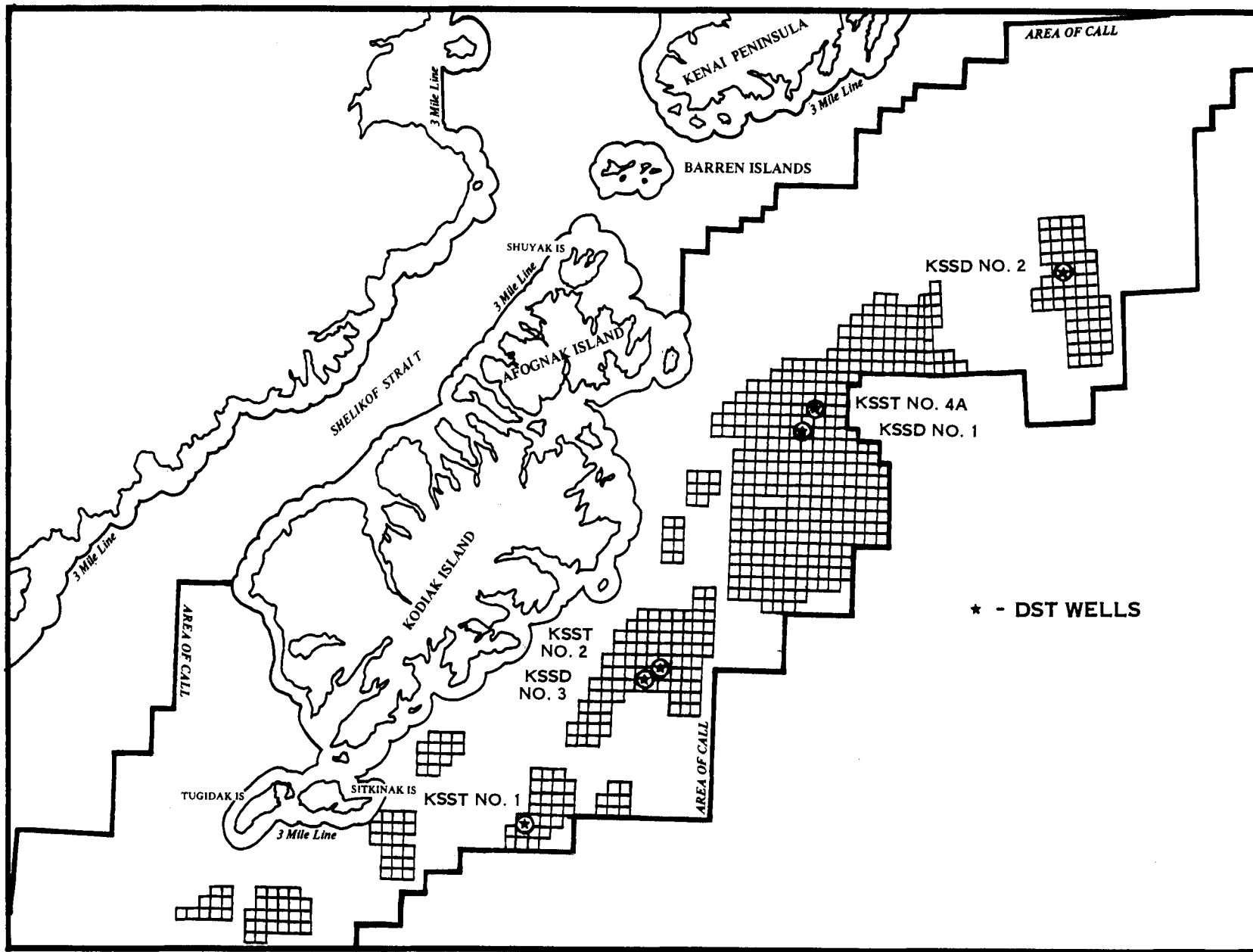


Figure 1. Proposed Lease Sale 46, Western Gulf of Alaska, Kodiak Shelf.

INTRODUCTION

Title 30, Code of Federal Regulations (CFR), paragraph 251.14, stipulates that geological data and processed geological information obtained from Deep Stratigraphic Test (DST) wells drilled on the Outer Continental Shelf (OCS) be made available for public inspection 60 calendar days after the issuance of the first Federal lease within 50 nautical miles of the well site or 10 years after completion of the well if no lease is issued. Six DST wells (often called COST wells) were drilled on the Kodiak shelf in support of proposed Lease Sale 46 (fig. 1), three in 1976 and three in 1977. The first series of wells, the KSST No. 1, KSST No. 2, and KSST No. 4A wells, was drilled by Exploration Services Company, Inc. (ESCI), to shallow depths and obtained relatively limited data. These data were made available for public inspection after 10 years, as required by CFR 251.14, but no formal report was issued at the time. The second series of Kodiak shelf wells, the KSSD No. 1, KSSD No. 2, and KSSD No. 3 wells, was drilled in 1977 by Sun Oil Company. These wells were drilled to much greater depths and acquired far more data. The last well was completed in October 1977. MMS interpretations of the data from all six wells are released in this report.

Lease Sales 46, 61, and 99 have all been cancelled. No lease sale for the Kodiak shelf area is scheduled in the current 5-year Oil and Gas Leasing Program.

1. REGIONAL PETROLEUM EXPLORATION HISTORY

EXPLORATION IN THE VICINITY OF KODIAK SHELF

Areas of petroleum exploration activity nearest the Kodiak shelf include the Kanatak district 160 miles northwest, the Shelikof Strait 120 miles northwest, the Iniskin Peninsula 200 miles north, the upper Cook Inlet and Kenai Peninsula district 250 miles to the north, an exploratory well drilled near Middleton Island about 100 miles northeast, the Katalla district 260 miles northeast, and the Gulf of Alaska lease sale areas 39 and 55, approximately 200 miles northeast. Figure 2 is a map showing the locations of the six Kodiak shelf test wells and the locations of nearby areas of petroleum exploration interest.

The first recorded oil and gas discoveries in Alaska were oil seeps found by the Russians in 1853 on the Iniskin Peninsula along the west side of Cook Inlet (Miller, Payne and Gryc, 1959). Drilling in this area took place over the intervals from 1902 to 1906, 1936 to 1939, and 1953 to 1960. The deepest well was drilled to 11,200 feet. The highest production reported was 50 barrels a day from a well completed in 1903.

A description of oil seeps reported by the Russians in 1869 "near Katmai" probably referred to the Kanatak district near Lake Becharof on the Alaska Peninsula (Miller, Payne and Gryc, 1959). In 1903 to 1904, four wells were drilled southeast of Lake Becharof, and in 1923 to 1926, five more were drilled south of the east end of Lake Becharof. No significant petroleum occurrences were reported. In 1940 and 1959, two more unsuccessful wells were drilled between the two areas of former activity. Sixteen other wells have been drilled on the Alaska Peninsula west and southwest of the Kanatak district, two in 1959, seven in the 1960's, five in the 1970's, one in 1981, and the most recent in 1985. None were reported to have discovered any producible hydrocarbons.

Gold prospectors discovered oil and gas seeps near Katalla about 1896 (Martin, 1921), and 44 wells were drilled in the area between 1901 and 1932. Production in the Katalla district, which amounted to approximately 154,000 barrels of oil, ceased in 1933 because of a fire that partially destroyed the refinery.

In 1957, oil was discovered on the Kenai Peninsula in the Swanson River field. Other major oil and gas discoveries were made

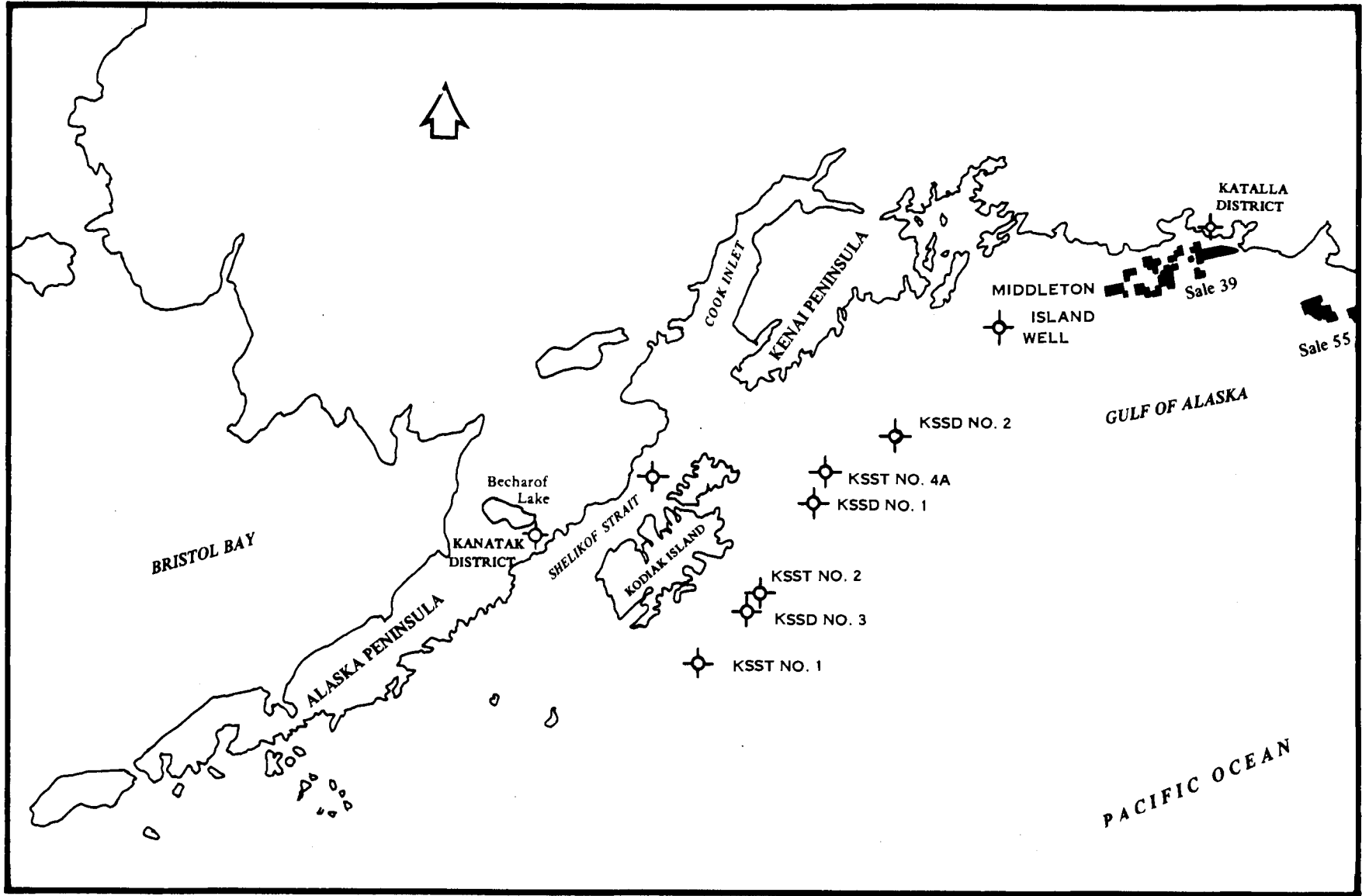


Figure 2. Locations of Kodiak Shelf COST wells and nearby petroleum districts.

in the next few years below upper Cook Inlet and production is still going on 30 years later.

In 1969, the Middleton Island well was drilled by Tenneco Oil Company at 59°41' north latitude, 146°26' west longitude, about 30 miles northwest of Middleton Island. No producible hydrocarbons were found.

In 1976, a COST well was drilled offshore in the Gulf of Alaska in the lease sale 39 area. Seven exploratory wells were drilled in this area in 1977 and 4 more were drilled in 1978. In 1983, one exploratory well was drilled in the lease sale 55 area. No producible hydrocarbons were found in any of these exploratory wells.

EXPLORATION ON KODIAK SHELF

To date, oil industry geophysical exploration in the Kodiak shelf area has produced 32,715 line miles of common-depth-point (CDP) data and 9,893 miles of high resolution (HRD) data. In 1976, the U. S. Geological Survey also gathered 2,212 miles of CDP data and 12,633 miles of HRD data in the area. No gravity and magnetic data have been gathered in this area.

Six DST wells were drilled on the Kodiak shelf in 1976 and 1977. Their locations, drilling company, depths, and completion dates are shown in table 1.

TABLE 1. COST wells drilled on the Kodiak shelf.

<u>Well Name</u>	<u>Location</u>		<u>Operator</u>	<u>Depth (feet)</u>	<u>Completion Date</u>
	<u>N lat</u>	<u>W long</u>			
KSST 1	56°23'39"	152°57'53"	Exploration Services	4,225	1 Aug 1976
KSST 2	57°00'18"	151°45'18"	Exploration Services	4,307	23 Aug 1976
KSST 4A	58°12'29"	150°19'46"	Exploration Services	1,391	19 Sep 1976
KSSD 1	57°59'53"	150°29'09"	Sun Oil	8,517	17 Jul 1977
KSSD 2	58°31'33"	148°48'42"	Sun Oil	10,460	8 Sep 1977
KSSD 3	56°57'16"	151°55'54"	Sun Oil	9,357	25 Oct 1977

In July 1971 the Deep Sea Drilling Project (DSDP) of the Joint Oceanographic Institutions for Deep Earth Sampling (JOIDES) drilled 5 core holes in the slope and abyssal plain south of the Kodiak shelf from the drill ship Glomar Challenger. Penetration depths beneath the sea floor ranged from 358 to 2,607 feet. Sites 179 through 182, drilled in water depths from 4,708 to 16,152 feet, are described at length in volume XVIII of the Initial Reports of the Deep Sea Drilling Project (Kulm and others, 1973).

No leases have been offered for sale in the Kodiak shelf area and no lease sales are scheduled for the immediate future.

2. OPERATIONAL SUMMARY OF THE KODIAK SHELF STRATIGRAPHIC DRILLING PROGRAM

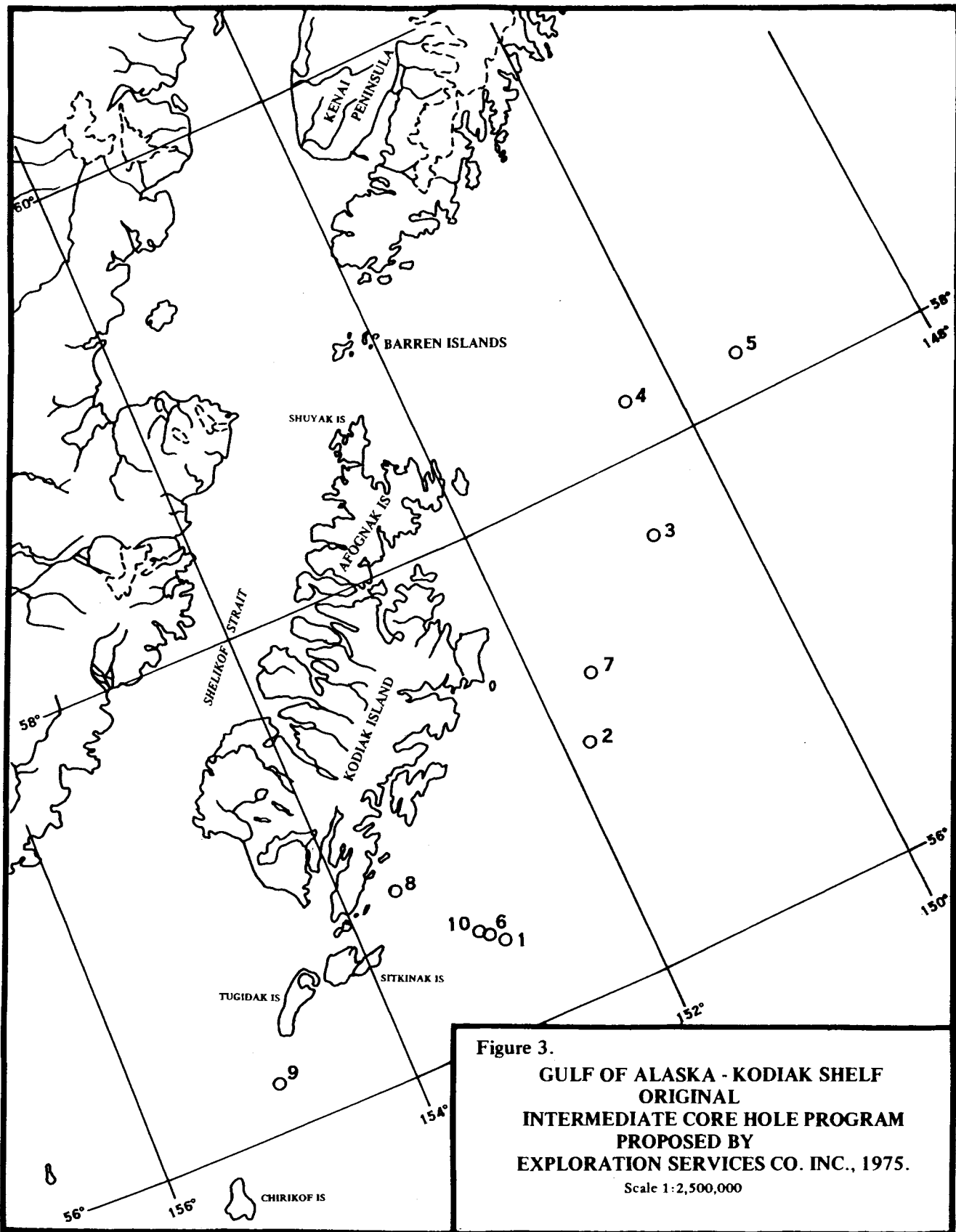
KSST WELLS

The Kodiak Shelf Stratigraphic Test (KSST) No. 1, 2, and 4A wells were drilled in 1976 to obtain geologic information prior to proposed Lease Sale 46. The three KSST wells were drilled from the Zapata Trader, a self-propelled shipshape drilling vessel owned by Zapata Offshore Company and built by William Pickersgill and Sons, Ltd., of Sunderland, England. The ship was converted to a drilling vessel by the Gulfport Shipbuilding Corp., Port Arthur, Texas, in 1975. The vessel is classified by the American Bureau of Shipping (ABS) as an A1 (E) (M) Drilling Unit suitable for moderate environmental and sea conditions and subpolar climates. The rig was designed to withstand 70-foot waves and 100-knot winds while drilling in 600 feet of water. The rated drilling depth is 20,000 feet with 5-inch drill pipe and 7-inch collars. The Zapata Trader was inspected by MMS (formerly the Conservation Division of the U.S. Geological Survey) personnel before drilling began. Operations were also inspected by MMS personnel throughout the drilling period to ensure compliance with Department of the Interior regulations and orders.

The KSST well program was operated by Exploration Services Company, Inc. (ESCI), with the following 10 oil companies sharing expenses:

- Amoco Production Company
- Cities Service Oil Company
- Gulf Oil Company, USA
- Union Oil Company of California
- Atlantic Richfield Company
- Exxon Corporation, USA
- Shell Oil Company
- Skelly Oil Company
- Standard Oil of California
- Sun Oil Company

On January 8, 1975, Exploration Services Company, Inc., submitted their original proposal to drill twenty 2,000-foot core holes in the Kodiak shelf area. Approval to drill the test holes was given on April 30, 1976, and was designated OCS Permit 76-35. This proposal was subsequently amended to extend the depth of the wells to 4,000 feet. The locations of the proposed sites are shown on figure 3. Only three holes were drilled under this permit from the approved



list of sites. All well depth measurements were made from the Kelly bushing (KB), which was 52 feet above sea level.

Kodiak, Alaska, was utilized as the primary shore base for personnel and equipment. Helicopters certified for instrument flights were used to transport personnel, groceries, and lightweight equipment between the rig and shore base. Personnel, equipment, and supplies were transported to and from the shore base and Anchorage, Alaska, via charter and common air carriers. Two sea-going supply boats supplied fuel, water, and miscellaneous cargo from the shore base to the rig.

KSST No. 1 Well

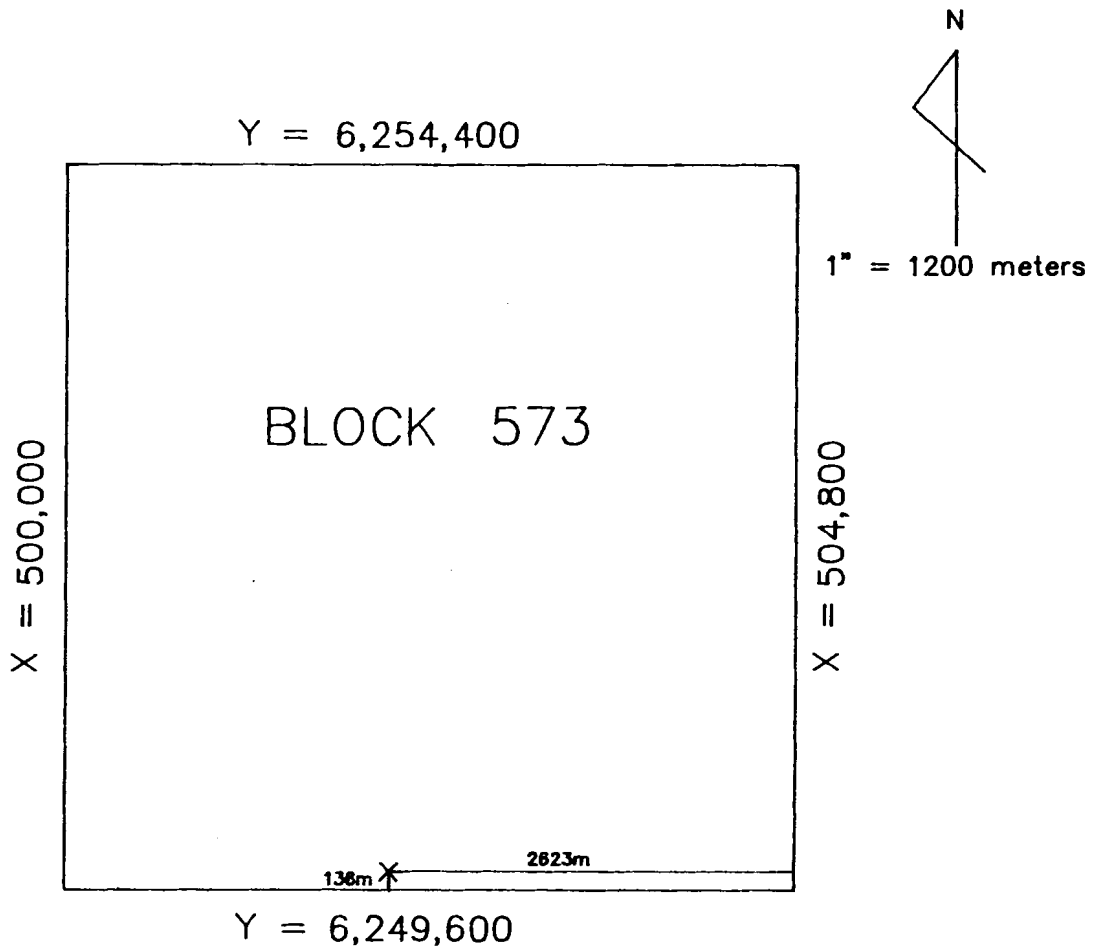
The location of the KSST No. 1 well was latitude $56^{\circ}23'38.9575''$ N and longitude $152^{\circ}57'53.0671''$ W, or UTM coordinates (Zone 5) X=502,176.68 meters and Y=6,249,736.55 meters. The well was located on Block 273 [OCS Protraction Diagram (OPD) Albatross Bank No. 5-8] in 162 feet of water (fig. 4). The KSST No. 1 well was spudded at 0100 hours on July 13, 1976, and reached a total depth of 4,225 feet on July 25, 1976, after 13 days of drilling. The well was permanently plugged and abandoned on August 3, 1976.

Drilling Program

The KSST No. 1 well was drilled using a total of seven bits ranging in size from 36 inches to 8 1/2 inches. The hole was spudded using a 36-inch bit to a depth of 238 feet, deepened to 327 feet with a 26-inch bit, then reamed out with the 36-inch bit to 327 feet. The well was further deepened with a 12 1/2-inch bit down to a depth of 1,260 feet, where the 9 5/8-inch casing was set, and then drilled to 4,210 feet with four 8 1/2-inch bits.

The average drilling rate was 45.3 feet per hour with a high rate of 65 feet per hour from 1,260 to 1,937 feet. A low rate of 10.5 feet per hour was experienced during the initial reaming-out of the hole prior to setting the 30-inch structure casing. The daily drilling progress for the well is shown on figure 5.

The 30-inch casing was set at 318 feet with 496 sacks of class G cement with 2 percent calcium chloride (CaCl_2); the 9 5/8-inch casing was set at 1,243 feet with 294 sacks of class G cement mixed with 4 percent gel, followed by 100 sacks of class G cement. Three cement plugs were set to plug and abandon the well. The first plug consisted of 150 sacks of class G cement with a slurry weight of 15.8 that was set between 2,614 and 2,714 feet. The second plug was a mixture of 132 sacks of class G cement and 600 pounds of calcium chloride that was set between 950 and 1,343 feet. The final plug consisted of 60 sacks of cement that were pumped down the drill pipe and placed between 320 and 470 feet. An unsuccessful attempt was made to cut the 30-inch casing at 240 feet. An explosive charge succeeded in separating the 30-inch casing at 218 feet. The casing and abandonment programs are shown in figure 6.



GEODETIC POSITION UNIVERSAL TRANSVERSE MERCATOR
COORDINATES, ZONE 5

LAT. 56° 23' 38.9575" N Y = 6,249,736.55 meters
LONG. 152° 57' 53.0671" W X = 502,176.68 meters

Figure 4. Final location plat showing the position of the KSST No. 1 well, OCS Protraction Diagram NO 5 - 8.

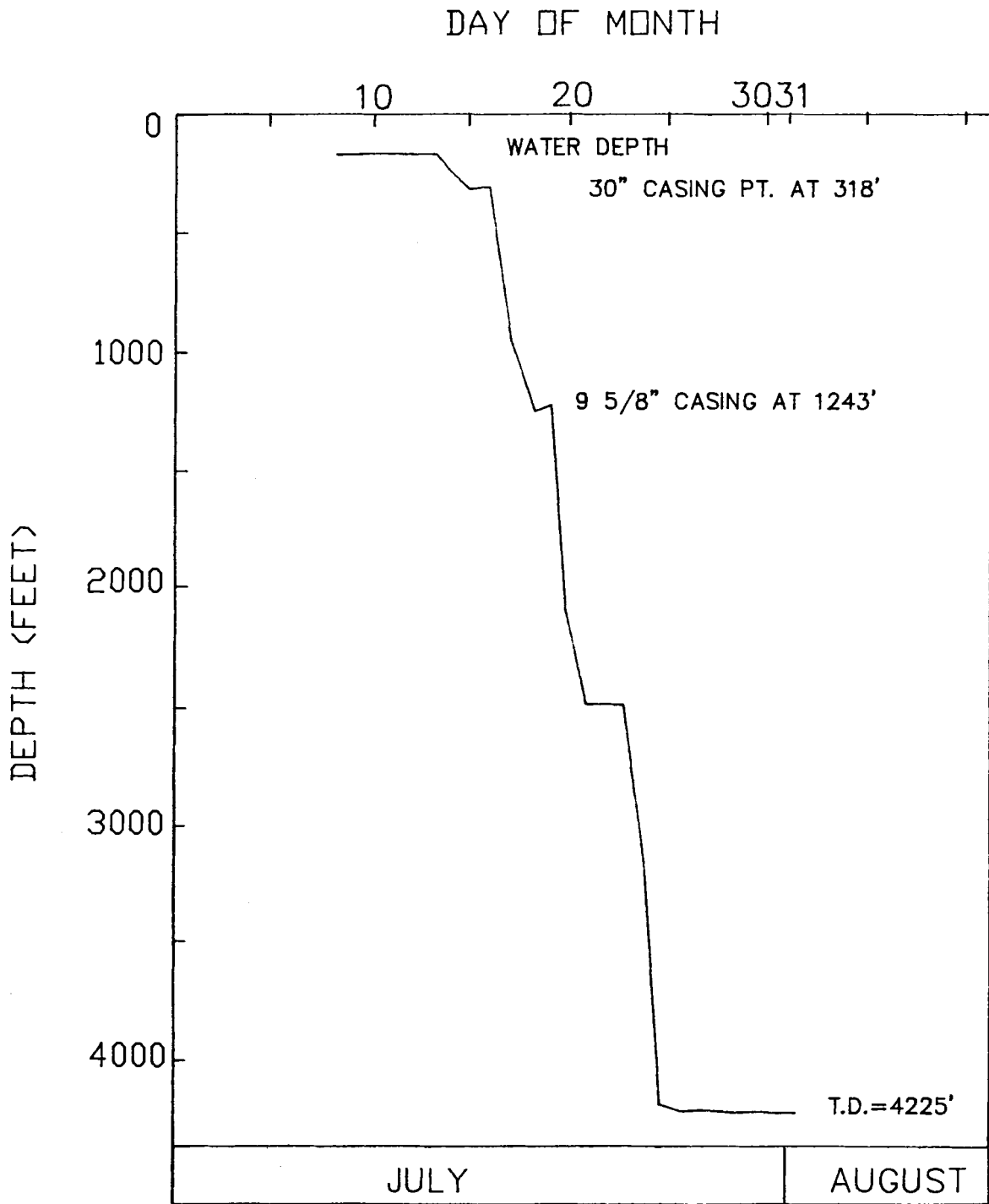


Figure 5. Daily drilling progress for the KSST No. 1 well.

KELLY BUSHING 0'
MEAN SEA LEVEL 52'
MUD LINE 214'

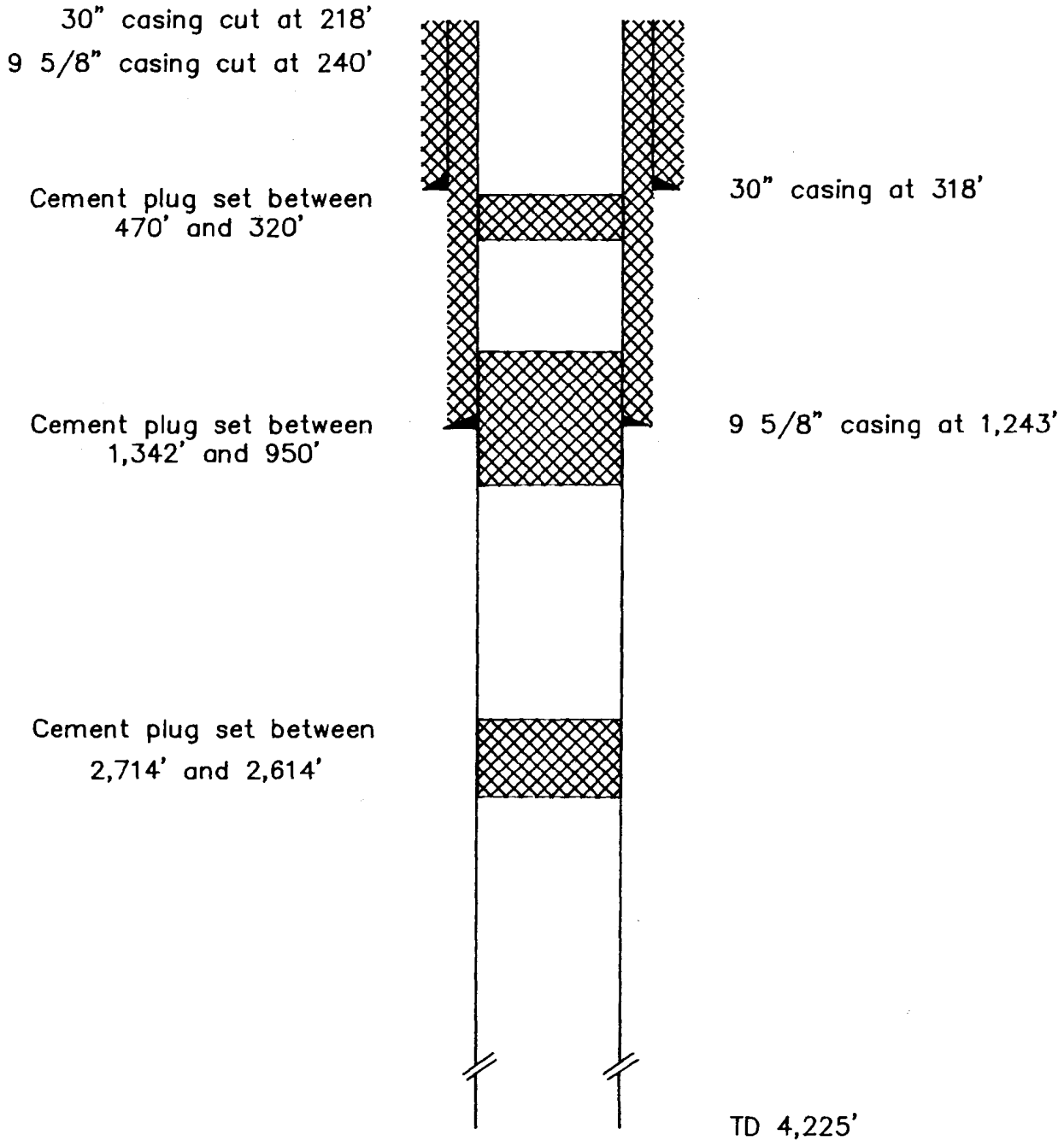


Figure 6. Schematic diagram showing casing strings, plugging and abandonment program, KSST No. 1 well.

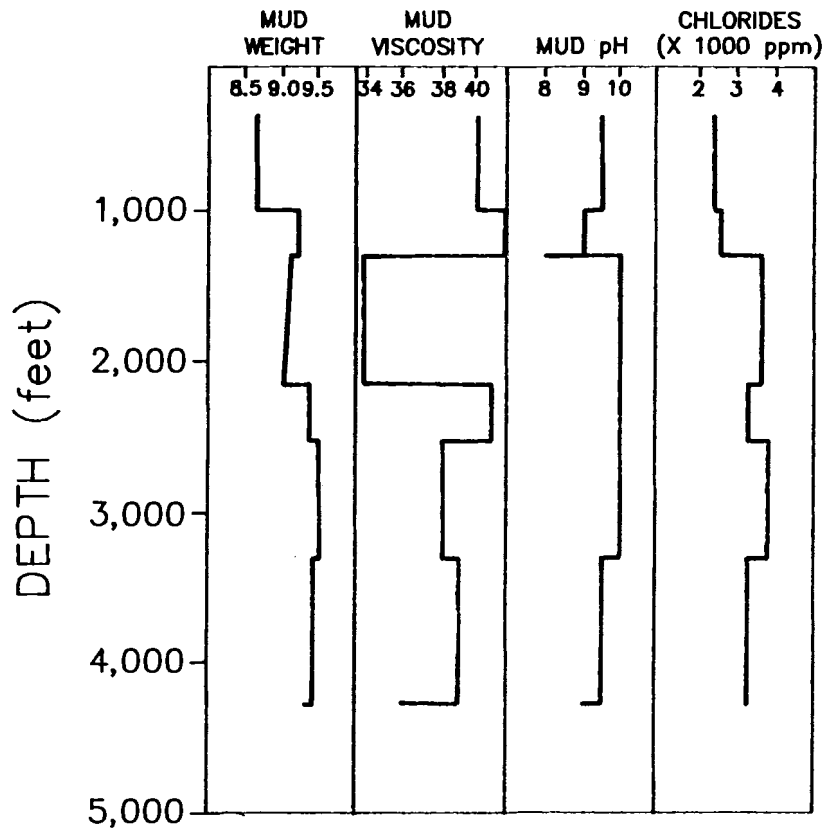


Figure 7. Changes of drilling mud properties with depth, including mud weight, viscosity, pH, and total chlorides, KSST No. 1 well.

Drilling Mud

The well was drilled with sea water to 330 feet, where sea water was replaced with a gel mud weighing 8.7 pounds per gallon (ppg) which was used to 838 feet. The mud was then "weighted up" with barite to 9.2 ppg and varied little thereafter. The final mud weight at TD was 9.3 ppg. Viscosity varied from 36 to 42 seconds throughout the well, with an average of approximately 38 seconds. Initial chloride concentrations were 2,300 parts per million (ppm), which increased to 3,800 ppm midway through the well, then decreased to 3,300 ppm at total depth. Calcium concentrations were generally limited to trace amounts except for a stringer located between 2,124 and 2,501 feet which raised the concentration level to 3,400 ppm. Mud pH values ranged between 8.0 and 10.0, averaging about 10.0 throughout most of the well. Selected drilling mud properties and their average changes with depth are shown in figure 7.

Samples and Tests

Drill cuttings were collected every 30 feet for lithologic and paleontologic analysis. Logging runs were made at depths of 1,260 and 4,225 feet. The types of logs and the intervals over which they were run are as follows:

Run 1 (318 to 1,250 feet) and

Run 2 (1,250 to 4,160 feet)

Dual Induction Laterolog (DIL)
Borehole Compensated Sonic (BHC)
Compensated Neutron/Formation Density (CNL/FDC)
High Resolution Dipmeter Tool (HDT)

There were no drill stem tests performed on this well.

Weather

KSST No. 1 operations were delayed for 30 hours from July 19 to July 20, 1976, because of high seas and winds. The rest of the drilling program was uninterrupted.

KSST No. 2 Well

The location of the KSST No. 2 well was latitude 57°00'17.78" N and longitude 151°45'17.88" W, or UTM coordinates (Zone 5) X=575,624 meters and Y=6,318,412 meters. The well was located on Block 984 (OPD Kodiak No. 5-6) in 237 feet of water (fig. 8). The KSST No. 2 well was spudded on August 3, 1976, and reached a total depth of 4,307 feet on August 19, 1976. It was abandoned on August 23, 1976, after 17 days of drilling.

Drilling Program

The KSST No. 2 well was drilled as a straight hole using a total of six drill bits ranging from 36 inches to 8 1/2 inches. A 26-inch drill bit was used to spud the well and to continue drilling down to

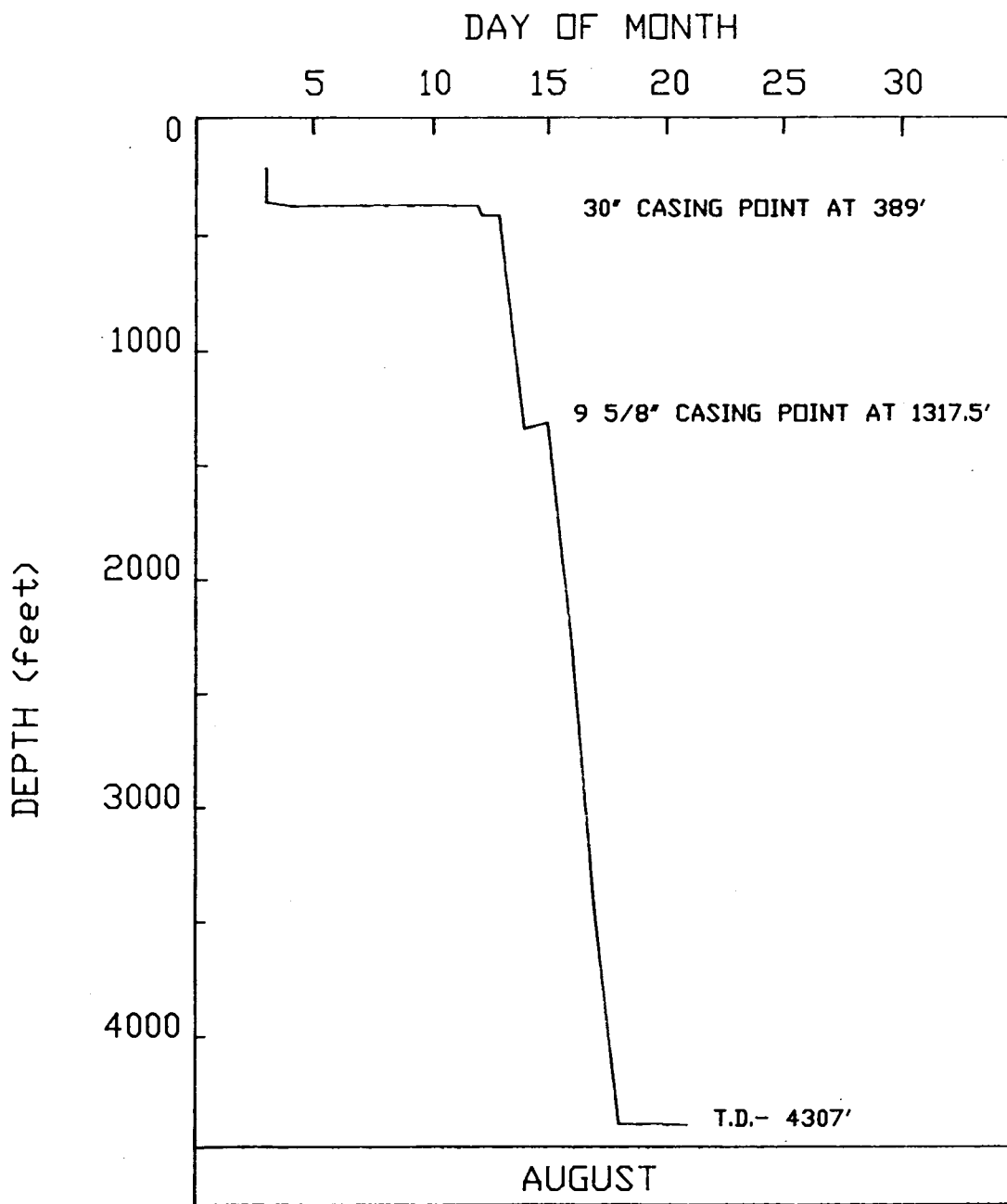


Figure 9. Graph showing daily drilling progress for the KSST No. 2 well.

377 feet, after which the hole was reamed open using a 36-inch hole opener assembly. The 36-inch bit was used to drill to 399 feet. A 26-inch bit was then used to drill to 1,338 feet, after which an 8 1/2-inch drill bit was used to the total depth of 4,307 feet.

The average drilling rate was 63.5 feet per hour, with a high rate of 109 feet per hour from 421 to 1,338 feet. A low rate of 5 feet per hour was experienced during the spudding of the well down to a depth of 377 feet. The daily drilling program for the well is shown in figure 9.

The casing program consisted of setting the 30-inch string at a depth of 389 feet with 280 sacks of class G cement with 2 percent calcium chloride. The 9 5/8-inch casing was set at 1,317.5 feet with 460 sacks of cement mixed with 4 percent gel followed by 100 sacks of neat cement. Four cement plugs were set to abandon the well. The first plug was set between 2,667 and 2,784 feet using 40 sacks of class G cement. The second plug was placed between 1,443 and 1,193 feet with 135 sacks of class G cement mixed with 2 percent calcium chloride. The third plug was placed between 387 and 535 feet with 56 sacks of class G cement mixed with 2 percent CaCl_2 . The surface plug, consisting of 168 sacks of class G cement mixed with 2 percent CaCl_2 , was set between 316 and 349 feet. The casing and abandonment programs are shown in figure 10.

Exploration Services Company, Inc., mechanically cut the 9 5/8-inch casing at 338 feet, but during removal the lower portion of the casing unscrewed and became detached from the rest of the string. This section was subsequently retrieved by using a 9 5/8-inch spear. The 30-inch conductor casing was then mechanically cut and recovered at 307 feet.

Drilling Mud

The mud program for the KSST No. 2 well was similar to that of the KSST No. 1 well. The initial spudding of the well used sea water for the first 377 feet of the hole. A problem with hole sloughing occurred at 421 feet and was remedied by using a gel mud system weighing 8.7 ppg. The mud weight was gradually increased over the well depth to a final weight of 9.6 ppg at TD. Viscosity varied from 48 seconds initially to 43 seconds at TD, with an average of approximately 44 seconds. Chloride concentration started at 3,100 ppm and decreased to 2,500 at total depth. Mud pH values ranged between 9.5 and 11.3, with the bulk of the values being recorded at a pH of 9.5. Selected drilling mud properties and their average changes with depth are shown in figure 11.

Samples and Tests

Drill cuttings were collected for lithologic and paleontologic analysis at 30-foot intervals from 450 to 4,307 feet (TD). Logging

KELLY BUSHING 0'
MEAN SEA LEVEL 52'
MUD LINE 284'

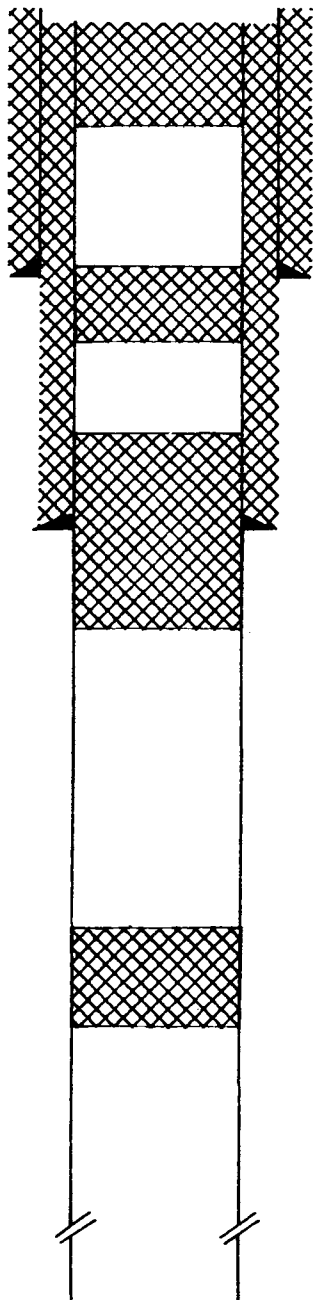
30" casing cut at 307'
9 5/8" casing cut at 338'

Cement plug set between
349' and 316'

Cement plug set between
535' and 387'

Cement plug set between
1,443' and 1,193'

Cement plug set between
2,784' and 2,667'



30" casing at 389'

9 5/8" casing at 1,317.5'

TD 4,307'

Figure 10. Schematic diagram showing casing strings, plugging and abandonment program, KSST No. 2 well.

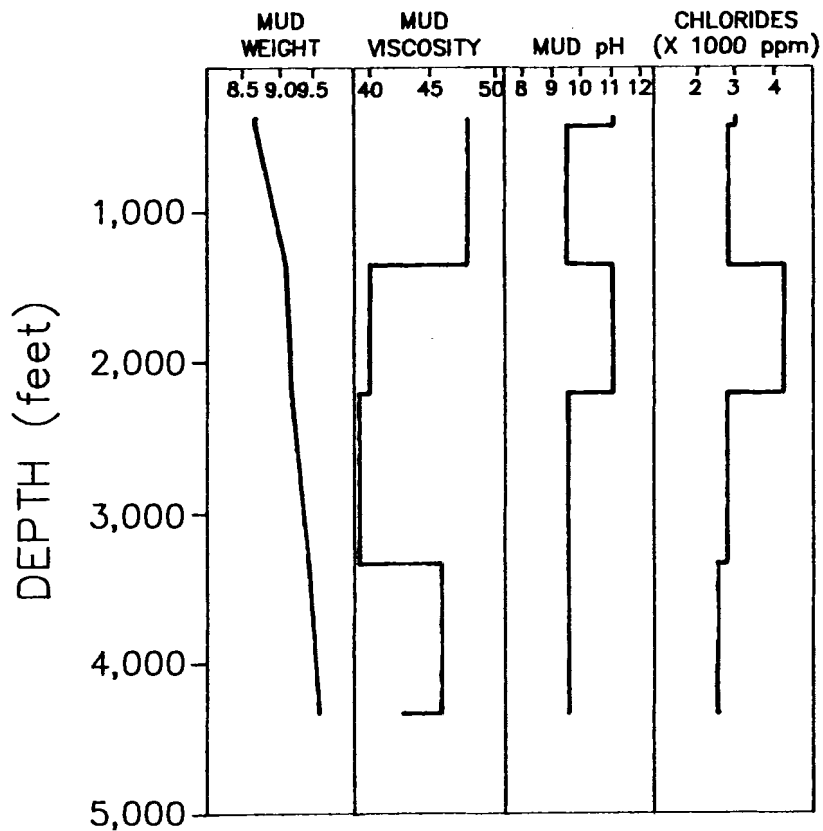


Figure 11. Changes of drilling mud properties with depth, including mud weight, viscosity, pH, and total chlorides, KSST No. 2 well.

runs were made at depths of 1,338 feet and 4,307 feet. The types of logs and the intervals over which they were run follow:

Run 1 (338 to 1,338 feet) and

Run 2 (1,344 to 4,307 feet)

Dual Induction-Laterolog (DIL)
Borehole Compensated Sonic (BHC)
Compensated Neutron/Formation Density (CNL/FDC)
High Resolution Dipmeter Tool (HDT)

No drill stem tests were performed on this well.

Weather

KSST No. 2 operations were delayed for 58 hours from August 5 to 8, 1976, because of high seas and winds.

KSST No. 4A Well

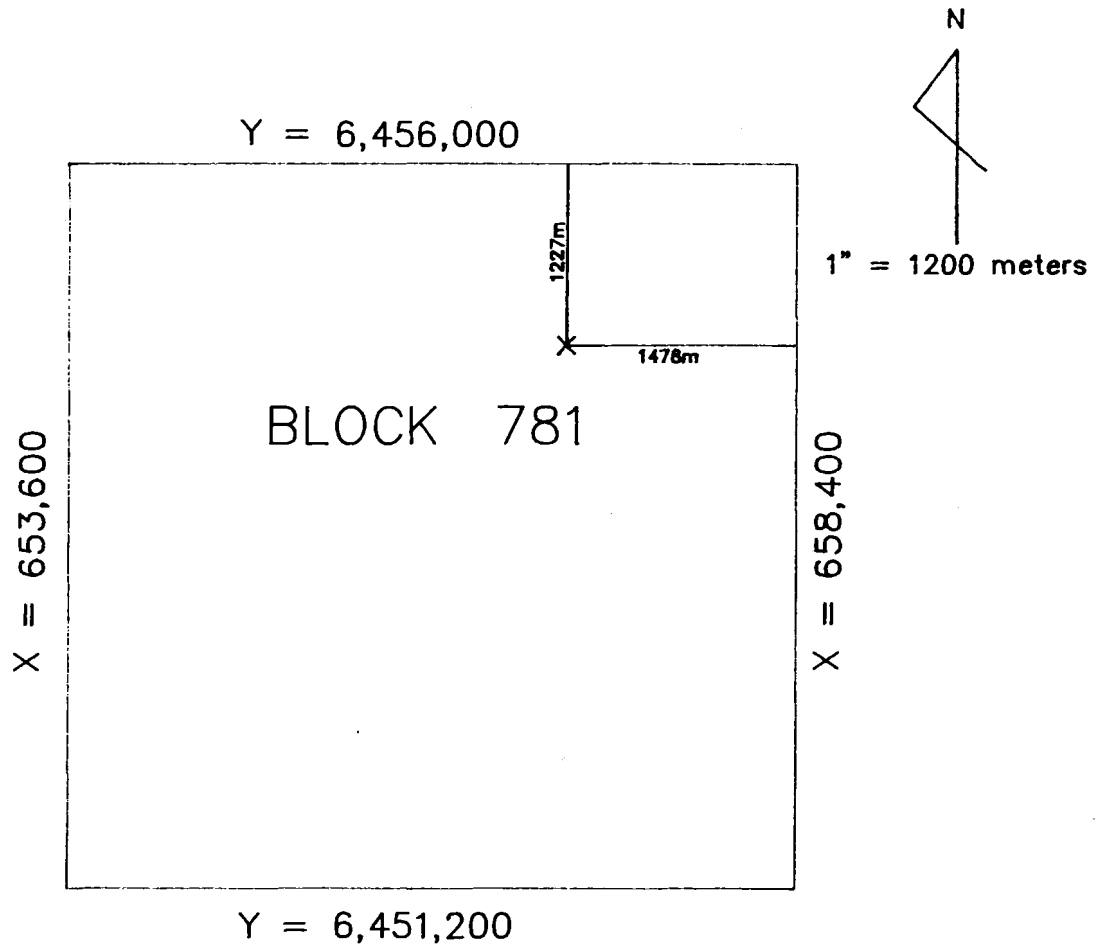
The KSST No. 4 well was spudded at 0730 hours on August 28, 1976, and was drilled to 477 feet where an attempt was made to set the 30-inch casing. Because of adverse hole conditions, the casing could not be run to total depth and subsequently parted while being pulled out of the hole. The hole was then abandoned. A second well, the KSST No. 4A, was spudded on August 30, 1976, approximately 50 feet from the original location, and reached a total depth of 1,391 feet on September 5, 1976, after 7 days of drilling. The well was plugged and abandoned on September 19, 1976. The location for the KSST No. 4A well was latitude $58^{\circ}12'28.98''$ N and longitude $150^{\circ}19'45.81''$ W, or UTM coordinates (Zone 5) X=659,922 meters and Y=6,454,773 meters. The well was located on Block 781 (OPD Afognak No. 5-4) in 307 feet of water (fig. 12).

Drilling Program

The first attempt by Exploration Services Company, Inc., to drill on Block 781 was abandoned when a section of 30-inch surface casing became separated while being removed from the hole. The original hole was drilled to a total depth of 477 feet. While running the casing into the hole, a bridge was encountered at 422 feet. As the string was being pulled so that the hole could be reamed back to 477 feet, the casing parted. This hole was subsequently plugged and abandoned. The vessel moved approximately 50 feet from the first location and spudded the KSST No. 4A well.

The KSST No. 4A well was drilled as a straight hole using a total of 3 drill bits. A 26-inch bit was used to drill to 479 feet, and the hole was then enlarged using a 36-inch hole opener assembly to a depth of 477 feet. A 12 1/2-inch bit was used to the total depth of 1,391 feet.

The average drilling rate for the KSST No. 4A well was 37.3 feet per hour, with a high rate of 86.3 feet per hour from 479 feet to



GEODETIC POSITION UNIVERSAL TRANSVERSE MERCATOR
COORDINATES, ZONE 5

LAT.	58° 12' 28.98" N	Y =	6,454,773 meters
LONG.	150° 19' 45.81" W	X =	656,922 meters

Figure 12. Final location plat showing the position of the KSST No. 4A well, OCS Protraction Diagram NO 5 - 4.

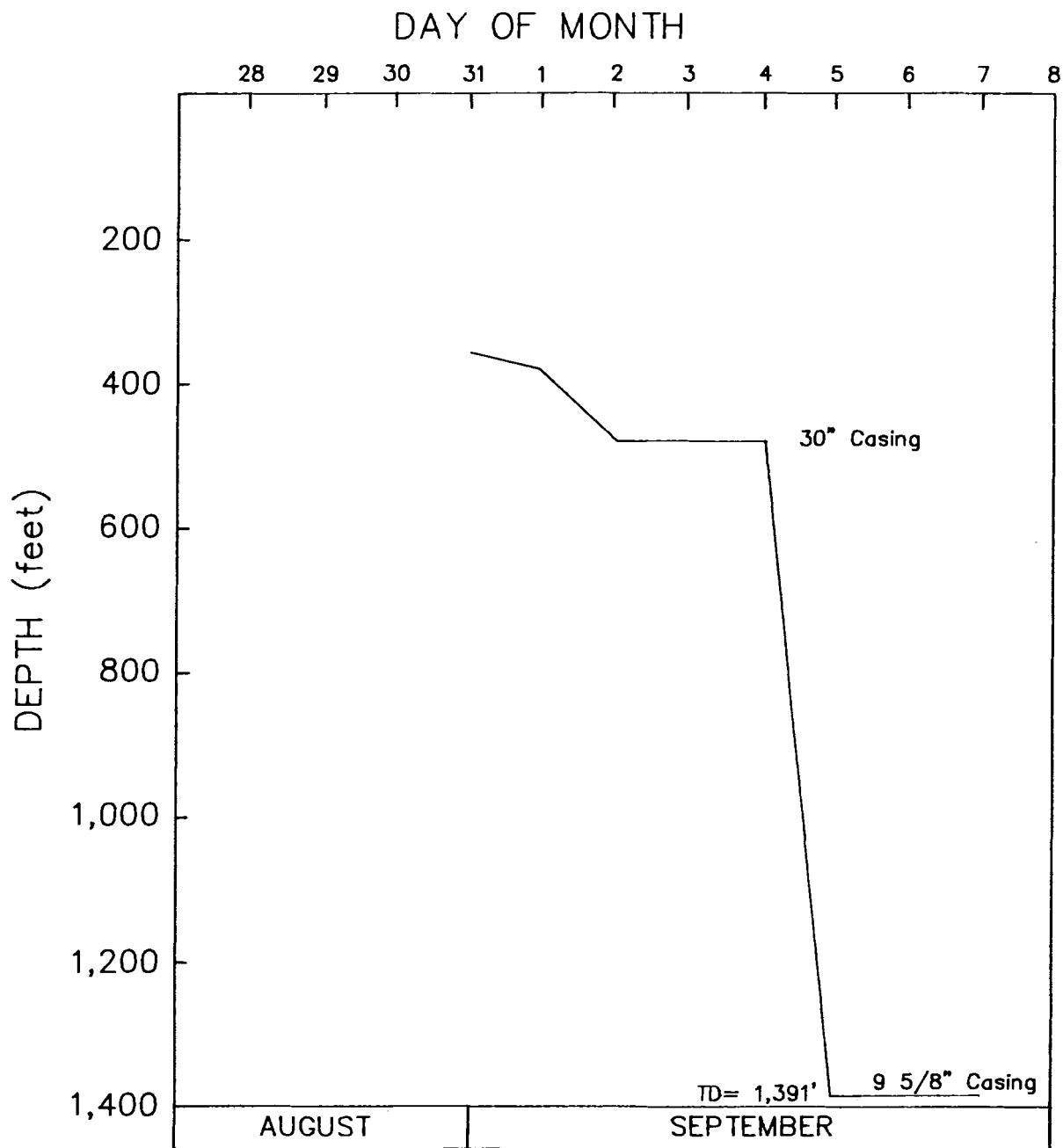


Figure 13. Graph showing daily drilling progress for the KSST No. 4A well.

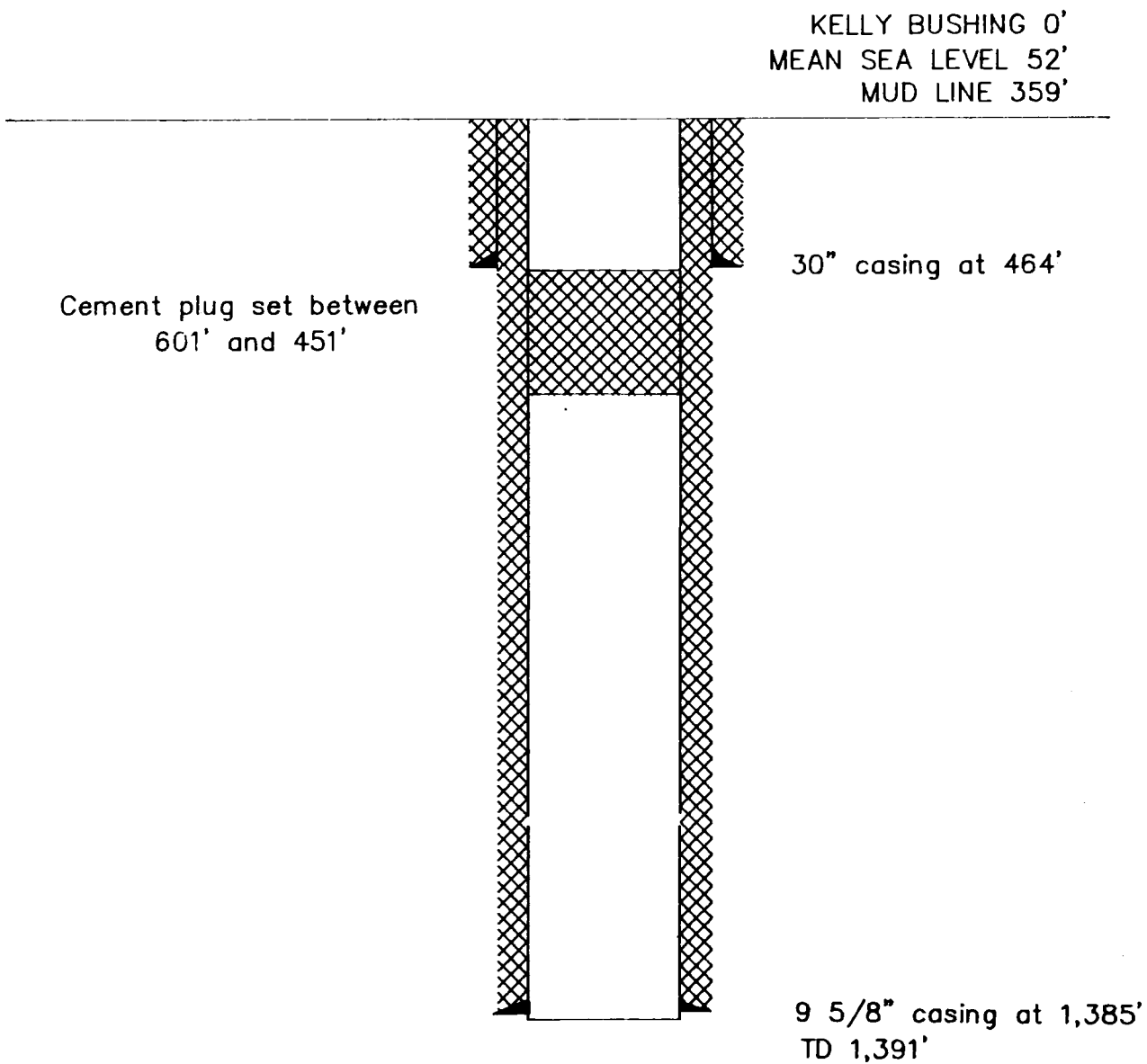


Figure 14. Schematic diagram showing casing strings, plugging and abandonment program, KSST No. 4A well.

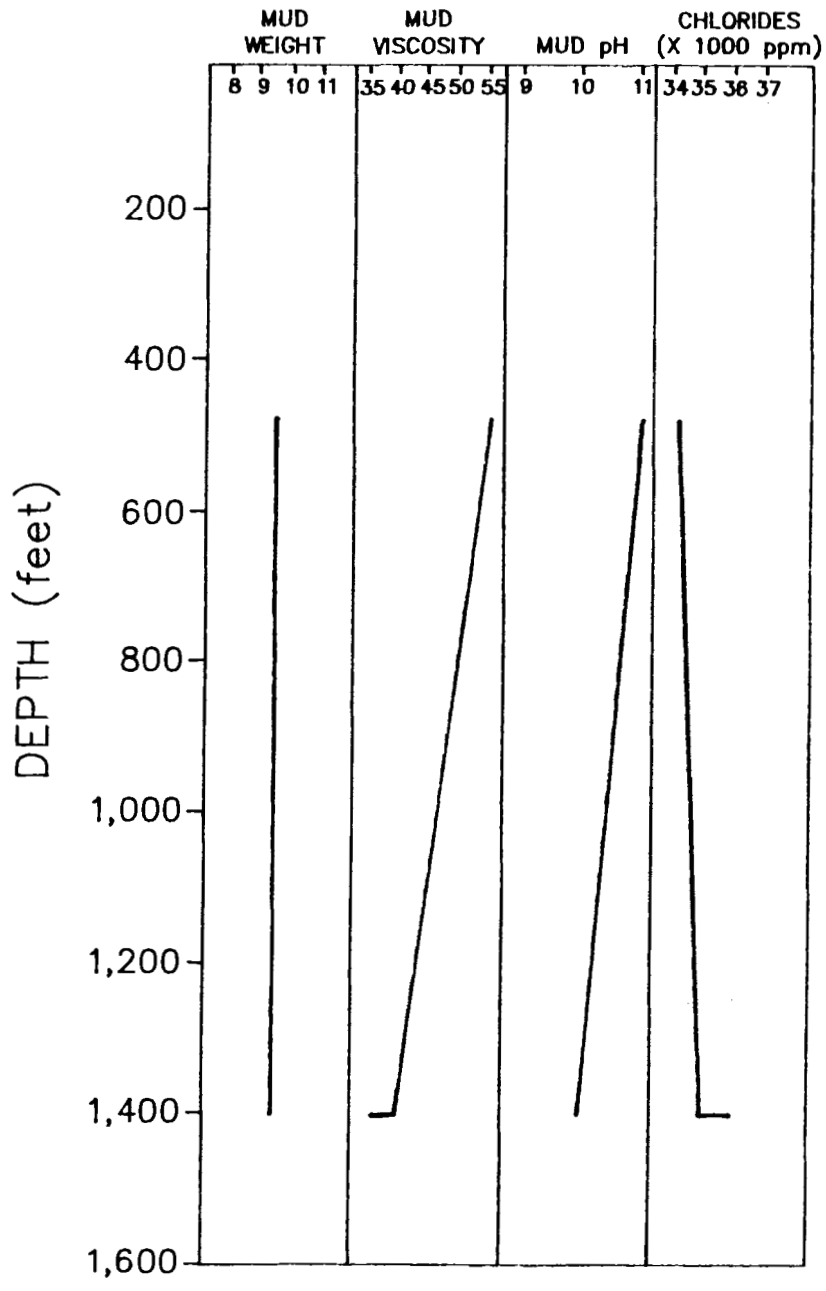


Figure 15. Changes of drilling mud properties with depth, including mud weight, viscosity, pH, and total chorides, KSST No. 4A well.

1,385 feet and a low rate of 6.9 feet per hour from 359 feet to 479 feet. The daily drilling program for the well is shown in figure 13.

The 30-inch casing string was set at a depth of 464 feet with 435 sacks of cement. The 9 5/8-inch casing was set at a depth of 1,385 feet with 344 sacks of class G cement with 4 percent gel, followed by 100 sacks class G cement with 2 percent CaCl_2 . The KSST No. 4A well was abandoned by setting 57 sacks of cement from 451 to 601 feet. No casing was recovered. The casing and abandonment programs for KSST No. 4A are shown in figure 14.

Drilling Mud

The well was drilled with sea water to 479 feet, where sea water was replaced with a gel mud weighing 8.7 ppg. After cementing the 30-inch casing, the gel mud was changed to a 9.4-ppg drilling mud. The mud weight varied little thereafter to the TD of 1,391 feet. Viscosity decreased from 55 seconds initially to 36 seconds at TD, with an average of approximately 42 seconds. Chloride concentrations gradually increased from 3,400 ppm at 479 feet to 3,600 ppm at total depth. Selected drilling mud properties of the KSST No. 4A well and their average changes with depth are shown in figure 15.

Samples and Tests

One series of conventional sidewall cores was taken between 479 and 1,400 feet. Thirty cores were attempted and 18 recovered.

The types of logs and the interval over which they were run are as follows:

Run 1 (470 to 1,390 feet)

- Dual Induction-Laterolog (DIL)
- Borehole Compensated Sonic (BHC)
- Compensated Neutron/Formation Density (CNL/FDC)
- High Resolution Dipmeter Tool (HDT)

There were no drill stem tests on this well.

Weather

KSST No. 4A operations were delayed due to high seas and winds for 57 hours from September 8 to 10, and for 72 hours from September 14 to 17.

KSSD WELLS

The KSSD No. 1, 2, and 3 wells were drilled in 1977 by Sun Oil from the SEDCO 708, a self-propelled, column-stabilized semisubmersible drilling unit. The SEDCO 708 was constructed in 1977 by Kaiser Steel Corporation and is classified by the American Bureau of Shipping (ABS) as A1 (E) (M) AMS. It was designed to withstand 110-foot waves and 100-knot winds in 600 feet of water.

The rated drilling depth is 25,000 feet. The KSSD wells were the first wells drilled by the SEDCO 708.

Sun Oil Company acted as operator for itself and the following 13 oil companies who shared expenses for the three KSSD wells:

Amerada Hess
Amoco Production Company
Atlantic Richfield Company
Chevron USA
Cities Service Company
Continental Oil Company
Exxon Corporation, USA
Getty Oil Company
Gulf Energy & Minerals Company, USA
Marathon Oil Company
Phillips Petroleum Company
Shell Oil Company
Texaco, Inc.

The primary shore base and air base for personnel and supplies was Kodiak, Alaska, which is approximately 61, 125, and 54 miles from the No. 1, No. 2, and No. 3 well sites, respectively.

Regulations and OCS Orders required Sun Oil to provide the Minerals Management Service with all well logs, samples, cores, and operational and technical reports at the same time it provided them to industry participants.

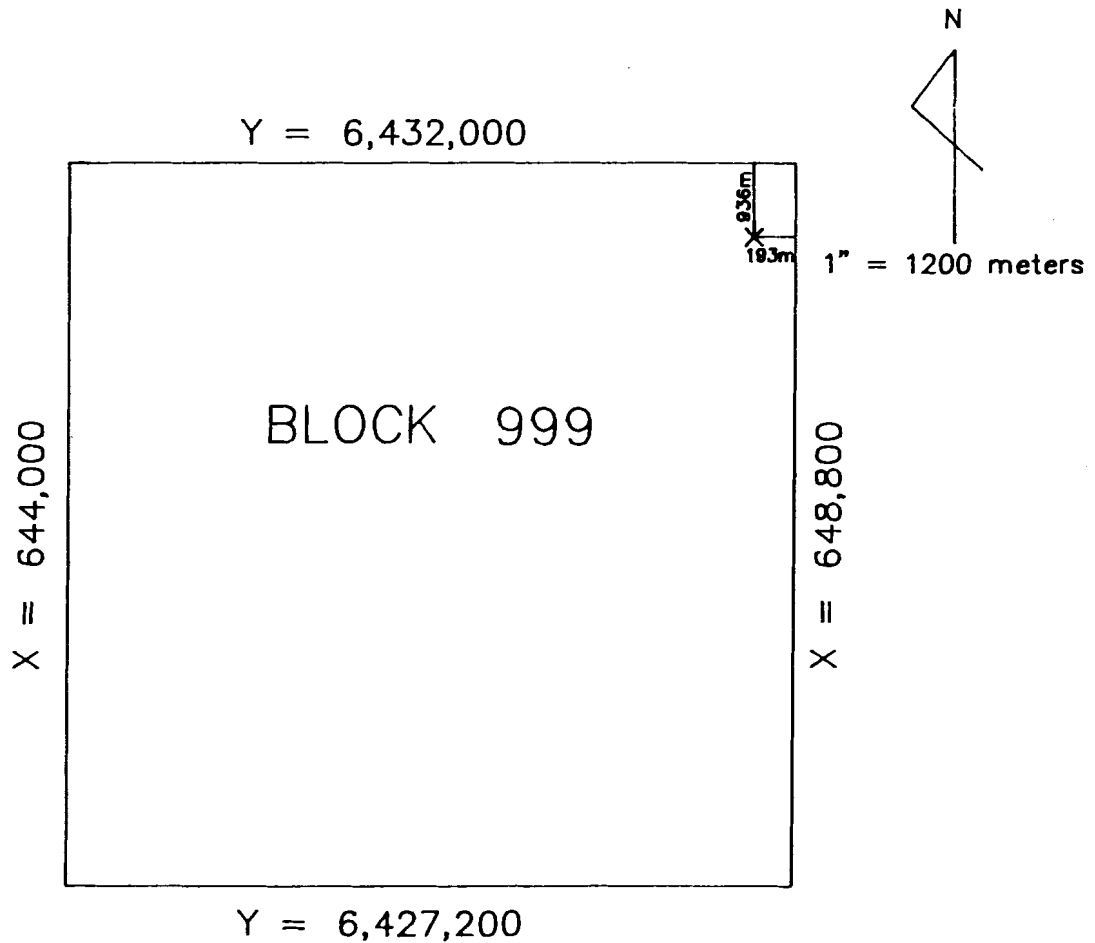
KSSD No. 1 Well

The location of the KSSD No. 1 well was latitude 57°59'53.4922" N and longitude 150°29'08.7375" W, or UTM coordinates (Zone 5) X=648,607 meters and Y=6,431,064 meters. The well was located on Block 999 [Official Protraction Diagram (OPD) NO5-6] in 526 feet of water (fig. 16). All measurements were made from the Kelly bushing (KB) which was 90 feet above sea level and 616 feet above the mud line. The KSSD No. 1 well was spudded at 2200 hours on May 25, 1977, and reached a total depth of 8,517 feet on July 11, 1977, after 47 days of drilling. The well was plugged and abandoned by 0800 hours on July 17, 1977. On July 18, 1977, the rig was under tow to the KSSD No. 2 well location.

Drilling Program

The KSSD No. 1 well was drilled as a straight hole using a total of 15 drill bits. A 26-inch bit was used to drill to a depth of 777 feet, after which the hole was opened using a 36-inch hole opener assembly. A 26-inch bit was used to 1,670 feet, 17 1/2-inch bits were used to 4,636 feet, and 12 1/2-inch bits were used to 8,517 feet (TD).

The average drilling rate was 28.4 feet per hour, with a high rate of 81 feet per hour from 1,670 to 4,634 feet and a low rate of



GEODETIC POSITION UNIVERSAL TRANSVERSE MERCATOR
COORDINATES, ZONE 5

LAT. 57° 59' 53.4922" N Y = 6,431,064 meters
LONG. 150° 29' 08.7375" W X = 648,607 meters

Figure 16. Final location plat showing the position of the KSSD No. 1 well, OCS Protraction Diagram NO 5 - 6.

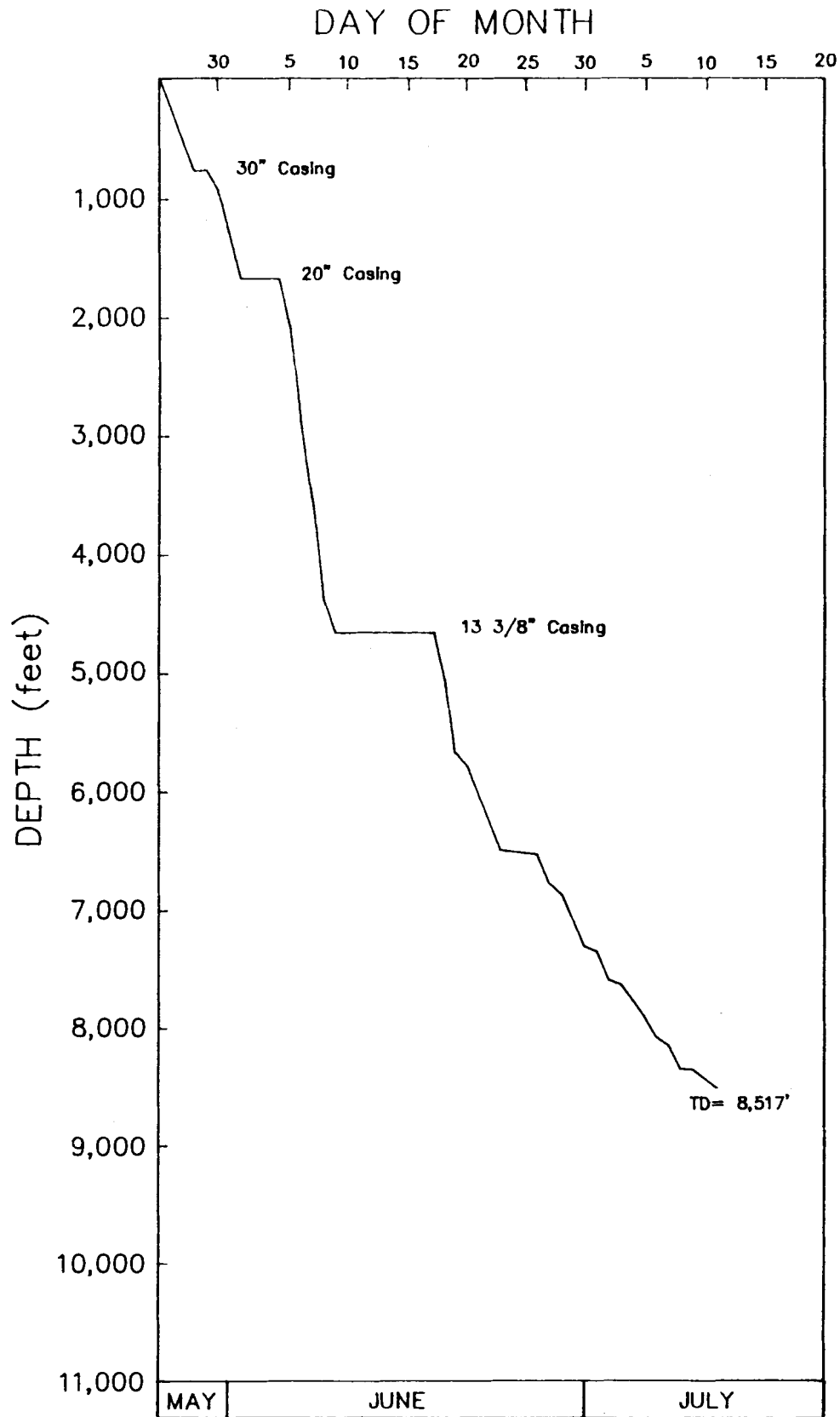


Figure 17. Graph showing daily drilling progress for the KSSD No. 1 well.

8.2 feet per hour from 8,140 feet to TD. Figure 17 shows the daily drilling progress.

The 30-inch casing string was set at a depth of 742 feet with 500 sacks of cement; the 20-inch was set at 1,619 feet with 1,735 sacks of cement; and the 13 3/8-inch was set at 4,584 with 1,805 sacks of cement. Two cement plugs were set to abandon the well. The first plug was set between 4,434 and 4,685 feet, the second between 761 and 911 feet. The hole between the plugs remained filled with drilling mud. The 20-inch and 30-inch casing strings were cut and pulled from 637 feet. The 13 3/8-inch casing was cut and pulled from 642 feet. The casing and abandonment programs are shown in figure 18.

Drilling Mud

The well was drilled with seawater to 1,670 feet, where the seawater was replaced with a gel mud weighing 9.2 pounds per gallon (ppg). The mud weight varied little over the course of the well, with a final weight at TD of 10.5 ppg. Viscosity varied from 50 seconds initially to 40 seconds at TD, with an average of approximately 43 seconds. Chloride concentrations started at 11,000 ppm at about 2,675 feet and decreased to less than 2,000 ppm from approximately 6,225 feet to TD. Mud-logging services were provided by NL Baroid Petroleum Services from approximately 1,670 feet to TD. The mud properties for this well are shown in figure 19.

Samples And Tests

One series of sidewall cores was taken between 1,680 and 4,614 feet. There were 59 cores recovered in 74 attempts. Six conventional cores were taken. The intervals cored and the footage recovered are shown in table 2. The cores were analyzed for mineralogy, paleontology, porosity and permeability, grain density, and diagenesis. Limited oceanographic and meteorological data were collected for this well.

TABLE 2. Conventional cores, KSSD No. 1 well.

<u>Core No.</u>	<u>Interval (feet)</u>	<u>Recovered (feet)</u>
1	5,775 - 5,785	8
2	5,785 - 5,823	38
3	6,496 - 6,508	8
4	6,508 - 6,514	4
5	8,140 - 8,155	12
6	8,155 - 8,177	22

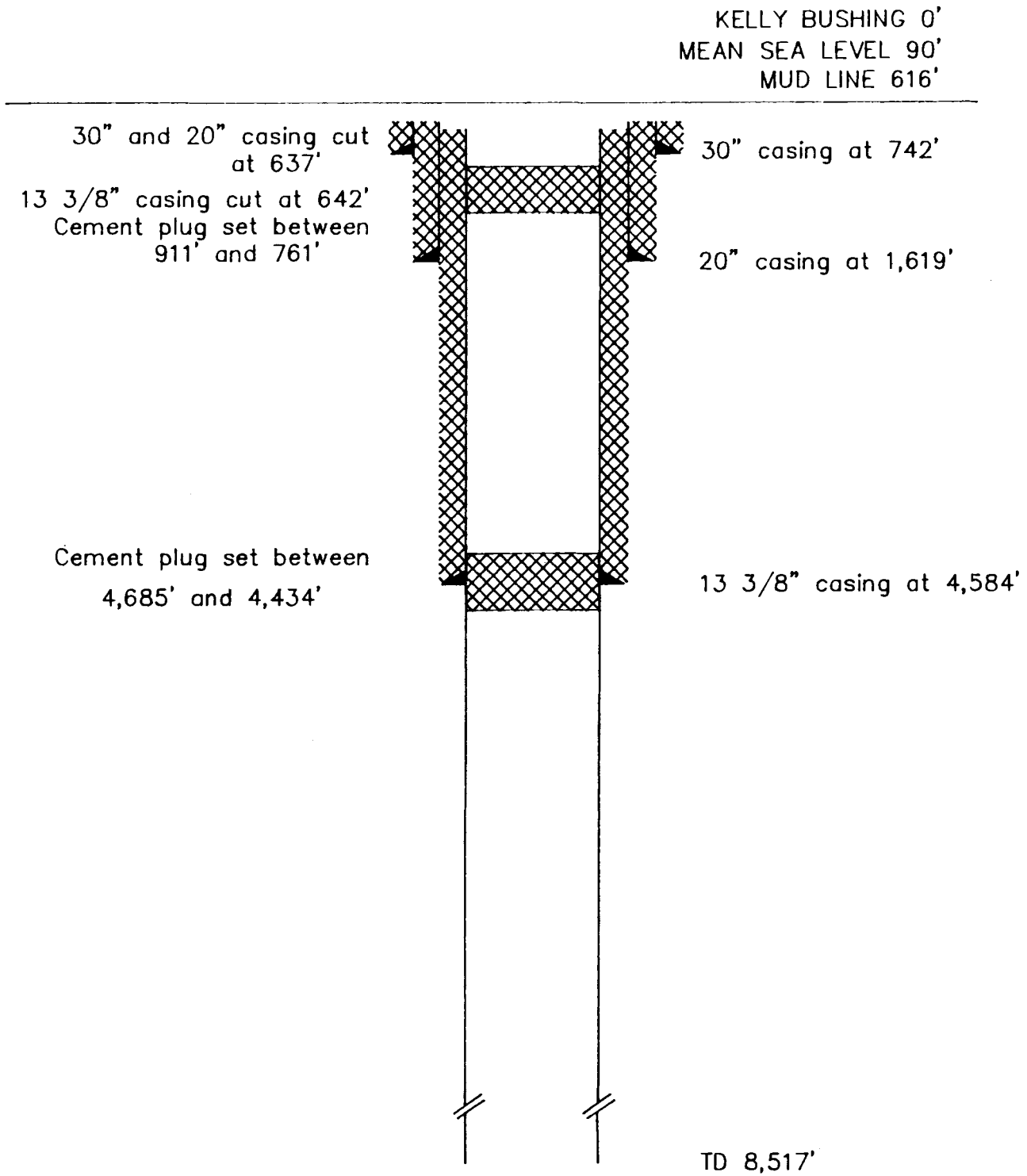


Figure 18. Schematic diagram showing casing strings, plugging and abandonment program, KSSD No. 1 well.

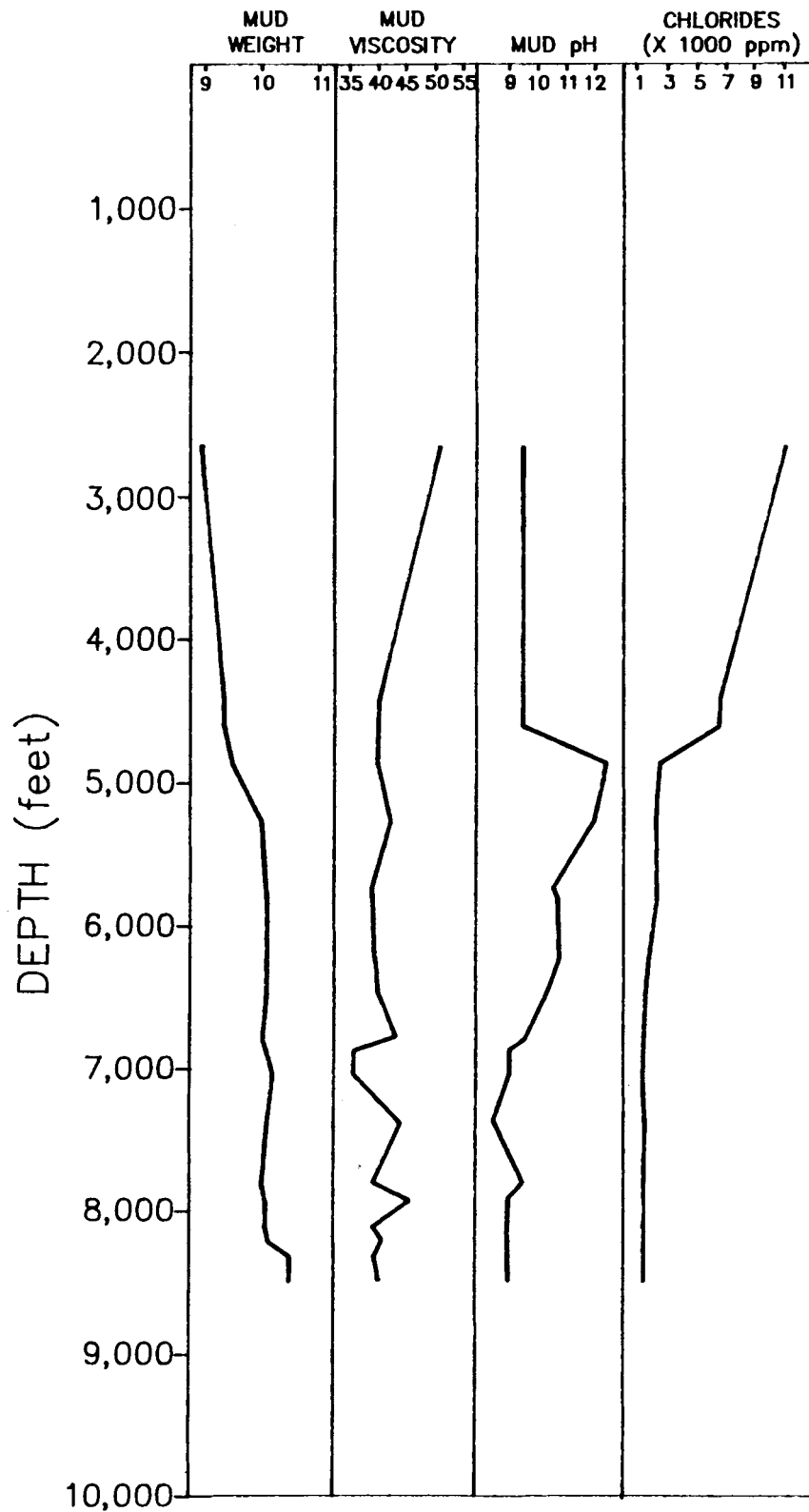


Figure 19. Changes of drilling mud properties with depth, including mud weight, viscosity, pH, and total chlorides, KSSD No. 1 well.

The types of logs and the intervals over which they were run are as follows:

Run 1 (1,618 to 4,630 feet) and

Run 2 (4,600 to 8,495 feet)

Dual Induction Laterolog (DIL)
Borehole Compensated Sonic (BHC)
Long Spaced Sonic (LSS)
Proximity Microlog (PML)
Compensated Neutron/Formation Density (CNL/FDC)
High Resolution Dipmeter Tool (HDT)

There were no drill stem tests run on this well.

KSSD No. 2 Well

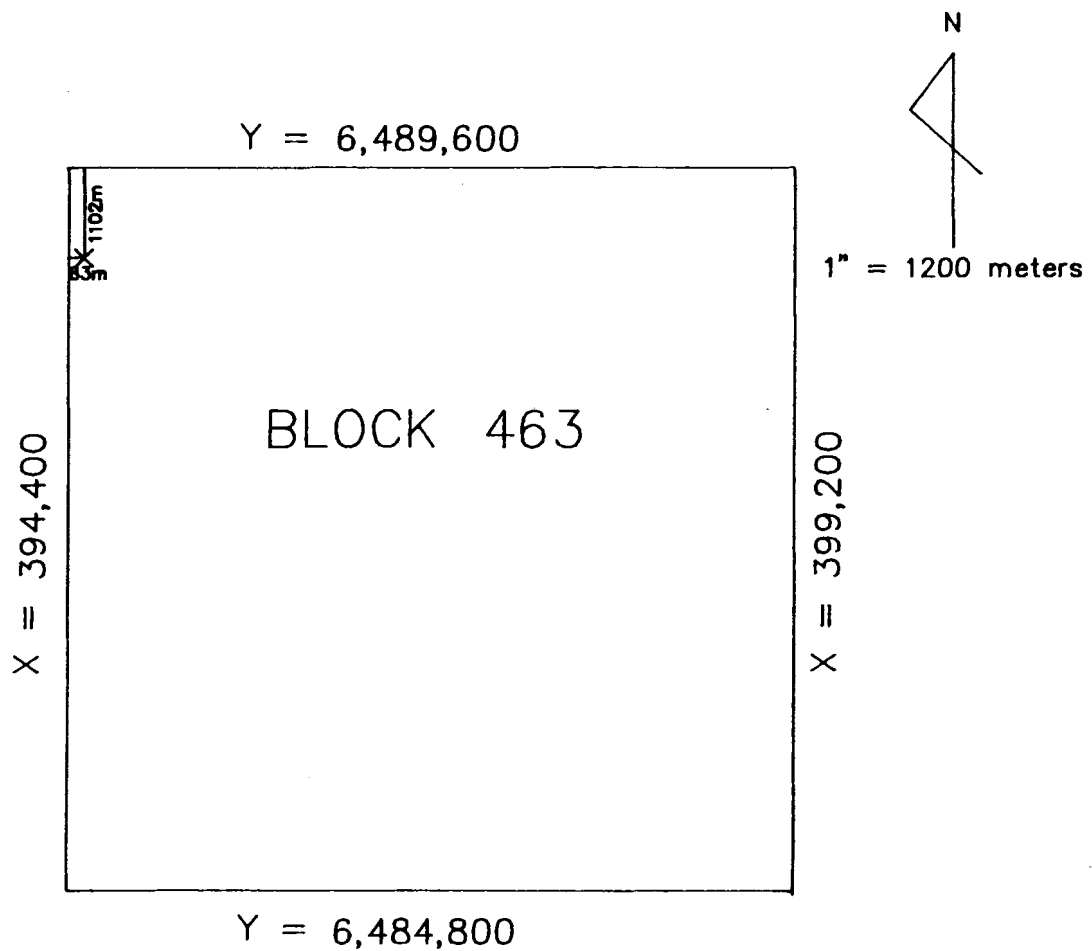
The site of the KSSD No. 2 well was latitude 58°31'33.9409" N and longitude 148°48'42.6226" W, or UTM coordinates (Zone 6) X=394,483 meters and Y=6,488,498 meters. The well was located on Block 463 (OPD NO6-3) in 375 feet of water (fig. 20). All measurements were made from the KB, which was 90 feet above sea level and 465 feet above the mud line. The KSSD No. 2 well was spudded at 0900 hours on July 22, 1977, and reached a TD of 10,460 feet on August 31, 1977, after 41 days of drilling. The well was plugged and abandoned by 1800 hours on September 7, 1977, and the rig was under tow to the KSSD No. 3 well location on September 8, 1977.

Drilling Program

The KSSD No. 2 well was drilled to TD as a straight hole. A total of 19 bits were used. A 26-inch bit was used to drill to 605 feet and the hole was then enlarged with a 36-inch hole opener assembly. A 26-inch bit was used to 1,465 feet, 17 1/2-inch bits to 4,465 feet, and 12 1/2-inch bits to 10,460 feet (TD).

The drilling rate varied from a high of 97 feet per hour to a low of 3.8 feet per hour. The average drilling rate over the entire well was approximately 38.2 feet per hour. Figure 21 shows the daily drilling progress.

The 30-inch casing string was set at a depth of 595 feet with 756 sacks of cement; the 20-inch was set at 1,424 feet with 1,735 sacks of cement; and the 13 3/8-inch was set at 4,431 feet with 1,645 sacks of cement. To abandon the well, four cement plugs were set: plug No. 1 from 7,740 to 8,010 feet; plug No. 2 from 5,572 to 5,920 feet; plug No. 3 from 4,308 to 4,533 feet; and plug No. 4 from 615 to 769 feet. An EZSV cement retainer was set at 4,358 feet. Drilling mud filled the open hole and the casing between the plugs. The 20-inch and 30-inch casings were cut at 491 feet and recovered. Because of difficulty in pulling the 30-inch casing, it was recovered from 480 feet. The 13 3/8-inch casing was cut and recovered from 505 feet. The casing and abandonment programs are shown in figure 22.



GEODETTIC POSITION UNIVERSAL TRANSVERSE MERCATOR
COORDINATES, ZONE 5

LAT. 58° 31' 33.9409" N Y = 6,488,498 meters
LONG. 148° 48' 42.6226" W X = 394,483 meters

Figure 20. Final location plat showing the position of the KSSD No. 2 well, OCS Protraction Diagram NO 5 - 3.

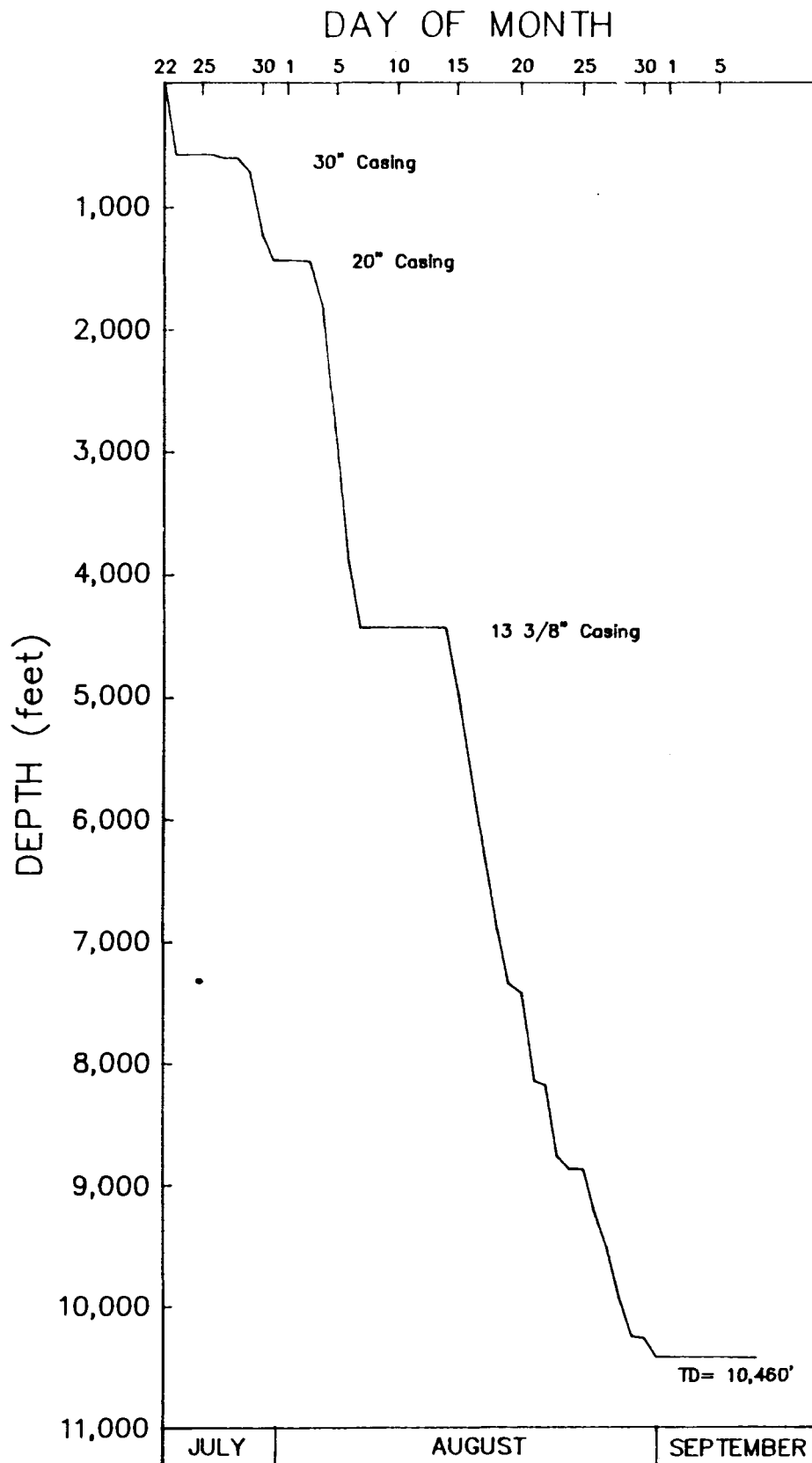


Figure 21. Graph showing daily drilling progress for the KSSD No. 2 well.

After the 13 3/8-inch casing was drilled out, gas was detected in the mud system. The mud weight was increased slightly to avoid potential problems. Prior to coring at 7,350 feet, the gas units had decreased somewhat, but a minor amount of hydrogen sulfide gas (H₂S) was encountered. The mud weight was increased again, which caused the hydrocarbon gas and H₂S levels to drop. The mud weight was gradually increased to TD to control what was perceived to be a low-volume gas influx.

Drilling Mud

Seawater was used to drill the well to 1,465 feet, where the seawater was replaced with a gel mud weighing 9.4 ppg. The mud weight was gradually increased to 13.9 ppg at TD. The initial viscosity was 43 seconds and the final viscosity 48 seconds. A low viscosity of 40 seconds was recorded at 7,358 feet and a high of 54 seconds at 10,460 feet. Chloride concentrations ranged from 2,000 to 4,000 ppm between approximately 1,800 feet and 7,400 feet, after which they averaged about 1,625 ppm to TD. Mud logging services were provided by NL Baroid Petroleum Services from approximately 1,465 feet to TD. Mud properties for this well are shown in figure 23.

Samples and Tests

Two series of sidewall cores were taken, the first between 1,482 and 4,441 feet, the second between 4,500 and 10,410 feet. In the first series, 125 cores were attempted and 100 recovered. In the second series, 71 cores were attempted and 67 recovered. Two conventional cores were taken. The intervals cored and the footage recovered are shown in table 3. The cores were analyzed for mineralogy, paleontology, porosity and permeability, grain density, and diagenesis.

TABLE 3. Conventional cores, KSSD No. 2 well.

<u>No.</u>	<u>Interval (feet)</u>	<u>Recovered (feet)</u>
1	7,350 - 7,380	18
2	10,275 - 10,293	18

The types of logs and the intervals over which they were run are as follows:

Run 1 (1,424 to 4,457 feet) and

Run 2 (4,420 to 10,460 feet)

Proximity Microlog (PML)

Long Spaced Sonic (LSS)

Borehole Compensated Sonic (BHC)

Dual Induction Laterolog (DIL)

Compensated Neutron/Formation Density (CNL/FDC)

KELLY BUSHING 0'
MEAN SEA LEVEL 90'
MUD LINE 465'

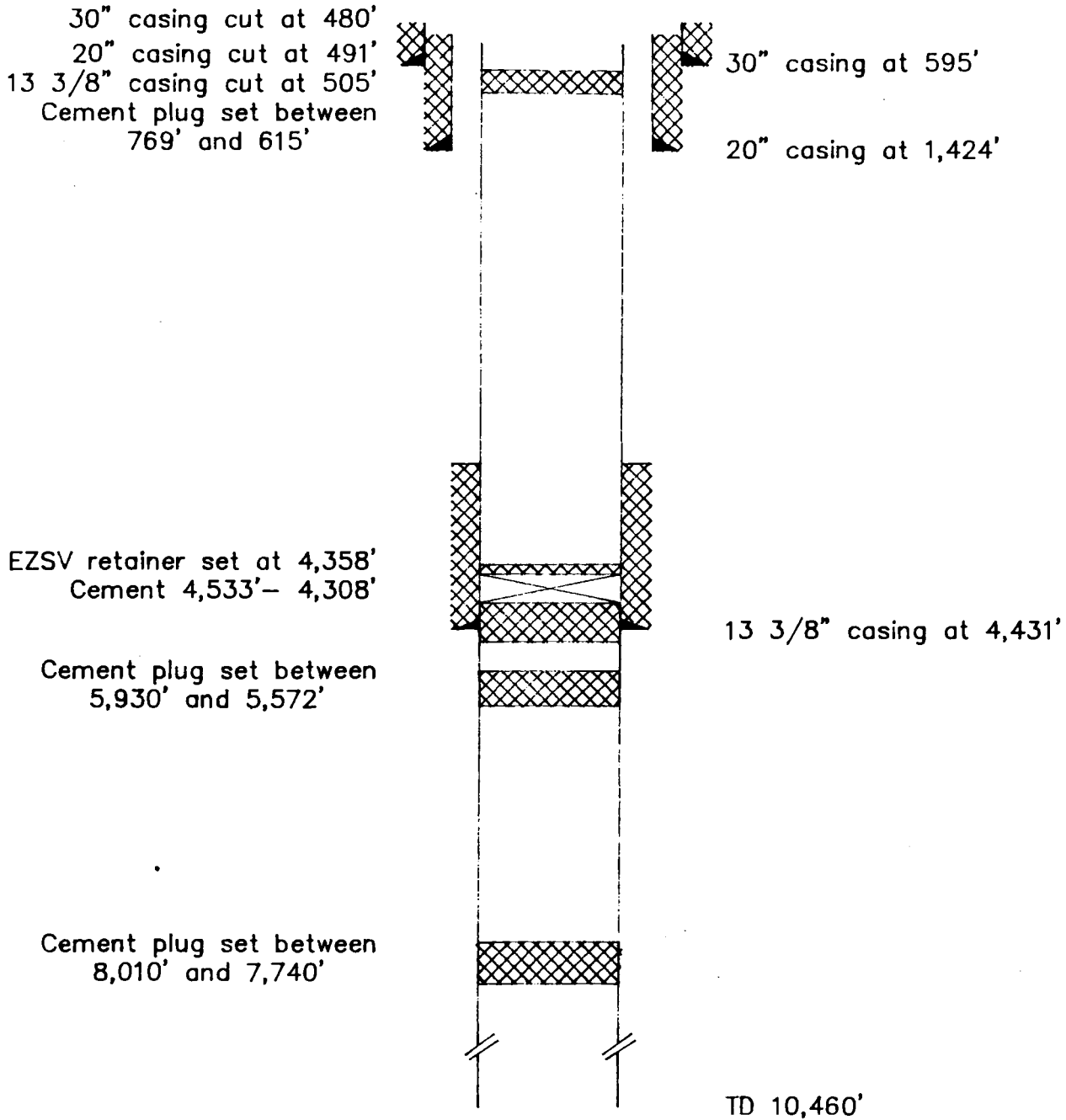


Figure 22. Schematic diagram showing casing strings, plugging and abandonment program, KSSD No. 2 well.

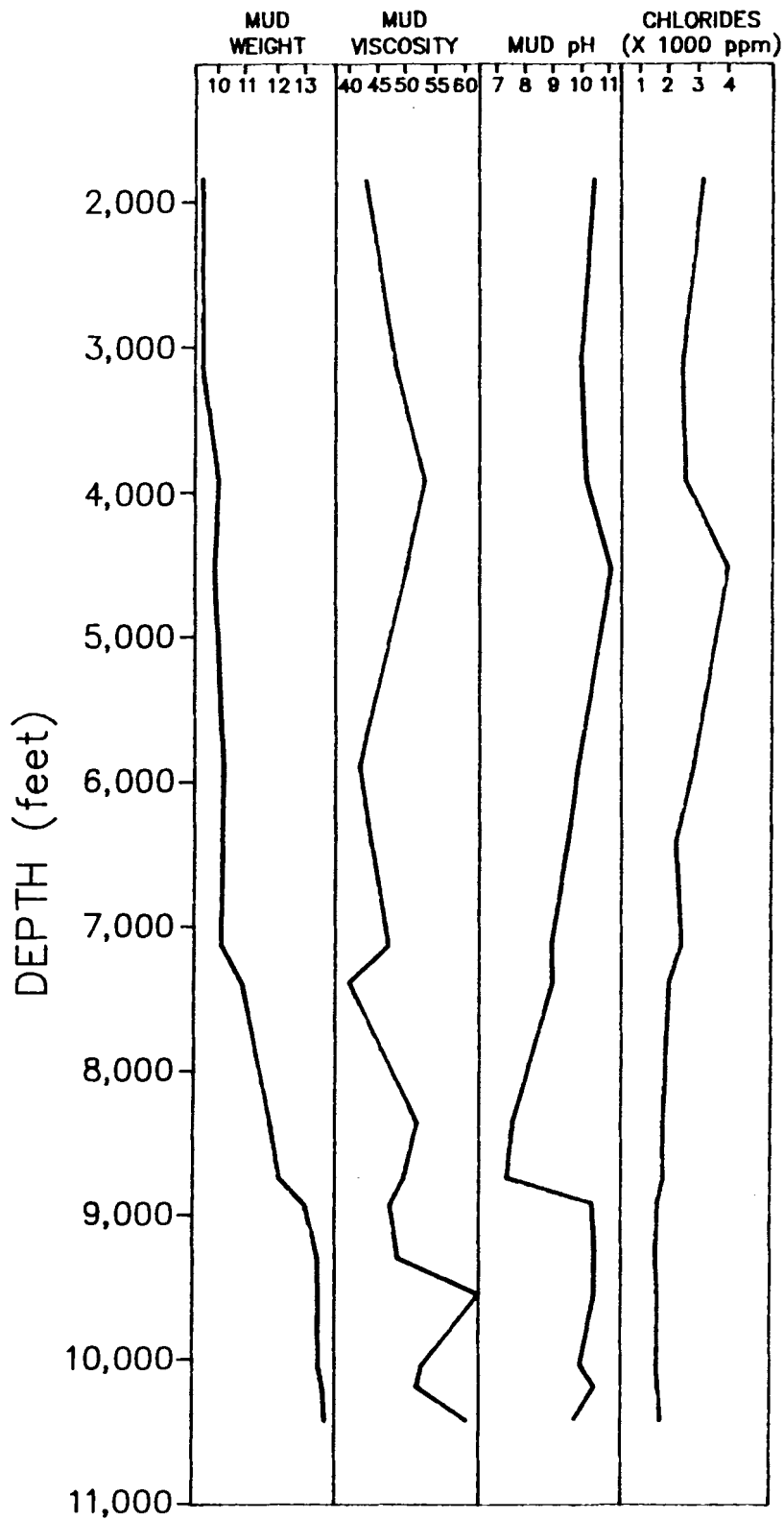


Figure 23. Changes of drilling mud properties with depth, including mud weight, viscosity, pH, and total chlorides, KSSD No. 2 well.

High Resolution Dipmeter Tool (HDT)
Repeat Formation Tester (RFT)
Temperature Log (TL)

There were no drill stem tests run on this well.

Weather

At one point, operations were halted for 1 1/2 days because of weather. The average maximum wind speed was 30.7 knots at this time, while the average maximum seas were 15.7 feet. Limited oceanographic and meteorological data were collected for this well.

KSSD No. 3 Well

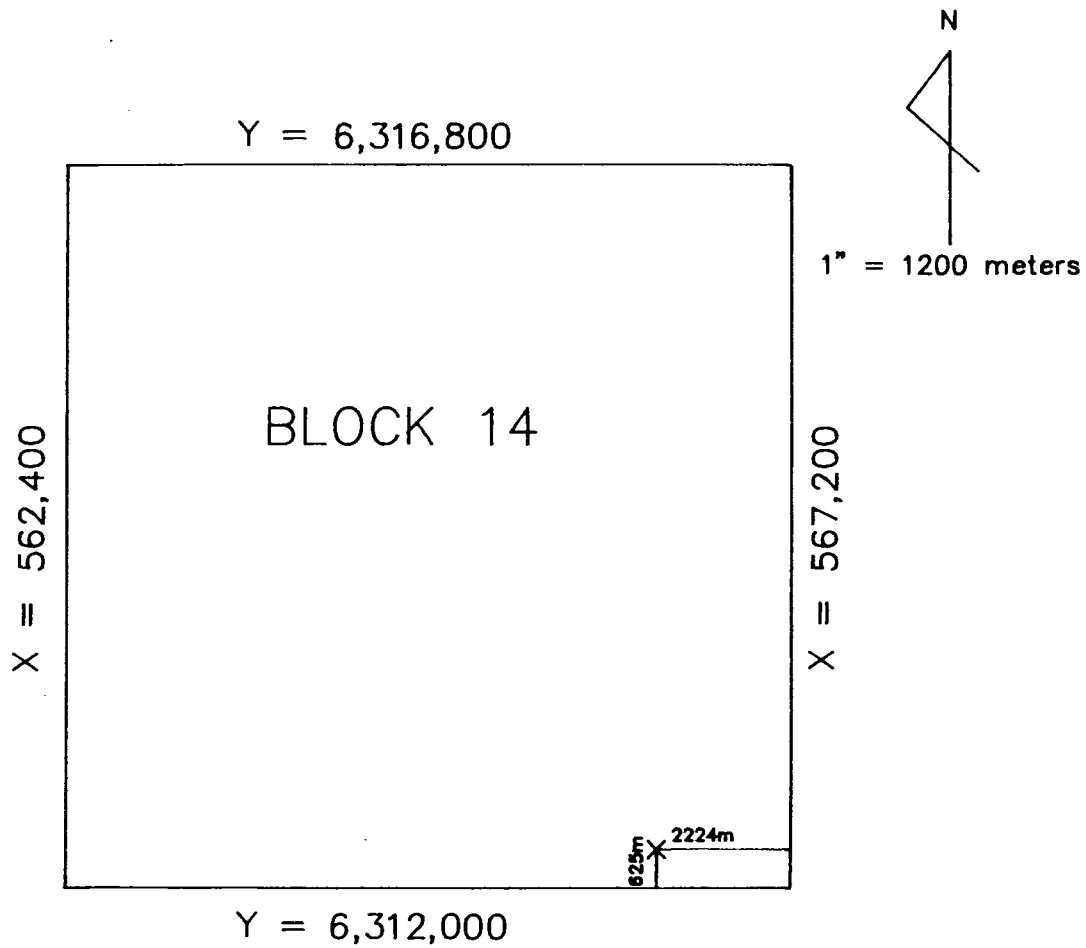
The KSSD No. 3 well site was at latitude 56°57'16.477" N and longitude 151°55'54.173" W, or UTM coordinates (Zone 5) X=564,976 meters and Y=6,312,625 meters. The well was located on Block 14 (OPD NO5-8) in 265 feet of water (fig. 24). All measurements were made from the KB, which was 90 feet above sea level and 355 feet above the mud line. The KSSD No. 3 well was spudded at 2300 hours on September 13, 1977, and reached a TD of 9,357 feet on October 20, 1977, after 37 days of drilling. The well was plugged and abandoned at 1930 hours on October 25, 1977.

Drilling Program

The KSSD No. 3 well was drilled to TD as a straight hole using 18 drill bits. The first 485 feet were drilled using a 26-inch bit followed by a 36-inch hole opener assembly. A combination of bits ranging in size from 26 to 8 1/2 inches were used to drill the hole to 9,357 feet (TD).

The average drilling rate for the first 500 feet of the well was 8 feet per hour. From approximately 1,370 to 6,264 feet, the average drilling rate was 56 feet per hour, and from 6,264 feet to TD, the average drilling rate was 11.8 feet per hour. These averages include coring time. Figure 25 shows the daily drilling progress.

The 30-inch casing was set at 485 feet using 600 sacks of cement, the 20-inch at 1,334 feet with 1,350 sacks of cement, and the 13 3/8-inch at 4,325 feet with 1,425 sacks of cement. Two cement plugs were set to abandon the well, the first between 4,200 and 4,425 feet, the second between 455 and 605 feet. The hole between the plugs remained filled with 10.5-ppg mud. The 30-inch casing was cut and pulled from 372 feet, the 20-inch casing was cut and pulled from 375 feet, and the 13 3/8-inch casing was cut and pulled from 395 feet. The casing and abandonment programs are shown in figure 26.



GEODETC POSITION UNIVERSAL TRANSVERSE MERCATOR
COORDINATES, ZONE 5

LAT.	56° 57' 16.477" N	Y = 6,312,625 meters
LONG.	151° 55' 54.173" W	X = 564,976 meters

Figure 24. Final location plat showing the position of the KSSD No. 3 well. OCS Protraction Diagram NO 5 - 8.

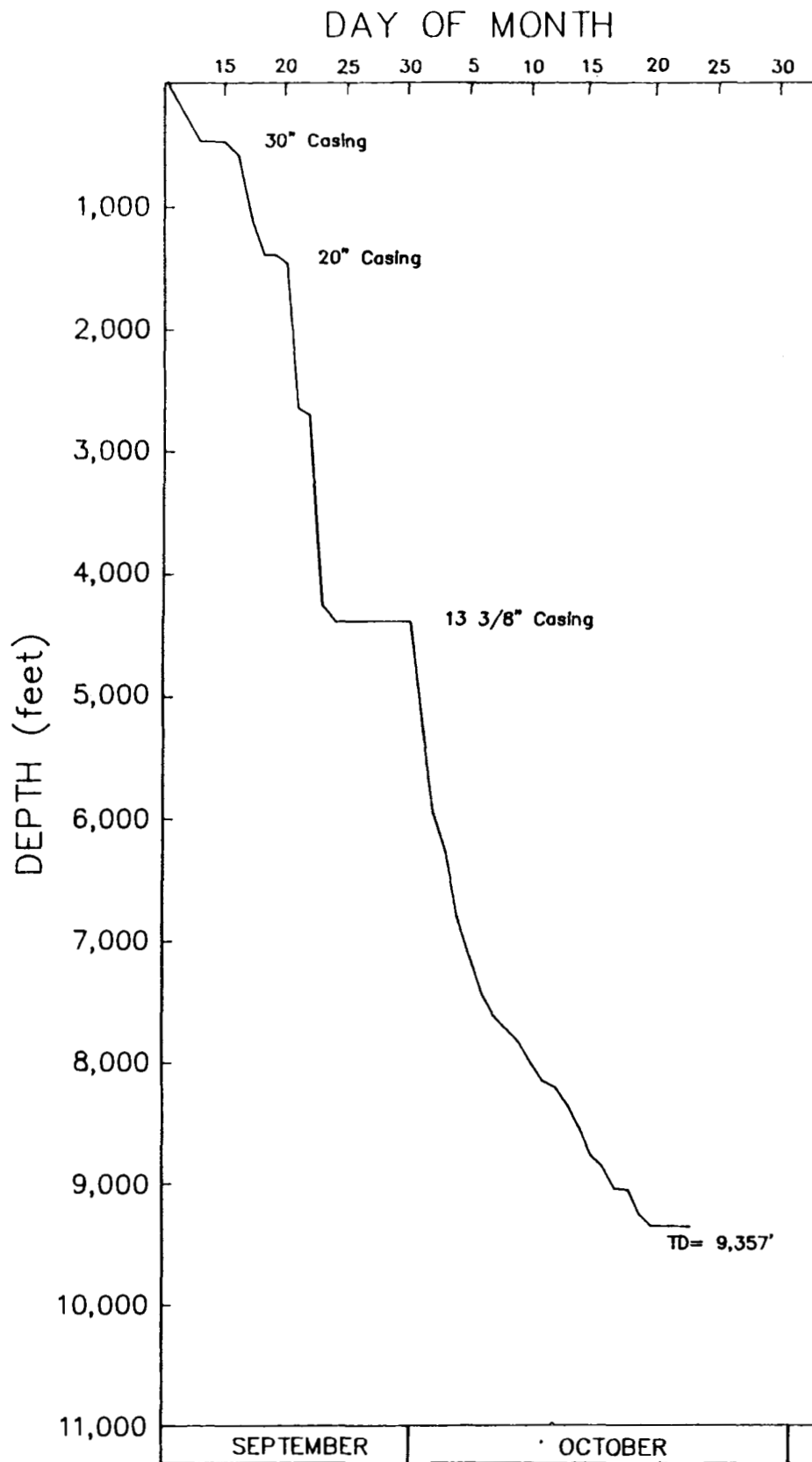


Figure 25. Graph showing daily drilling progress for the KSSD No. 3 well.

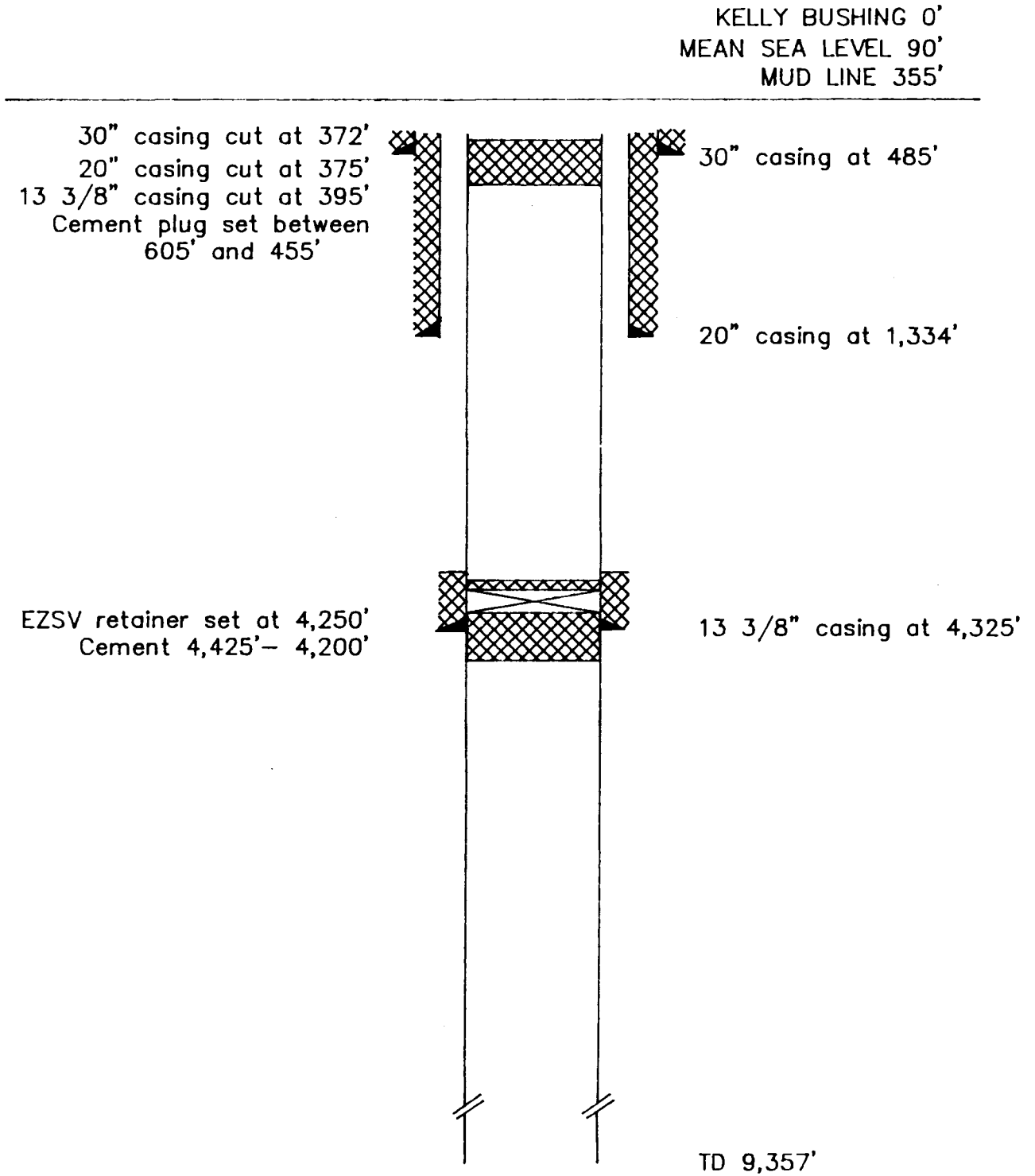


Figure 26. Schematic diagram showing casing strings, plugging and abandonment program, KSSD No. 3 well.

Drilling Mud

The well was drilled to 1,365 feet using seawater, which was then replaced with a gel mud. The mud weight averaged 9.6 ppg between 2,300 and 4,550 feet, and 10.5 ppg from 5,000 feet to TD. The average viscosity over the well was 53 seconds. The chloride concentrations ranged from a low of 1,155 ppm at 2,300 feet to a high of 3,100 ppm at 8,675 feet, with an overall average of 2,588 ppm. Mud logging services were provided by NL Baroid Petroleum Services from approximately 1,365 feet to TD. Mud properties for the well are shown in figure 27.

Samples and Tests

Four series of sidewall cores were taken. In the first series, 57 cores were attempted and 51 recovered between 4,462 and 7,681 feet. The second series attempted 34 cores and recovered 26 over the interval from 4,489 to 9,300 feet. The third series was shot between 4,400 and 9,340 feet, and 43 cores were recovered out of 50 attempts. The fourth series attempted and recovered 104 cores between 1,405 and 4,372 feet.

Four conventional cores were taken in the KSSD No. 3 well. The intervals cored and the footage recovered are shown in table 4. These cores were analyzed for mineralogy, paleontology, porosity and permeability, grain density, and diagenesis.

TABLE 4. Conventional cores, KSSD No. 3 well.

<u>No.</u>	<u>Interval (feet)</u>	<u>Recovered (feet)</u>
1	6,264 - 6,277	12
2	7,601 - 7,627	26
3	8,175 - 8,205	26
4	9,044 - 9,064	19

The types of logs and the intervals over which they were run are as follows:

Run 1 (1,333 to 4,387 feet) and

Run 2 (4,316 to 9,360 feet)

Dual Induction Laterolog (DIL)
Borehole Compensated Sonic (BHC)
Compensated Neutron/Formation Density (CNL/FDC)
High Resolution Dipmeter Tool (HDT)
Long Spaced Sonic (LSS)
Proximity Microlog (PML)
Repeat Formation Tester (RFT)
Temperature Log (TL)

There were no drill stem tests run on this well.

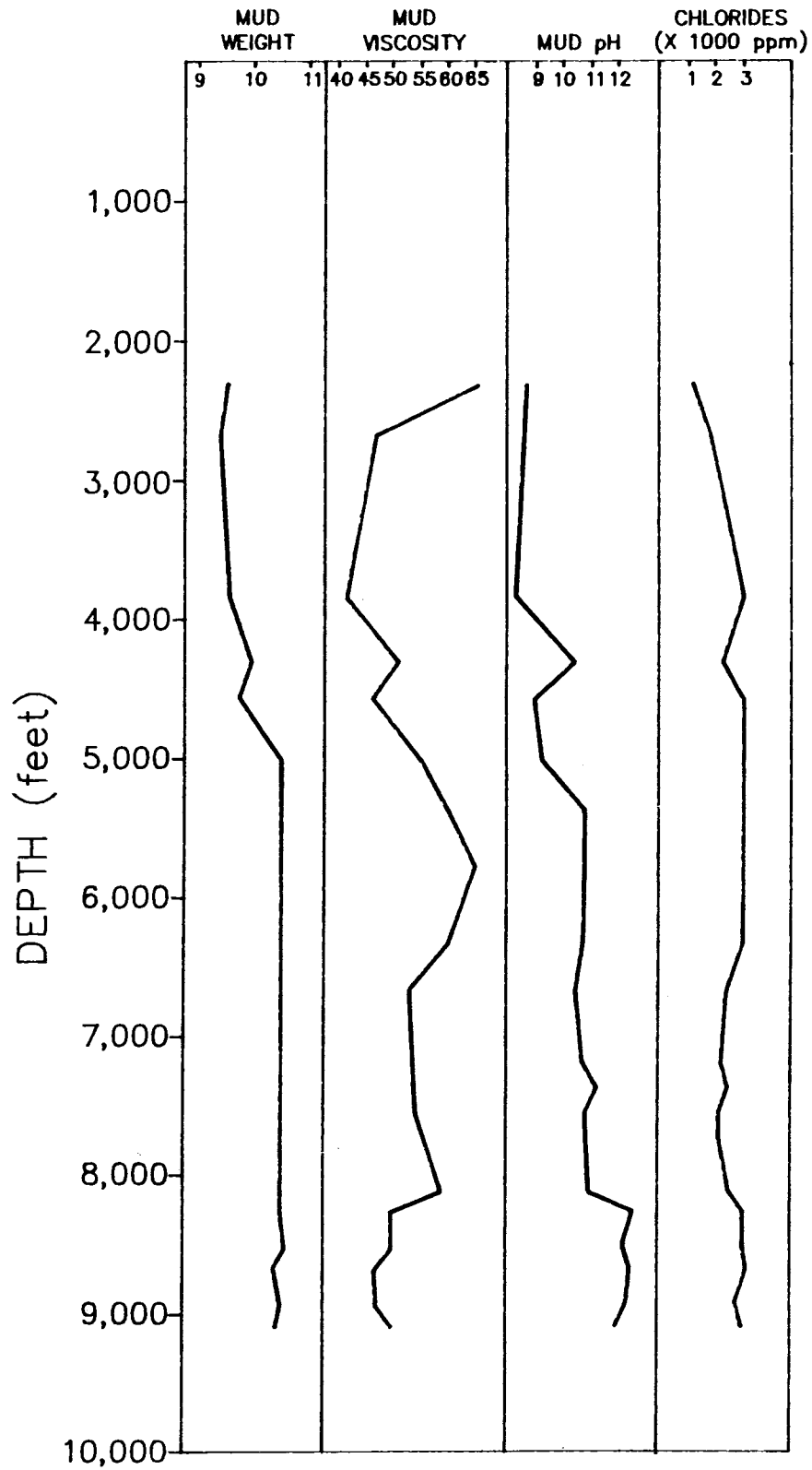


Figure 27. Changes of drilling mud properties with depth, including mud weight, viscosity, pH, and total chlorides, KSSD No. 3 well.

Weather

Only limited oceanographic and meteorological data were collected for this well.

3. LITHOLOGIC SUMMARY

The sedimentary section penetrated by the six Kodiak shelf COST wells consists of sedimentary rocks derived from volcanic, metamorphic, plutonic and sedimentary source terranes. The sedimentary section does not contain good petroleum reservoir or source rocks. Extremely fine grain size, abundant clay, poor sorting, and the formation of authigenic minerals have all contributed to creating low permeabilities.

The lithologic descriptions of the six Kodiak shelf COST wells are based on the study of drill cuttings and reports made by Core Laboratories for Exploration Services Company, Inc., and Sun Oil Company (Core Laboratories Inc., 1976a,b; 1977a,b; 1978). The petrographic classification scheme utilized was unspecified.

Six conventional cores were taken from the KSSD No. 1 well, two from the KSSD No. 2 well, and four from the KSSD No. 3 well. No conventional or sidewall core samples or thin sections were made available to MMS personnel for study, and the present location of this material could not be ascertained by Sun Oil Company personnel. No conventional cores were taken from the three KSST wells. Figures 28 through 33 are lithologic columns and descriptions of the six Kodiak shelf wells. Appendix 1 contains descriptions of the conventional cores and thin sections, and permeability, porosity, grain density, and X-ray diffraction data from samples taken from conventional and sidewall cores from the three KSSD wells. Also shown in Appendix 1 are permeability, porosity, and grain density data for sidewall core samples taken from the KSST No. 1 and No. 2 wells.

The Pleistocene sediments of the Kodiak shelf are predominantly glaciomarine deposits. The Miocene and Pliocene marine sediments of the KSSD and KSST wells represent the Kodiak shelf equivalents of the Narrow Cape and Tugidak Formations that are exposed on Kodiak Island and vicinity. The Miocene sandstones of the Narrow Cape Formation have a mean composition of 57 percent quartz, 21 percent feldspar, and 22 percent lithics (Fisher, 1980, p. 1149). The lithic clasts consist of approximately 48 percent sedimentary fragments and 47 percent volcanic and plutonic fragments. The feldspar is about 75 percent plagioclase. No data are available on the composition of the Pliocene Tugidak sandstones. Fisher (1980, fig. 6) documented a trend of a progressive rise in the quartz content and compositional

maturity of sandstones in successively younger formations on Kodiak Island. This maturation trend probably reflects the progressive exposure and recycling of older Cretaceous and Tertiary sediments and the unroofing of the Kodiak batholith and satellite plutons.

The sandstones of the Miocene and younger sediments of the KSSD and KSST wells appear similar in composition to those reported by Fisher (1980) from the Narrow Cape Formation. Although no point-counts were conducted in the petrographic analyses of the sandstones from the Kodiak shelf strata, visual estimates of mineral composition and X-ray diffraction analyses allow a general comparison. Visual estimates from thin sections of Miocene and younger sandstones in the KSSD No. 3 well indicated an average composition of about 60 to 65 percent quartz and chert, 20 to 25 percent feldspars, and 10 to 15 percent lithics (Appendix 1). X-ray diffraction data indicate an average composition of 62 percent quartz, 23 percent feldspar, and 15 percent clays, micas, carbonates, and accessory minerals (Appendix 1, KSSD No. 3 well). The lithics consist largely of fine, randomly oriented feldspar laths in a clay-rich matrix. These probably represent highly altered volcanic rock fragments recycled from older volcanoclastic sediments. The larger feldspar grains are predominantly plagioclase; however, in some of the samples they consist of as much as 50 percent orthoclase. This suggests a significant input from a plutonic source such as the Kodiak batholith or perhaps the volcano-plutonic terrane of the Alaska-Aleutian Peninsula. A deviation in the general trend of increasing quartz content in younger sandstones was noted in the basal sandstones of middle Miocene age (see Well Log Interpretation chapter). These sandstones are more quartz rich than the younger sandstones in the well, apparently because of higher contents of detrital chert and silica cement. The high influx of detrital chert suggests that significant erosion of older sediments occurred in the middle Miocene.

A shift in the direction of sediment dispersal occurred at the KSSD No. 3 well, in the Albatross Basin, in the late Miocene or early Pliocene (see Well Log Interpretation chapter). Sediment dispersal in the Miocene was from the northwest; in the Pliocene and early Pleistocene it was from the northeast. Because no accompanying shift in composition of the sandstones was noted, it is assumed that the sources were similar terranes. Farther to the northeast in the Stevenson Basin, the Miocene sandstones in the KSSD No. 1 well appear to have lower quartz contents, which may indicate some difference in provenance. The average composition from X-ray diffraction analyses (Appendix 1) is 43 percent quartz, 33 percent feldspar, and 21 percent clays and micas. However, only three samples of sandstones were available for analysis, and these consisted of shaly and silty, very fine grained sandstone.

The Eocene sediments penetrated in the KSSD wells appear to represent the Kodiak shelf equivalents of the Sitkalidak Formation, which is exposed on Kodiak Island and vicinity. However, the incomplete and generally qualitative nature of the data precludes a detailed comparison of the KSSD and Sitkalidak Formation lithologies

with those of the possibly equivalent Eocene Zodiac Fan deposits of the Aleutian abyssal plain at DSDP site 183 (Stewart, 1976; Moore and others, 1983). This is unfortunate in that this data might be useful in unraveling the histories of the Prince William and Yakutat block tectonostratigraphic terranes. The sandstones of the Sitkalidak Formation are relatively rich in feldspar and lithic fragments; an average composition from 27 samples of fine-grained sandstone is 31 percent quartz, 30 percent feldspar, and 39 percent lithics (Moore and others, 1983, table 3). The lithics are composed of approximately equal numbers of volcanic and sedimentary clasts, and minor amounts of plutonic and metamorphic clasts. The feldspar is about 85 percent plagioclase. The composition of the Sitkalidak sandstones suggests a provenance of a partially eroded magmatic arc along a continental margin (Dickinson and Suczak, 1979).

Compositions of the Eocene sandstones from the KSSD wells appear generally similar to those of the Sitkalidak Formation (Appendix 1), although direct quantitative comparisons are difficult because no petrographic point-count analyses were conducted on the KSSD well samples. Mineral content determinations from X-ray diffraction analyses provide some basis for quantitative comparison, although the two analysis techniques are considerably different. Relative percentages of quartz, feldspar, and various clays, micas and accessory minerals for sands and silts of the KSSD wells are as follows:

	<u>KSSD No. 1 well</u> <u>(18 samples)</u>	<u>KSSD No. 2 well</u> <u>(3 samples)</u>	<u>KSSD No. 3 well</u> <u>(3 samples)</u>
Quartz	46	42	39
Feldspar	33	29	38
Clay, etc.	21	29	23

The Eocene sandstone of the KSSD No. 3 well, which is the nearest to Kodiak Island, exhibits the closest resemblance to the Sitkalidak sandstone, with a nearly equal ratio of quartz to feldspar. Sandstones of the KSSD No. 1 and No. 2 wells, farther to the northeast, are somewhat more quartz rich. This may suggest a closer proximity to a continental sediment source to the northeast in the Eocene, although the sparsity of these data make such a conclusion highly speculative.

The Core Laboratories geologist who described core 4 from the KSSD No. 3 well noted structures that "resemble algal boundstones, although such an interpretation is not borne out by X-ray diffraction data" in a thin section from 9,051 feet, and stated that in a thin section from 9,060 feet "the clotted texture, along with the high clay content and the short irregular (desiccation?) fractures, suggest a possible algal origin with frequent subaerial exposure" (Appendix 1). This analysis is not supported by the paleontologic interpretation of the sediments penetrated by these wells. The fossils found at these depths indicate middle to late Eocene outer neritic to lower bathyal deposition. However, a subsequent analysis of cuttings from the cored interval revealed the presence of minor

amounts (small flakes) of brown, micritic limestone and finely laminated siltstones that might be algal in origin. Field samples of age-equivalent strata exposed on the nearby Alaska Peninsula collected in 1984 by the U. S. Geological Survey indicate the presence of small algal heads (Jim Case, personal commun., 1987), and Plafker (in press) reports the presence of shallow-water reef organisms, including corals, coralline algae, and bryozoans, from Eocene age samples dredged from the Gulf of Alaska continental slope. Therefore, on paleoecological grounds, Eocene algal mat deposition in the area was possible and the "algal boundstone" reported by Core Laboratories could represent shallow-water material carried downslope by turbidity currents.

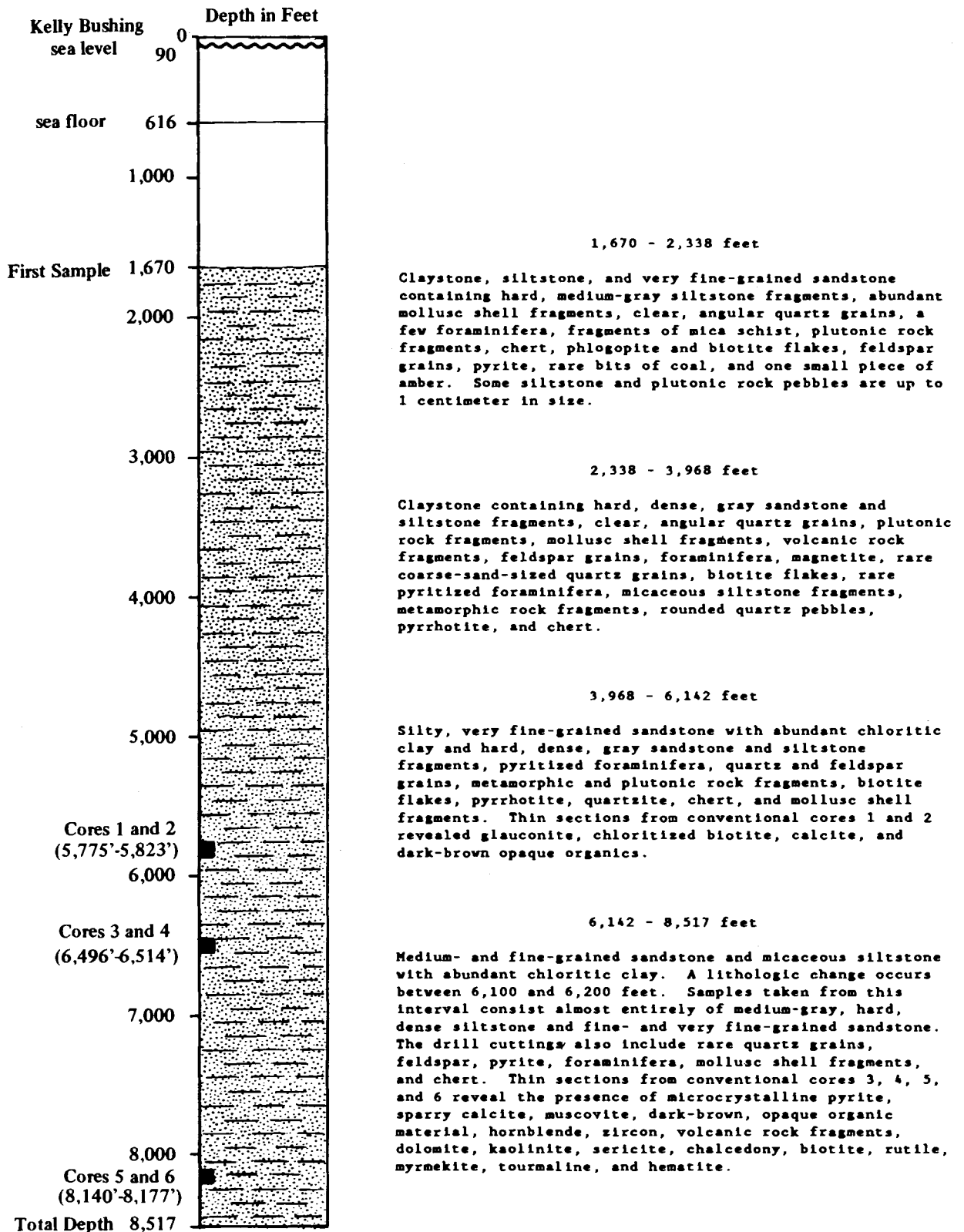


Figure 28. Lithologic description and core locations of the KSSD No. 1 well.

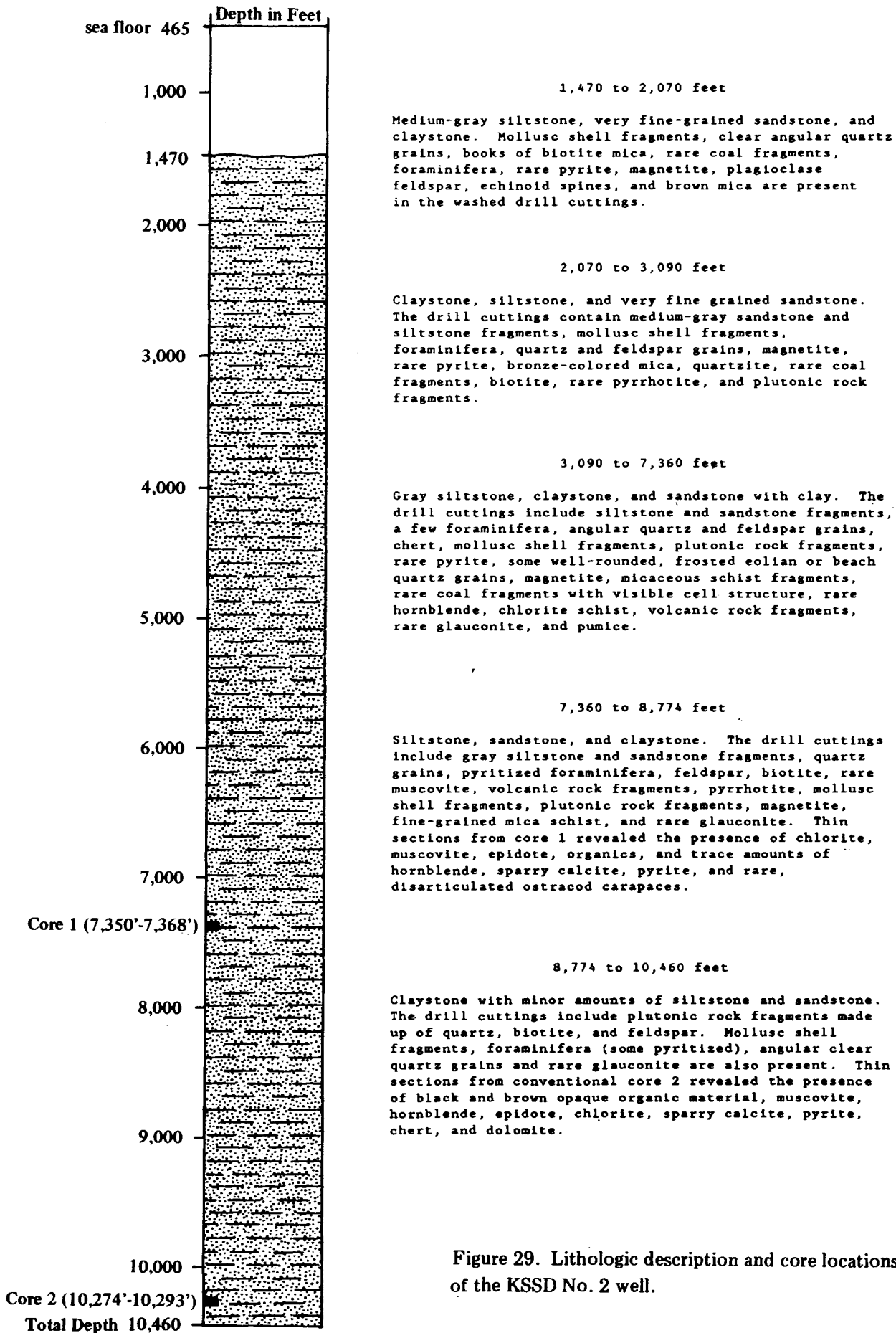


Figure 29. Lithologic description and core locations of the KSSD No. 2 well.

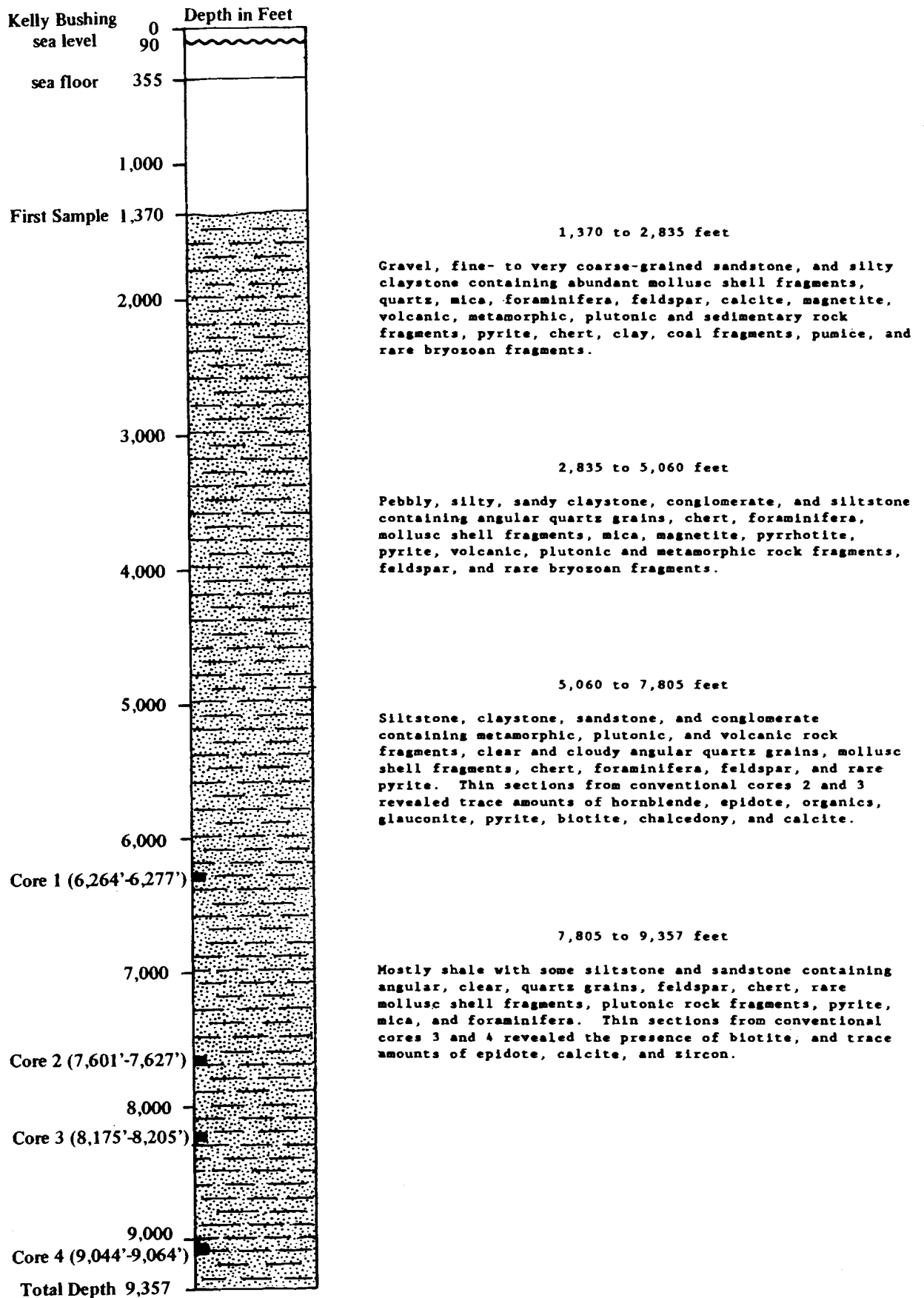
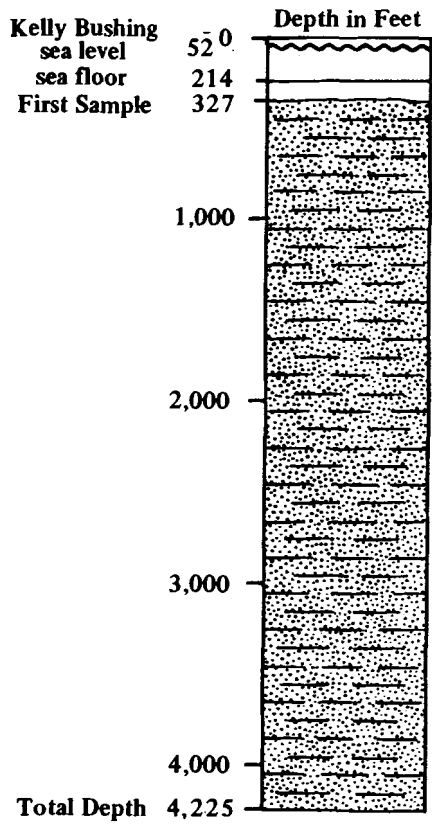
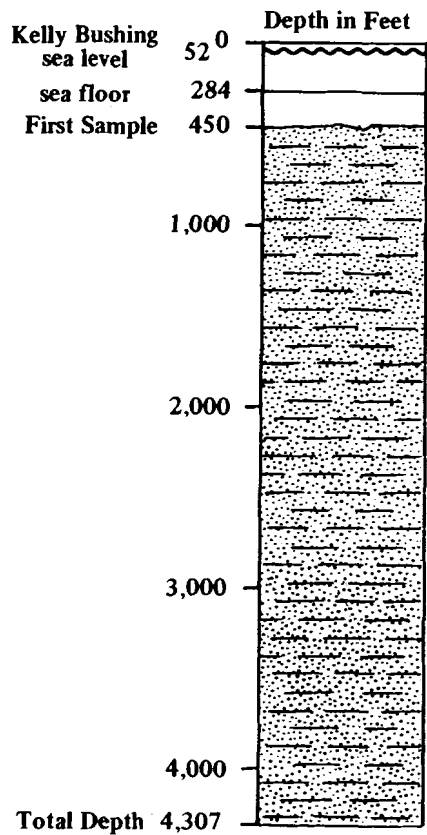


Figure 30. Lithologic description and core locations of the KSSD No. 3 well.



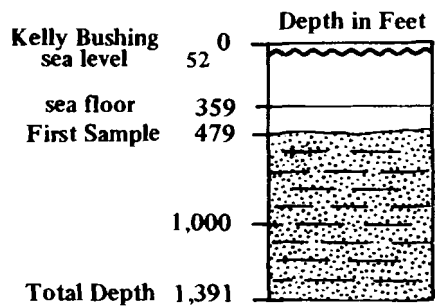
Claystone, siltstone, and sandstone containing clear, angular quartz grains, well-rounded, frosted quartz grains, plutonic rock fragments, mollusc shell fragments, rare pyrite, feldspar, mica, chert, foraminifera, pumice, and pink rhyolite.

Figure 31. Lithologic description of the KSST No. 1 well.



Gravel, siltstone, claystone, and sandstone containing mollusc shell fragments, plutonic rock fragments, subangular quartz grains, feldspar, foraminifera, volcanic rock fragments, chert, biotite, pumice, hornblende, pyrrhotite, phlogopite, pink rhyolite, Bryozoa, ostracods, and rare pyrite and chalcopyrite.

Figure 32. Lithologic description of the KSST No. 2 well.



Siltstone, claystone, mudstone, and sandstone containing angular quartz grains, chert, feldspar, volcanic rock fragments, mollusc shell fragments, foraminifera, plutonic rock fragments, mica, and rare pyrite.

Figure 33. Lithologic description of the KSST No. 4A well.

4. VELOCITY ANALYSIS

Seismic velocities in strata penetrated by the KSST and KSSD wells were evaluated for the purpose of time-to-depth conversion and to facilitate correlation between significant lithologic and biostratigraphic horizons in the wells and seismic reflection profile data. The data used in this interpretation consisted of the long-spaced sonic logs from the wells. Unless specified otherwise, depths in this chapter are measured from mean sea level.

For each of the six wells, root mean square (RMS) velocities (figs. 34 to 39) and time-depth curves (figs. 40 to 45) were generated by computer from the digitized sonic logs. Interval velocities were calculated from the RMS velocities using the Dix equation (Dix, 1955), and are shown along with the time-depth curves in figures 40 through 45. Also shown in figures 40, 41, 43, and 44 are interval velocities calculated from unreversed sonobuoy refraction profiles shot near the wells by the U.S. Geological Survey (Holmes and others, 1978) (fig. 46). The interpretation of the crustal structure as derived from the sonobuoy data is included in this discussion because the paucity of non-proprietary seismic data across the Kodiak shelf makes it otherwise difficult to extrapolate lithologic and paleontologic well data.

In the KSST No. 1 well, interval velocities calculated from the RMS velocities increase with depth down to approximately 1,500 feet (fig. 40). From that depth to TD (4,225 feet), the interval velocities remain relatively uniform. Travel-time data recorded on the sonic log show the presence of a high-velocity zone from approximately 1,500 to 2,300 feet (fig. 47, p. 73). This zone does not show up well in figure 40 because of the relatively broad, 200-millisecond increments used in the calculation of the interval velocities. In this zone, interval velocities average almost 10,000 feet per second, which is anomalously high for seismic velocities at those depths. A comparison of sonic velocities measured in shales penetrated by this well with sonic velocities in the KSSD No. 1 and KSSD No. 3 wells suggests that between 3,000 and 5,000 feet of uplift and erosion has occurred at the KSST No. 1 well site (see Abnormal Formation Pressure chapter). The analysis presented in the Abnormal Formation Pressure chapter also uncovered the presence of a fault zone cutting the well bore between 1,720 and 1,925 feet, with a mineralized zone possibly associated with it. Thus the anomalously high sonic velocities measured below

1,500 feet can probably be attributed to the combined effects of the exhuming of deeper, well-compacted sedimentary rocks, and mineralization related to a fault zone and the resulting induration of the associated sediments.

Interval velocities calculated from an unreversed seismic refraction profile shot near the KSST No. 1 well (fig. 46) show a similar, although much less detailed, velocity profile (fig. 40). This simpler interpretation of the crustal structure is the result of the inability of the seismic refraction technique to discriminate small velocity contrasts and to detect thin layers or velocity reversals. In the velocity profile calculated from the refraction data, the inflection in the velocity gradient occurs at a slightly shallower depth than does the inflection apparent in the sonic log data. This difference is most likely caused by the refraction profile not having been shot directly across the well site.

Interval velocities calculated from the sonic logs from the KSST No. 2 and the KSST No. 4A wells (figs. 41 and 42) increase gradually with depth without any significant reversals or discontinuities. Interval velocities calculated from a sonobuoy refraction profile shot near the KSST No. 2 well agree fairly well with the velocity gradient calculated from the sonic log (fig. 41). A major unconformity also seen in the KSSD wells is represented in the refraction profile by the velocity increase recorded at 5,500 feet. The KSST No. 2 well was not drilled deep enough to penetrate the unconformity.

In the KSSD No. 1 and the KSSD No. 3 wells, interval velocities increase gradually with depth to the base of the Neogene section at 6,052 and 7,715 feet, respectively (figs. 43 and 44). In each well, an increase in the interval velocity measured from the sonic logs coincides roughly with the depth of the unconformity at the base of the Neogene section as determined from the well logs. This increase is subtle, however, and the depth of the unconformity cannot be recognized solely on the basis of the velocity data. Spurious sonic travel times caused by instrument problems during the logging of the KSSD No. 1 well may have been introduced into the velocity calculations for the section of the well below 4,600 feet (below KB). This possible error is manifested by the apparent velocity discontinuity at that depth which also coincides with a change in the logging runs. These possibly spurious travel times do not appear to have significantly altered the velocity contrast across the unconformity.

The unconformity is also manifested in the interval velocity curve derived from sonobuoy refraction data shot near the KSSD No. 1 well (fig. 43). In those data, the depth of the unconformity is represented by the 13,900 feet per second velocity measured at 5,700 feet. This depth does not coincide with the depth of the unconformity determined from well log data both because of the geometry of the refractor and because the refraction profile was not shot directly across the well site. The apparent high interval

velocity calculated from the refraction data as compared to the in situ sonic velocities below the unconformity is a consequence of the geometry of the refractor and the refraction profile having been shot updip. In the seismic refraction profile shot near the KSSD No. 3 well (fig. 44), the 12,000 feet per second velocity at approximately 5,300 feet coincides with the boundary between the Plio-Pleistocene turbidite sequence and the Miocene turbidite sequence discussed in the Well Log Interpretation chapter (plate 7).

Interval velocities calculated from the KSSD No. 2 well sonic log are unusually uniform from the top of the data to TD at 10,460 feet (fig. 45). The interval velocities calculated for the Neogene section of the well are comparable to the interval velocities in the same section of the KSSD No. 1 and No. 3 wells, but the interval velocities calculated for the deeper section of the well are uncharacteristically low. In contrast with the sedimentary section penetrated by the KSSD No. 1 and 3 wells (which included claystone, sandstone, siltstone, shale, and gravel), the section penetrated by the KSSD No. 2 well was almost exclusively claystone. The low and uniform sonic velocities that are characteristic of the deeper section of the KSSD No. 2 well could have been caused by either formation alteration or overpressuring of the claystone. An analysis of the physical properties of shales penetrated by the KSSD No. 2 well presented in the Abnormal Formation Pressure chapter reveals the presence of an overpressured interval starting at 6,500 feet. The top of this overpressured interval coincides with the approximate depth above which sonic velocities measured in the KSSD No. 2 well are comparable to the sonic velocities measured in the other Kodiak shelf wells. Accordingly, the apparent uniformity of the sonic velocities measured in the KSSD No. 2 well is attributed to anomalously low velocities measured in the lower part of the well.

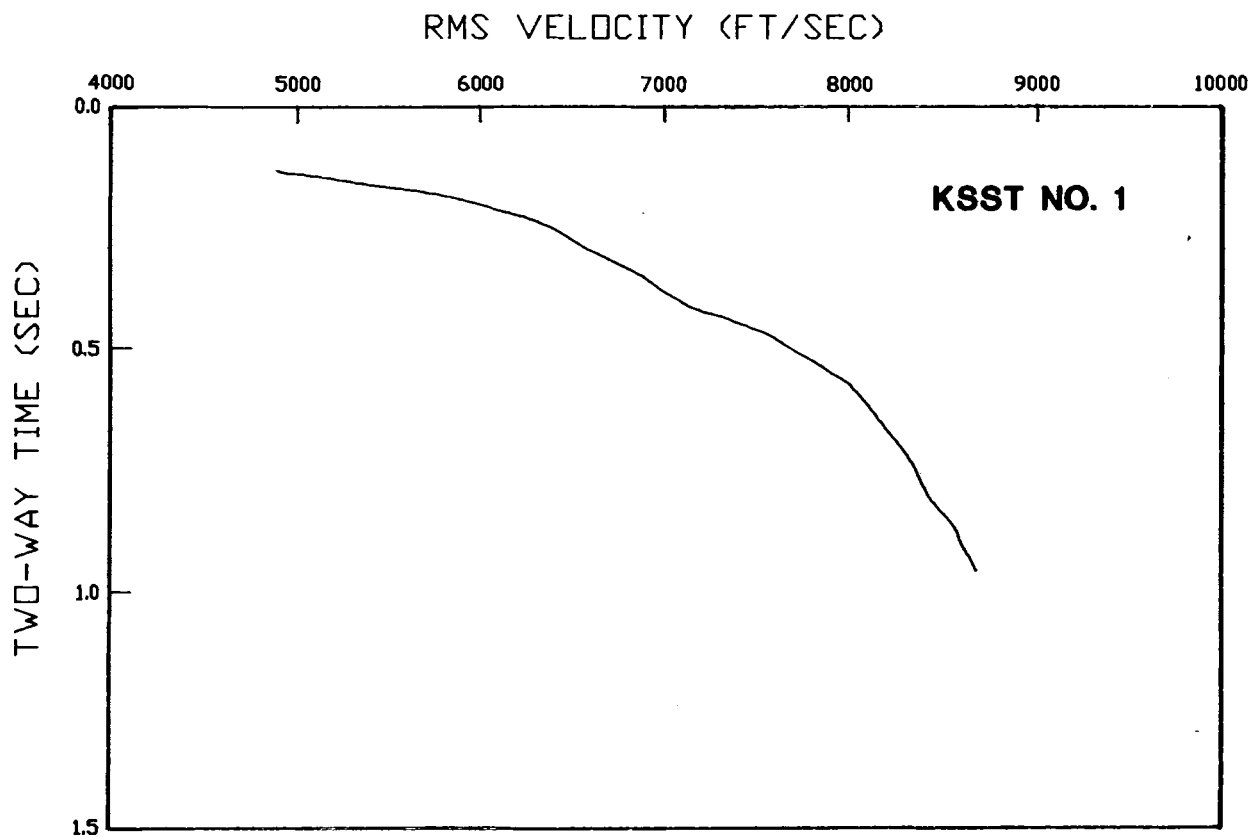


Figure 34. RMS velocity calculated from the long-spaced sonic log from the KSST No. 1 well. Depths are measured relative to mean sea level.

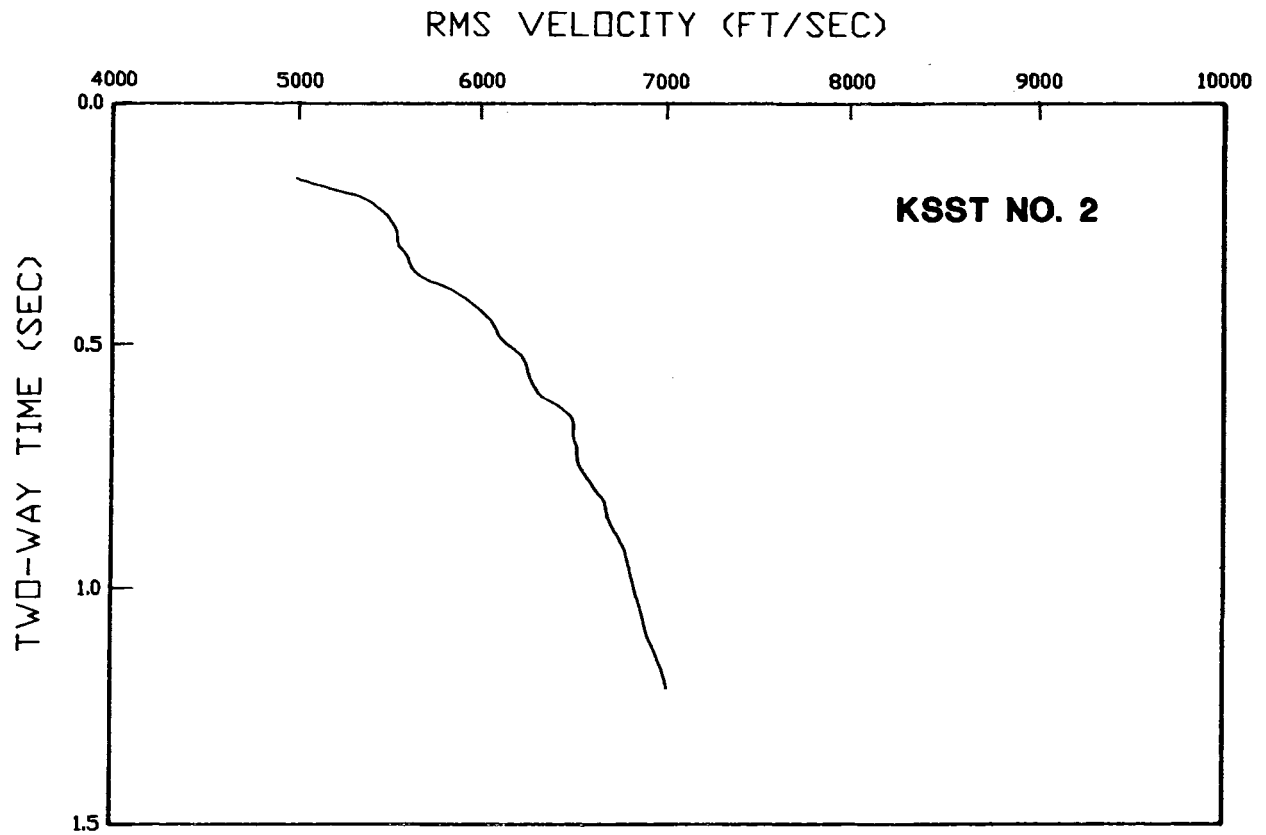


Figure 35. RMS velocity calculated from the long-spaced sonic log from the KSST No. 2 well. Depths are measured relative to mean sea level.

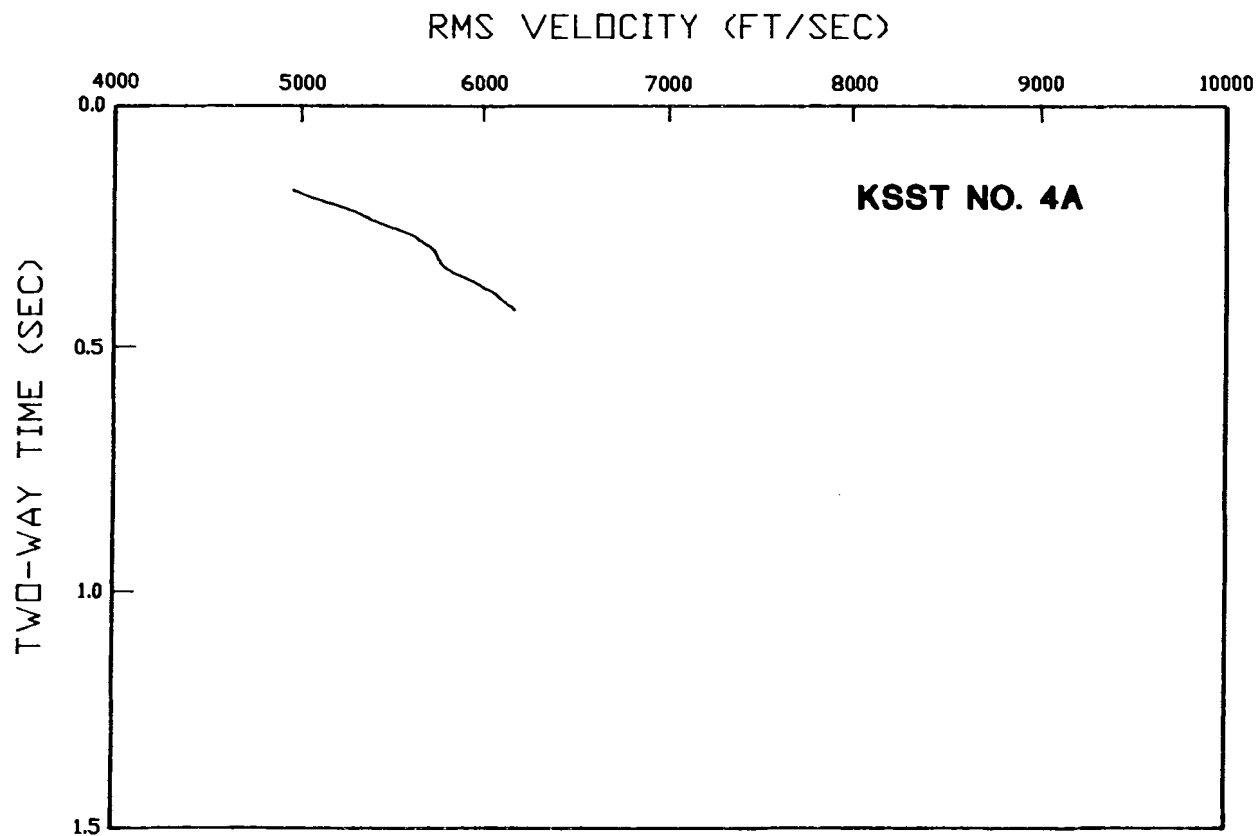


Figure 36. RMS velocity calculated from the long-spaced sonic log from the KSST No. 4A well. Depths are measured relative to mean sea level.

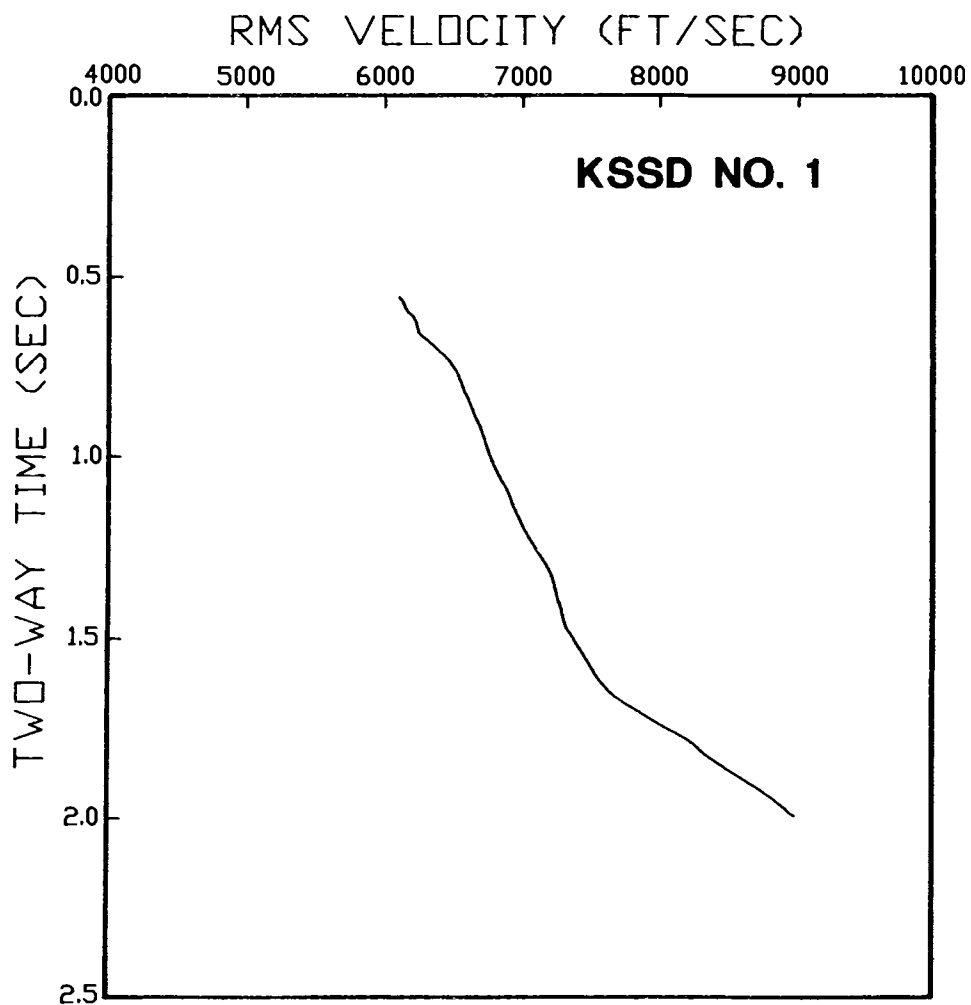


Figure 37. RMS velocity calculated from the long-spaced sonic log from the KSSD No. 1 well. Depths are measured relative to mean sea level.

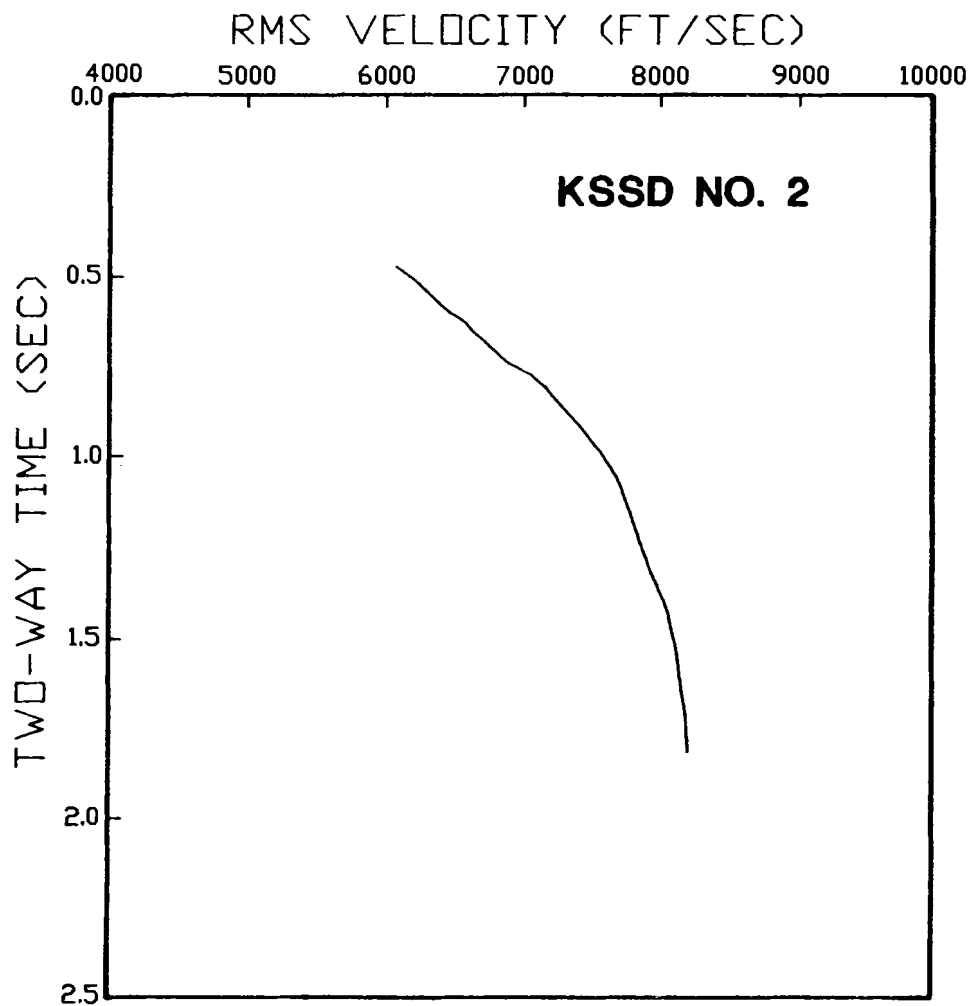


Figure 38. RMS velocity calculated from the long-spaced sonic log from the KSSD No. 2 well. Depths are measured relative to mean sea level.

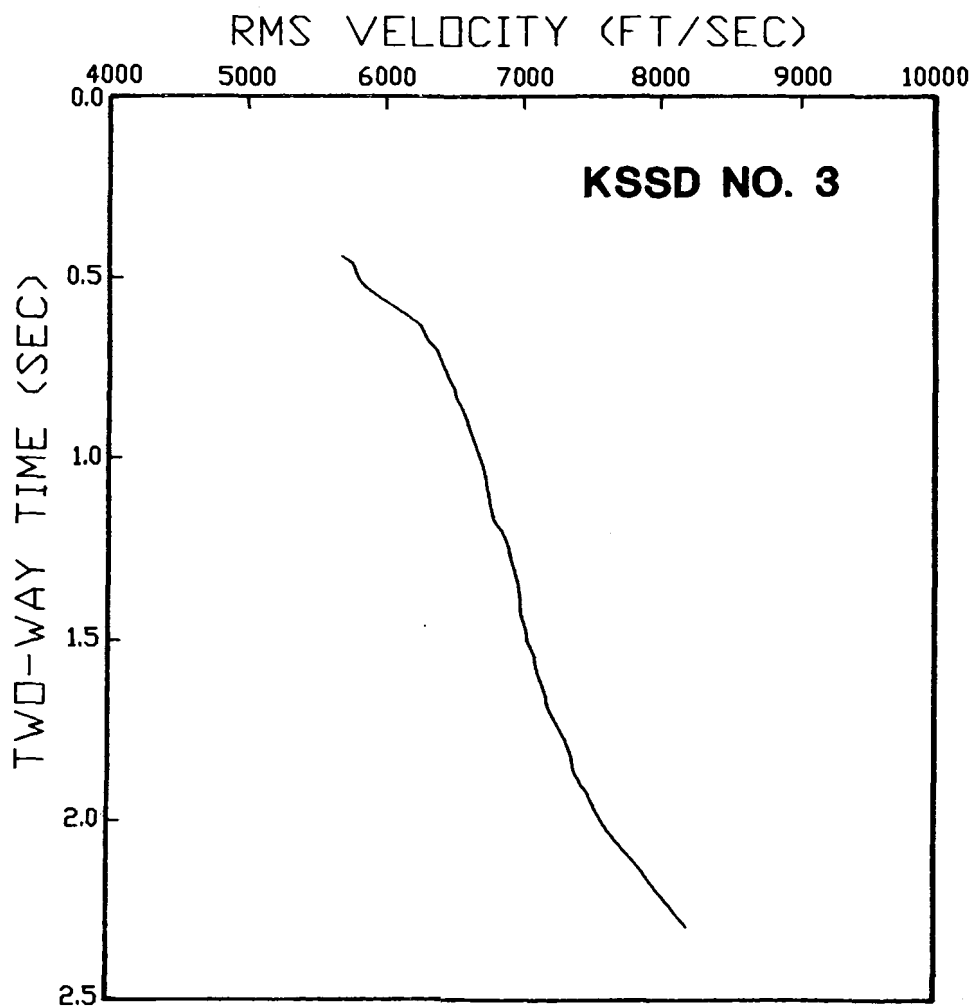


Figure 39. RMS velocity calculated from the long-spaced sonic log from the KSSD No. 3 well. Depths are measured relative to mean sea level.

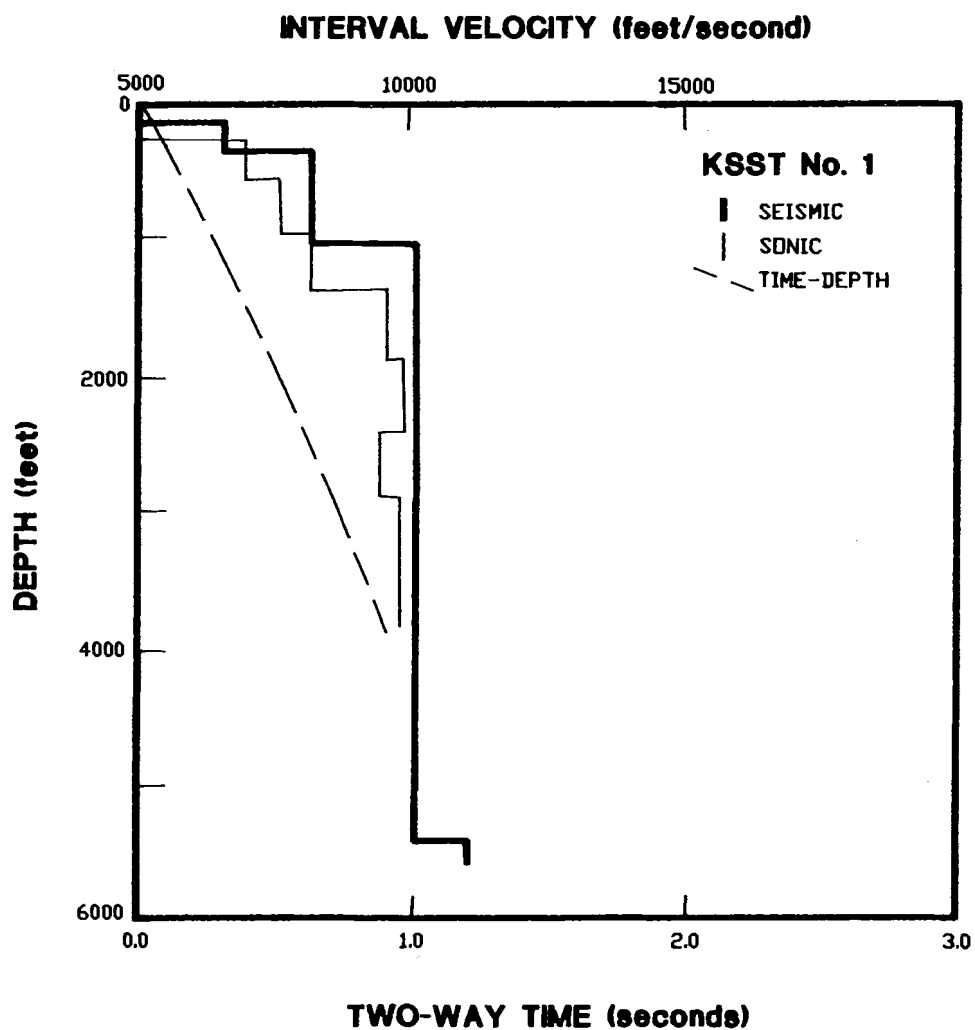


Figure 40. Interval velocities and a time-depth curve calculated from interval transit time data from the long-spaced sonic log of the KSST No. 1 well. Also shown is an interval velocity curve calculated from an unreversed sonobuoy refraction profile shot near the well (Holmes and others, 1978). Depths are measured relative to mean sea level.

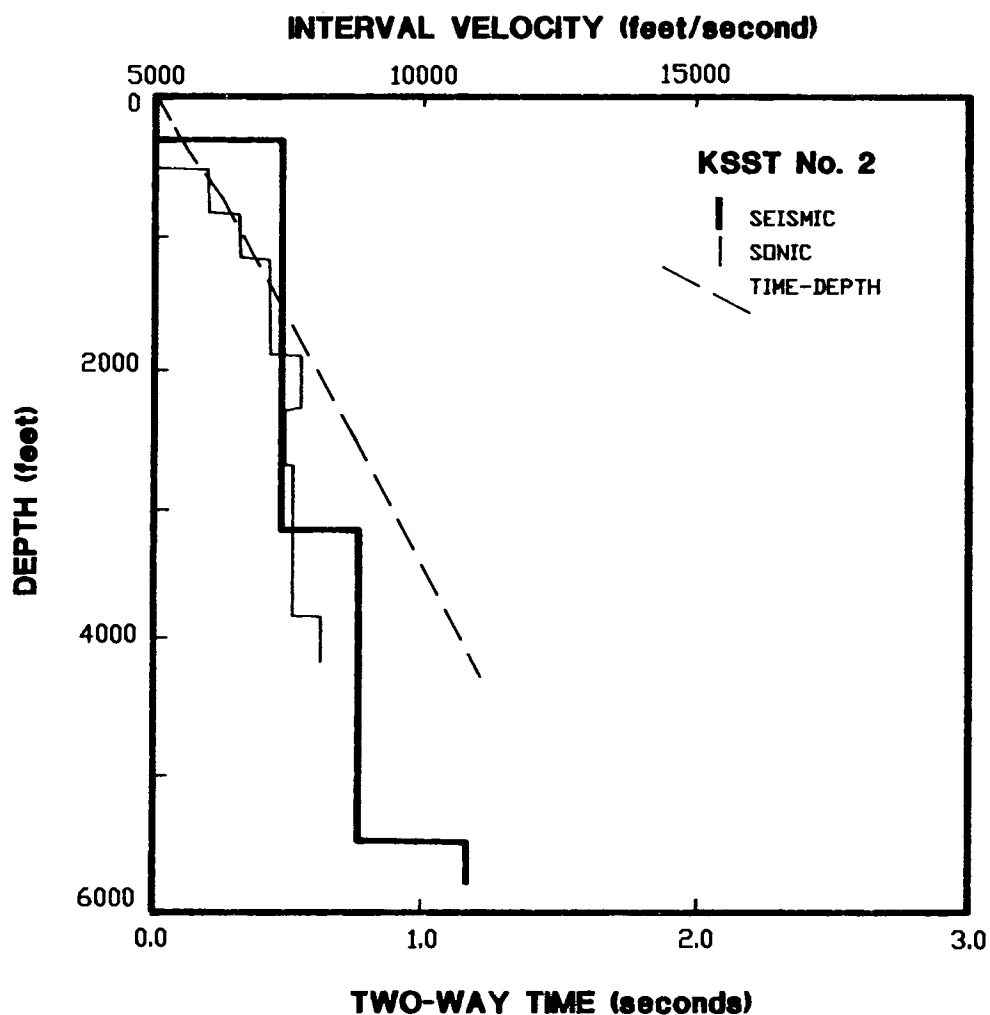


Figure 41. Interval velocities and a time-depth curve calculated from interval transit time data from the long-spaced sonic log of the KSST No. 2 well. Also shown is an interval velocity curve calculated from an unreversed sonobuoy refraction profile shot near the well (Holmes and others, 1978). Depths are measured relative to mean sea level.

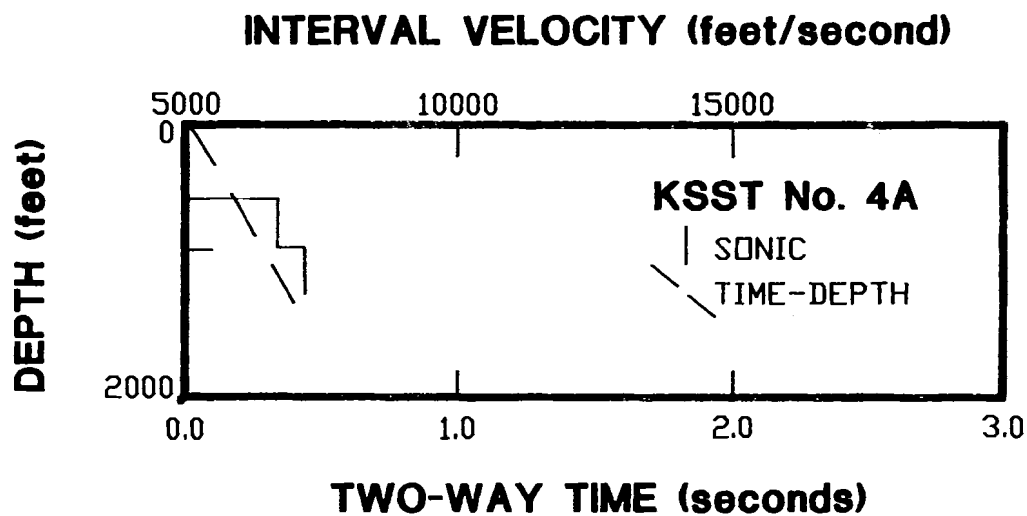


Figure 42. Interval velocities and a time-depth curve calculated from interval transit time data from the long-spaced sonic log of the KSST No. 4A well. Depths are measured relative to mean sea level.

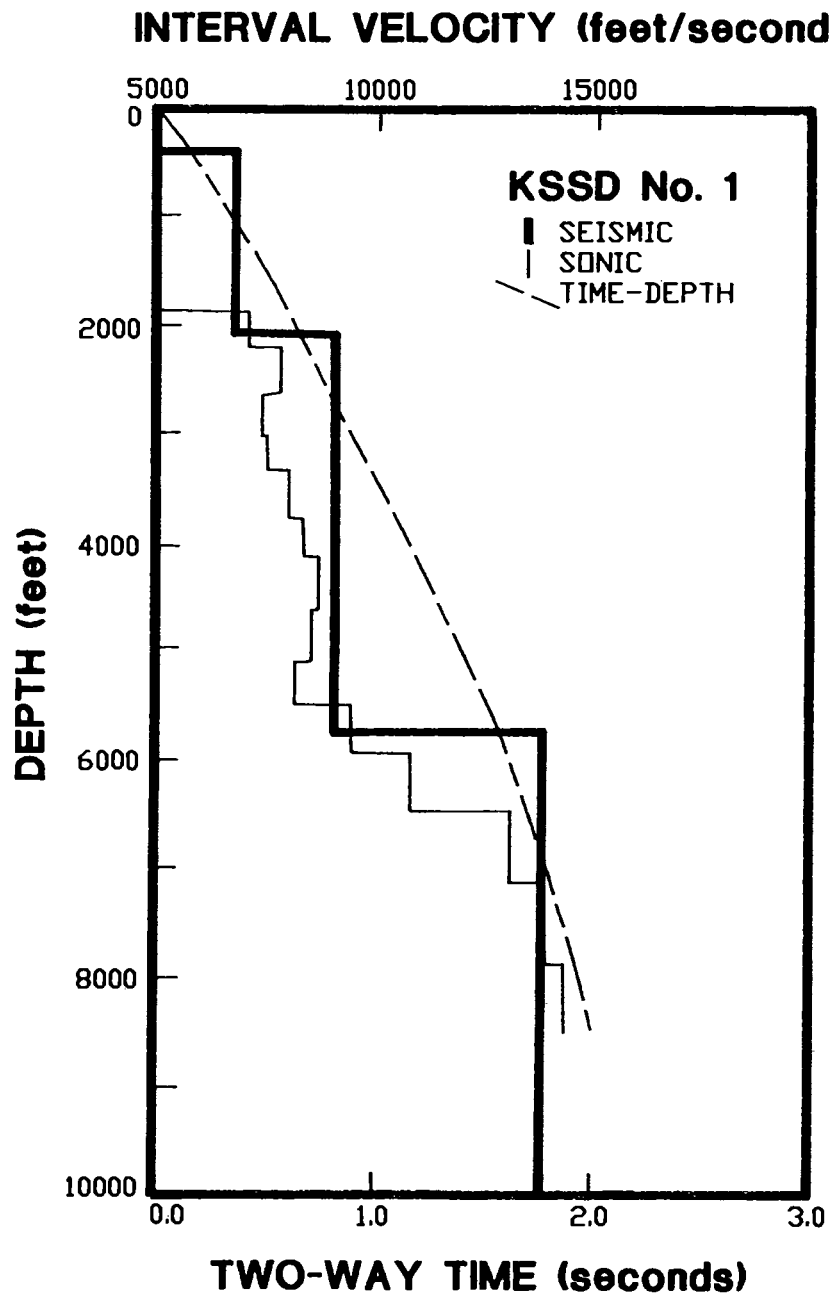


Figure 43. Interval velocities and a time-depth curve calculated from interval transit time data from the long-spaced sonic log of the KSSD No. 1 well. Also shown is an interval velocity curve calculated from an unreversed sonobuoy refraction profile shot near the well (Holmes and others, 1978). Depths are measured relative to mean sea level.

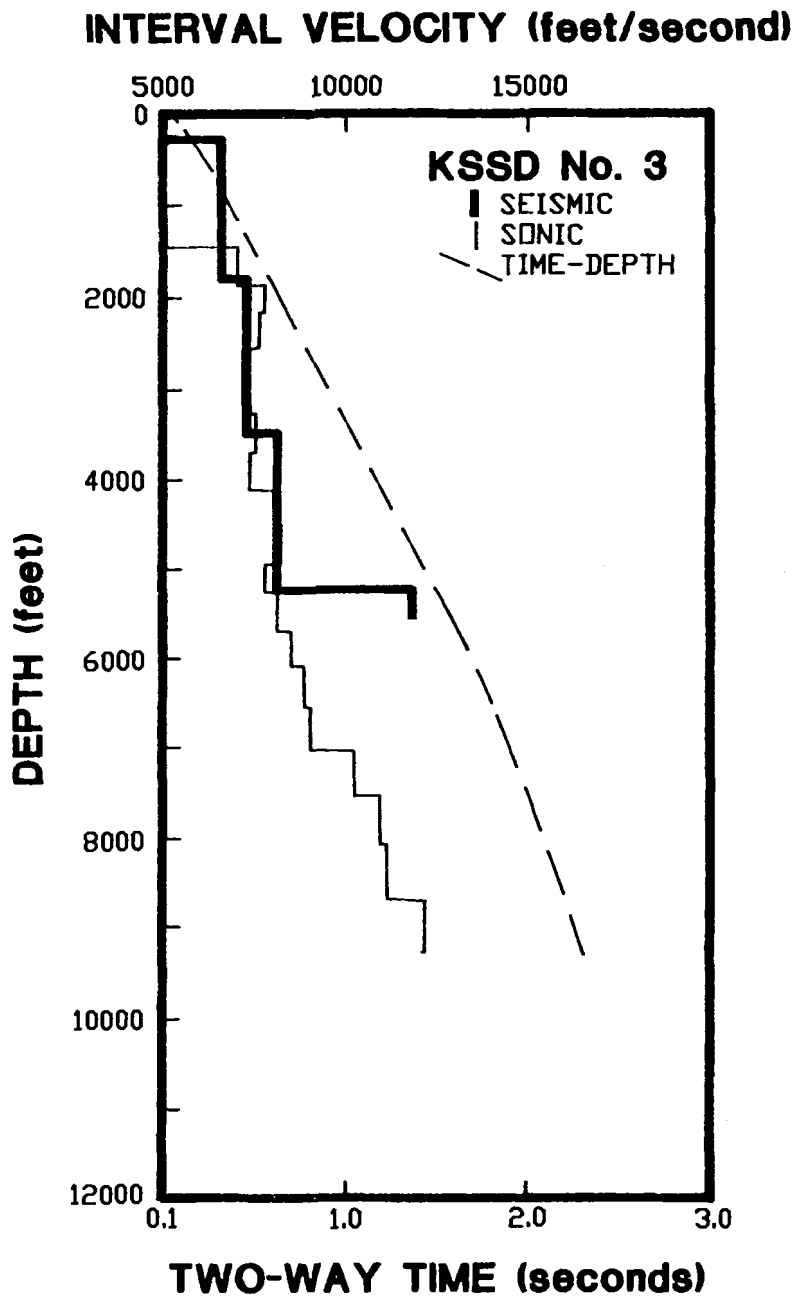


Figure 44. Interval velocities and a time-depth curve calculated from interval transit time data from the long-spaced sonic log of the KSSD No. 3 well. Also shown is an interval velocity curve calculated from an unreversed sonobuoy refraction profile shot near the well (Holmes and others, 1978). Depths are measured relative to mean sea level.

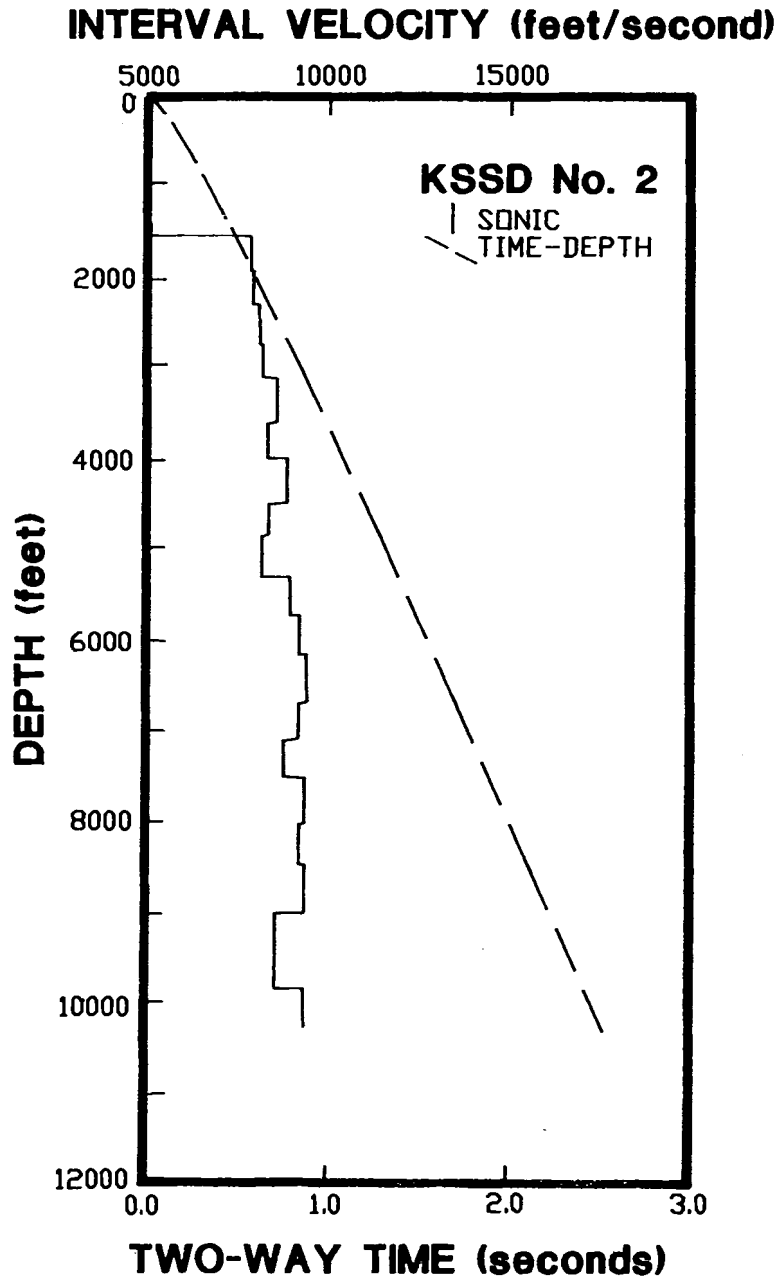


Figure 45. Interval velocities and a time-depth curve calculated from interval transit time data from the long-spaced sonic log of the KSSD No. 2 well. Depths are measured relative to mean sea level.

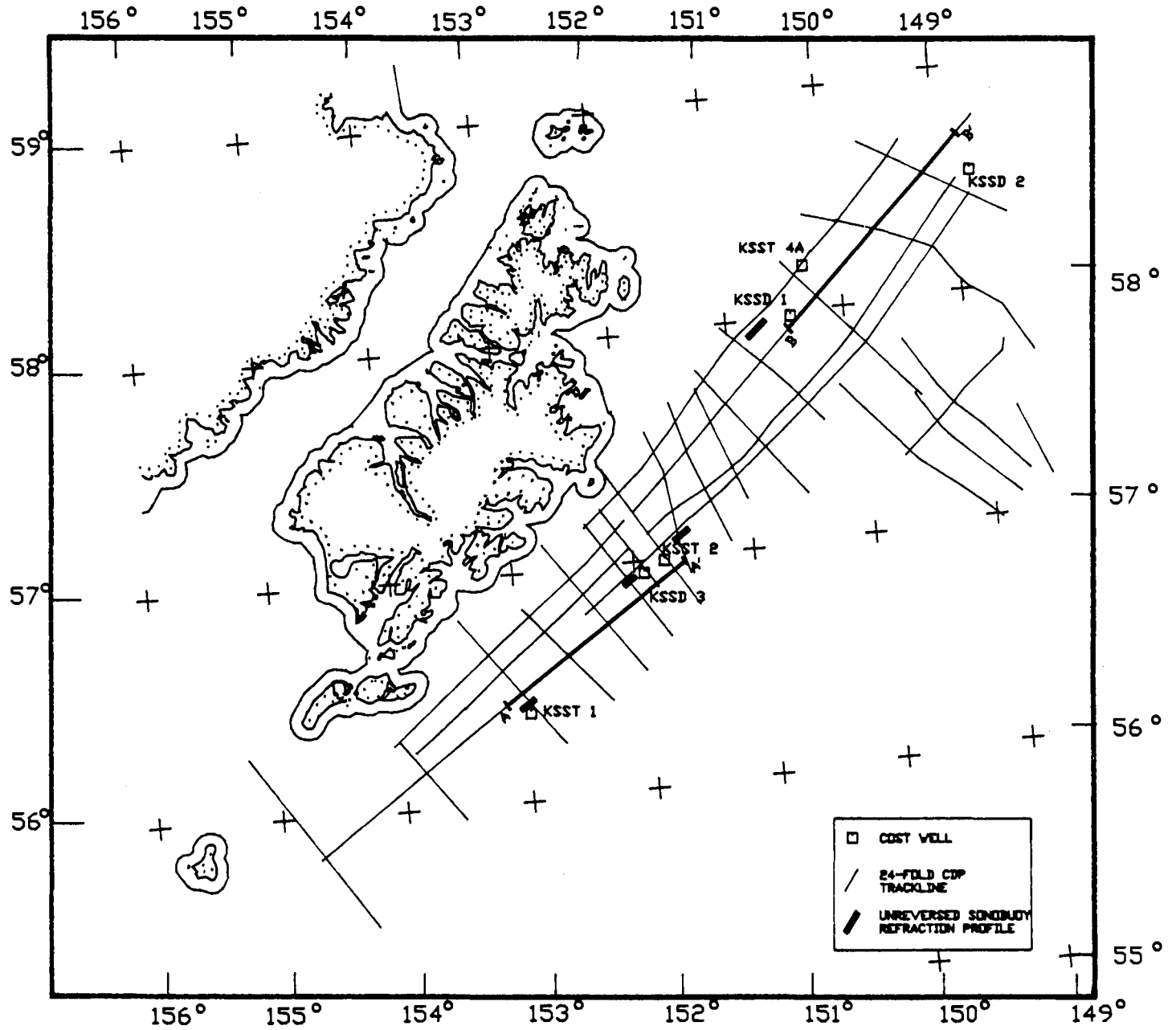


Figure 46. Map showing trackline coverage of 24-fold seismic reflection profile data across Kodiak shelf. Also shown are the locations of unreversed sonobuoy refraction profiles shot near wells.

5. SEISMIC STRATIGRAPHY AND TECTONIC EVOLUTION OF THE KODIAK SHELF

The Cenozoic strata underlying the Kodiak shelf comprise two seismic sequences separated by an unconformity of regional extent. These seismic sequences represent the tectonically deformed Paleogene stratigraphic sequence, which constitutes the basement complex that underlies most, if not all, of the shelf, and the relatively undeformed Neogene stratigraphic sequence that overlies it. Synthetic seismograms were generated for the purpose of correlating the data from the KSST and KSSD wells with nearby non-proprietary seismic reflection data. However, because of the structural complexity of the Kodiak shelf and the distances separating the wells from the seismic lines (1.5 to 8.5 miles), only rough correlations could be made.

The synthetic seismograms were generated by Minerals Management Service personnel using data from the long-spaced sonic logs. Logs with a scale of 5 inches per 100 feet were digitized with an accuracy estimated to be approximately 1 microsecond per foot in transit time and 1.0 foot in depth. Reflection coefficients were determined from the travel time data while assuming constant density. Reflection coefficients were then convolved with a standard 8 to 55 Hz Ricker wavelet in a computer program that generates synthetic seismograms without multiples. The program assumes horizontal strata and planar incident waves that are propagating normal to the reflecting surfaces. This assumption, however, is not valid for the Paleogene section of the wells, where the presence of steeply dipping strata is indicated in the dipmeter data. The synthetic seismograms are displayed in both normal and reverse polarity in figures 47 to 52.

Figures 53 and 54 show parts of two 24-fold seismic reflection profiles shot parallel to the shelf in 1975 by the U.S. Geological Survey (fig. 46). The seismic profile shown in figure 53 transects the Albatross basin and was shot within 5, 3.5, and 4 miles, respectively, of the KSST No. 1, KSST No. 2, and KSSD No. 3 wells. The locations of the wells are projected into the profile shown in the figure. Three geologically significant horizons penetrated by the wells, here designated A', A, and C, are shown on the profile. Horizons A and C correspond to horizons A and C of Fisher and von Huene (1980) and represent the top of strata of late Pliocene age and a regional unconformity, respectively.

The seismic profile shown in figure 54 transects the Stevenson basin and was shot within 2, 8, and 8.5 miles, respectively, of the KSSD No. 1, KSST No. 4A, and KSSD No. 2 wells. The locations of the wells are projected into the seismic profile shown in the figure. The Stevenson basin is bisected by the Portlock anticline which is indicated in the figure. In this figure, the depths of seismic horizons A and C were determined on the basis of the paleontologic interpretation from only the KSSD No. 1 well (see Biostratigraphy chapter); the paleontologic interpretation of the KSSD No. 2 well was not used for this purpose because a major fault between the well and the seismic line made correlation unreliable.

Horizon A' corresponds to the base of the Pleistocene glaciomarine shelf sequence discussed in the Well Log Interpretation chapter. This sequence is composed of upward-fining sequences of interbedded mudstone and conglomerate or mudstone and sandstone. Paleontologic data indicate that the base of this sequence is middle Pleistocene in age. On the seismic profile shown in figure 53, horizon A' cannot be followed across the entire Albatross basin because of an intervening basement uplift over which the Neogene seismic sequence has been folded. East of the uplift, the reflections comprising the stratigraphic sequence overlying horizon A are truncated at the sea floor as a consequence of that folding.

Horizon A is a prominent reflection that can be traced across most of the Kodiak shelf. In the KSSD No. 1 and KSST No. 2 wells, horizon A coincides with the boundary between strata of early Pleistocene age and strata of late Pliocene age. The other Kodiak shelf wells were not used to date this horizon because poor reflection continuity, steeply dipping reflections, or substantial distances separating the wells from the seismic data made correlation tenuous.

The widespread occurrence of horizon A indicates that the geological phenomenon that it represents must have occurred nearly simultaneously across the entire Kodiak shelf. Beginning at approximately 1.2 Ma, Middleton Island, 120 miles northeast of the Kodiak shelf, was covered by a large continental glacier (Molnia, 1979). The glaciation of the Middleton shelf region occurred simultaneously with the appearance of an increase in glacially derived detritus sampled in piston cores from the North Pacific abyssal plain (Molnia, 1979). These events roughly coincided with the formation of horizon A, suggesting that horizon A may represent a significant oceanographic event, perhaps a lowering of sea level or an intensification of circulation across the shelf, associated with that climatic degradation.

Horizon C is a regional unconformity that separates deformed Paleogene strata from relatively undeformed Neogene strata (figs. 53 and 54). Fisher and Holmes (1980) detected a marked velocity discontinuity in seismic refraction data at the depth of horizon C. Velocities measured above horizon C were typically 2.5 kilometers per second (8,200 feet per second), whereas velocities measured below horizon C were typically 4.0 kilometers per second (13,100 feet per

(text continued on p. 89)

second). On the basis of similar high velocities measured by refraction profiles shot near Kodiak Island, presumably through Eocene and Oligocene rocks of the Sitkalidak and Sitkinak Formations, and from the presence of Paleogene strata penetrated at the Tenneco Middleton Island State No. 1 well 120 miles to the northeast, those investigators interpreted that the higher velocities measured beneath the Kodiak shelf were caused by the presence of strata of Paleogene age. Elsewhere in this report, evidence in the well data of moderately to steeply dipping strata and of highly compacted shale beds, in the absence of evidence from kerogen maturity data corroborating an earlier history of deep burial, is interpreted to indicate that the rocks below horizon C have experienced tectonic dewatering and compaction (see Abnormal Formation Pressure chapter). The velocity discontinuity at horizon C detected by Fisher and Holmes (1980) is also a manifestation of that difference in the degree of dewatering and compaction and, hence, in the tectonic histories between the strata above and below that discontinuity.

THE ORIGIN OF THE HORIZON C UNCONFORMITY AND TECTONIC MODELS

Field mapping in widely separated regions of the plate margin along southwestern Alaska indicates that a major episode of tectonic deformation and uplift occurred along that margin sometime during Eocene through Miocene time. In addition, other evidence also shows that at least one other episode of tectonic deformation and uplift occurred locally. Gates and Gibson (1956) described a major unconformity in the Aleutian Islands separating rocks of early to middle Tertiary age from those of late Tertiary age, an unconformity which DeLong and McDowell (1975) later attributed to a middle Tertiary orogeny. Burk (1965) noted that strata of late Oligocene and early Miocene age were missing on the Alaska Peninsula, which he interpreted to reflect deformation, uplift, and erosion. Other evidence of early to middle Tertiary tectonics reported by Burk (1965) and also by Brockway and others (1975) is thick sequences of volcanoclastic sediments of Eocene and Oligocene age underlying parts of the Alaska Peninsula. Reed and Lanphere (1973) reported that during middle Tertiary time, plutonic rocks ranging in composition from quartz diorite to granite were emplaced along the trend of the Alaska-Aleutian Range. Barnes and Payne (1956) and Barnes (1962) described evidence from the Matanuska Valley, 260 miles north of the Kodiak shelf, which indicated that a major episode of folding and uplift, accompanied by the erosion of Mesozoic and early Tertiary strata, took place at some time between middle Eocene and late Oligocene times. Kirschner and Lyon (1973) and Fisher and Magoon (1978) also reported that the Cook Inlet region, which includes the Matanuska Valley, was deformed and uplifted within that time frame. Keller and others (1984) described micropaleontologic evidence for a hiatus of early Oligocene (33 Ma) to late Oligocene (24 Ma) age in samples from the Tenneco Middleton Island well, which could also be a manifestation of tectonic activity and uplift at that time. Further east in the Gulf of Alaska, the Pliocene to Miocene Yakataga Formation unconformably overlies the Miocene to late Eocene Poul Creek Formation. In the Kodiak Island region, Fisher and Holmes

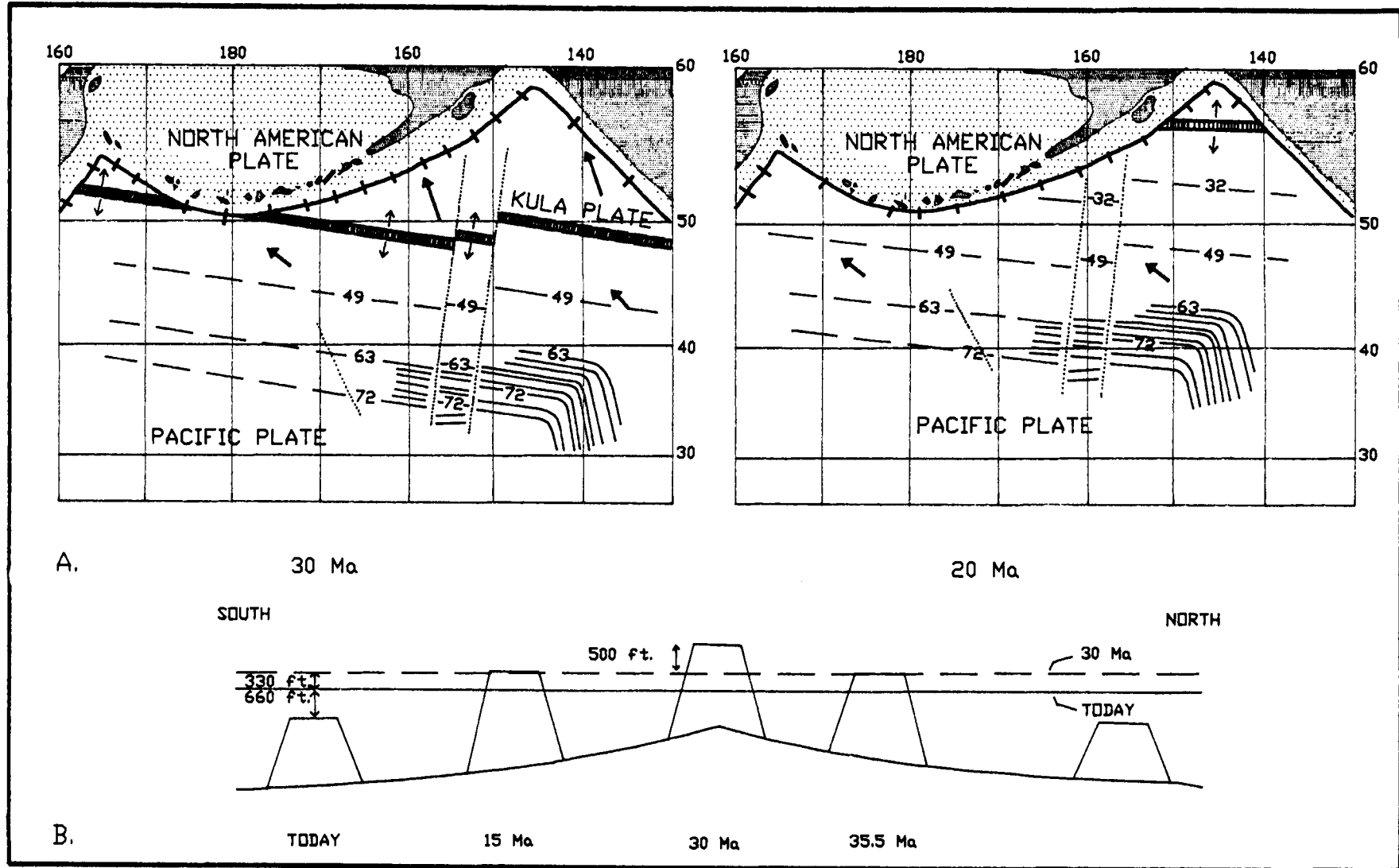


Figure 55. A. The theoretical configuration of the northern Pacific region at 30 Ma and 20 Ma (after Grow and Atwater, 1970). The bold line represents the Kula-Pacific spreading center. The solid arrows indicate the directions of motion of the plates relative to North America. The magnetic anomalies shown as the solid lines represent anomalies presently observed in the North Pacific. The magnetic anomalies shown as the dashed lines represent anomalies in oceanic crust that have been subsequently subducted at the Aleutian trench. B. A schematic model showing the uplift and subsidence history of a section of the Aleutian arc summit platform which overrode the subducting Kula-Pacific spreading center at 30 Ma (after DeLong and others, 1978).

(1980) and Moore and Allwardt (1980) reported that uplift during Oligocene time is manifested by the deposition of non-marine sediments of the middle and late Oligocene Sitkinak Formation on top of an unconformity that truncates "offscraped" slope and submarine fan deposits of the Eocene Sitkalidak Formation.

These widespread examples of deformation and uplift have been alternatively attributed to the subduction of the Kula ridge (Reed and Lanphere, 1973; Grow and Atwater, 1970; DeLong and others, 1978, 1980); the obduction of an offscraped, trench-filling submarine fan complex (Moore and Allwardt, 1980); and the underplating of the overriding North American plate by deep-sea sediments offscraped from the subducting oceanic plate (Byrne, 1986). Reed and Lanphere (1973) speculated that the magmatic activity along the Alaska-Aleutian arc during middle Tertiary time was related to the northward underthrusting of the Kula plate and the subsequent subduction of the Kula ridge. Grow and Atwater (1970) and DeLong and others (1978, 1980) presented models relating the geology of the Alaska-Aleutian arc to the hypothetical consequences of the subduction of the Kula-Pacific spreading center along the Aleutian trench. Although those two models differ somewhat, particularly in their interpretations of the effects of the subduction of a spreading center on magma generation along the arc, both models embrace the same sequence of events: an initial phase of deformation followed by regional uplift and subaerial erosion (producing an areally extensive unconformity), followed in turn by subsidence and deposition of a shallow-marine clastic sequence. In both models, uplift and subaerial erosion would occur as the Aleutian arc overrode progressively younger and consequently shallower oceanic crust across the northern flank of the Kula ridge spreading center (fig. 55B). The studies of Grow and Atwater (1970) and DeLong and others (1978) both recognized the ramifications of subducting a roughly east-west oriented ridge beneath a southwardly convex arc to the tectonics of that plate margin. In their models, they employed this geometry to explain why geologic evidence shows that the timing of the orogeny occurred progressively later northeastward up the arc (fig. 55A).

Moore and Allwardt (1980) proposed a different model in order to explain the tectonic deformation that took place across the Kodiak shelf during Paleogene time. They envisioned that the deformation, uplift, and subsidence of the shelf was caused by the obduction of submarine fan deposits offscraped from the subducting plate. They formulated this interpretation on the basis of field mapping on Kodiak and neighboring islands which revealed that the Eocene Sitkalidak Formation is composed of two distinct structural units, an intensely deformed unit with disrupted strata and a moderately deformed but relatively intact unit. They concluded that the intensely deformed unit, which is situated in the more seaward structural position, represents an offscraped, trench-filling submarine fan complex, whereas the less deformed unit, which is situated in the more landward structural position, represents a slope basin deposit (fig. 56). Unconformably overlying both structural units are non-marine strata composing the Oligocene Sitkinak Formation. Moore and Allwardt (1980) interpreted that the two

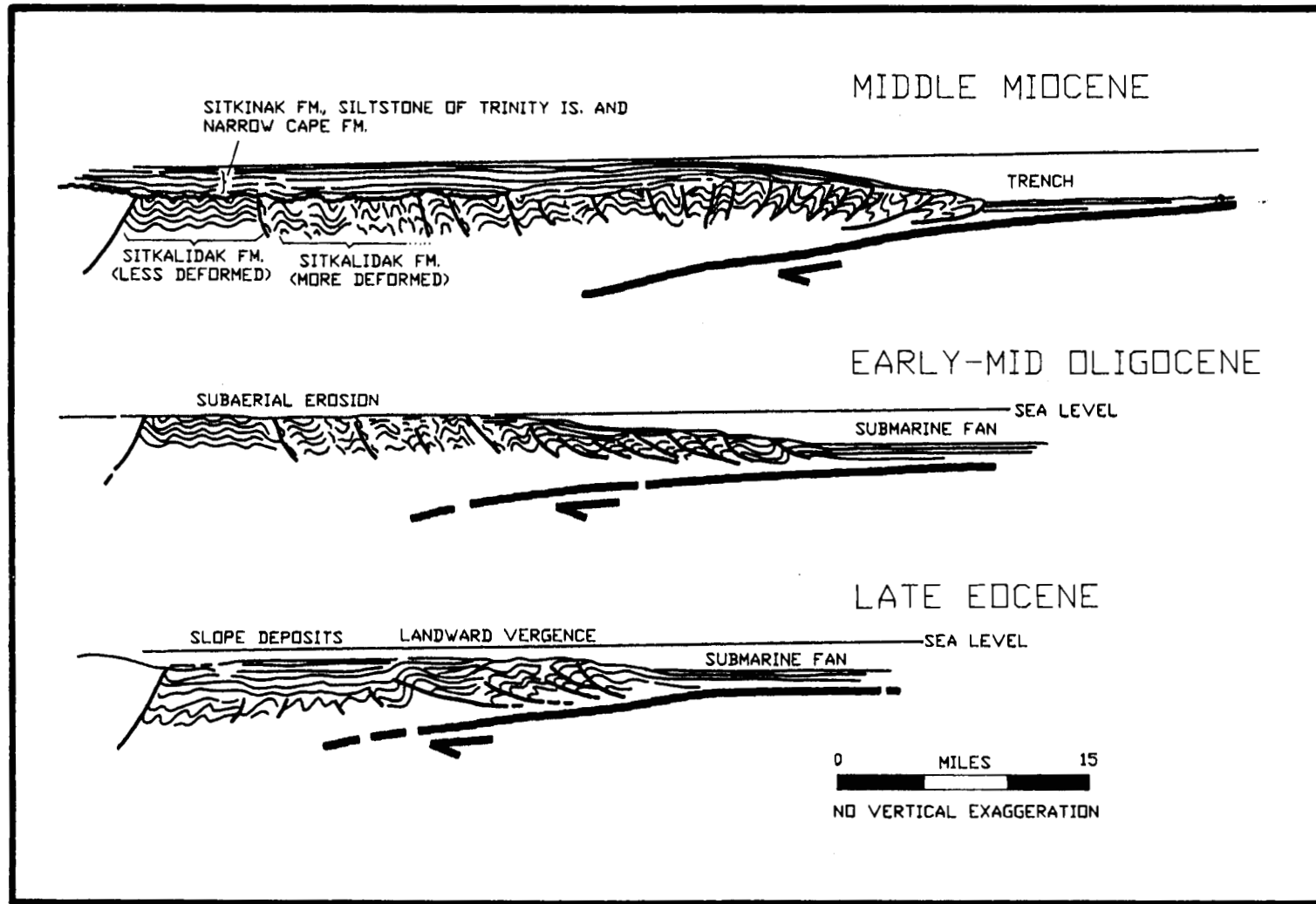


Figure 56. Tectonic evolution of the Kodiak shelf (after Moore and Allwardt, 1980) illustrating the development of the more deformed and less deformed units of the Sitkalidak formation.

contrasting sites of deposition (trench and slope basin) represented by the two structural units of the Sitkalidak Formation and the unconformable deposition across them of non-marine sediments reflects a history of rapid deposition during Eocene time followed by uplift and erosion during Oligocene time.

Byrne (1986) proposed a third mechanism for the uplift of the Kodiak shelf region. He cited structural characteristics of the Late Cretaceous to Paleocene Ghost Rocks Formation that indicate that most, if not all, of the rocks underlying the Kodiak Islands and adjacent continental shelf were uplifted vertically without the landward tilting or imbrication typical of many convergent margins (e.g., Seely and others, 1974; Seely, 1977). In order to account for those structural relationships, Byrne proposed that a series of 7- to 12-mile-deep, landward-dipping reflectors apparent on seismic reflection data shot northeast of Kodiak Island (event "A" of Fisher, von Huene, Smith, and Bruns, 1983) represents the top of a sediment package composed of turbidite fan deposits offscraped from the subducting oceanic plate and underplated beneath the Kodiak shelf. In an earlier report, Fisher, von Huene, Smith, and Bruns (1983) proposed that those deep reflections could be either from a detached piece of oceanic crust or from rocks associated with the subducting Pacific plate. In a subsequent evaluation of a different set of seismic reflection data across the same transect, Fisher and others (1987) determined that those reflections could not have been from the subducting plate and were more likely from underplated rocks. In the model of Byrne (1986), the underplating of those deposits between early Eocene and early Oligocene times produced the observed regional uplift of Kodiak Island in the absence of landward tilting (fig. 57).

The unconformity modeled above is present across much of the southern Alaskan plate margin from the Aleutian Islands to the Kenai Peninsula. On the basis of geologic data, DeLong and others (1978) estimated that in the Aleutian Islands west of the Alaska Peninsula, the age of that unconformity is approximately 30 Ma (late Oligocene). In the Kodiak shelf region, the situation is more complex, and two unconformities appear to be present. On Sitkinak Island, one unconformity separates the highly deformed deep-sea rocks of the Eocene to Oligocene Sitkalidak Formation from the less deformed non-marine rocks of the Oligocene Sitkinak Formation (Moore, 1969; Moore and Allwardt, 1980). At Narrow Cape near the eastern end of Kodiak Island, Oligocene strata of the Sitkinak Formation are absent, and the Sitkalidak Formation is unconformably overlain by shallow-marine strata of the Miocene Narrow Cape Formation. A controversy exists regarding the nature of the contact between the Narrow Cape Formation and the Sitkinak Formation. In the Trinity Islands, the Sitkinak Formation is conformably overlain by a shallow-marine siltstone unit of late Oligocene or early Miocene age (Allison, 1976) which Moore (1969) originally included in the Narrow Cape Formation, but to which Armentrout later assigned the informal designation "siltstone of the Trinity Islands" (J.M. Armentrout, personal commun., 1979, cited in Moore and Allwardt, 1980). Because of the difference in age between the "siltstone of the Trinity Islands" and the Narrow Cape Formation, and the large distance separating the

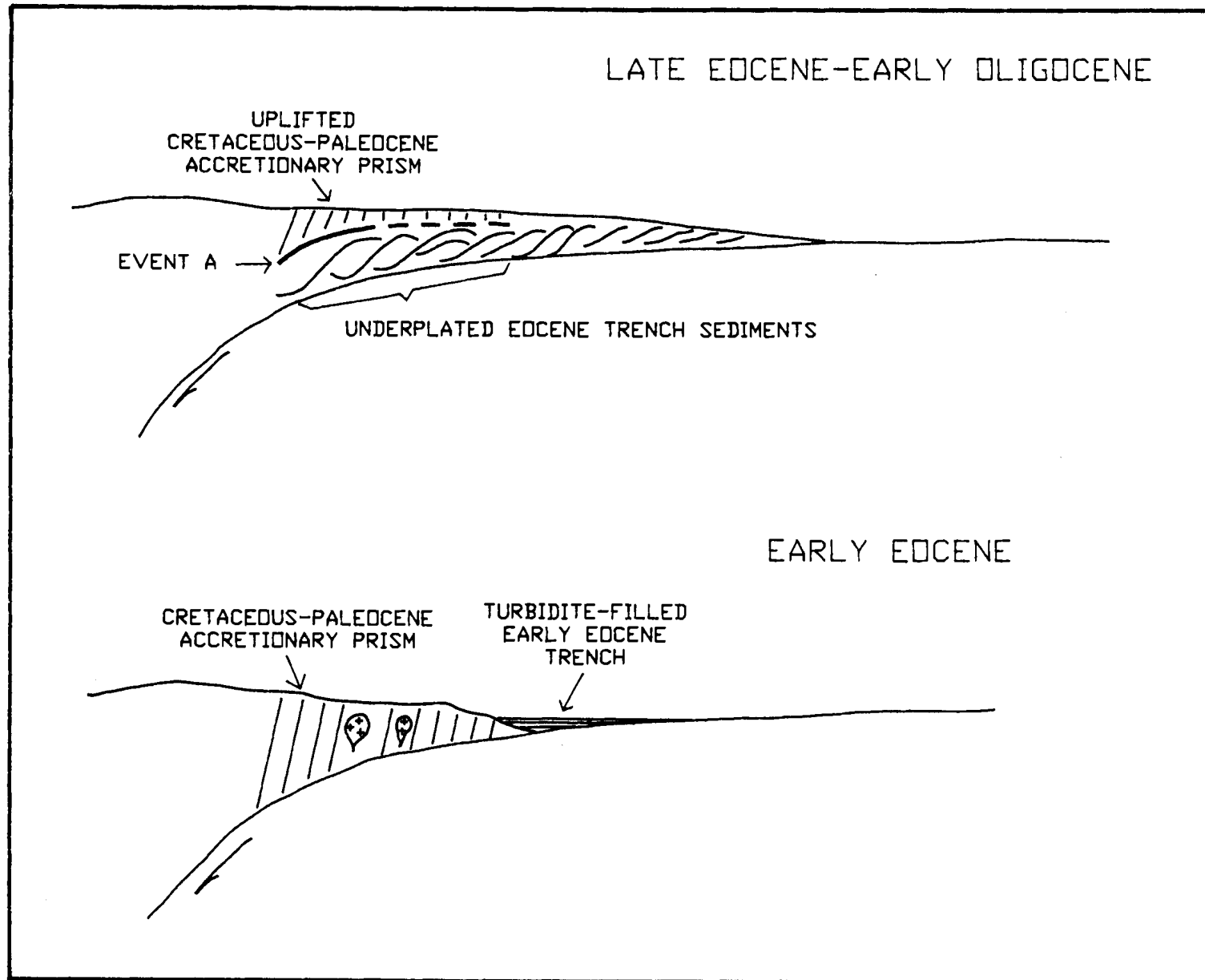


Figure 57. Schematic model for the uplift of the Kodiak shelf caused by regional-scale underplating (after Byrne, 1986).

Trinity Islands from the type section of the Narrow Cape Formation, Moore and Allwardt (1980) preferred the later designation of Armentrout over the original one of Moore (1969). As a consequence of that discrepancy, and because the contact between the Sitkinak and the Narrow Cape Formations has not been mapped, it is not clear whether one or two unconformities are present. Offshore on the Kodiak shelf, Oligocene strata are also absent in the KSSD wells, and Miocene and Eocene rocks are separated by the horizon C unconformity. Because of the controversy regarding what stratigraphic unit overlies the Sitkinak Formation in the Trinity Islands, the nature of the contact between strata of the Oligocene Sitkinak Formation and the Miocene Narrow Cape Formation is not understood. Hence, either a single, time-transgressive unconformity separates the Sitkalidak Formation from the Sitkinak Formation near the southwestern end of the Kodiak shelf and also from the younger Narrow Cape Formation near the northeastern end of the shelf, or, more likely, a second, younger and as yet unmapped unconformity separates the Narrow Cape and Sitkinak Formations.

Fisher and Holmes (1980) attributed the unconformity found offshore to the uplift and exposure of the shelf during middle and late Miocene time as a consequence of the growth of an ancient shelf-break structure situated landward of the present shelf break. An evaluation of paleontologic data presented elsewhere in this report (see Biostratigraphy chapter) enables the timing of the uplift and erosion of the Kodiak shelf region to be constrained better than has been possible with previously published data. The study presented in this report identified the presence of microfossils of middle Miocene age in the KSSD No. 3 well, and of middle or possible early Miocene age in the KSSD No. 1 and KSSD No. 2 wells. Byrne (1986) pointed out that because of the paucity of fossils in the underlying Sitkalidak Formation, the timing of the initial uplift in that region is poorly understood and may have occurred any time between early Eocene (50 Ma) and late Oligocene (30 Ma) times. The present study also established that the age of the strata underlying the horizon C unconformity is late Eocene in the KSSD No. 2 and KSSD No. 3 wells (and possible middle Eocene in the KSSD No. 1 well). Thus, on the basis of new data presented in this report, the episode of uplift (or episodes if two unconformities are present) manifested by the horizon C discordance occurred after late Eocene time and prior to middle or possibly early Miocene time.

In the Albatross basin and in a small unnamed basin flanking the Central Shelf Uplift (fig. 58), horizon C is underlain by coherent reflections representing relatively undeformed stratified rock. In contrast, in many regions, particularly in the uplifted areas flanking the shelf basins, horizon C is underlain by an acoustically unresolvable basement complex. Paleontologic data presented elsewhere in this report indicate that these acoustically unresolvable rocks, which underlie much of the Kodiak shelf, are composed, at least in part, of strata coeval with the Sitkalidak Formation. The age and lithology of the relatively undeformed stratified rock is problematic, but these rocks may represent

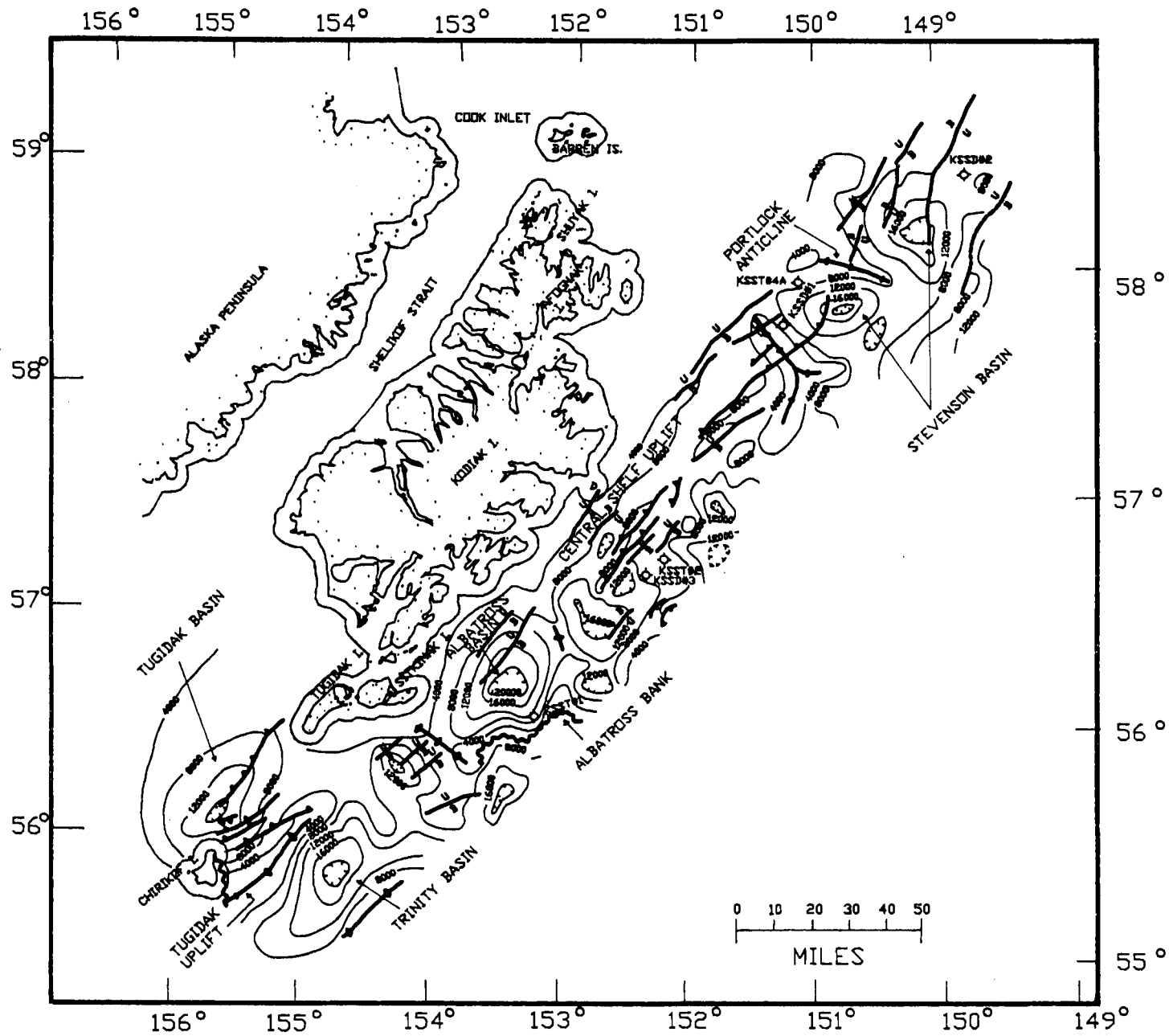


Figure 58. Structure-contour map of horizon C (after W. Horowitz, unpublished MMS interpretation).

either a relatively intact slope-basin deposit within the Sitkalidak Formation or part of the Oligocene Sitkinak Formation.

Much of the strata that compose the acoustically unresolvable basement complex is believed to be allochthonous. Recent geological and geophysical investigations indicate that much of the western North American continent is made up of a collage of allochthonous tectonostratigraphic terranes (e.g., Jones and Silberling, 1979; Coney and others, 1980). These tectonostratigraphic terranes are suspected to have originated elsewhere and were subsequently transported to and accreted onto the continental margin. The mechanism by which these terranes were transported large horizontal distances may have been either through the relative motions of lithospheric plates upon which they passively rode or as fault slivers translated along the inner trench wall (Jarrard, 1986). Previous investigators recognized that the rocks exposed on Kodiak and in the Shumagin Islands have lithologic and paleontologic affinities with similar rocks exposed elsewhere along southern Alaska which, together, make up linear belts that extend parallel to the continental margin (Jones and others, 1978; Coney and others, 1980; Jones and others, 1981). Microfossils from sediments of Pleistocene age sampled in the KSST No. 1 well include reworked, "tropical", shallow-water microfossils of probable Eocene age (see Biostratigraphy chapter: Unusual Reworked Fossil Elements). The presence of these Paleogene microfossils may reflect the accretion of terranes originally deposited at lower latitudes and lend support to an allochthonous origin for the underlying acoustically unresolvable rock.

Most of Kodiak Island and the adjacent continental shelf are underlain by two tectonostratigraphic terranes, the Prince William and Chugach terranes (fig. 59). Since early Mesozoic time, the accretion of such belts of arc-derived turbidite deposits and allochthonous tectonostratigraphic terranes has progressively broadened the shelf towards the southeast. The Prince William terrane, the more seaward of the two and, hence, the one more recently emplaced, is made up of a sequence of melange, turbidites, and volcanics of Paleocene age and a submarine fan complex of Eocene to possible early Oligocene age (Moore and others, 1983). This terrane underlies the continental shelf seaward of Kodiak Island and extends northeastward into Prince William Sound and its borderland and, presumably, southwestward along the edge of the Shumagin shelf, although at present its exact boundaries are poorly defined.

Paleomagnetic data from early Paleocene volcanic rocks of the Ghost Rocks Formation, a component of the Prince William terrane exposed on Kodiak Island, indicate that those rocks were originally emplaced approximately 25 degrees south of their present location (Plumley and others, 1982; Moore and others, 1983). Moore and others (1983) presented three models for the northward translation of the Kodiak accretionary complex following that magmatic event. In their models, the Kodiak accretionary complex arrived at its present latitude during early middle Eocene time (approximately 48 to 50 Ma). Keller and others (1984) also addressed the Paleogene northward

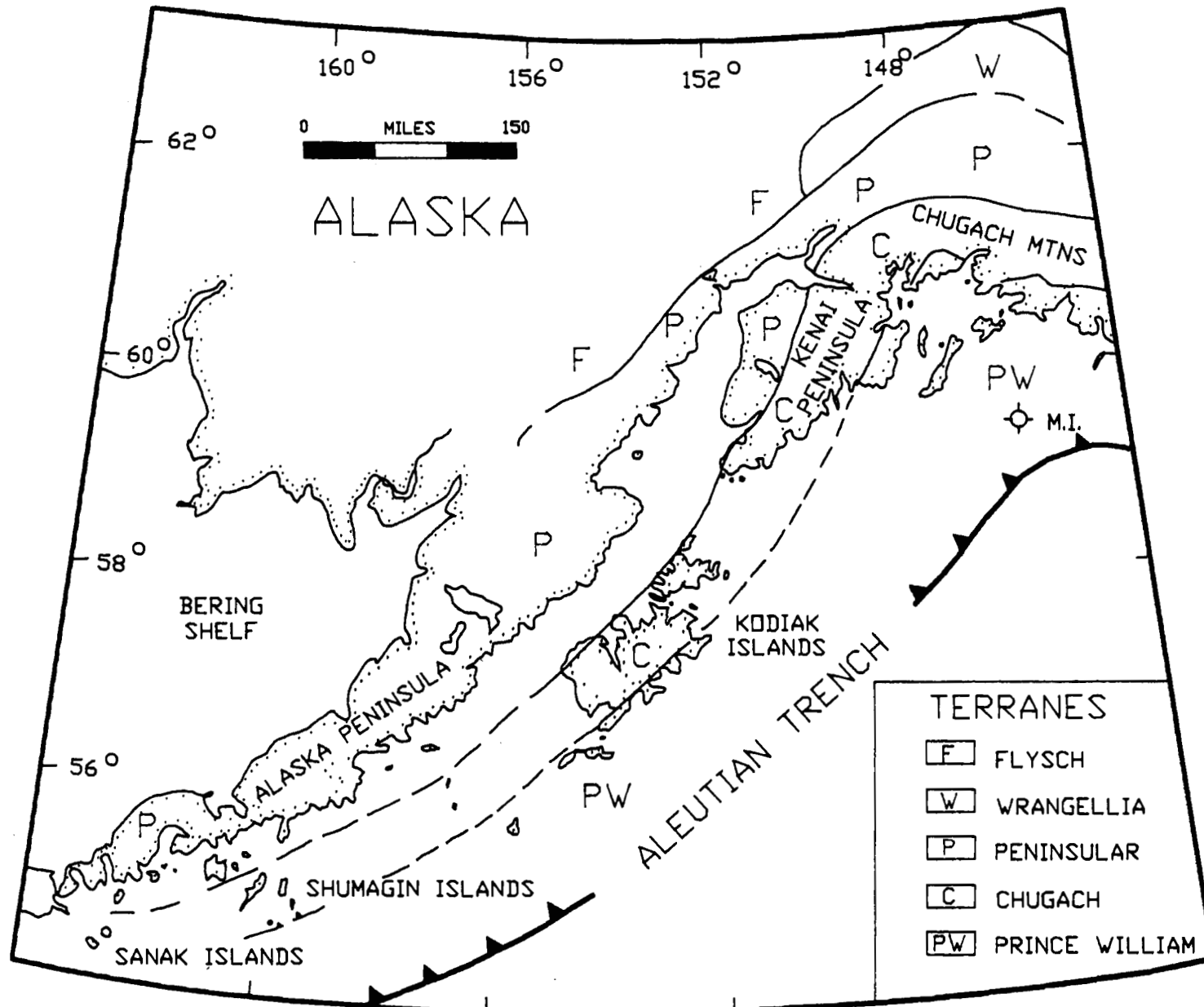


Figure 59. Tectonostratigraphic terranes underlying southwestern Alaska (after Jones and others, 1981). The location of the Tenneco Middleton Island State No. 1 well is also shown.

motion of the Prince William terrane. Those investigators compared microfossil assemblages sampled in the Middleton Island well (fig. 59) with marine sequences exposed onshore in California, Oregon, and Washington and with the present distribution of planktonic faunal provinces in order to determine the paleolatitude of the Prince William terrane at the time of deposition of those microfossils. On the basis of that evaluation, those investigators postulated that the Prince William terrane reached its present position somewhat later, during late middle Eocene time (40 to 42 Ma). Unconformably overlying the Prince William terrane is the Neogene stratigraphic sequence which was deposited in its present location following the accretion of the Prince William terrane.

The Chugach terrane, the more landward of the two terranes underlying the Kodiak shelf, is composed of two subterranes: a strongly folded but coherent turbidite sequence of Late Cretaceous age, and a melange unit of mid-Late Cretaceous age (Plafker and others, 1977; Nilsen and Moore, 1979). These two southwest-northeast-trending subterranes are juxtaposed along the Uganik thrust fault. On Kodiak Island, the turbidite sequence, the more extensive of the two subterranes, was designated the Kodiak Formation by Moore (1969). This turbidite sequence is one component of an extensive turbidite terrane that extends across most of southern Alaska and elsewhere comprises the Shumagin Formation (Moore, 1974), the Valdez Group (Clark, 1972, 1973), the Yakutat Group (Plafker and others, 1976), and the Sitka Graywacke (Loney and others, 1975). Moore (1972) postulated that this extensive turbidite terrane was deposited in an oceanic trench along the continental margin of Alaska during Cretaceous time. The second subterrane, the melange, was originally designated the Uyak Formation by Moore (1969), but was later modified to the Uyak Complex by Connelly (1978) because of its highly complicated internal structure. The melange is a disrupted polymictic assemblage of basic volcanic rocks, chert, ultramafics, limestone, and plutonic rocks in a cherty and tuffaceous argillite matrix. Plafker and others (1977) informally correlated the melange with similar rocks of Cretaceous age exposed further east along southern Alaska which previously had been designated the Chugach terrane by Berg and others (1972). Connelly (1978) proposed that the Uyak Complex on Kodiak Island is correlative with the McHugh Complex on the Kenai Peninsula to the northeast (Clark, 1973; Moore and Connelly, 1976) on the basis of similarities in lithology, style of deformation, degree of metamorphism, and tectonic setting. He suggested that the Uyak-McHugh Complex melange subterrane represents a subduction complex emplaced sometime after mid-Early Cretaceous time.

Underlying the abyssal north Pacific sea floor immediately south of the Kodiak shelf and the Aleutian Trench lies a submarine fan complex of late Eocene through at least early Oligocene and possibly late Oligocene age (Stevenson and others, 1983). This fan complex, the Zodiac fan, occupies an area of sea floor equivalent to roughly seven-tenths of the land area of the state of Alaska. With average and maximum thicknesses of 800 and 5,000 feet, respectively, and a total sediment volume of approximately 64,000 cubic miles, the Zodiac

fan represents a significant depositional artifact of the history of the interaction between the Pacific and the North American plates. On the basis of an evaluation of the sedimentologic characteristics of the fan, Stewart (1976) interpreted that the constituent turbidite sands represent the first-order products of the erosion of a plutonic terrane. He also interpreted, on the basis of the uniform composition of the constituent sand grains, that the fan was derived from the same source terrane for its entire depositional history, which spanned nearly 20 million years. On the basis of similarities in the mineralogy of the framework grains, he proposed that the Sitkinak and Sitkalidak Formations represent the proximal equivalents of the distal turbidite sands that make up the fan, and, accordingly, that the Zodiac fan was deposited in roughly its present location with little or modest relative motion having occurred between the Pacific and North American plates.

Stevenson and others (1983) presented a somewhat different interpretation of the origin and tectonic significance of the Zodiac fan. Those investigators critiqued other models of Tertiary plate motion formulated on the basis of world-wide magnetic anomalies, hot-spot tracks, paleomagnetic data, and the displacement of equatorial sedimentation patterns in light of new constraints on plate motion derived from the fan. In the earlier models, the deposition site of the Zodiac fan would have been 900 to 1,800 miles from the nearest terrigenous sediment source which seemed unlikely in terms of the morphology and sediment texture of the fan. Contrary to those models, which also required large amounts of convergence between the Pacific and North American plates along the Aleutian Trench, Stevenson and others (1983) proposed that the source of the Zodiac fan sediments was a large, proximal, northward-drifting landmass which moved in concert with the Zodiac fan deposition site. This geometry eliminated the awkward interpretation that required turbidity currents to transport sediments many hundreds of miles. On the basis of paleomagnetic data, those investigators suggested that the landmass that acted as the source terrane now underlies the Alaska Peninsula and parts of southern Alaska. Thus, their model allowed for a both a proximal northern source terrane and a short sediment transport distance.

In a more recent study, von Huene and others (1985) argued that the Zodiac fan could not have been sourced from the previously mobile landmass that now forms parts of southern Alaska because that region, the Prince William terrane, had already been accreted to nuclear Alaska by middle Eocene time. Alternatively, they proposed that the Zodiac fan was probably derived from somewhere in the vicinity of present-day Washington State or British Columbia. In his study of a possible provenance for the Zodiac fan turbidites, Stewart (1976) determined that although the coeval rocks exposed in western Washington and Oregon and on Vancouver Island were derived from volcanic terrane, which makes them unlikely equivalents of the fan, the plutonic rocks of British Columbia made ideal candidates for the parent rocks of the fan. In order to provide a conduit to shunt sediments from that source region to the deposition site of the fan, von Huene and others (1985) invoked the allochthonous Yakutat block

which is presently undergoing accretion to the southern Alaskan plate margin. It is safe to say at this juncture that no proposed model satisfies all of the constraints currently judged significant by various researchers. However, some data from the Kodiak shelf wells, while neither collected nor analyzed for the purpose of evaluating plate tectonics models, may shed some light on the problem (see Lithologic Summary and Biostratigraphy chapters, particularly reworked elements in the KSST No. 1 well and Eocene environments in the KSSD wells).

SUMMARY

The Kodiak shelf is underlain by two principal seismic sequences representing a basement complex and the overlying shelf sediments. The basement complex is composed of a pair of juxtaposed, allochthonous, tectonostratigraphic terranes, whereas the overlying Neogene shelfal sediments were deposited in situ. The more seaward of the two allochthonous terranes, the Prince William terrane, may have originated as far as 25 degrees farther south than its present position and was emplaced by late Eocene time. The unconformity that separates the two seismic sequences formed prior to middle or possibly early Miocene time and may truncate an older unconformity exposed on Kodiak and the neighboring islands. Two areally extensive seismic horizons are present within the upper seismic sequence. The older horizon may represent a significant early Pleistocene oceanographic event associated with the advance of continental glaciers across the shelf. The younger horizon corresponds to the base of a Pleistocene glaciomarine shelf sequence.

6. WELL LOG INTERPRETATION

Wireline well log data from the six Kodiak shelf COST wells were interpreted to determine the lithology, reservoir characteristics, and stratigraphy of the sedimentary rocks that underlie the Kodiak shelf. The petrophysical logs were supplemented by sidewall and conventional core data, and descriptions of rock cuttings from drilling mud logs. Wireline log traces fundamental to stratigraphic and petrophysical interpretations were manually digitized at 0.5-foot increments on magnetic tapes to allow processing by computer. Reduced-scale plots of the principal wireline log traces, a stratigraphic column, and a summary chart of geologic data from cores and rock cuttings of each well are shown on plates 1 to 7. Each Kodiak COST well is discussed in the order in which the well was drilled. Stratigraphic interpretations in this chapter are based on an integration of the well log analysis with micropaleontologic, petrographic, and petrophysical analyses of cores and drill cuttings that are discussed in other chapters of this report. Depths given are measured depths below kelly bushing unless specified otherwise.

The stratigraphic section penetrated by the three shallow Kodiak COST wells (KSST Nos. 1, 2, and 4a) consists of relatively undeformed Plio-Pleistocene glaciomarine sediments that mantle the Kodiak shelf. The three deep COST wells (KSSD Nos. 1, 2, and 3) penetrated Miocene and Eocene sedimentary rocks, in addition to the Plio-Pleistocene strata. The Plio-Pleistocene and Miocene sections are composed of the acoustically resolvable strata that fill the forearc basins of the Kodiak shelf. Eocene strata are structurally deformed. Dipmeter logs of the KSSD wells indicate that the Eocene strata dip steeply (15 degrees to nearly vertical), and in two of the wells are apparently folded and faulted. No strata of Oligocene age were penetrated by the Kodiak COST wells. Lower to middle Miocene strata rest with angular unconformity on underlying upper Eocene strata in the three KSSD COST wells.

The Plio-Pleistocene and Miocene section is made up of clastic marine sediments that were deposited in neritic to bathyal depths. The predominant lithology in all but the KSSD No. 3 and nearby KSST No. 2 wells is silty mudstone to muddy siltstone that characteristically contains matrix-supported pebbles of igneous and metamorphic origin. In the KSSD No. 3 and KSST No. 2 wells, substantial sections of sandstone and conglomerate that are interpreted to represent shallow marine shelf and deep-sea fan

deposits are present. The bulk of the Plio-Pleistocene sediment, and perhaps the Miocene sediment as well, appears to represent glacial detritus that has been reworked by marine processes, although airborne volcanic ejecta and erosion of sedimentary bedrock from submarine outcrops along submarine structural highs probably also supplied significant amounts of sediment. The Plio-Pleistocene to Miocene section is largely equivalent in age to the shallow marine shelf strata of the Tugidak (late Pliocene to Pleistocene) and Narrow Cape (lower and middle Miocene) Formations that crop out on Tugidak and Chirikof Islands (Moore, 1969). The bathyal strata of the Neogene section on the Kodiak shelf probably represent deep-water facies equivalents of the Tugidak and Narrow Cape Formations.

The Paleogene section penetrated by the KSSD wells consists of structurally deformed Eocene strata. These rocks consist of shale, siltstone, and sandstone that are highly indurated except where overpressured conditions exist (see Abnormal Formation Pressure chapter). Coeval strata that are exposed on Kodiak, Sitkalidak, and Sitkinak Islands are represented by the Sitkalidak Formation (Moore, 1969). The strata of the Sitkalidak Formation are believed to represent deep-sea turbidite deposits on the basis of lithofacies (Nilsen and Moore, 1979; von Huene and others, 1980a), although microfossil assemblages suggest shallower neritic environments (von Huene and others, 1980a). Microfossil assemblages from the Eocene strata in the KSSD wells are also somewhat ambiguous as to depositional environments, but on the basis of their relative seaward stratigraphic position from exposures of the deep-sea fan facies of the Sitkalidak Formation, these structurally deformed strata probably also represent deep-sea deposits.

KSSD NO. 1 WELL

The KSSD No. 1 well was located adjacent to the southwestern edge of Albatross basin, along the steep northern flank of Albatross Bank. The well was drilled to a total depth of 4,225 feet and penetrated Pleistocene to late Pliocene clastic sediments that are coeval with the Tugidak Formation which is exposed on Tugidak Island approximately 55 miles to the northwest. Albatross Bank is the most tectonically active area of the Kodiak shelf, and as much as 3 kilometers of uplift (9,800 feet) may have occurred since the late Miocene or Pliocene (Fisher and von Huene, 1980; McClellan and others, 1980). The strata at the well site have been structurally tilted to the northwest by the uplift of Albatross Bank and dip steeply toward the deepest part of Albatross basin. The dipmeter log indicates that structural dip magnitudes average about 25 to 35 degrees, with dip directions generally between north 20 degrees west and north 30 degrees west.

Mudstone was the predominant lithology encountered in the KSSD No. 1 well (pl. 1). Most of the sidewall cores recovered were described as mudstone or silty mudstone, and the drill cuttings consisted predominantly of clay- and silt-sized sediment. Scattered granule- to pebble-sized fragments of metamorphic and volcanic rocks

were noted in the mudstones throughout most of the well and probably reflect ice-rafting and other glacial processes. The spontaneous potential (SP) and gamma ray logs were relatively inactive and displayed responses at or near shale baseline values over most of the well. The Dual Induction Laterolog (DIL) recorded low resistivities characteristic of shales or shaly siltstones and sandstones and displayed little or no separation between the shallow- and deep-investigation resistivity curves, indicating lithologies too impermeable to allow invasion of the drilling mud filtrate into the formation. Stratigraphic intervals containing higher contents of sand and silt, such as that shown between 1,250 and 1865 feet on the lithologic column of plate 1, were identified on the logs on the basis of slightly higher resistivities, slightly lower gamma ray values, and increases in sand and silt content recorded in the drilling mud log. The neutron-density porosity curves display smaller separation in these intervals, which may also indicate higher contents of sand. However, the neutron-density log curves also exhibit large and somewhat erratic swings in these intervals (pl. 1), which, in combination with the rough and enlarged borehole conditions indicated by the caliper log, suggests that some of the neutron-density log data may be invalid.

The only substantial interval of permeable sandstone in the KSST No. 1 well was encountered at the top of the logged interval between 318 and 395 feet in strata of probable middle to late Pleistocene age. Three sidewall cores from this interval exhibited porosity ranging from 28.8 to 30.8 percent and permeability ranging from 62 to 170 millidarcies (Core Laboratories, Inc., 1976a). Porosity calculated from the density log in this interval ranges from 16 to 26 percent, but neutron porosity values are higher, generally about 36 percent, because of shaliness. The modest permeability obtained from the sidewall cores in a sandstone as shaly as this is probably a result of shallow burial and only slight compaction. Deeper in the well, below 400 feet, only a few sidewall cores recovered very fine- to fine-grained, silty sandstone. Porosity and permeability measured from sidewall cores taken from these more deeply buried sands ranged from 18.6 to 24.8 percent and 11 to 41 millidarcies (Core Laboratories, Inc., 1976a). The SP and gamma ray logs of these deeper sandstone intervals display little difference in response from that of adjacent mudstone intervals and indicate that, overall, the intervals are probably too thin, shaly, and impermeable to represent reservoir rock.

KSST NO. 2 WELL

The KSST No. 2 well was located about 55 miles northeast of the KSST No. 1 well, near the southwestern end of the Dangerous Cape high, a positive structural feature that separates Albatross and Stevenson basins. The Dangerous Cape high contains a relatively thin section of seismically resolvable strata. The KSST No. 2 well was drilled to a total depth of 4,307 feet and penetrated clastic sediments of Pleistocene to late Pliocene age that are coeval with strata of the Tugidak Formation which crops out about 105 miles to

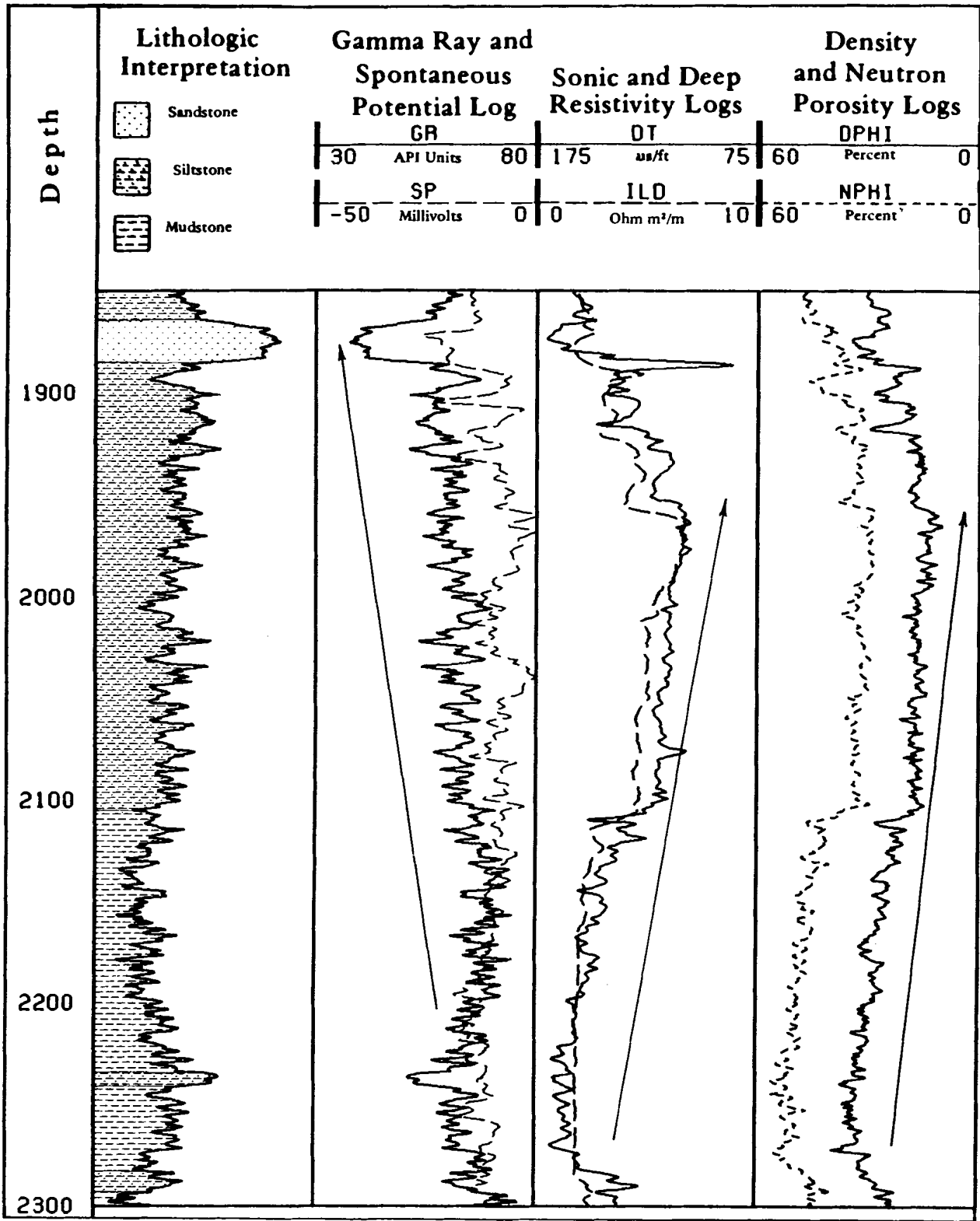


Figure 60. LITHOLOGY AND WIRELINE LOG RESPONSES FROM A PROGRADATIONAL SEDIMENTARY SEQUENCE IN THE KSST NO. 2 WELL. Arrows illustrate the overall log trends which display funnel-shaped patterns indicative of an upward-coarsening grain-size profile.

the southwest on Tugidak Island. The KSST No. 2 well was located in a saddle on the northeastern side of a small basin in an area of possible wedge-out of shallow horizons.

The sedimentary section penetrated by the well consisted of interbedded mudstone, siltstone, and sandstone to a depth of 3,100 feet, and dominantly mudstone from 3,100 feet to total depth (pl. 2). Microfossils from the sandier section above 3,100 feet indicate deposition in environments ranging from upper bathyal to inner neritic. Microfossils from the mudstone section below 3,100 feet indicate deposition mainly in upper bathyal environments. Sidewall cores from the sandier section above 3,100 feet recovered silty to sandy, pebbly mudstone, pebbly siltstone, and very fine- to fine-grained, silty, pebbly sandstone. The mud logger's description characterized the gravel-sized fraction of the sediment from the sandy section of the well as subangular to well-rounded, granule- to pebble-sized igneous and metamorphic rock fragments. Sidewall cores from the mudstone section below 3,100 feet mainly recovered silty, mottled mudstone.

The wireline logs in the KSST No. 2 well display a succession of funnel-shaped patterns which indicate that many of the strata were deposited as coarsening-upward progradational sequences (fig. 60). The funnel-shaped log patterns are most pronounced on the resistivity, sonic, density, and neutron-density logs (pl. 2, fig. 60). The coarsening-upward cycles indicated by the funnel-shaped log patterns vary in thickness from 20 to as much as 400 feet, but are generally over 50 feet thick.

Each of the vertical, coarsening-upward cycles represented by the funnel-shaped log patterns is interpreted as a sequence of strata deposited in environments of progressively higher energy. In the nearby KSSD No. 3 well, similar upward-coarsening sequences are inferred to represent submarine fan deposits because of the deep-water microfossils they contain and the similarities in the log and dipmeter patterns to those of documented submarine fan deposits (see discussion of the KSSD No. 3 well in this chapter). However, in this well, the microfossils indicate a wide range in paleobathymetry from shallow to deep marine. Consequently, a submarine fan origin for the upward-coarsening sequences of this well is uncertain. The wide range in paleobathymetry indicated by the microfossils could be a result of shallow water organisms being swept into deeper water by turbidity currents, or a result of large sea-level changes. Most of these progradational sequences are Pleistocene in age, so it is certain that large-scale glacioeustatic fluctuations did occur during their deposition. Therefore, it seems probable that these strata contain both shallow shelf and deep-marine deposits.

The tops of the progradational sequences are generally capped by sandstone beds which in several sections of the well attain significant thickness and have fair porosity and permeability. Porous sandstones, such as in the interval from 2,580 to 2,600 feet (pl. 2), are indicated on the logs by large negative SP deflections

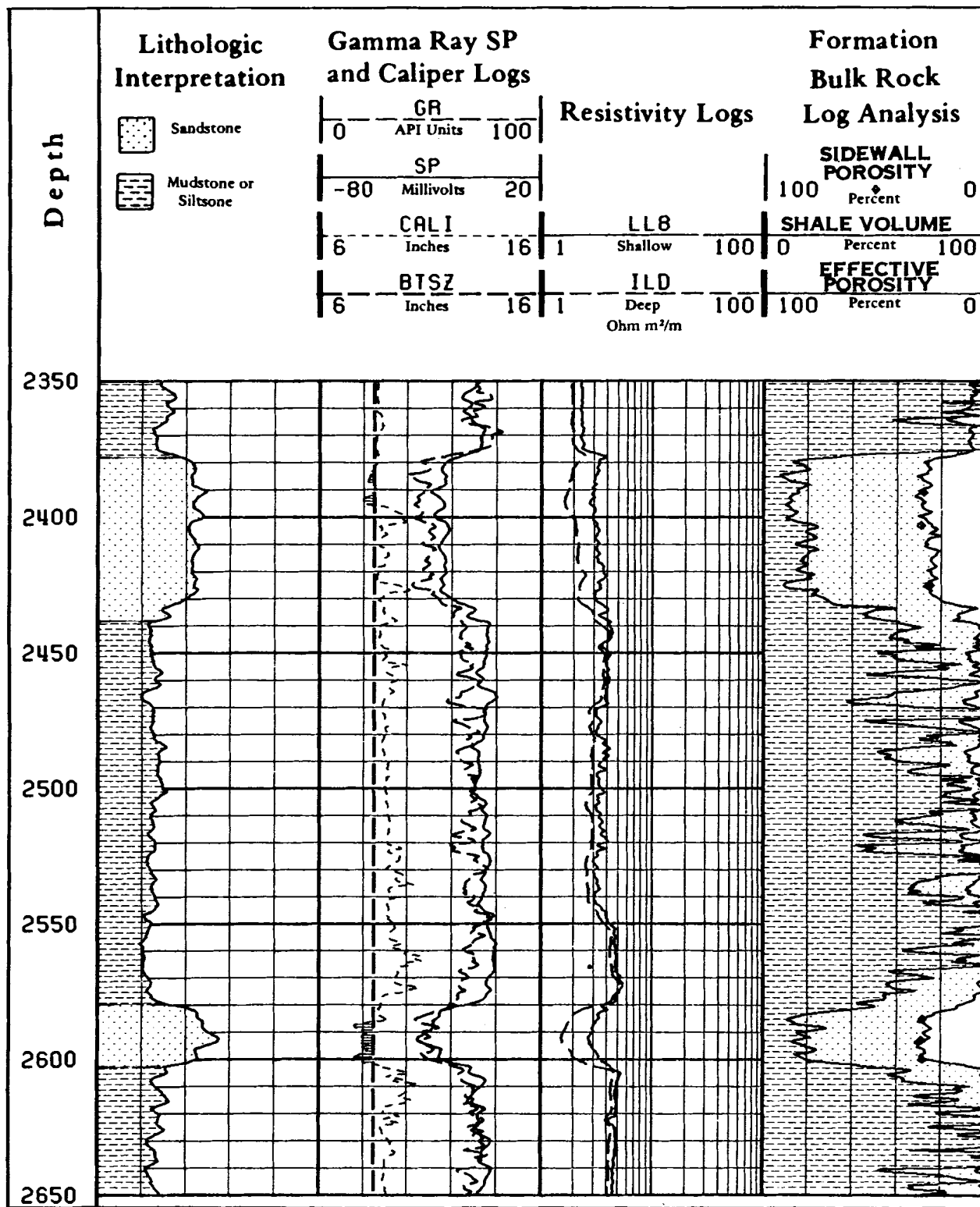


Figure 61. WIRELINE LOG RESPONSES AND FORMATION ANALYSIS OF SANDSTONE IN THE KSST NO. 2 WELL. Permeable sandstones are indicated by SP log deflections, resistivity curve separations, and the presence of mudcake (shaded areas between the caliper curve and bitsize trace). Shale volume in the formation analysis derived from the gamma ray log and effective porosity from the density log. Sidewall core porosity from Core Laboratories Inc., 1976b.

coupled with deflections toward low values of resistivity, sonic velocity, and density.

Sandstone beds over 5 feet thick that showed indications of permeability on the DIL log as manifested by resistivity curve separations (mud-filtrate invasion) and by SP curve deflections were analyzed for reservoir potential. Because these sandstones contain varying amounts of clay and silt, the recorded log porosity required correction for shale effects. Sandstone shaliness was evaluated using the gamma ray log as a clay indicator. Endmember log responses for clean sandstone and clay shale were estimated from the total range of the gamma ray log in the well. An index of sandstone shaliness was then obtained for each sandstone from the value of the gamma ray log response relative to the endmember responses. The respective endmember gamma ray log values used for clean sandstone and clay shale in this well were 38 and 70 API units. A nonlinear, empirically based relationship that is characteristic of Tertiary sedimentary rocks (Dresser Atlas, 1979; Asquith and Gibson, 1982) was assumed between the endmember values and the interpreted shale volume:

$$V_{sh} = 0.083x[2\exp(3.7xIGR)-1]$$

where: V_{sh} = shale volume
IGR = gamma ray index or relative position between endpoints
exp = exponent

An effective porosity was then calculated by correcting the total porosity recorded by the density log for the shale volume (Dresser Atlas, 1979):

$$PHI_e = [(RH_{Oma}-RH_{Ob})/(RH_{Oma}-RH_{Of})] - V_{sh}[(RH_{Oma}-RH_{Osh})/(RH_{Oma}-RH_{Of})]$$

where: V_{sh} = shale volume
 PHI_e = effective porosity
 RH_{Oma} = matrix density of formation
 RH_{Ob} = bulk density of formation
 RH_{Of} = fluid density
 RH_{Osh} = bulk density of shale

The results of this log interpretation method for two sandstone beds that occur in the interval between 2,350 and 2,650 feet (pl. 2) are displayed graphically on figure 61. Both beds show indications of permeability on the logs. Invasion of the sandstones by drilling mud filtrate is indicated by the separation of the deep (ILD) and shallow (LL8) resistivity curves and by the mudcake development that is signaled by the smaller value of the caliper curve (CALI) relative to that of the bitsize trace. The presence of SP curve deflections opposite the sandstones also indicates permeability. Six sidewall cores from the two sandstone beds were described as very fine- to fine-grained and silty, with measured permeabilities ranging from 15 to 157 millidarcies (Core Laboratories, Inc., 1976b). Sandstone

porosity obtained from both logs and cores ranges between about 25 and 30 percent (fig. 61).

A tabulation of the results of the log interpretation of sandstone reservoir potential in the well are shown in table 5 (p. 135). The KSST No. 2 well contained a total of 276 feet of sandstone in beds ranging from 6 to 83 feet thick. Of this total, the net thickness of sandstone that contains less than 40 percent shale and at least 10 percent effective porosity accounts for 221 feet. Over half of the total sandstone was contained in two beds between 60 and 83 feet thick.

Although the total porosity of the sandstones in table 5 (p. 135) is high, over 30 percent, the logs and cores indicate that the sandstones are silty and shaly. The shale content calculated from the logs averages 24 percent. Because of this shale content, as much as a quarter of the total porosity consists of ineffective microporosity contained in the intergranular shale matrix. Effective porosity calculated from the logs averages only about 23 percent (table 5). Because of the silty, fine-grained character of these sandstones, a significant fraction of the effective porosity is probably distributed in small silt-sized pores, and the permeability is generally low to moderate. Permeability derived from the logs averages about 12 millidarcies, and measurements from the sidewall cores average about 49 millidarcies (table 5). Measurements of permeability from sidewall cores tend to be too high because the sidewall-coring process tends to fracture and disrupt the rock fabric and thereby increase permeability. Because no conventional core data were available to calibrate these log-derived permeabilities, they should be considered only as a qualitative index of permeability.

The sandstones of this well appear to possess low to moderate reservoir potential because of the small pore size of the sandstones. Sandstones in which the porosity consists mainly of microporosity make poor reservoirs because they typically have low permeability and high irreducible water saturations, and only a small fraction of the in situ hydrocarbon can be recovered.

KSST NO. 4A WELL

The KSST No. 4A well was located on the southwestern flank of Portlock Anticline, which separates Stevenson basin into two subbasins. The well was drilled to a depth of 1,391 feet and penetrated Pleistocene and late Pliocene strata along the northern margin of the southwestern subbasin of Stevenson basin. The strata in the KSST No. 4A well, like those of the other two KSST wells, are coeval with the Tugidak Formation on Tugidak Island, which lies southwest of Kodiak Island. The sediment that fills the southwestern subbasin apparently came from high-standing areas of the Dangerous Cape high, because seismic reflectors indicate that, regionally, strata dip in a landward direction (von Huene and others, 1980a, p. 25). The structural dip at the KSST No. 4A well site is difficult to interpret because plots of dips from the dipmeter log exhibit

considerable scatter in magnitude (1 to 40+ degrees) and direction, but overall most dip directions are to the south.

The sedimentary section sampled by the KSST No. 4A well was primarily mudstone (pl. 3). All of the sidewall cores from the well recovered mudstone lithologies. Most of the mudstone samples were described as silty to sandy, with occasional pebble-sized rock fragments. The drilling mud log recorded significant amounts of granule- to pebble-sized rock fragments throughout the well except in the interval from 950 to 1,040 feet. This pebble-free mudstone interval is manifested on the wireline logs by low resistivity, longer sonic interval transit times, lower density, and higher neutron-density porosities (pl. 3). On the logs, the base of this pebble-free mudstone section appears as a sharp contact, but the upper contact is gradational with the overlying pebbly mudstone section, and together these two sections form a coarsening-upward sequence (1,040 to 480 feet, pl. 3). The underlying section of the well appears to be the upper part of a similar sequence.

The log patterns of these two coarsening-upward mudstone sequences are similar to those interpreted as progradational sequences in the KSST No. 2 well. The microfossil data display two distinct regressive patterns (pl. 3) that approximately coincide with the upward-coarsening sequences. The microfossil assemblage indicates upward-shoaling deposition in water depths ranging from upper bathyal to middle neritic (see Biostratigraphy chapter). The paleobathymetry suggests that these sequences probably represent outer shelf, slope, and basinal deposits. If these deposits are chiefly slope facies, then disrupted bedding characteristic of syndepositional deformation may account for the random, widely scattered dips obtained from the dipmeter log.

The SP and gamma ray logs are relatively featureless through the well, and the shallow- and deep-investigation resistivity curves display little separation, which indicates that no permeable intervals are present. Because no sandstones were recovered by the sidewall cores, no porosity and permeability measurements were conducted on sidewall samples from the well.

KSSD NO. 1 WELL

The KSSD No. 1 well was located approximately 16 miles southwest of the KSST No. 4A well, on the western margin of the southwestern Stevenson subbasin. The well was drilled to a depth of 8,517 feet and encountered deep-water marine, clastic sediments ranging from Pleistocene to Eocene in age. The sedimentary section penetrated by the well consists of a Quaternary and Neogene section separated from a Paleogene section by an angular unconformity at 6,142 feet. The Quaternary to Neogene section (Pleistocene to Miocene) is composed of relatively undeformed basin-fill that represents the acoustically resolvable strata of Stevenson basin. The dipmeter log indicates that the structural dip of the Quaternary and Neogene strata at the well site is generally 5 to 15 degrees to the northwest or west. The

Paleogene section contains structurally deformed Eocene strata that floor the Stevenson basin. The dipmeter log indicates that at the well site the Eocene strata are steeply dipping (generally 50 to 80 degrees) and may be faulted at several depths.

Quaternary and Neogene Strata

The Quaternary and Neogene section of the KSSD No. 1 well can be subdivided into three zones of differing lithofacies, depositional environments, and wireline log responses. The upper zone consists of coarse-grained, glaciomarine shelf and slope deposits; the lower two zones of fine-grained, deep-water marine, basinal deposits.

The uppermost zone includes the interval from 1,670 feet (depth of first sample) to 2,338 feet and includes middle to late Pleistocene strata (pl. 4). These strata are composed of calcareous, silty mudstones, muddy siltstones, silty, pebbly sandstones, and sandy, pebble conglomerates that were deposited in middle neritic to upper bathyal water depths. The wireline logs suggest that the mudstones at the base of the upper zone are in sharp contact with those of the underlying zone. The sonic, resistivity, density, and neutron logs all display marked changes (pl. 4) that indicate an increase in density and hardness, probably as a result of higher contents of silt and calcite cement. The sandstones and conglomerates above 2,020 feet represent the only porous and permeable intervals in the KSSD No. 1 well. The gamma ray and SP logs of these coarser grained intervals display funnel-shaped profiles (pl. 4) that are indicative of upward-coarsening progradational sequences. The log profiles of these sandstones and conglomerates are similar to those displayed in the KSST No. 2 well and probably reflect similar depositional environments. Both the coarsening-upward lithology and shoaling-upward paleobathymetry (pl. 4) of this zone reflect an overall regressive depositional pattern.

The middle zone spans the interval from 2,338 to 3,968 feet and contains strata of Pleistocene and Pliocene age. This zone is composed predominantly of mudstone deposited in middle to lower bathyal water depths (pl. 4). Mudstones recovered in sidewall cores and drill cuttings were described as slightly silty to nonsilty clays that were generally noncalcareous. The wireline logs are relatively inactive through the zone and display responses indicative of shale or shaly lithologies (pl. 4). The base of the zone was picked at a subtle log break that approximately coincides with a shoaling of paleobathymetry at 3,980 feet (pl. 4). The log break is characterized by slight decreases in resistivity, sonic velocity (interval transit time), and formation density relative to the underlying zone. The small shift in the petrophysical properties of the mudstone may be a result of slight lithologic and diagenetic changes related to the change in depositional environment. The log break might also record a depositional hiatus or disconformity.

The basal zone of the Quaternary to Neogene basin-fill spans the interval from 3,968 to 6,142 feet and includes strata of Miocene and

early Pliocene age (pl. 4). The strata of this zone are composed predominantly of mudstone deposited in upper to middle bathyal water depths (pl. 4). The lower two-thirds of the zone, below about 4,600 feet, appears to contain interbeds of muddy sandstone or siltstone. The SP log displays small deflections in this zone that are not apparent in the overlying logged interval (pl. 4). Although this suggests that the lower zone is sandier, the higher activity of the SP log in the lower zone is probably largely a result of the lower salinity mud used in drilling the well below 4,600 feet. The resulting greater resistivity contrast between the drilling-mud filtrate and formation water in the second logging run has resulted in better lithologic definition over most of the lower zone of the Neogene section.

Another difference in log response between the two logging runs is apparent on the BHC sonic log (DT curve) in the lower zone (pl. 4). The DT curve is offset an average of 15 to 20 microseconds per foot slower below 4,600 feet. The borehole was larger when the second logging run was made, and the offset of the BHC sonic log is a result of borehole condition and size. The long-spaced sonic (LSS) log, which sees deeper into the formation and is less affected by near-borehole formation condition, was not offset. An increase in the compaction gradient is evident on the sonic and density logs below about 5,300 feet (pl. 4) in the lower zone (see Abnormal Formation Pressure chapter). This steeper compaction gradient may be a result of a disconformity. The basin-fill of the southwestern Stevenson subbasin is reported by von Huene and others (1980a, p. 25) and Hoose and others (1984, p. 19) to be separated into two sequences by a channel-like unconformable reflection on seismic profiles. Perhaps the change in compaction gradient in this zone is the result of this unconformity.

Two conventional cores cut from the interval 5,750 to 5,824 feet contained interbeds of very fine grained, silty, and shaly sandstone (Core Laboratories, Inc., 1977a). These fine-grained muddy sandstones probably represent distal turbidite deposits. Porosity and permeability measured from core samples of these sandstones indicate that they have poor reservoir potential. Porosity from three conventional core samples ranged from 13.7 to 15.5 percent, but permeability was only 0.79 to 8.4 millidarcies and may have been increased by fractures (Core Laboratories, Inc., 1977a). This low permeability indicates that the pore spaces are probably constricted by intergranular shale and silt.

The only Quaternary to Neogene sandstones in the KSSD No. 1 well with sufficient thickness, porosity, and permeability to have any reservoir potential occur in the Pleistocene glaciomarine section of the upper zone. However, these shallow strata are probably not prospective for hydrocarbon accumulations because they are thermally immature and lack sealing horizons.

Paleogene Strata

The boundary between the Quaternary to Neogene and the Paleogene sections is an angular unconformity. The unconformity is at 6,142 feet and is indicated on the dipmeter log by large shifts in dip magnitude and direction. Lower to middle Miocene strata just above the unconformity dip 7 to 15 degrees northeast; Eocene strata below the unconformity dip 50 to 70 degrees northwest. Large shifts on the resistivity, sonic, density, and neutron logs are also evident at the unconformity (pl. 4). The high resistivity, density, and sonic velocity recorded in Eocene strata below the unconformity indicate that these sedimentary rocks are highly indurated. Abrupt changes in dip direction or magnitude recorded by the dipmeter log at 7,000, 7,780, and 8,100 feet indicate that faulting and folding occur within the Eocene section of the well.

The Eocene section consists mainly of siltstone and shale with minor amounts of silty, shaly, very fine grained sandstone. Sandstone samples from three conventional cores possessed low porosity and permeability; porosity ranged from 0.1 to 6.6 percent and permeability was generally 0.5 millidarcy or less (Core Laboratories, Inc., 1977a). The wireline logs display no indications of porosity and permeability in the Eocene sandstones.

Microfossil data indicate that the Eocene strata are marine and probably bathyal. Coeval strata of the Sitkalidak Formation exposed on Kodiak, Sitkalidak, and Sitkinak Islands are interpreted as deep-water marine turbidite deposits (Nilsen and Moore, 1979), and the Eocene strata of the KSSD No. 1 well probably represent similar, if not deeper water, depositional environments.

KSSD NO. 2 WELL

The KSSD No. 2 well was located on the northeastern flank of the northern Stevenson subbasin, approximately 70 miles northeast of the of the KSSD No. 1 well and 55 miles northeast of the KSST No. 4A well. The KSSD No. 2 well was drilled to a depth of 10,460 feet and penetrated a deep-water marine, clastic sedimentary section ranging from Pleistocene to Eocene in age. The section penetrated by the well consists of two sections separated by an unconformity at 8,774 feet. The upper, Quaternary to Neogene, section contains strata ranging from Pleistocene to Miocene in age (pl. 5). This section contains the relatively undeformed, acoustically resolvable basin-fill of Stevenson basin. Dip plots from the dipmeter log, although somewhat erratic, indicate that the structural dip of this upper section is generally 3 to 5 degrees to the northeast. The lower, Paleogene, section contains Eocene strata that dip between 15 and 30 degrees to the northwest.

Quaternary to Neogene Strata

The Quaternary to Neogene section in the KSSD No. 2 well is predominantly composed of mudstone that was deposited in deep-water

marine environments. Microfossil assemblages indicate three general paleobathymetric zones are present (1,470 to 3,090 feet, 3,090 to 7,368 feet, and 7,368 to 8,774 feet, pl. 5) that record the gradual shoaling of depositional environments from lower bathyal to outer neritic depths as the basin was progressively filled.

Late Pleistocene strata from about 1,470 to 2,070 feet were deposited chiefly in outer neritic depositional environments and contain the coarsest grained sediment of any strata observed in the well. Drill cuttings from this interval contained over 50 percent sand and gravel, but the sidewall cores recovered were mainly sandy siltstones and shales that contained occasional-to-common pebbles composed of varied igneous, metamorphic, and sedimentary rock fragments. The remainder of the lithologically similar Pleistocene strata (from 2,070 to 3,090 feet) represent outer neritic to upper bathyal depositional environments and contain lower pebble contents. Wireline log and core data suggest that the lithology of this zone probably consists of sandy, pebbly mudstone and siltstone. No sandstone or conglomerate beds are indicated by deflections on the SP or gamma ray logs. However, the SP log response was suppressed in the upper part of the well (above 4,420 feet, pl. 5) because of the higher relative salinity of the drilling mud used in that interval. Therefore, the siltstone and thin sandstone interbeds indicated by the SP log lower in the well may also be present in the upper zone.

The section between 3,090 and 7,360 feet represents upper bathyal deposits ranging from Pleistocene to Miocene in age (pl. 5). The sidewall cores and drill-cuttings log indicate that the sand content of the mudstones and siltstones gradually diminishes downward in this zone. The SP log provides better definition of lithology below 4,420 feet and displays frequent low-amplitude, negative deflections and occasional thin, high-amplitude deflections (pl. 5), a pattern which indicates interbeds of siltstone or shaly sandstone and occasional thin interbeds of sandstone or conglomerate. The gamma ray log response through most of these intervals differs little from that of adjacent mudstone or shale intervals, which indicates that the sandstone and siltstone interbeds have high clay contents. The siltstones and sandstones probably represent turbidite deposits. Below 6,500 feet, the strata of this zone are overpressured (see Abnormal Formation Pressure chapter).

The lower to middle Miocene strata between 7,360 and 8,774 feet are middle to lower bathyal deposits that represent the basal section of the basin-fill. These strata are lithologically similar to the mudstone or shale of the superjacent zone. The gamma ray log records a generally higher radioactivity level, which suggests that these mudstones may be more clay-rich than other strata in the well.

Gas shows were recorded on the drilling mud log from two intervals (7,000 to 7,150 feet and 7,890 to 8,015 feet) in the Neogene section of the well. These shows are probably related to the overpressured condition of the strata below 6,500 feet. The gas from the upper interval consisted entirely of methane, and the gas from the lower interval had very high ratios of methane to other heavier

gas fractions. Wireline logs, sidewall cores, and drill cuttings indicate that the gas shows occurred in intervals that were chiefly shales or claystones. The SP log recorded one or two deflections in each gas show interval, which suggests the presence of thin, 4- to 8-foot-thick, porous, permeable beds. However, sidewall cores recovered only clay, silty clay, and pebbly clay from the intervals displaying these SP deflections. Porosity from the density log ranges from 14 to 20 percent, but if corrected for the high shale content, effective porosity would be very low. It is probable that these zones have little, if any, reservoir potential.

Paleogene Strata

The boundary between the Neogene and Eocene strata is a regional angular unconformity. The dipmeter log indicates that strata just above the unconformity (8,774 feet) dip 5 to 10 degrees east-northeast, and strata just below the unconformity dip about 15 to 25 degrees northwest. In the KSSD No. 1 well, large shifts on the wireline logs (pl. 5) indicate that the strata beneath the unconformity are highly indurated. However, in the KSSD No. 2 well, the rocks below the unconformity are less resistive and dense, and exhibit longer interval transit times on the sonic log (pl. 5) than do younger rocks above the unconformity. These log shifts are the opposite of what normally occurs when logging from older to younger rocks, and are probably a result of the abnormal formation pressures in this section of the well.

Drill cuttings, sidewall cores, and a conventional core (10,274 to 10,923 feet) indicate that these older strata consist primarily of claystone or shale, with secondary amounts of siltstone and very fine grained, silty sandstone. The gamma ray log exhibits a significant shift at the unconformity and records levels of radioactivity that average about 10 API units lower in these older rocks (pl. 5). The lower levels of radioactivity are probably a result of the higher average content of quartz in the claystones or shales of these rocks relative to the overlying younger rocks. X-ray diffraction analysis of claystones from the two conventional cores indicate that the quartz contents average 11 percent higher in the older rocks (Core Laboratories, Inc., 1977b). Below the unconformity, the average separation between the neutron and density porosity logs decreases by about 4 porosity percentage points (pl. 5), which also suggests higher quartz contents in the older claystones.

The only significant sandstone in the Paleogene section occurs just beneath the unconformity between about 8,800 and 8,885 feet (pl. 5). Sidewall cores from this interval recovered silty, very fine- to fine-grained sandstone, but porosity and permeability were not measured. The caliper log indicated that the borehole was caved in this interval and recorded hole sizes generally in excess of 18 inches. Consequently, the large deflections displayed by the gamma ray, sonic, density, and neutron logs (pl. 5) probably do not represent valid data. The gas peak recorded by the drilling mud log in this interval is probably mainly attributable to "trip gas", which characteristically occurs when drilling has resumed after the drill

pipe is pulled from the hole and replaced during the process of changing the drill bit.

KSSD NO. 3 WELL

The KSSD No. 3 well was located near the border of the Dangerous Cape high and the Albatross basin, approximately 9 miles southwest of the KSST No. 2 well. The KSSD No. 3 well was drilled to a depth of 9,357 feet and penetrated a marine, clastic sedimentary section. The upper, Quaternary to Neogene, section of the well contains sediments that are Pleistocene to Miocene in age and represents the relatively undeformed, acoustically resolvable strata that mantle the Dangerous Cape high and fill the Albatross basin. The lower, structurally deformed Paleogene section is Eocene in age. The dipmeter log indicates that the strata of the basin-fill sequence dip 2 to 8 degrees southwest to southeast. Below a regional angular unconformity at 7,805 feet, the Eocene strata dip 15 to 70 degrees northwest.

Quaternary and Neogene Strata

The Quaternary to Neogene section of the KSSD No. 3 well consists of sequences of interbedded mudstone, siltstone, sandstone, and conglomerate that were deposited in marine environments ranging from middle neritic to middle bathyal (pl. 6). Drill cuttings and sidewall and conventional cores recovered silty to sandy, pebbly mudstone, pebbly siltstone, and very fine- to fine-grained, generally silty, pebbly sandstone or sandy conglomerate. The gravel-sized sediment fraction consists of angular to rounded granule- to pebble-sized igneous and metamorphic rock fragments. Rounding of the gravel-sized rock fragments appears to increase downward in the section. Wireline logs indicate that numerous sandstone or conglomerate beds were encountered, more than in any of the five other stratigraphic test wells drilled on the Kodiak shelf. Sandstone and conglomerate beds over 5 feet thick that showed indications of permeability on the Dual Induction Laterolog log (DIL) were analyzed to determine their reservoir potential. The same log analysis techniques that were discussed in the section on the nearby KSST No. 2 well were used to evaluate the porosity, permeability, and shaliness of sandstones in the KSSD No. 3 well.

Three major Quaternary to Neogene stratigraphic sequences were recognized in the KSSD No. 3 well on the basis of dipmeter patterns, large-scale wireline log patterns, and microfossil paleobathymetry. The upper glaciomarine stratigraphic sequence contains Pleistocene middle to outer neritic microfossils, exhibits random to polymodal dip azimuth patterns, and displays predominantly bell-shaped, upward-fining wireline log profiles (pl. 7). The second sequence is Plio-Pleistocene in age and is composed of strata that contain outer neritic to upper bathyal microfossils, exhibit consistent southwestward dip azimuth patterns, and display funnel-shaped, upward-coarsening wireline log profiles (pl. 7). The strata of the second sequence are interpreted to represent turbidite deposits.

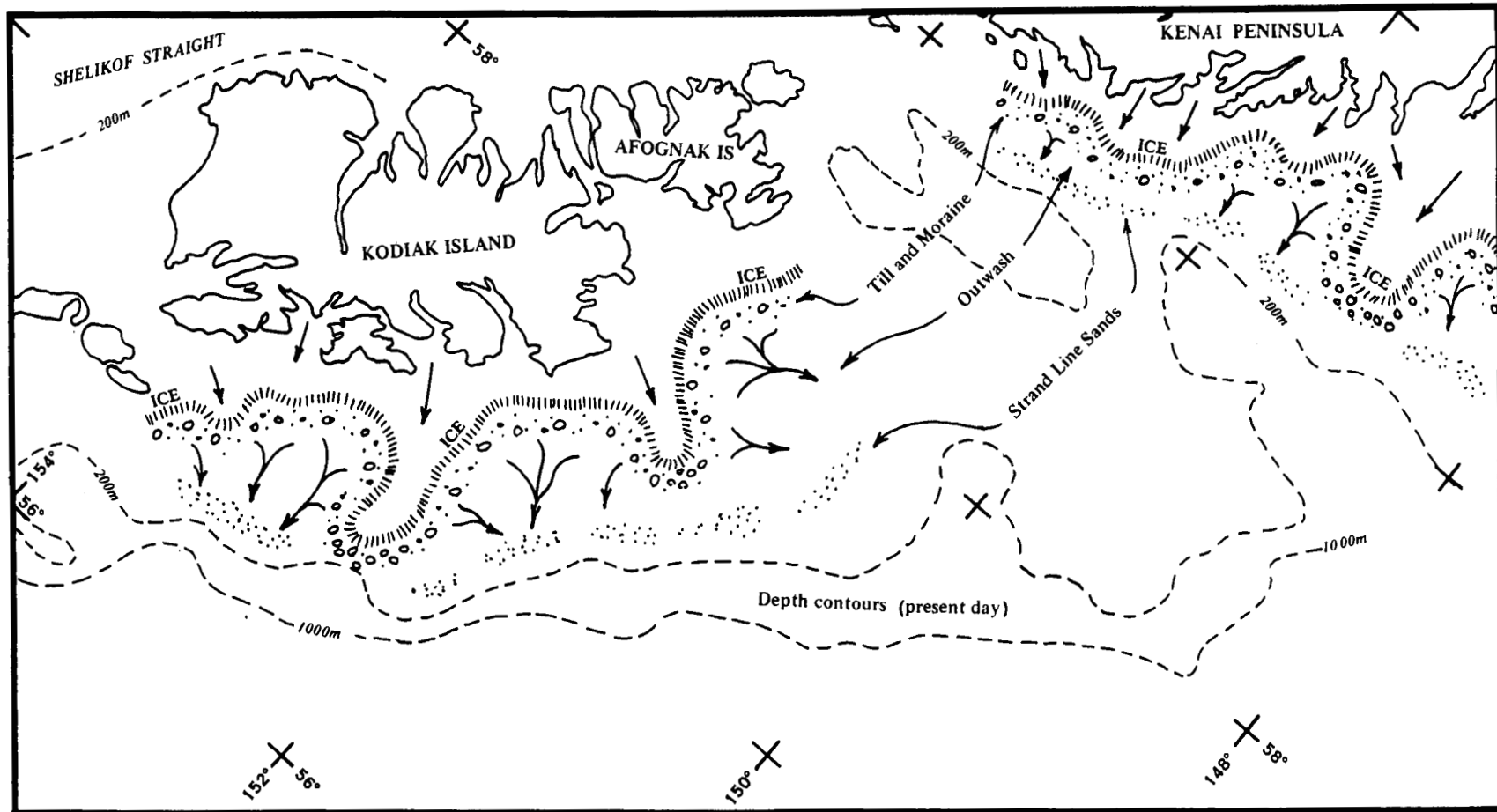


Figure 62. Schematic paleogeographic map of the Kodiak shelf area showing texture and genesis of shelf sediments during the Pleistocene. Glacial pathways and end moraines from Hampton and others (1979), and Thrasher (1979).

The third sequence, also interpreted as a turbidite sequence, is Miocene in age and composed of strata that contain outer neritic to middle bathyal microfossils, exhibit consistent southeastward dip azimuth patterns, and display a mixture of bell- and funnel-shaped wireline log patterns.

Pleistocene Glaciomarine Shelf Sequence

The upper sequence from the first sample at 1,370 feet to 2,835 feet includes shelf deposits of middle to late Pleistocene age (pl. 6 and 7). The sediment from this sequence is the most gravel-rich of any sequence in the well. The drilling mud log recorded abundant gravel that ranged from angular to rounded, although most was angular to subangular. The SP log indicates that much of the sand or conglomerate occurs in beds 15 feet thick or less, although one bed is over 50 feet thick. On a somewhat larger scale, the logs display serrate, bell-shaped vertical profiles (pl. 7) that indicate upward-fining and upward-shaling sequences of interbedded mudstone and conglomerate or sandstone. The thin conglomerate and pebbly sandstone beds probably represent shelf strandline and storm-wave deposits and submarine shelf channel fills.

The upward-shaling profiles of these conglomerate-mudstone sedimentary sequences reflect systematic waning of depositional energy, probably as a result of marine transgressions. The occurrence of abundant coarse-grained conglomeratic sediment in strata that were deposited in offshore shelf settings where depositional slopes were low and currents were generally insufficient to transport gravel-sized particles suggests that these sediments are relict. It is probable, considering the Pleistocene age of these strata and the angularity of the gravel-sized detritus, that most of the sediment is of glacial origin. The sediment was probably originally transported and deposited by glacial or periglacial processes when the shelf was either exposed or very shallow during the sea-level lowstands that accompanied glacial advances (fig. 62). The sediment was reworked, transported, and modified by marine processes during subsequent interglacial marine transgressions.

Seismic-reflection profiles indicate that the Pleistocene glaciomarine shelf strata are flat-lying, so the dips obtained from dipmeter log data are sedimentary rather than structural in origin. As a result, the random patterns exhibited by rose diagrams of dip directions (azimuth frequency diagrams, pl. 7) from these strata are probably indicative of the complex series of sedimentary processes these sediments have undergone. Glacial sediments are typically poorly stratified and poorly sorted to begin with, and the bioturbation and variable currents characteristic of marine shelf environments would probably not greatly increase the abundance of sedimentary structures with consistent dip orientations. Random to polymodal current-bedding orientation is characteristic of marine shelf sands and tends to result in random dipmeter patterns (Goetz and others, 1977).

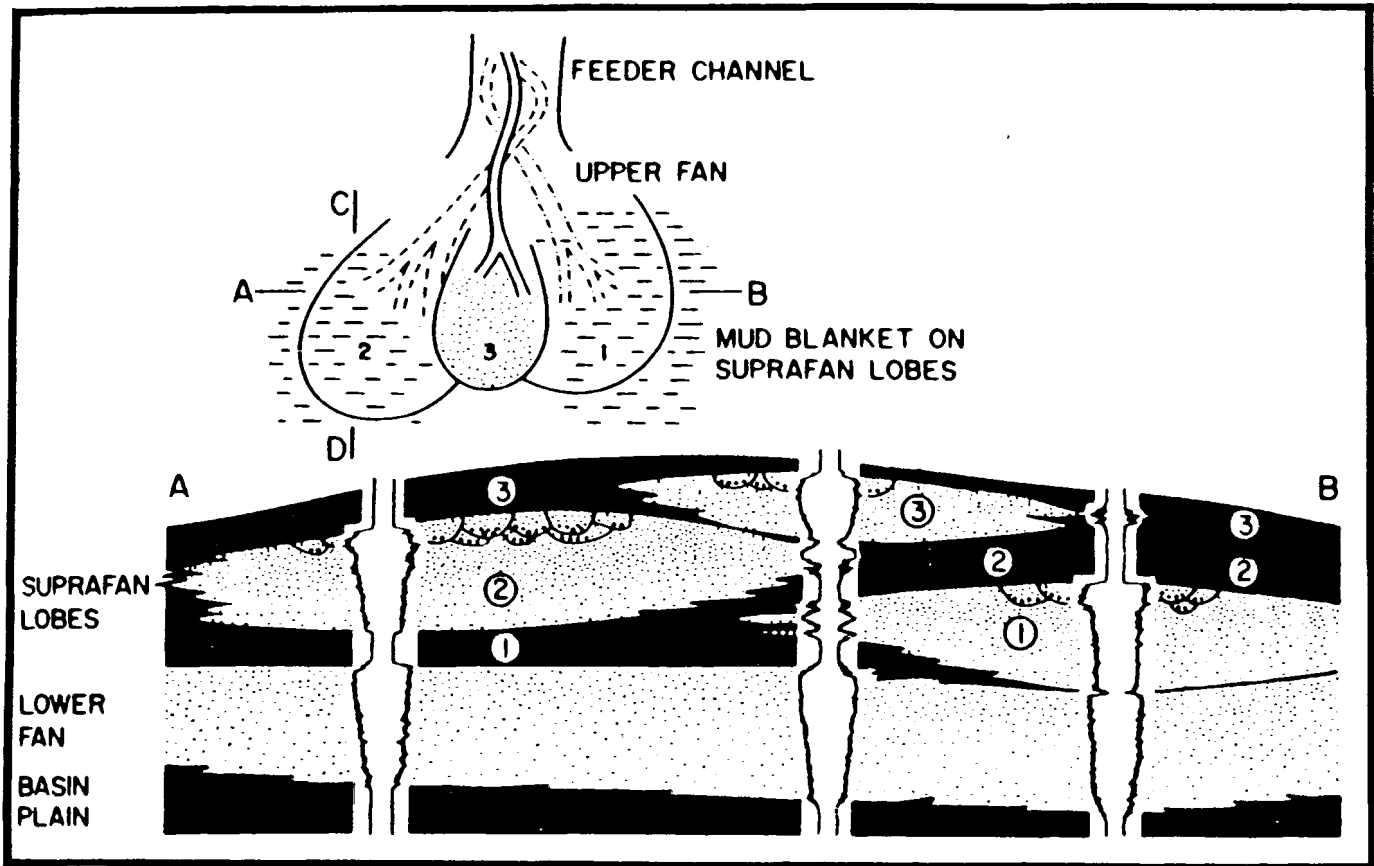


Figure 63. Hypothetical vertical cross section across prograding lower and middle-fan system (from Walker 1978, fig. 18). Lower-fan sequence is coarsening-upward, and each suprafan lobe has coarsening-upward sequence, from thin-bedded turbidites to channelized massive and pebbly sandstones. Each suprafan-lobe sequence also shales out laterally into mudstone drape that covers adjacent parts of fan. Sequence shown in cross section is result of suprafan lobe switching from position 1, to 2, to 3 (see plan view, upper part of diagram). Lobe switching may be related to changing meander patterns in upper-fan channel. Hypothetical electric logs illustrate coarsening-upward prograding-lobe sequences, fining-upward channel-fill sequences, and highlight problems of correlation in such a system (after Nelson and Nilsen, 1984).

The Pleistocene glaciomarine shelf sequence contains a total of 237 feet of sandstone and conglomerate in beds ranging from 6 to 58 feet thick (table 6, p. 136). Of this total, the net thickness of sandstone and conglomerate that contains less than 40 percent shale and at least 10 percent effective porosity accounts for 189 feet. Descriptions of sidewall core samples indicate that these shallow-marine shelf sandstones are generally shaly and silty. Shale content calculated from the logs averages 20 percent (table 6, p. 136). Total porosity from the density log averages 27 percent, but because of the shaliness, the average effective porosity derived from the logs is reduced to about 21 percent. The average effective porosity indicated by the sidewall cores is somewhat higher at 24 percent. Log-derived permeability averages about 10 millidarcies (md). Sidewall core permeabilities average considerably higher at 154 md, but most of the sidewall permeabilities are less than 10 md and the average is skewed higher by several high values (Appendix 1).

Plio-Pleistocene Turbidite Sequence

This sequence spans the interval between 2,835 and 5,060 feet and contains strata of late Pliocene to early Pleistocene age (pl. 7). The drilling mud log indicated that gravel and coarser grained detritus like that in the overlying sequence are also present in the upper part of this sequence. However, the amount of gravel-sized sediment rapidly diminishes downward in the sequence. Microfossils from this Plio-Pleistocene sequence indicate that there is a parallel downward increase in paleobathymetric depths (pl. 7). Overall, the strata record an upward-coarsening and shoaling pattern which reflects a regressive phase of the basin history (pl. 7). Sedimentation rates evidently exceeded subsidence rates and the basin was infilled.

On a somewhat smaller scale, the wireline logs display repetitive funnel-shaped profiles (pl. 7) similar to those described in the KSST No. 2 well (pl. 2, fig. 60). These funnel-shaped log profiles record upward-coarsening progradational sedimentary cycles, and the entire Plio-Pleistocene sequence appears to be composed of these cycles. The progradational cycles, or sequences, are generally over 50 feet thick and range upward to 300 feet (pl. 7). Microfossil data indicate that the progradation occurred in relatively deep water, in outer shelf, slope and basinal environments. Therefore, these upward-coarsening stratification sequences probably represent turbidite or submarine-fan deposits. The repeated cycle of fan lobe buildup and abandonment that occurs during the progradation of submarine-fan depositional systems characteristically results in a series of stacked, upward-coarsening sedimentary cycles (fig. 63) (Walker, 1978; Nelson and Nilsen, 1984) similar to those recorded by the funnel-shaped wireline log motifs of this sequence (pl. 7).

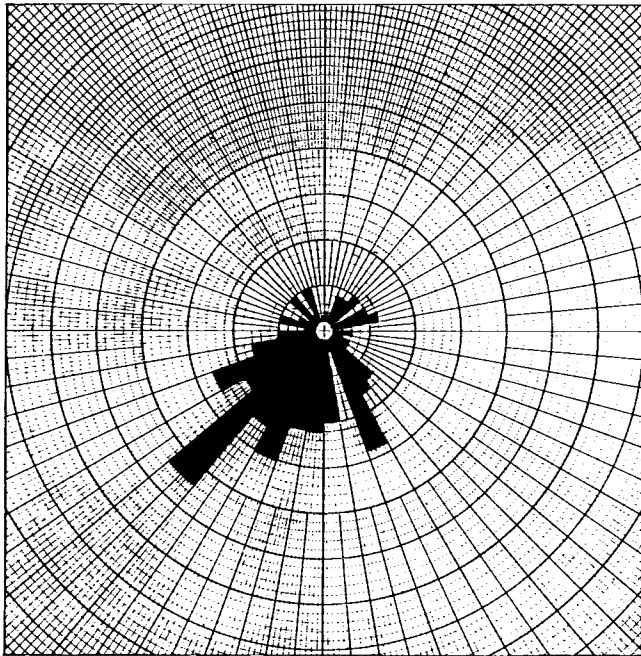
Rose diagrams of dip directions constructed from dip azimuth frequencies obtained from the dipmeter log show a consistent southwesterly trend in this sequence (pl. 7). This trend appears to be indicative of the original paleoslope and direction of progradation. Low-angle dip magnitudes of 5 degrees or less mainly

represent the present structural attitude of these strata: Higher angle dip magnitudes are inferred to be mainly the result of such primary and secondary sedimentary features as foreset bedding on inclined slopes of fan lobes, foreset crossbedding in submarine distributary mouth bar and channel point-bar deposits, current crossbedding, and compactional drape of bedding over sandstone bodies. Because rose diagrams of dip azimuth frequencies from both of these structural (low angle) and sedimentary (high angle) types of dips contain essentially equivalent directional trends (fig. 64), it seems probable that they represent the original depositional trend of these geologically young strata. On this basis, the strata of the Plio-Pleistocene sequence are inferred to have been deposited on a southwesterly sloping surface by a submarine fan complex which prograded from the northeast in the area of the Dangerous Cape High.

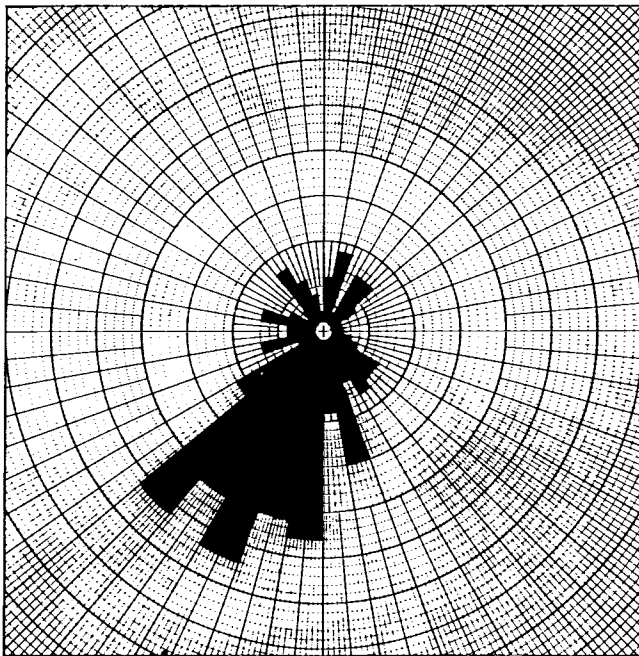
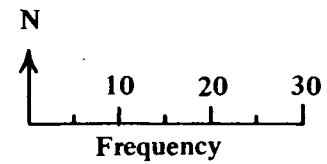
Numerous sandstone beds are associated with the upper sections of these progradational sequences. The sandstone beds range in thickness from a few feet to over 110 feet, form an aggregate thickness of 606 feet, and compose 27 percent of the Plio-Pleistocene turbidite sequence. Several different sandstone facies are present which are probably related to depositional locales on or near a submarine fan. Selley (1979) was able to distinguish upper-, middle-, and lower-fan depositional environments from North Sea submarine-fan sandstones using gamma ray, SP, and dipmeter log motifs (fig. 65). Sandstones with similar log motifs, or patterns, are present in the progradational cycles of this sequence, and the criteria recognized by Selley (1979) were used to interpret the depositional environments of these sandstones.

The log and dipmeter motifs of sandstones in the upper section of the sequence between 2,835 and 3,670 feet (pl. 7) resemble those of the upper- and mid-fan sandstone facies of figure 65 (pts. I and II). For example, the sandstone at 3,060 feet (fig. 66) displays log and dip motifs which appear analogous to those of upper- or mid-fan sandstone facies. This 94-foot-thick pebbly sandstone exhibits a uniform SP log profile with sharp upper and lower contacts similar to those of upper fan, base-of-slope massive conglomeratic sandstones (fig. 65, pt. I). However, the sonic log trace is serrate, indicating internal bedding, and as a result the dipmeter data are not random. The dip pattern has a preferred southwesterly orientation and upward-decreasing motifs, which are more analogous to mid-fan, turbidite in-filled channels (fig. 65, pt. II) than upper-fan channel-fills. This combination of facies suggests that this sandstone may represent a channel deposit from a transitional upper- to mid-fan position.

The sandstones of the middle part of the Plio-Pleistocene turbidite sequence, between 3,670 and 4,455 feet (pl. 7), are thin bedded and exhibit log and dipmeter motifs that resemble those of the lower-fan, distal turbidite deposits of figure 65 (pt. III). For example, the upward-coarsening sequence that is illustrated on figure 67 is capped by a series of thin sandstones less than 10 feet thick. The upward-coarsening log profiles of these sandstones are analogous to those of the distal-fan turbidites of figure 65 (pt. III),



Directional trends of low-angle dips ($< 5^\circ$) which chiefly represent structural dips.



Directional trends of high-angle dips ($> 5^\circ$) which chiefly represent sedimentary dips.

Figure 64. Rose diagrams of dip azimuth frequencies from high resolution dipmeter log data, 2,835 – 5,060 feet, KSSD No. 3 well. Equivalent directional trends of both structural and sedimentary dips suggest that sedimentary progradation was from the northeast to the southwest.

although the dipmeter motifs are not as evident in this example. These sandstones and the other thin sandstones of this section are interpreted to represent distal turbidites of lower-fan lobes.

The lower part of the Plio-Pleistocene turbidite sequence, between 4,455 and 5,060 feet, contains sandstone beds that are thicker than those of the lower-fan deposits of the overlying section (pl. 7). Individual sandstone beds display a combination of log and dipmeter motifs that suggests deposition in a mid-fan setting. For example, the 95-foot-thick sandstone at 4,500 feet (fig. 68), the thickest bed in this section, displays an upward-coarsening log profile and an upward-increasing dipmeter motif in the lower part of the bed that resembles those of the mid- and lower-fan prograding facies of figure 65 (pts. II and III). However, the upper part of the sandstone above 4,570 feet displays a fairly uniform log profile and some upwardly decreasing dip motifs that resemble the channel facies of the mid-fan deposits of figure 65 (pt. II). This suggests that it may reflect deposition in a transitional setting near the mid- and lower-fan boundary.

The somewhat problematical 95-foot-thick sandstone bed of figure 68 may represent either a distributary channel-fill amalgamated with a fan like that of the lower sandstone of part II, figure 65, a fan lobe deposit, or perhaps, a submarine analogue of a deltaic distributary-mouth-bar deposit. Distributary-mouth-bar deposits in a submarine fan system would be most likely to occur at the mid- to lower-fan boundary where steeper gradients exist at the distal ends of suprafan lobes (radial profile, fig. 65). A distributary-mouth-bar deposit represents a high-energy depositional environment in a deltaic setting and probably would in a submarine-fan setting as well. The massive character of the upper section of this sandstone and the 20- to 30-degree dips suggest a high-energy depositional environment. However, few examples of channel-mouth bar deposits are documented from submarine fan systems (Nelson and Nilsen, 1984, p. 203). Whatever the depositional origins of this sandstone bed, it appears to have the best reservoir potential of any of the sandstones in the Plio-Pleistocene turbidite sequence. The average shale content is low (13.3 percent) and average effective porosity (24 to 27 percent) and permeability (19 to 200 md) are high relative to most of the other sandstones (table 7, p. 137). The average shale content for the 500 net feet of sandstone in the Plio-Pleistocene turbidite sequence is about 23 percent (table 7). Sidewall core descriptions indicate that these submarine-fan sandstones are generally shaly and silty, like the shelf sandstones of the overlying sequence. The total porosity obtained from the density log averages about 26 percent for these sandstones, but because of the shaliness, the average effective porosity derived from the logs is reduced to about 19 percent. The average effective porosity indicated by the sidewall cores is somewhat higher at 24 percent. Log-derived permeability averages about 6 millidarcies (md). Sidewall core permeabilities average considerably higher at 110 md. Overall, the sandstones of the Plio-Pleistocene sequence appear to have low to moderate reservoir potential, although a few of the thicker beds have moderate to good potential.

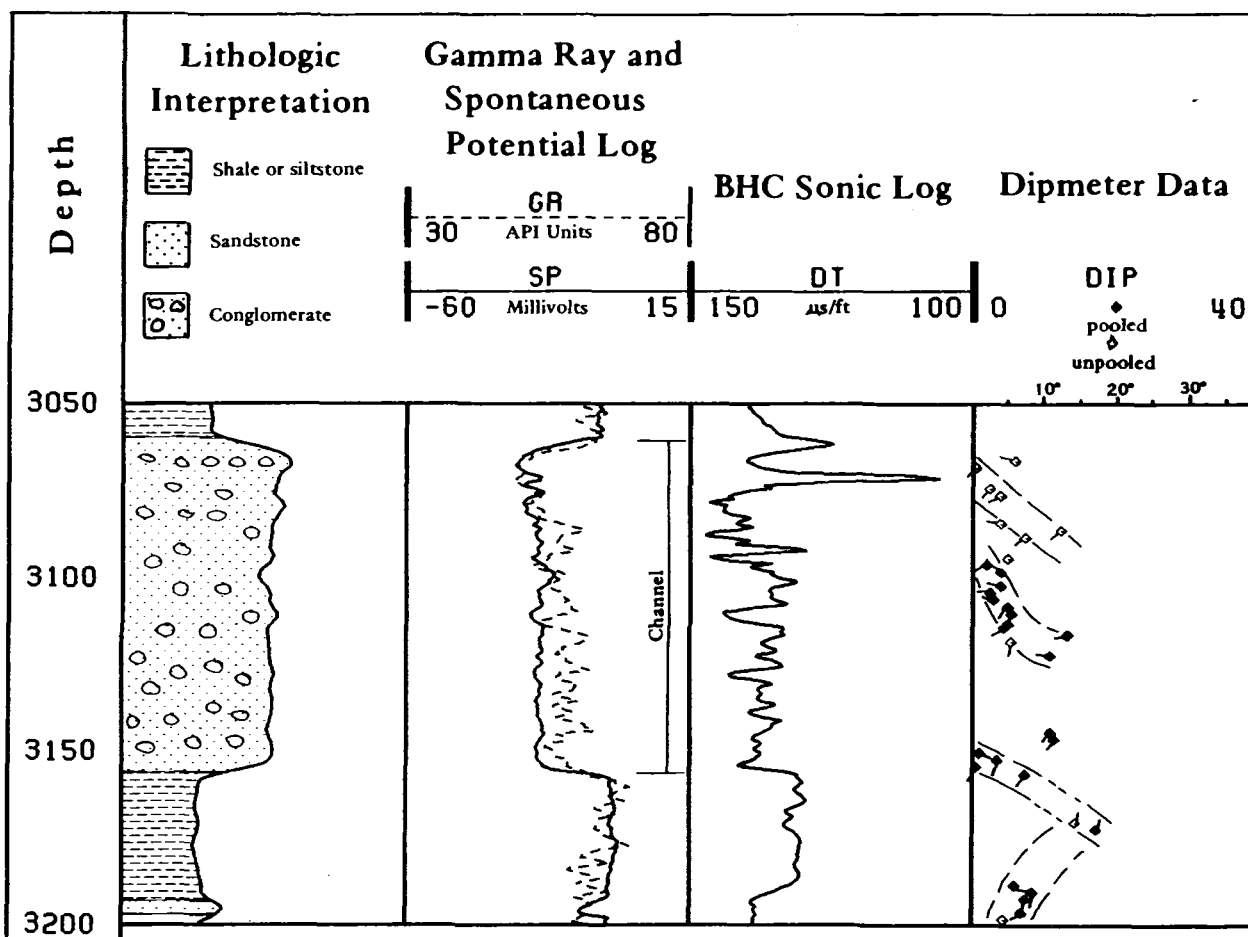


Figure 66. LOG OF SUBMARINE UPPER- TO MID-FAN CHANNEL DEPOSIT, PLIO-PLEISTOCENE TURBIDITE SEQUENCE, KSSD NO. 3 WELL. Example of a channel sandstone that displays log and dip motifs similar to both upper- and mid-fan channel sandstones (fig. 65, pts. I and II). The sandstone displays a massive SP log profile that resembles an upper-fan channel facies, but the serrate sonic log profile and the upward-decreasing dip motifs suggest an affinity with mid-fan channel facies. The sandstone may represent a channel facies transitional to the two environments.

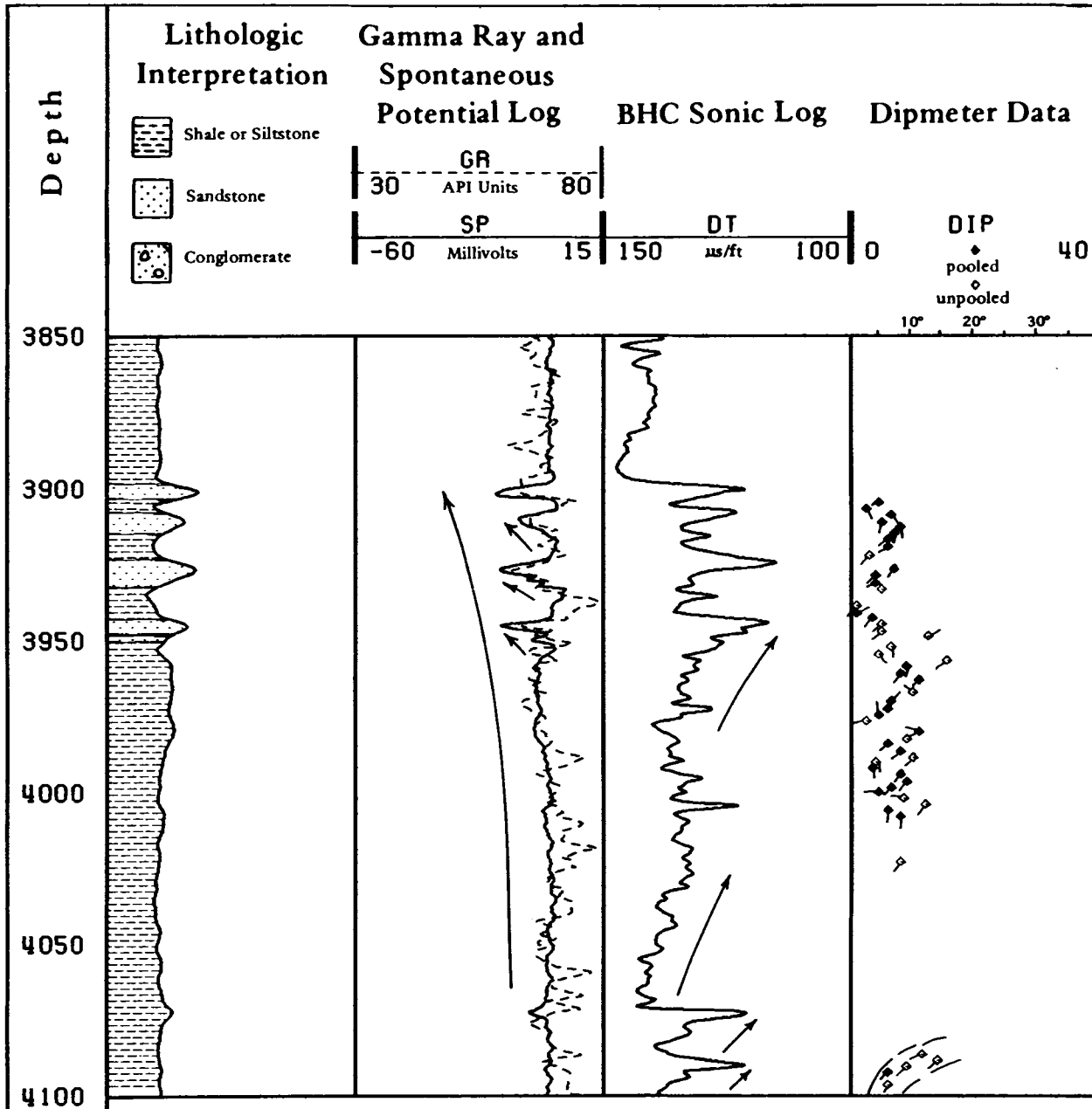


Figure 67. LOG OF A SUBMARINE LOWER-FAN FACIES ASSOCIATION, PLIO-
 PLEISTOCENE TURBIDITE SEQUENCE, KSSD NO. 3 WELL. Example of thin, distal-
 fan turbidite sandstones at the top of a lower-fan sequence. Compare with fig. 65, pt.
 III. The logs in this example display characteristic upward-coarsening trends that indicate
 a progradational sequence, but the upward-increasing dip motifs are not generally apparent.

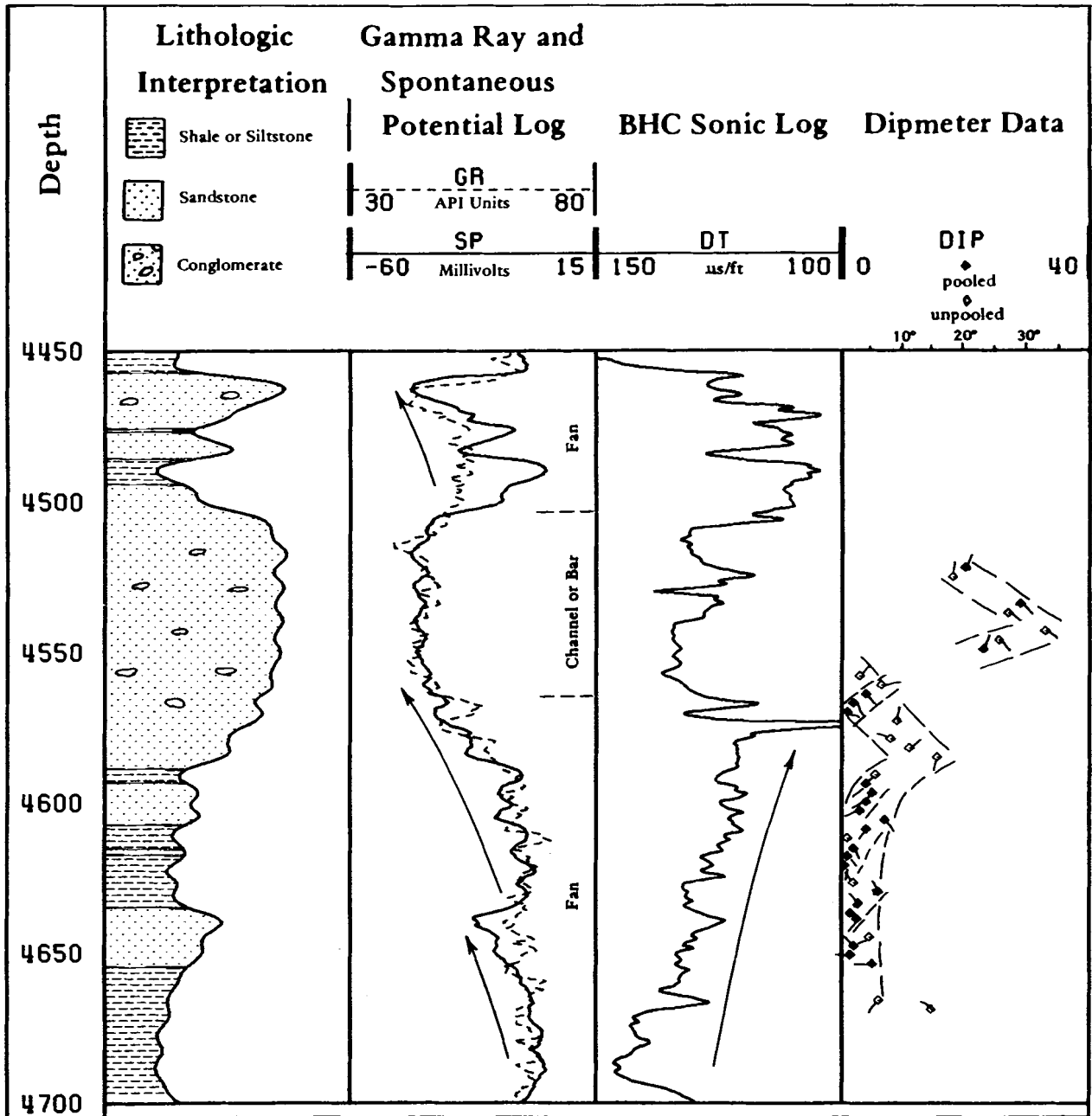


Figure 68. LOG OF A SUBMARINE MID-FAN FACIES ASSOCIATION, PLIO - PLEISTOCENE TURBIDITE SEQUENCE, KSSD NO. 3 WELL. Example of progradational fan facies and a thick mid-fan channel or bar deposit. Compare with fig. 65, pts. II and III. The fan lobe deposits exhibit upward-coarsening log trends and upward-increasing dip motifs which may indicate a transitional environment near a channel mouth in the mid- to lower-fan position.

Miocene Turbidite Sequence

This sequence spans the interval between 5,060 and 7,805 feet and includes strata of middle Miocene and late Miocene age (pl. 6). The lithology of this turbidite sequence is similar to that of the overlying Plio-Pleistocene turbidite sequence, that is, pebbly sandstone, siltstone, and mudstone. Microfossils indicate that most of the sediments were deposited in middle to upper bathyal depths, although an interval near the middle of the sequence may have been deposited in slightly shallower outer neritic to upper bathyal depths (pl. 7). These strata, like those of the overlying sequence, are interpreted to have been deposited by a submarine-fan system.

Besides the age difference between the Miocene and Plio-Pleistocene turbidite sequences, these sequences can be distinguished by divergences in dip directions indicated by azimuth frequency rose diagrams, and by differences in large-scale log patterns (pl. 7). The directional trend of dips in the Miocene sequence is predominantly to the southeast and represents a 90 degree shift in trend from that of the Plio-Pleistocene sequence. Dips that reflect the present structural attitude of the Miocene strata appear to be generally less than 5 degrees. For the same reasons enumerated in the discussion of the Plio-Pleistocene sequence, the southeasterly dip trend of the Miocene sequence is assumed to represent the original paleoslope and direction of progradation. This suggests that the sediment source was to the northwest, from the Kodiak Island area. However, given the somewhat greater age of the Miocene turbidite sequence and the highly active tectonic setting of the Kodiak shelf, the possibility of post-depositional structural tilting of this sequence cannot be ruled out. Strata of Pliocene to late Pleistocene age in the KSST No. 1 well 54 miles to the southwest have been structurally tilted by the uplift of Albatross Bank, and von Huene and others (1980a) have recognized large-scale post-depositional tilting of stratigraphic sequences in the same area of Albatross basin based on reconstructions from seismic records. In any case, the divergence in dip trends between the Miocene and Plio-Pleistocene turbidite sequences, whether structural or stratigraphic in origin, indicates that a significant shift in sedimentation occurred at the boundary between the sequences, and further suggests that the resultant angular discordance represents an unconformity.

The wireline logs in both the Plio-Pleistocene and Miocene turbidite sequences display large-scale funnel-shaped coarsening-upward vertical profiles that indicate progradational sedimentation patterns. The Miocene sequence, however, also contains some large-scale bell-shaped fining-upward profiles that suggest transgressive patterns (pl. 7). In most cases, it is uncertain whether or not these larger-scale fining-upward patterns actually represent relative sea level rises. However, in one case between about 6,100 and 6,300 feet, a fining-upward sedimentary cycle does coincide with a transgressive pattern of paleobathymetry that is indicated by the microfossil data (pl. 7). The other fining-upward cycles may be the result of sea level transgressions too small to be detected by

microfossil data or simply the result of the normal in-filling of submarine channels by turbidites (fig. 65, pt. II).

The SP log indicates that the Miocene turbidite sequences contain numerous sandstones (pl. 7). Most of the sandstone occurs in beds between 20 and 100 feet thick (table 8, p. 138). The aggregate sandstone thickness is about 1,120 feet and represents 40 percent of the strata. Most of the thick sandstone beds exhibit log and dipmeter motifs that resemble those of the mid-fan facies association of fig. 65, pt. II. For example, in the sandstone sequence of figure 69 the log motifs indicate an upward-coarsening fan facies (below 6,250 feet) that is succeeded by upward-fining channel-fill facies. This type of vertical facies association is repeated throughout the Miocene turbidite sequence. This sedimentary pattern is interpreted to result from the cyclic progradation and abandonment of suprafan lobes, which is believed to be a characteristic pattern of the mid-fan environment (fig. 65) (Selley, 1979).

Although the Miocene turbidite sandstones exhibit essentially equivalent log and dipmeter patterns, significant differences in petrophysical properties exist between those in the upper and those in lower parts of the sequence. The upper Miocene sandstones, between 5,060 and 6,890 feet, display smaller scale deflections on the gamma ray and SP logs than do the middle Miocene sandstones between 6,890 and 7,805 feet (pl. 7). This appears to be a result of higher contents of quartz and chert and lower contents of shale and clay in the basal middle Miocene sandstones. Shale contents calculated from the logs of sandstones below 6,890 feet range between about 10 and 17 percent, whereas in the upper Miocene sandstones, shaliness generally ranges between 20 and 30 percent (table 8, p. 138). Petrographic descriptions of core samples (Core Laboratories, Inc., 1978) indicate that the middle Miocene sandstones contain a greater fraction of detrital chert in the grain framework than the upper Miocene sandstones. Detrital chert generally makes up from 15 to 35 percent of the grain framework of middle Miocene sandstones and 15 percent or less in the upper Miocene sandstones. Petrographic descriptions also suggest that the middle Miocene sandstones tend to be more highly cemented, primarily with silica, than the upper group.

A summary of the reservoir potential of the two groups of sandstones in the Miocene turbidite sequence is tabulated in table 8, (p. 138). The upper Miocene shaly sandstones contain an aggregate thickness of 658 feet in beds ranging from 9 to 135 feet in thickness. The net thickness of sandstones containing less than 40 percent shale and having an effective porosity of at least 10 percent is 596 feet. The average shale content of the net sandstone is about 24 percent, and the average effective porosity calculated from the logs is 17 percent. Log-derived permeability ranges from 0.1 to 10 md, and sidewall cores indicate permeability is less than 5 md in all but one bed which had a measured permeability of 208 md. The single measurement obtained from a conventional core cut from these strata indicated a porosity of only 3.5 percent and a permeability of only 0.04 md (conventional core 1, Appendix 1).

The relatively clean, well-cemented sandstones of the middle Miocene in table 8 (p. 138) attain an aggregate thickness of 462 feet in beds ranging from 20 to 127 feet in thickness. The net sandstone thickness is 388 feet. The logs indicate that the net sandstone contains an average shale content of about 14 percent and an average effective porosity of 17 percent. Sidewall cores indicate an average effective porosity that is somewhat higher at 22 percent. However, the data that were obtained from two analyses of conventional core 2 (Appendix 1), which was cut from the basal sandstone of the lower group (sandstone at 7,565 feet, table 8), suggest that the sidewall porosities may be too high. The conventional core porosity averages 9.4 percent, while the sidewall core porosity from this same bed averages a much higher 21.4 percent. The log-derived effective porosity averages 13.3 percent and is in somewhat better agreement with the conventional core data. Despite the disparity in the porosity data from this bed, the permeability data is in reasonably close agreement. The permeability averages 3.0 md from the conventional core, 2.7 md from the sidewall core, and 0.3 md from the logs. Log-derived calculations from the other beds of the lower sandstone group suggest similar low permeabilities in the range of a few millidarcies (table 8). By contrast, the sidewall permeabilities are higher, commonly in the range of 20 to 55 md, and if accurate, they indicate fair reservoir potential. However, the more optimistic sidewall core permeabilities from the cleaner sandstones of the lower group stand a greater chance of being artificially high than the less consolidated shaly sandstones of the upper group. The well-cemented sandstones of the middle Miocene are probably more brittle than the upper sandstones, and are probably more susceptible to fracturing and fabric disruption from the sidewall coring process.

To summarize, the reservoir potential of the shaly, submarine-fan sandstones from the upper part of the Miocene turbidite sequence appears to be generally low because of low permeability. The reservoir potential of the relatively clean submarine-fan sandstones from the basal strata of the Miocene turbidite sequence is probably also low because of permeability reduction as a result of porosity constriction by silica and calcite cementation. However, the permeability data from the logs and cores of the lower group of sands are more ambiguous and suggest that some of these lower sands might contain fair potential with permeabilities in the range of 20 to 55 md.

Paleogene Strata

The Paleogene section of the KSSD No. 3 well consists of Eocene strata that are separated from the Neogene sequence by a regional angular unconformity marked on the dipmeter log by a large shift in dip magnitude and direction. Dipmeter log data indicate that the middle Miocene strata that overlie the unconformity dip about 2 to 4 degrees east or southeast, whereas the Eocene strata below the unconformity dip 15 to 65 degrees northwest. However, locating the precise depth of the unconformity from dipmeter data is not possible because it occurs within a 185-foot interval that is devoid of discernable dips. Because of this, the depth of the unconformity was

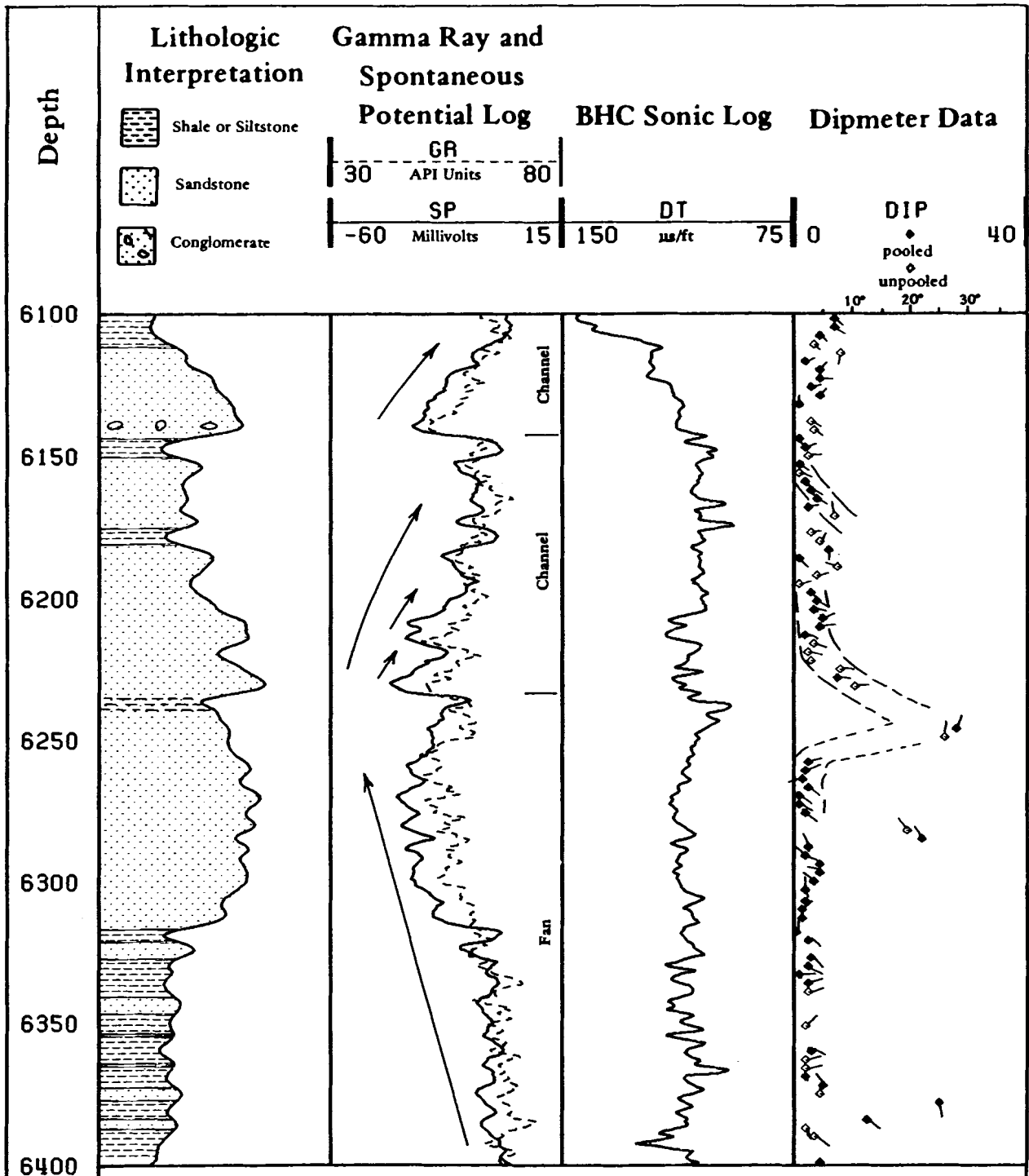


Figure 69. LOG OF A SUBMARINE MID – FAN FACIES ASSOCIATION, MIOCENE TURBIDITE SEQUENCE, KSSD NO. 3 WELL. Example of a succession of turbidite in-filled channel sandstones overlying a fan-lobe deposit. Compare with fig. 65, pt. II. The fan facies displays an upward-coarsening trend on the gamma ray log, but upward-increasing dip motifs are not readily apparent except perhaps near the top of the fan-lobe. The channel facies exhibit serrate, upward-fining log trends and upward-decreasing dip motifs.

picked from the sonic log at 7,805 feet, where the log displays a downward shift to a serrate, higher velocity profile (pl. 6) that indicates highly indurated and thinly bedded, or, perhaps, highly fractured, rocks.

The Eocene section consists of shale, siltstone, and minor amounts of sandstone. The sandstone is shaly, silty, very fine to fine grained, and highly cemented. The wireline logs indicate that these rocks are hard, dense, and resistive. There is little or no SP log response across sandstone intervals (pl. 6), which suggests that the sandstones are essentially impermeable.

Microfossil data indicate that these strata are deep-water marine, probably bathyal. Coeval strata of the Sitkalidak and Sitkinak Formations which are exposed on Kodiak, Sitkalidak, and Sitkinak Islands are interpreted as deep-water marine turbidite deposits (Nilsen and Moore, 1979), and the strata of the KSSD No. 1, 2, and 3 wells appeared, from the limited log and core data, to contain similar lithofacies. However, conventional core no. 4 in the KSSD No. 3 well (pl. 7, Appendix 1) recovered mudstone that was reported to contain a texture of oriented clots of organic fragments that suggest an algal origin (Core Laboratories, Inc., 1978) (see Lithologic Summary chapter). These same mudstones were also reported to contain short irregular fractures resembling desiccation cracks, features indicative of intertidal deposition. If these mudstone samples represent in situ deposits, then the Eocene section of the KSSD No. 3 well contains strata that were deposited in shallow marine environments. However, their most likely origin is as clasts swept in by turbidity currents.

TABLES 5, 6, 7, and 8. Gross sandstone thickness includes intervals with a negative SP log deflection of at least 10 millivolts, and net thickness includes sandstone within the interval that contains at least 10 percent effective porosity and less than 40 percent shale. Shaliness was obtained from the gamma ray log. Total log porosity was obtained from the density log, and effective log porosity was obtained from density-porosity corrected for shale. Log-derived permeability was calculated from the Wyllie-Rose equation (Wyllie and Rose, 1950).

TABLE 5. Summary of wireline log interpretations of sandstone reservoir potential in the KSST No. 2 well. Sidewall core data are from Core Laboratories, Inc. (1976b).

DEPTH TO TOP (feet)	THICKNESS (feet)		SHALINESS (% volume)	POROSITY (% volume)				PERMEABILITY (md)		
	Gross	Net		Total (logs)	Effective		Logs	Logs	SW core*	
					Logs	SW core*				
830	83	76	26.1	36.2	26.5	----	---	16	---	---
1,870	21	15	9.5	31.0	28.1	28.6	(3)	21	21	(3)
1,900	6	5	33.1	23.1	15.2	22.9	(1)	0.8	1.3	(1)
2,378	60	54	17.9	29.3	25.2	27.4	(3)	12	99	(3)
2,580	22	20	19.8	30.9	26.3	28.4	(3)	16	52	(3)
2,902	22	20	31.4	21.1	14.1	21.4	(2)	0.4	25	(2)
2,967	38	15	34.7	20.3	12.4	23.8	(1)	0.2	28	(1)
3,828	12	8	31.1	21.5	14.5	----	---	0.4	--	---
4,210	<u>12</u>	<u>8</u>	<u>31.6</u>	<u>32.3</u>	<u>21.9</u>	<u>21.1</u>	<u>(1)</u>	<u>9.0</u>	<u>86</u>	<u>(1)</u>
Total or (Average)	276	221	24.0	31.3	23.3	25.9	(14)	12	49	(14)

*The number in parentheses indicates the number of cores in the interval.

TABLE 6. Summary of wireline log interpretations of sandstone reservoir potential in the Pleistocene glaciomarine shelf sequence, KSSD No. 3 well. Sidewall core data are from Core Laboratories, Inc. (1978).

DEPTH TO TOP (feet)	THICKNESS (feet)		SHALINESS (% volume)	POROSITY (% volume)				PERMEABILITY (md)		
	Gross	Net		Total (logs)	Effective		Logs	SW core*	Logs	SW core*
1,578	10	10	17.2	33.9	28.3	20.4	(1)	29	0.3	(1)
1,601	33	19	23.4	26.9	19.5	21.2	(2)	7.3	1.3	(2)
1,716	27	12	18.8	29.7	23.3	21.5	(1)	16	1.5	(1)
1,872	58	56	18.0	28.5	22.9	22.8	(4)	11	275	(4)
2,174	6	6	23.6	24.7	18.2	21.7	(1)	1.8	0.2	(1)
2,200	16	11	27.5	24.9	17.7	18.7	(1)	1.4	<0.1	(1)
2,450	20	17	22.2	28.8	21.5	21.8	(3)	10	550	(3)
2,492	11	9	31.4	28.9	19.9	26.9	(1)	4.3	9.0	(1)
2,568	12	11	21.2	25.8	20.0	21.3	(2)	3.2	4.5	(2)
2,716	22	18	22.5	23.5	17.0	23.2	(2)	2.0	3.0	(2)
2,812	22	20	23.9	24.3	17.4	20.6	(2)	2.0	<0.1	(2)
Total or (Average)	237	189	19.5	27.4	20.8	24.4	(18)	9.8	154	(18)

*The number in parentheses indicates the number of cores in the interval.

TABLE 7. Summary of wireline log interpretations of sandstone reservoir potential of the Plio-Pleistocene turbidite sequence, KSSD No. 3 well. Sidewall core data are from Core Laboratories, Inc. (1978).

DEPTH TO TOP (feet)	THICKNESS (feet)		SHALINESS (% volume)	POROSITY (% volume)			PERMEABILITY (md)			
	Gross	Net		Total (logs)	Effective		Logs	SW core*	Logs	SW core*
					Logs	SW core*				
2,942	76	61	27.4	26.0	17.1	20.9	(3)	4.1	1.0	(3)
3,060	96	96	21.4	27.5	21.2	24.8	(4)	5.8	55	(4)
3,225	29	26	26.9	23.3	16.1	22.6	(2)	0.9	5.6	(2)
3,380	27	23	24.0	21.3	14.8	23.5	(3)	0.6	204	(3)
3,431	38	30	29.3	21.7	13.9	19.6	(1)	0.4	0.7	(1)
3,480	84	50	26.8	23.6	16.2	24.1	(3)	1.4	26	(3)
3,669	15	15	23.4	24.8	18.5	18.0	(2)	2.0	2.7	(2)
3,732	6	6	30.3	22.6	14.6	21.9	(1)	0.5	0.9	(1)
4,119	6	6	16.9	24.3	18.7	26.7	(2)	3.9	629	(2)
4,458	28	23	12.7	26.5	22.3	26.9	(1)	8.5	115	(1)
4,494	113	83	13.3	29.2	24.2	27.5	(6)	19	200	(6)
4,700	68	66	24.7	26.9	19.9	23.0	(4)	4.2	32	(4)
4,910	<u>20</u>	<u>15</u>	<u>32.8</u>	<u>25.8</u>	<u>17.1</u>	<u>20.9</u>	<u>(1)</u>	<u>1.2</u>	<u><0.1</u>	<u>(1)</u>
Total or (Average)	606	500	22.7	25.9	19.3	24.5	(33)	6.3	110	(33)

*The number in parentheses indicates the number of cores in the interval.

TABLE 8. Summary of wireline log interpretations of sandstone reservoir potential of the Miocene turbidite sequence, KSSD No. 3 well. Sidewall core data are from Core Laboratories, Inc. (1978).

DEPTH TO TOP (feet)	THICKNESS (feet)		SHALINESS (% volume)	POROSITY (% volume)				PERMEABILITY (md)	
	Gross	Net		Total (logs)	Effective		Logs	SW core*	
UPPER MIOCENE SHALY SANDSTONES									
5,060	17	17	16.3	28.8	24.4	21.0	(2)	10.0	0.8 (2)
5,084	46	43	23.4	24.4	17.9			2.0	
5,342	28	28	26.1	27.9	20.7	18.0	(2)	3.7	<0.1 (2)
5,430	36	26	28.8	23.0	15.2	19.6	(1)	0.9	0.5 (1)
5,690	82	70	25.9	25.6	18.7	22.7	(4)	2.2	2.7 (4)
5,797	9	9	27.7	22.4	14.7	18.7	(1)	0.8	<0.1 (1)
5,832	121	117	22.5	22.1	15.9			1.0	
6,108	34	31	23.9	24.1	17.8	20.3	(1)	1.6	0.5 (1)
6,149	25	8	30.2	19.5	11.6	18.5	(1)	0.1	<0.1 (1)
6,180	135	130	21.4	22.8	16.6	28.4	(2)	1.6	208 (2)
6,489	102	100	22.1	23.2	17.1	20.2	(2)	1.4	1.0 (2)
6,640	<u>23</u>	<u>17</u>	<u>28.2</u>	<u>19.4</u>	<u>12.0</u>			<u>0.1</u>	
Total or (Average)	658	596	23.6	23.7	17.0	21.4	(16)	1.8	27 (16)
MIDDLE MIOCENE CLEAN SANDSTONES									
6,892	28	28	14.0	22.7	18.7	22.7	(3)	2.4	55 (3)
6,935	51	51	16.2	21.5	16.9	23.8	(2)	1.4	25 (2)
6,996	20	20	14.8	20.8	16.5	20.1	(1)	1.2	5.5 (1)
7,054	59	59	12.0	22.2	18.7	24.4	(3)	2.2	38 (3)
7,250	38	38	14.6	22.8	18.7	27.2	(2)	2.2	40 (2)
7,335	29	29	9.7	22.0	18.8	22.6	(3)	2.8	20 (3)
7,416	110	71	10.7	21.2	17.5	19.9	(3)	2.8	1.1 (3)
7,565	<u>127</u>	<u>92</u>	<u>17.3</u>	<u>18.0</u>	<u>13.3</u>	<u>21.4</u>	<u>(3)</u>	<u>0.3</u>	<u>2.7</u> (3)
Total or (Average)	462	388	13.8	21.2	17.0	22.8	(20)	1.8	24 (20)

*The number in parentheses indicates the number of cores in the interval.

7. BIOSTRATIGRAPHY

INTRODUCTION

Six deep stratigraphic test wells were drilled on the Kodiak shelf between 1976 and 1977. The locations of these wells are shown in figure 2 (p. 4). Exploration Services Company, Inc., drilled the KSST Nos. 1, 2 and 4A wells in 1976, and Sun Oil Company drilled the KSSD Nos. 1, 2, and 3 wells in 1977. Paleontological data from these wells are the basis of this report. Rotary drill bit cuttings from the wells were processed for foraminifera and siliceous microfossils by the MMS using standard techniques. The initial microfaunal identification and interpretation for the three KSST wells was done by Ronald F. Turner (in 1977) and updated for this report by Turner and John A. Larson, both of the MMS. The bryozoan identifications were made by Ronald F. Turner. Because of different stipulations in the older drilling permit, the Government did not receive any consultant paleontological reports for the KSST wells. Palynological data were obtained for the MMS from selected KSST well samples by the Bujak Davies Group (written commun., 1987).

In 1977, Anderson, Warren and Associates did a detailed paleontological analysis for the participants in the KSSD drilling program. The results of these comprehensive studies were revised, updated, and supplemented by MMS personnel and by using subsequently published biostratigraphic zonations (Barron, 1980, 1985; Rouse, 1977; Williams and Bujak, 1977; Perch-Nielsen, 1985; Haq, 1980; Bujak, 1984; Bukry, 1973, 1975; Bujak Davies Group, 1987). Selected samples from the KSSD wells were also reprocessed and investigated by the Bujak Davies Group for the MMS. The siliceous microfossil interpretation for all six wells was done by Donald L. Olson of the MMS.

The Kodiak shelf siliceous microfossil assemblage thus far recovered (diatoms, radiolarians, silicoflagellates, and ebridians) is characterized by low diversity and low abundance relative to the siliceous assemblages identified from wells on the Bering Sea shelf (Turner and others, 1983a,b, 1984a,b,c). Because this assemblage did not contain most of the primary and secondary biostratigraphic marker species, the occurrences of less diagnostic taxa were used in the integrated biostratigraphy.

Strata are discussed in the order in which they were encountered. All depths are taken from the Kelly bushing.

Fossil occurrences are listed as highest and lowest stratigraphic occurrences and are expressed in relative frequency as follows: isolated (I), 1 specimen; rare (R), 2 to 10 specimens; frequent (F), 11 to 32 specimens; common (C), 32 to 100 specimens; and abundant (A), 100 to 320 specimens present in a sample. The wells are discussed in chronological (drilling) order as follows: KSST No. 1 (fig. 70, p. 146), KSST No. 2 (fig. 71, p. 151), and KSST No. 4A (fig. 72, p. 154), KSSD No. 1 (fig. 73, p. 165), KSSD No. 2 (fig. 74, p. 175), and KSSD No. 3 (fig. 75, p. 185). A preliminary correlation (fig. 76, p. 187) is discussed at the end of this chapter.

Paleobathymetry

For the most part, paleoenvironmental determinations are based on foraminiferal data and expressed in the following bathymetric terms: inner neritic (0 to 60 feet), middle neritic (60 to 300 feet), outer neritic (300 to 600 feet), upper bathyal (600 to 1,500 feet), and middle bathyal (1,500 to 3,000 feet). Where the data do not allow a precise bathymetric determination, the depth curve is placed on the appropriate boundary indicating a broadened depth range that includes the depth zones to either side of the line (e.g., outer neritic to upper bathyal).

Sampling and Paleoenvironment

The 30-foot aggregate ditch sample intervals in the six Kodiak COST wells were insufficient to establish a finely calibrated Plio-Pleistocene paleoclimatic curve because many of the samples in the upper parts of the wells contain a mixture of fossil materials from glacial and interglacial intervals. The net result is, for some of the wells, an apparent contradiction between periods of known glaciation (e.g., late Pleistocene) and a paleontologically indicated climatic regime of cool-temperate. Data from Deep Sea Drilling Project Leg 19 indicate that glaciation in the Bering Sea may have begun as early as the middle Pliocene (Scholl and Creager, 1973). Similar data exist for the Gulf of Alaska (Yakataga Formation) as far back as the late Miocene. The present-day climate of the Alaska Peninsula is defined as maritime (Karlstrom, 1964) to sub-polar maritime (Mitchell, 1958, cited in Detterman, 1986). Present circulation patterns of the Kodiak shelf are probably broadly similar to those that existed during glaciation. Evidence from Lower Cook Inlet, the Alaska Peninsula, and Kodiak Island indicates that most of the area was ice covered during glacial episodes. Recovery of vegetation in the area could have occurred within a relatively short time after glacial retreats, fed from refugia in southcentral Alaska or on Kodiak Island (Karlstrom, 1964; Karlstrom and Ball, 1969). These rapid changes in vegetation could have produced the above-noted mixture of glacial and interglacial fossil materials within sample intervals.

KSST NO. 1 WELL

KSST No. 1 well samples were processed by the MMS and examined by Ronald F. Turner and Donald L. Olson, but yielded no in situ,

precisely age-diagnostic foraminifera or diatoms. Most of the species recovered were long ranging. A major portion of the foraminiferal biostratigraphy for this well was developed by tabulating the coiling-direction trends in populations of the planktonic foraminifera Neogloboquadrina pachyderma. Ericson (1959) and Bandy (1960) established that the coiling directions in Recent and fossil forms of Neogloboquadrina pachyderma populations are indicative of the temperature of the water mass in which they lived. Because dextrally coiled forms dominate the population in warm water and sinistrally coiled forms dominate in cold water, these workers were able to use the changes in coiling ratios through time to document paleoclimatic cycles in the fossil record. When the warm- and cold-water trends revealed by such coiling direction changes in the KSST No. 1 well and other Kodiak wells are compared with conventional Neogene paleoclimate curves such as the one presented by Ingle (1967, p. 315), a general biostratigraphic zonation of the late Neogene sections for the wells can be erected (fig. 76, p. 187). The biostratigraphy of the sparse, low-diversity siliceous microfossil assemblage identified from the KSST No. 1 well generally supports that derived from foraminifera. The paleontological data and interpretations made in 1977 for the majority of the participants in the drilling program for the KSST wells were not made available to MMS (then USGS Conservation Division) geoscientists. Limited dinocyst and palynomorph data from studies conducted in 1987 for the MMS by the Bujak Davies Group are used here.

Unusual Reworked Fossil Elements

Reworked microfossils are relatively common in both the KSST and KSSD wells and have also been recovered from shallow core holes and bottom samples in the Gulf of Alaska. The reworking is related to both tectonic and glacioeustatic mechanisms. The most obvious and least confusing examples involve Paleogene fossils in Pleistocene and Holocene sediments. Reworked, pyritized Eocene benthic foraminifera are particularly conspicuous in the KSST No. 1 well. The relatively common presence of recycled palynomorphs as well as the late Eocene to late Miocene diatom Melosira clavigera (at 1,050 feet) is further evidence of substantial reworking in this well.

Perhaps the most interesting element of the reworked assemblage is worn and broken specimens of the tropical (to subtropical), shallow-water foraminifer Amphistegina. This genus was first recognized in Alaska in samples from the KSST No. 1 well (at 420, 480, and 570 feet) and the KSST No. 2 well (at 2,670 feet) by Turner (1976), who considered them to probably be reworked Tertiary forms possibly related to Amphistegina californica or Amphistegina simiensis, although the specimens did not compare well with very limited examples of these species from California examined from a collection held by Richard Brooks of ARCO Alaska. No thin sections were made nor were any available for study. The initial interpretation of these specimens being reworked was based on four factors: (1) the presence of reworked Eocene foraminifera throughout the well, (2) the association of some Amphistegina

specimens with a worn specimen of the Eocene-Oligocene species Cibicides cf. C. elmaensis (at 420 feet), (3) the established paleogeographic range of the two common Pacific coast Eocene species of Amphistegina (California, Washington, and Oregon; Cushman and Hanna, 1927; Cushman and McMasters, 1936; Todd, 1976), and (4) the worn condition of the specimens. Although the presence of a commonly reef-dwelling organism in Alaska could be considered somewhat unusual, Stoneley (1967) had previously reported a middle Eocene orbitoid foraminifera from a detrital limestone collected onshore in the nearby Yakutat district of the Gulf of Alaska, and Plafker (in press) reported the presence of in situ Amphistegina sp. and Discocyclusina sp. associated with late and middle Eocene fossils (including coral, coralline algae, bryozoans, etc.) in dredge samples from the Gulf of Alaska continental slope. The fact that the Kodiak shelf specimens and those from the Yakutat area of the Gulf of Alaska occur within a few hundred miles and two degrees of latitude of each other and represent the northernmost recorded occurrences of the genus was construed as circumstantial support for the interpretation that the Kodiak specimens are reworked Eocene elements and are conspecific with the Gulf of Alaska (Yakutat block) specimens.

As part of a reevaluation of the Kodiak microfossil assemblage for this report, the Amphistegina specimens were sent to C. W. Poag of the U.S. Geological Survey for identification. Poag (personal commun., 1987) suggested that they might represent a new species with affinities to Amphistegina bicirculata, a species described from the Recent of the Gulf of Elat (northern Red Sea) and the Pliocene of Jamaica (Larsen, 1976, 1978). He also suggested that the specimens be sent to Arne Rosenkrands Larsen of Dansk Olie and Gasproduktion for further examination. The specimens were subsequently sent to Dr. Larsen along with representative specimens dredged from the Gulf of Alaska supplied by George Plafker of the U.S. Geological Survey. Larsen (personal commun., 1988) stated that there were two species in the Kodiak Shelf assemblage, an inflated form that appeared to be Eocene or Oligocene in age, and a more lenticular form that has affinities with Amphistegina aucklandica. Amphistegina aucklandica has been described from middle Oligocene to middle Miocene sections in New Zealand, Midway Island, and Israel and is probably synonymous with Amphistegina vulgaris from the Miocene of France and Amphistegina bohdanowiczi from the Miocene of Poland. Larsen also indicated that the Eocene Gulf of Alaska specimens (all inflated forms) appeared to be older than those from the Kodiak wells, but that this might just be because of preservational differences. These observations are significant for a number of reasons, most of them ultimately related to elucidating the phylogeny, paleoecology, and biogeography of Amphistegina. There are, however, larger questions involved. For instance, is the presence of Amphistegina aff. A. aucklandica and Amphistegina spp. in Alaska primarily of paleoclimatologic/paleo-oceanographic significance (tropical-subtropical Tertiary) or of tectonostratigraphic significance (accretion of terranes originally deposited at much lower latitudes)?

There is currently a great deal of confusion concerning the identity of the Gulf of Alaska specimens; to date, they have not been figured or classified to the specific level in the published literature. Plafker (personal commun., 1987) believes that the Gulf of Alaska specimens are conspecific with (or closely related to) Amphistegina californica, a species reported from the Eocene of Washington. Keller and others (1984) and von Huene and others (1985) consider the Washington Amphisteginas to actually occur in the late Paleocene and, therefore, not to be coeval with the Yakutat dredge samples. Keller and others (1984) suggest instead that the Yakutat specimens are the same as the late middle to late Eocene Amphistegina parvula reported by Blondeau and Brabb (1983) from near San Jose, California. Because there are (at least) two quite different Gulf of Alaska tectonostratigraphic reconstructions that use the presence and "identity" of the dredged Amphisteginas to bolster their paleolatitudinal determinations, the unequivocal identity of the Alaskan species is important. The unfortunate fact may be that the poor preservational state of these specimens may preclude a definitive identification, although it might prove beneficial for Alphonse Blondeau or Earl Brabb of the U.S. Geological Survey to compare the Alaskan specimens with their California material and material from Washington. If, for instance, the inflated Kodiak specimens (found in the Prince William terrane) and those recovered from the Yakutat block (an apparently different terrane) were to prove to be the same species, this might well place new constraints on absolute and relative plate motions (timing and direction) and/or suggest a reevaluation of the Eocene paleoclimate.

To consider a rather extreme hypothesis, if Amphistegina aff. A. aucklandica in the KSST No. 2 well was to prove to be in situ, it would suggest a far warmer Pliocene marine climate in Alaska than has heretofore been recognized. Turner (1978), in a Gulf of Alaska exploratory well, recorded the presence of a juvenile delphinid tooth associated with an early Pleistocene to late Pliocene interglacial foraminiferal assemblage characterized by dextrally coiled populations of Neogloboquadrina pachyderma. The dolphin tooth was identified as belonging to an extant, warm-water species that does not presently range north of Point Conception, California (Donald Calkins, Alaska Department of Fish and Wildlife, personal commun., 1978). Modern Amphisteginas are limited by the 14 °C winter isotherm (Larsen, 1976), which roughly coincides with the latitude of Point Conception. In fact, Crouch and Poag (1979) reported the previously known northernmost occurrence of Amphistegina on the Pacific coast of North America from just south of Point Conception from a core taken offshore on the Santa Rosa-Cortes Ridge. Though highly unlikely, a much warmer Alaskan Neogene marine climate cannot be entirely ruled out without further study.

Another interesting area of speculation is the possible migration path of Amphistegina to Alaska. Porosorotalia, initially a tropical, shallow water genus first described from the Eocene of New Zealand, apparently moved northward along the western Pacific margin and evolved Neogene species (described from the Miocene of

Sakhalin Island, U.S.S.R. and various COST wells in the Alaska OCS) that were tolerant of cooler conditions. Perhaps the Alaskan Amphisteginas, particularly Amphistegina aff. A. aucklandica, represent an analogous Indo-Pacific dispersion. Alternatively, they could have come up from the Caribbean via a submerged isthmus as suggested by Crouch and Poag (1979) for Amphistegina gibbosa.

Another possibility is that Amphistegina aff. A. aucklandica is reworked from Miocene or Oligocene strata that have been completely eroded from Kodiak Island and are absent (or have yet to be encountered) offshore in the subsurface. This seems as plausible as an Eocene origin and more plausible than a subtropical Pliocene.

The Amphistegina aff. A. aucklandica specimens are presently considered to be reworked Tertiary elements. The inflated, probable Eocene Amphistegina species may be the same as those recovered nearby in the Yakutat dredge samples, although Larsen (personal commun., 1988) tends to discount this possibility. The presence of these tropical, shallow-water forms in Alaska, whatever their ages and taxonomic affinities, raises a host of tectonostratigraphic, biostratigraphic, paleoecologic, paleontologic, and biogeographic questions.

Late Pliocene to Early Pleistocene

The unsampled interval from the seafloor to 327 feet is considered to be late Pliocene to early Pleistocene (and Holocene) in age, in continuity with the interval directly underlying it. Shale velocity evidence from this and other Kodiak shelf wells indicates probable uplift of 3,000 to 5,000 feet resulting in the erosion of younger sediments (see Abnormal Formation Pressure chapter). The interval from 327 to 2,850 feet is late Pliocene to probable early Pleistocene in age (fig. 70, p. 146), based on the presence of dextrally coiled forms of Neogloboquadrina pachyderma, which are indicative of warmer water, interglacial conditions. The benthic foraminiferal assemblage includes Buccella frigida, Buccella inusitata, Cassidulina californica, Cassidulina limbata, Cassidulina norcrossi, Cassidulina reflexa, Cassidulina teretis, Cassidulina translucens, Cribrostomoides veleronis, Dentalina sp., Elphidiella hannah, Elphidium bartletti, Elphidium clavatum, Elphidium hughesi, Elphidium oregonense, Epistominella pacifica, Elphidium subarcticum, Epistominella smithi, Haplophragmoides spp., Lagena cf. L. sulcata, Pyrgo sp., Quinqueloculina arctica, Quinqueloculina seminulum, Recurvoides turbinatus, Rotalia subcorpulenta, Technitella melo, Trichohyalus bartletti, Trifarina fluens, Uvigerina cushmani, and Uvigerina juncea. Planktonic forms present include Globigerina sp., Globigerinita cf. G. glutinata (at 1,170 feet), and dextrally coiled Neogloboquadrina pachyderma. Echinoid spines, mollusc shell fragments, and arenaceous foraminiferal fragments are also present.

The dinocyst assemblage includes Filisphaera filifera, Impagidinium japonicum, Lingulodinium machaerophorum, Operculodinium centrocarpum, Reticulosphaera actinocoronata,

Spiniferites membranaceus, Spiniferites ramosus ramosus, and the brackish to freshwater species Peridinium sp. A. Also present are reworked specimens of Achomospaera spongiosa and the Eocene species Areosphaeridium diktyoplokus. Pollen and spores present are Betulaceoipollenites betuloides/infrequens, Cyathidites/Deltoidospora spp., Laevigatosporites ovatus, Lycopodiumsporites annotinioides, Osmundacidites claytonites, Piceaepollenites spp., Pinuspollenites spp., Alnipollenites spp. (= Polyvestibulopollenites verus), Selaginellaites selaginoides, Stereisporites antiquasporites, Taxodiaceaeipollenites hiatus, and Tsugaepollenites igniculus, and possibly reworked Polyodiidites favus, along with the fungal spores Exesisporites spp. and Microthyrites sp., and the marine alga, Tasmanites globulus.

The first siliceous microfossils were recovered at 780 feet. The assemblage is dominated by long-ranging species that are known from the middle Oligocene to the Pleistocene. Diatoms in this interval with ages ranging as young as late Pleistocene include Actinocyclus ehrenbergii, Actinocyclus ingens, Actinoptychus splendens, Actinoptychus cf. A. undulatus, Arachnoidiscus ehrenbergii, Aulacodiscus sp., Cocconeis costata, Cocconeis scutellum, Coscinodiscus marginatus, Grammatophora sp., Melosira sulcata, Navicula cf. N. pennata, Pinnularia sp., Stephanopyxis turris, Synedra sp., Thalassionema nitzschioides, and Thalassiothrix longissima. Additional specimens include reworked Melosira clavigera and Thalassionema cf. T. hirosakiensis. Also present are numerous siliceous spicule types. A fragment of the diatom Coscinodiscus pustulatus at 2,010 feet suggests that the interval from 2,010 to 2,850 feet could be as old as late Pliocene. The interval from 2,760 to 2,970 feet was not examined for diatoms because of insufficient sample material.

No calcareous nannofossil data were available.

Environment. The paleobathymetry ranged from inner to middle neritic between 327 and 450 feet, middle to outer neritic from 450 to 510 feet, upper bathyal from 510 to 1,380 feet, inner to middle neritic from 1,350 to 1,650 feet, and alternated between outer neritic to upper bathyal and middle to outer neritic from 1,650 to 2,850 feet (fig. 70). Miospore data indicate a cool-temperate climate.

Late Pliocene

The interval from 2,850 to 4,225 feet (TD) is late Pliocene in age on the basis of a foraminiferal assemblage similar to that of the overlying section, but characterized by the presence of deep-water arenaceous species. These deep-water forms include Bathysiphon sp., Cyclammina cancellata, Haplophragmoides sp., and Martinottiella cf. M. palida, along with increased numbers of upper bathyal calcareous species such as Epistominella pacifica, Epistominella smithi, and Uvigerina cf. U. hootsi. Haplophragmoides trullisata, which has been noted in the late Pliocene in other Kodiak shelf and Gulf of Alaska wells, is also present. The absence of sinistrally coiled Neogloboquadrina

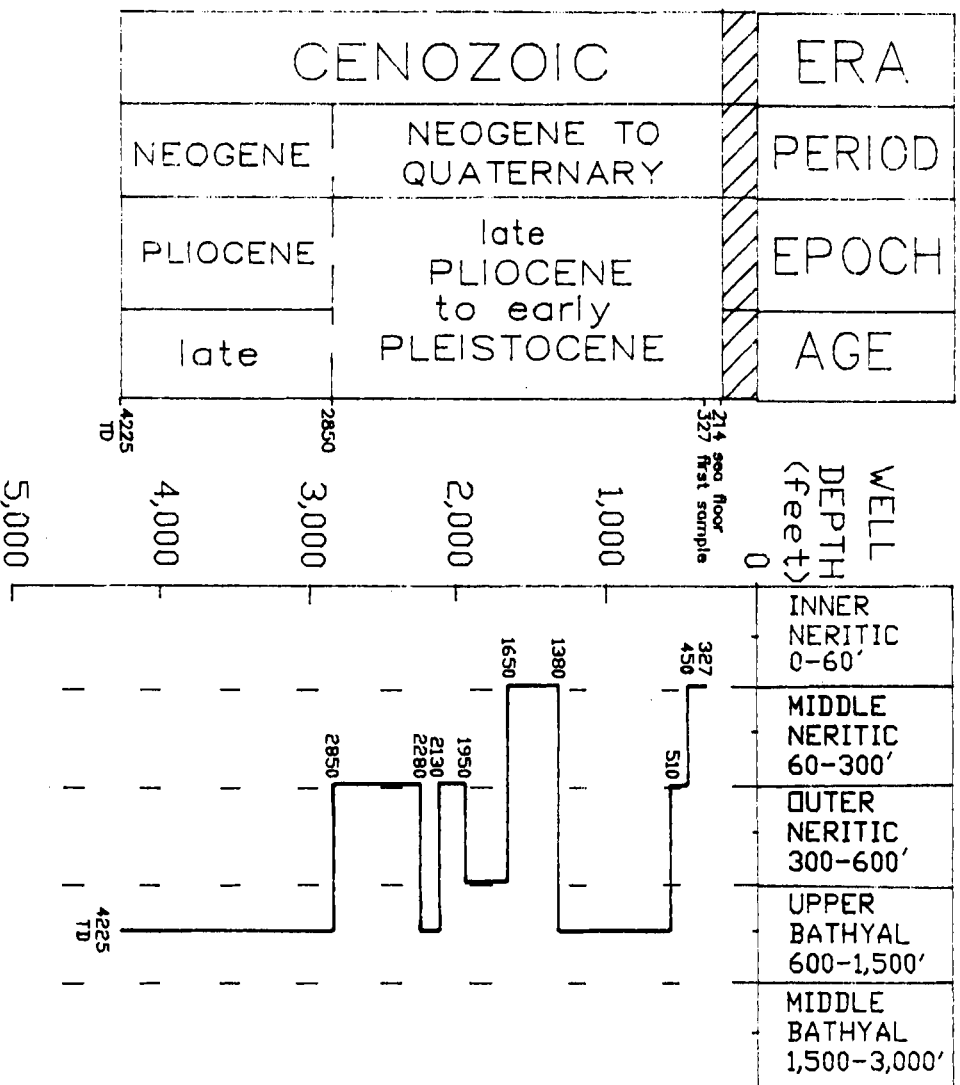


Figure 70. Biostratigraphy and paleobathymetry of the KSSST No. 1 well.

pachyderma, and the presence (at 3,270 feet) of the warm-water benthic species Bolivina interjuncta bicostata, suggest that this section represents a deep-water biofacies of a relatively warm water mass. Additional arenaceous foraminifera present in the interval include Ammonium? sp., Proteonia? sp., Psammosphaera? sp., and Reophax aff. R. scorpiurus. Additional calcareous foraminifera appearing in the late Pliocene interval include Cassidulina delicata, Elphidiella groenlandica, Nonionella turgida digitata, and Pyrgo cf. P. rothalia. Fragments of bivalves, gastropods, and echinoids are also present.

The dinocyst assemblage is similar to that of the overlying interval. Taxa first encountered in this interval are generally non-diagnostic or long ranging, with the exception of Filisphaera pilosa, which supports a late Pliocene age. Other species present include Spiniferites hexatypicus and possibly reworked Phthanoperidinium sp. An occurrence of Impagidinium cornutum at 2,970 feet, if not reworked, might suggest a late Miocene age but would contradict data from other fossil groups. Pollen and spores occurring in the interval include Carpinipites cf. C. spackmaniana and Ericipites antecursorioides, which generally support a Pliocene age. Also present are Compositae, Liquidambarpollenites sp., the freshwater alga Pediastrum boryanum, and fungal spores of the genus Pluricellaesporites.

A fragment of the diatom Thalassiosira cf. T. antiqua at 3,540 feet also supports a late Pliocene age for this interval. The diatom assemblage is similar to that of the overlying interval, with the addition of Synedra cf. S. ulna and Aulacodiscus cf. A. concentricus.

Environment. Paleoenvironments were upper bathyal throughout the Pliocene interval (fig. 70). Although there is insufficient palynomorph data to define a paleoclimate, there are some indications that this interval was somewhat warmer than the overlying Pleistocene section.

KSST NO. 2 WELL

Samples from the KSST No. 2 well contain few age-diagnostic foraminifera or diatoms. Major biostratigraphic divisions are based on rare diatom occurrences. The foraminiferal biostratigraphy is based primarily on paleoclimatic trends indicated by coiling-direction ratios in populations of the planktonic foraminifera Neogloboquadrina pachyderma (Ericson, 1959; Bandy, 1960; Bandy and others, 1969). These trends are similar to those described in the KSST No. 1 well. Other evidence comes from the occurrence of cold-water, benthic species such as Protoelphidium orbiculare, primarily an arctic species, and of the far less common Elphidium alaskense. Reworked specimens are common in this well, as they were in the KSST No. 1 well.

Pleistocene

The Pleistocene section of the KSST No. 2 well is subdivided into late Pleistocene (seafloor to 630 feet) and early to middle Pleistocene (630 to 2,160 feet) on the basis of diatoms, foraminifera, and stratigraphic position.

Late Pleistocene

The unsampled interval from the seafloor to the first sample at 450 feet is probably late Pleistocene (and Holocene) in age, in continuity with the interval directly underlying it. From 450 to 630 feet, the interval is late Pleistocene, with the bottom of the interval being based on diatom occurrences. The presence of the benthic foraminifera Elphidium alaskense above 630 feet suggests that this section was deposited in cold water. Other foraminifera in this interval include Buccella frigida, Buccella inusitata, Cassidulina californica, Cassidulina limbata, Cassidulina norcrossi, Cassidulina teretis, Cibicides fletcheri, Dentalina baggi, Elphidiella arctica, Elphidiella hannai, Elphidium bartletti, Elphidium clavatum, Elphidium frigidum, Elphidium oregonense, Nonionella labradorica, Oolina lineata, Quinqueloculina akneriana, Quinqueloculina arctica, Rotalia columbiensis, Trichohyalus bartletti, Trifarina angulosa, and Trifarina cf. T. hughesi. Other fossil material includes molluscan shell fragments, bryozoans, ostracodes, small bivalves and gastropods, barnacle fragments, spicules, echinoid spines and fragments, and serpulid worm tubes.

The only dinoflagellate observed in the late Pleistocene section is a reworked specimen of the late Jurassic dinoflagellate Gonyaulacysta jurassica. Pollen and spores occurring in the interval include Alnipollenites spp. (= Polyvestibulopollenites verus), Betulaceoipollenites betuloides/infrequens, Cyathidites/Deltoidospora spp., Laevigatosporites ovatus, Lycopodiumsporites annotinioides, Osmundacidites claytonites, Piceaepollenites spp., Pinuspollenites spp., Selaginellaites selaginoides, and reworked Ilexpollenites margaritus.

The siliceous microfossil assemblage is dominated by long-ranging species. Siliceous microfossils occurring in this interval with ages that range as young as late Pleistocene or Recent include Goscinodiscus marginatus, Melosira sulcata, and Thalassiosira cf. T. oestrupii.

Environment. Deposition of this section took place in cold water. Paleodepths were inner to middle neritic from 450 to 480 feet, middle to outer neritic from 480 to 600 feet, and inner to middle neritic from 600 to 630 feet (fig. 71, p. 151). The miospore assemblage indicates a cool-temperate climate.

Early to Middle Pleistocene

The interval from 630 to 2,160 feet is early to middle Pleistocene in age on the basis of diatom and dinoflagellate

occurrences. The top of the interval is based on the highest stratigraphic occurrence of Rhizosolenia cf. R. curvirostris (at 630 feet) and Actinocyclus oculatus and Thalassiosira nidulus (at 720 feet). The rest of the siliceous microfossil assemblage is similar to that of the overlying interval, with the addition of Actinocyclus cf. A. curvatulus, Actinocyclus ochotensis, Actinoptychus cf. A. undulatus, Arachnoidiscus ehrenbergii, Chaetoceros didymus, Cocconeis costata, Coscinodiscus cf. C. curvatulus, Coscinodiscus excentricus, Coscinodiscus cf. marginatus, Coscinodiscus cf. C. oculus iridis, Cymbella sp., Denticulopsis seminae, Navicula optima, Pterotheca sp., Rhizosolenia cf. R. barboi, Rhizosolenia hebetata hiemalis, Rhizosolenia cf. R. styliiformis, Thalassionema nitzschioides, Thalassiosira gravaida, Thalassiosira cf. T. nordenskioldii, Thalassiothrix longissima, the silicoflagellate Distephanus speculum, numerous siliceous microfossil fragments, and the reworked diatoms Coscinodiscus cf. C. symbolophorus, Cymbella debyi, Rhaphoneis sachalinensis, Rhizosolenia hebetata semispina, Thalassionema cf. T. hirosakiensis, Thalassiosira antiqua, and Thalassiosira gravaida (flat).

The foraminiferal assemblage is similar to that of the overlying interval, with the addition of Bucella depressa, Bucella cf. B. peruviana, Cassidulina delicata, Cassidulina reflexa, Cibicides conoides, Cibicides lobatulus, Dentalina decepta, Elphidiella groenlandica, Elphidium subarcticum, Epistominella pacifica, Epistominella smithi, Epistominella vitrea, Eponides cf. E. cribrorepandus, Fissurina lucida, Gaudryina arenaria, Glandulina laevigata, Karrerriella baccata, Lagena gracillima, Lagena semilineata, Lagena striata, Nonionella auricula, Nonionella basispinatum, Oolina melo, Polymorphina charlottensis, Protoelphidium orbiculare, Pullenia malkinae, Pullenia salisburyi, Pyrgo lucernula, Pyrgo rotalaria, Recurvoides turbinatus, Sigmomorphina trilocularis, Trichohyalis ornatissima, Trifarina fluens, Uvigerina cushmani, Uvigerina juncea, Uvigerina subperegrina, Virgulina complanata, and the planktonic species Globigerina bulloides. Frequent Pullenia malkinae occur between 1,800 and 1,890 feet. This species, although generally rare, has been noted in the Pliocene and early Pleistocene sections of other Kodiak COST wells and in some Gulf of Alaska wells. Rare, sinistrally-coiled Neogloboquadrina pachyderma, along with rare Elphidium alaskense and rare to abundant Protoelphidium orbiculare, indicate cold water conditions. Epistominella pacifica and Pullenia salisburyi are frequent to common over a short span between 690 and 780 feet. Increased populations of these species, particularly Epistominella pacifica, have been characteristic of the deeper water early Pleistocene to late Pliocene section of the other Kodiak COST wells. However, this short interval of abundance, which appears to be in a younger section here, may indicate an interglacial resurgence of an Epistominella pacifica population in the area. Deeper in the well, Epistominella pacifica does reappear in common to abundant numbers in a section dated as late Pliocene. Other fossil material in the early to middle Pleistocene interval includes molluscan shell fragments, bryozoans,

ostracodes, small bivalves and gastropods, barnacle fragments, and echinoid spines and fragments.

Well-preserved, disarticulated zoaria of the bryozoan Microporina articulata were recovered over the interval from 870 to 960 feet. The fossil specimens are identical to modern specimens from the present day Kodiak shelf. The erect, branching colonies are made up of short, tapering segments connected by flexible, chitinous joints (not preserved in the fossil material). This zoarial type, referred to as cellariiform, is generally considered an adaptation to moderately strong marine currents. The modern Kodiak specimens were collected in 1976 from water depths of 130 to 295 feet on the Northern Albatross Bank (Cuffey and Turner, 1987). Microporina articulata has been reported from arctic and subarctic waters worldwide (Osborn, 1950, 1952; Kluge, 1962). No previous fossil occurrence could be found in the literature, although it is not surprising that the species extends back at least into the Pleistocene.

A specimen of the dinocyst Impagidinium japonicum at 1,830 feet supports an age of no younger than early Pleistocene, although Jonathan Bujak (written commun., 1987) says it is possible that this species may not occur later than the Pliocene in the area, and therefore this may be a recycled specimen. No other dinocysts were recovered in this interval. Other palynomorphs first occurring in this interval are the fern spores Botrychium lanceolatum and Polypodioidites favus.

Environment. Between 630 and 1,660 feet, the paleobathymetry of this interval alternates between inner to middle neritic, middle neritic, and middle to outer neritic, with an interval of outer neritic to upper bathyal between 690 and 930 feet. From 1,650 to 2,160 feet, paleodepths were middle to outer neritic (fig. 71). Generally cold water conditions prevailed. The climate was cool-temperate, similar to that of the overlying section.

Probable Late Pliocene

The section from 2,160 to 4,307 feet (TD) is probably late Pliocene in age on the basis of diatoms and planktonic foraminifera. This age is based on the highest stratigraphic occurrences of the diatom Coscinodiscus cf. C. pustulatus and the silicoflagellate Ammodochium rectangulare at 2,160 feet, and the diatoms Coscinodiscus pustulatus, Stephanopyxis cf. S. horridus, Thalassiosira cf. T. decipiens, and Thalassiosira cf. T. usatschevii at 2,250 feet. This assemblage is similar to that found in the late Pliocene interval of the KSSD No. 1 and No. 3 wells. Ammodochium rectangulare is also present in the late Pliocene of the KSSD No. 1 well. The remainder of the siliceous microfossil assemblage is similar to that of the overlying interval, with the addition of the diatoms Arachnoidiscus cf. A. ehrenbergii, Denticulopsis cf. D. kamtschatica, Grammatophora sp., Porosira cf. P. glacialis, Stephanopyxis turris, Thalassiosira cf. T. gravis (flat), Xanthiopyxis cf. X. ovalis, the silicoflagellates Distephanus cf. D. speculum and Distephanus

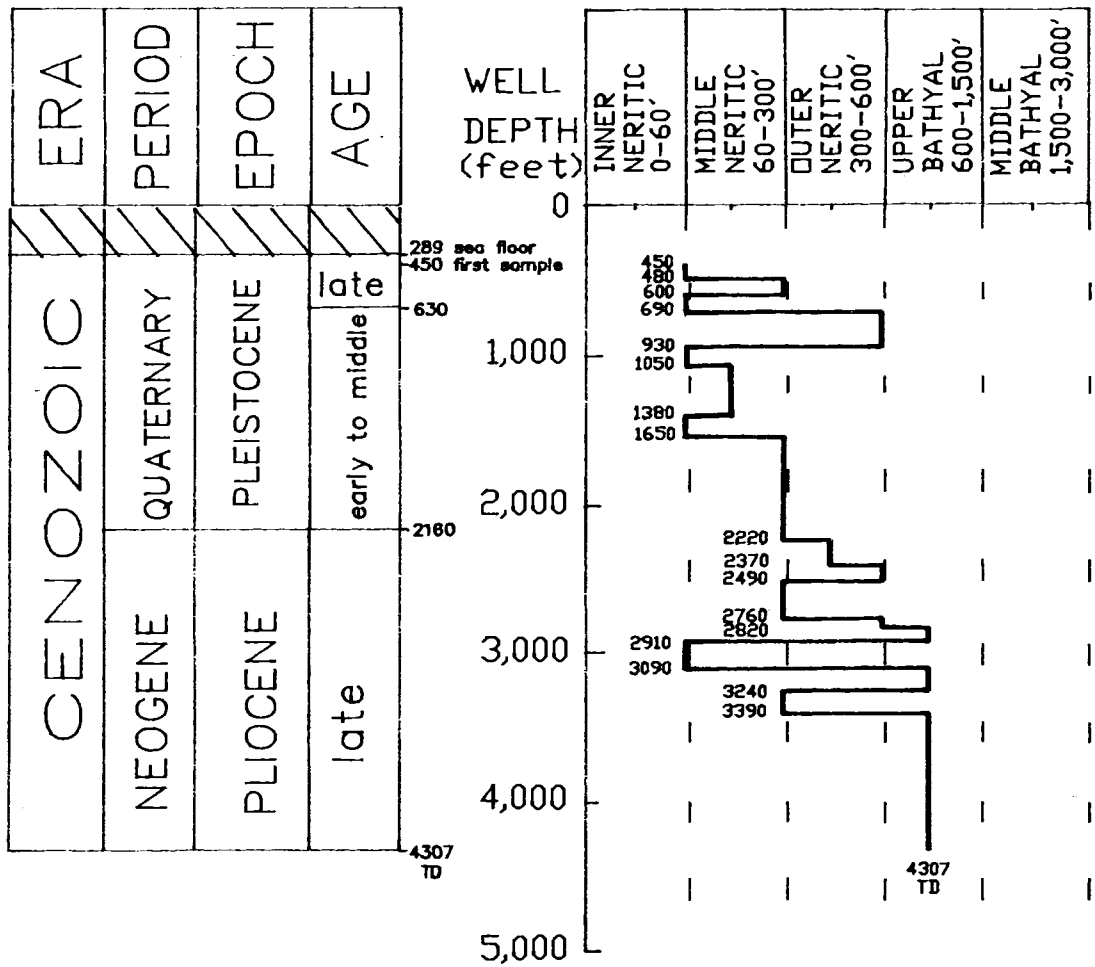


Figure 71. Biostratigraphy and paleobathymetry of the KSST No. 2 well.

speculum cf. longispinis, and the reworked diatom Cymbella cf. C. debyi.

Below 2,820 feet, several samples contained relatively abundant, predominantly dextrally coiled Neogloboquadrina pachyderma populations, which indicate warmer water conditions. This supports a probable late Pliocene age for the lower part of the well. The benthic foraminiferal assemblage from 2,160 to 4,307 feet is similar to that of the interval above, with the addition of Dentalina cf. D. pauperata, Elphidium cf. E. incertum, Fissurina cucurbitaesema, Nonionella miocenica stella, Nonionella cf. N. pulchella, Quinqueloculina seminulum, Rotalia subcorpulenta, and Triloculina tricarinata. Below 2,310 feet, Epistominella pacifica is frequent to common. Reworked specimens of Amphistegina aff. A. aucklandica, which was observed in several samples in the upper part of the KSST No. 1 well, occur at 2,670 feet (see discussion in KSST No. 1 well section). Other fossil remains present include bivalve fragments and small bivalves, echinoid fragments and spines, barnacle plates, and ostracodes.

The dinocyst assemblage is similar to that of the interval above. Additional species present include Filisphaera pilosa, which indicates a possible age of no younger than late Pliocene, Filisphaera filifera, Impagidinium sp., Spiniferites membranaceus, Spiniferites ramosus ramosus, the reworked Eocene species Areosphaeridium diktyoplokus and the reworked Miocene species Impagidinium cornutum. The pollen and spore assemblage is also similar to that of the overlying section, with the addition of the long-ranging moss spore Stereisporites antiquasporites. The fungal genus Microthyrites also has its highest occurrence in this interval.

Environment. Paleoenvironments were middle to outer neritic from 2,160 to 2,220 feet. Conditions varied between outer neritic to upper bathyal and middle to outer neritic between 2,220 and 2,910 feet, and inner to middle neritic depths prevailed from 2,910 to 3,090 feet. From 3,090 to 4,307 feet, the paleoenvironments were upper bathyal with one short middle to outer neritic interval from 3,240 to 3,390 feet (fig. 71). The presence of dextrally coiled Neogloboquadrina pachyderma throughout the interval indicates generally warmer water conditions.

KSST NO. 4A WELL

The foraminiferal biostratigraphy of the rather shallow KSST No. 4A well is similar to that of the KSST No. 1 and KSST No. 2 wells in that few age-diagnostic species are present. Diatom occurrences and paleoclimatic comparisons based on coiling direction ratios of Neogloboquadrina pachyderma were the primary basis for age determinations.

Pleistocene

The Pleistocene section is subdivided into probable early to middle Pleistocene (seafloor to 479 feet) and early Pleistocene (479 to 1,010 feet) on the basis of foraminifera and stratigraphic position.

Probable Early to Middle Pleistocene

The section from the seafloor to 479 feet was not sampled. This interval is considered to be probable early to middle Pleistocene (and Holocene) in age on the basis of its stratigraphic position overlying sediments of early Pleistocene age.

Early Pleistocene

The interval from 479 to 1,010 feet is early Pleistocene in age on the basis of dominantly dextrally coiled Neogloboquadrina pachyderma that appear at 590 feet and persist to the base of the section. Epistominella pacifica and Pullenia salisburyi are common to abundant below 680 feet. Pullenia malkinae, which is present in the Pliocene and early Pleistocene in some of the other wells in the Gulf of Alaska area, appears at 890 feet. The foraminiferal assemblage present is quite similar to that observed in the early Pleistocene to late Pliocene section of the KSST No. 1 and KSST No. 2 wells. Additional species observed in the KSST No. 4A well include Buliminella elegantissima, Eosyrinx curta, Fissurina marginata, Lagena apiopleura, and Pullenia salisburyi. Also present are molluscan shell fragments, barnacle plates, echinoid spines, spicules, a fish tooth (salmonid?) and rare Radiolaria.

No dinocysts were found in the samples analyzed. The spore and pollen assemblage consists of non-diagnostic or long-ranging species that indicate a Plio-Pleistocene age. The microflora includes Alnipollenites spp. (= Polyvestibulopollenites verus), Cyathidites/Deltoidospora spp., Laevigatosporites ovatus, Lycopodiumsporites annotinioides, Osmundacidites claytonites, Piceapollenites spp., Pinuspollenites spp., Pterocaryapollenites stellatus, (= Polyatriopollenites stellatus), possibly reworked specimens of Carpinipites cf. C. spackmaniana, and possibly reworked specimens of Caryapollenites simplex and Tsugaepollenites igniculus, the marine alga Tasmanites globulus, and the fungal spore Exesisporites spp.

The siliceous microfossil assemblage, like those of the KSST No. 1 and KSST No. 2 wells, consists of species that range into the late Pleistocene. Diatom species present include Actinocyclus ochotensis, Cocconeis costata, Coscinodiscus cf. C. excentricus, Coscinodiscus cf. C. pustulatus, Melosira sulcata, Thalassiosira cf. T. oestrupii, Thalassiothrix longissima, and reworked specimens of Actinocyclus oculatus and Denticulopsis cf. D. dimorpha.

Environment. Paleodepths range from middle to outer neritic from 479 to 530 feet, and outer neritic to upper bathyal from 530 to 650 feet. Upper bathyal environments begin at 650 feet and

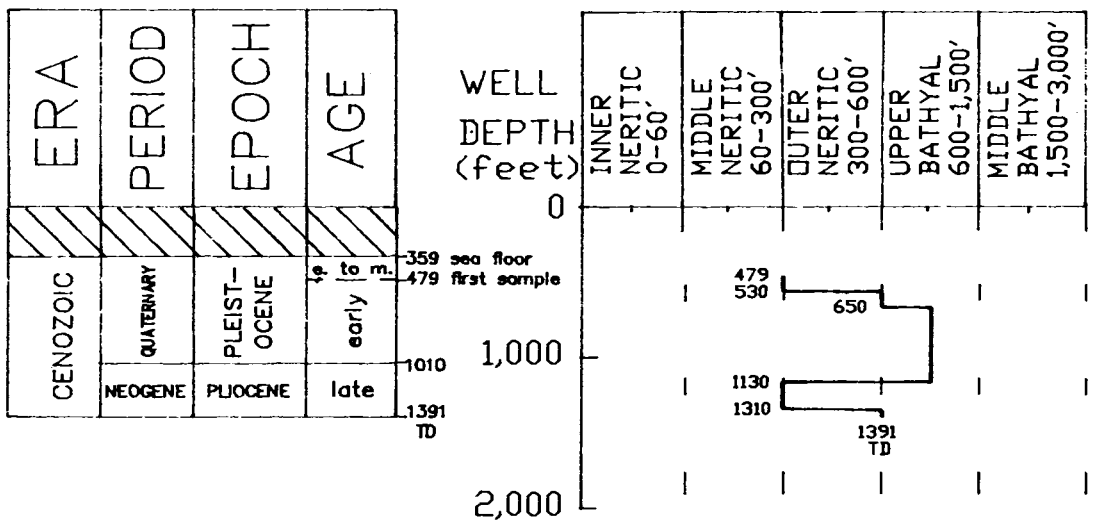


Figure 72. Biostratigraphy and paleobathymetry of the KSST No. 4A well.

continue to 1,010 feet (fig. 72). The paleoclimate was probably cool-temperate.

Late Pliocene

The interval from 1,010 to 1,391 feet (TD) is late Pliocene in age on the basis of diatom and foraminifera occurrences. This age is based on the highest stratigraphic occurrence of the diatoms Coscinodiscus cf. C. pustulatus, Stephanopyxis cf. S. horridus, and Thalassiosira cf. T. antiqua (at 1,010 feet) and Thalassiosira antiqua (at 1,100 feet). This assemblage is similar to that found in the late Pliocene of the KSST No. 2 and KSSD No. 1 and No. 3 wells. Additional diatom species with highest occurrences in this interval include Actinocyclus cf. A. curvatulus, Bacteriosira fragilis, Coscinodiscus cf. C. excentricus, Coscinodiscus marginatus, Denticulopsis seminae, Grammatophora sp., Stephanopyxis turris, Tabellaria sp., Thalassiosira antiqua, Thalassiosira gravis, Thalassiosira oestrupii, and Xanthiopyxis ovalis.

The foraminiferal assemblage in the late Pliocene interval of the KSST No. 4A well is similar to that of the overlying section and to the early Pleistocene and late Pliocene assemblages in the KSST No. 1 and No. 2 wells, with Elphidiella nitida being the only additional species. Epistominella pacifica is rare to common, and rare, dextrally coiled Neogloboquadrina pachyderma are present.

The pollen and spore assemblage is similar to that of the overlying section.

Environment. Upper bathyal paleoenvironments are indicated from 1,010 to 1,130 feet, middle to outer neritic environments from 1,130 to 1,310 feet, and outer neritic to upper bathyal environments from 1,310 to 1,391 feet (fig. 72). Although there are no other paleoclimate indicators, the presence of dextrally coiled Neogloboquadrina pachyderma indicates warmer water conditions compared with the overlying interval.

KSSD NO. 1 WELL

The biostratigraphic interpretations of the KSSD No. 1, KSSD No. 2, and KSSD No. 3 wells are primarily based on the integration of a study by Anderson, Warren, and Associates (1977a,b,c) with data from a recent study conducted for the MMS by the Bujak Davies Group (1987). The foraminifera and diatom assemblages were also investigated by John A. Larson and Donald L. Olson of the MMS. The Bryozoa were identified by Ronald F. Turner of the MMS. Extensive reworking, caving, and the absence of most age-diagnostic index microfossils preclude assignments of specific biostratigraphic microfossil zones.

Pleistocene

The Pleistocene section of the KSSD No. 1 well is subdivided into late Pleistocene (seafloor to 1,850 feet), middle Pleistocene

(1,850 to 2,660 feet), and early Pleistocene (2,660 to 3,110 feet) on the basis of diatoms, foraminifera, and stratigraphic position.

Late Pleistocene

The unsampled interval from the seafloor to 1,670 feet is considered to be possible late Pleistocene (and Holocene) in age, in continuity with the sampled interval immediately below it. From 1,670 to 1,850 feet, the section is probably late Pleistocene in age. The microfossils recovered are generally non-age-diagnostic, often ranging into the Holocene. A late Pleistocene age was inferred primarily from the stratigraphic position of the interval.

Diatom species within this interval with age ranges as late as late Pleistocene are Coscinodiscus excentricus, Coscinodiscus marginatus, Coscinodiscus oculus iridis, Stephanopyxis turris, Thalassiosira gravida, Thalassiosira oestrupii, and Thalassiothrix longissima.

The calcareous nannofossils identified from this interval are Coccolithus carteri and Gephyrocapsa caribbeanica, both of which range as late as the Pleistocene.

The dinocysts recovered in situ from this interval are generally long-ranging, non-age-diagnostic forms. Reworked older species include the Cretaceous species Ovoidinium verrucosum and Sirmiodinium grossii. The pollen and spores within this interval are also mostly long ranging. These include Alnipollenites sp. (= Polyvestibulopollenites verus), Betulaceoipollenites sp., Caryapollenites sp., Ericipites sp. (tetrad), Laevigatosporites spp., Lycopodiumsporites spp., Nyssapollenites sp., Osmundacidites sp., Piceapollenites sp., Pinuspollenites sp., Polypodiaceae, Sphagnumsporites sp., Taxodiaceapollenites sp., Tsugaepollenites sp., and undifferentiated bisaccate pollen. Also present are marine algae assignable to the Tasmanaceae. Probable reworked pollen in the interval include Boisduvalia sp., Ilexpollenites sp., Juglanspollenites sp., Pterocaryapollenites sp., and Ulmipollenites sp.

The foraminifera in this section of the well include Bolivina decussata, Buccella frigida, Buccella tenerrima, Cassidulina californica, Cassidulina minuta, Cassidulina cf. C. norcrossi, Cassidulina subglobosa, Cassidulina teretis, Cibicides conoides, Cibicides fletcheri, Elphidiella cf. E. frigidum, Elphidiella hannai, Elphidiella cf. E. oregonense, Elphidium cf. E. bartletti, Elphidium clavatum, Elphidium cf. E. discoidale, Epistominella bradyana, Epistominella pacifica, Lagena spp., Nonionella auricula, Quinqueloculina compacta, Rotalia columbiensis, and Trifarina fluens. Planktonic foraminifera include Globigerina bulloides. Molluscan shell fragments are frequent to common throughout the interval, and sponge spicules and echinoid fragments are consistently present.

Environment. The environment of deposition indicated by the foraminiferal assemblages was middle to outer neritic from 1,670 to 1,850 feet (fig. 73, p. 165). The Bujak Davies Group considered the climate to be cool-temperate on the basis of palynology.

Middle Pleistocene

The interval from 1,850 to 2,660 feet is considered to be middle Pleistocene based on the occurrence of the diatom Thalassiosira nidulus (at 1,850 feet) and the silicoflagellate Distephanus octonarius (at 1,940 feet). Thalassiosira nidulus occurs in the middle Pleistocene in the KSSD No. 2 and KSSD No. 3 wells. Distephanus octonarius is also a middle Pleistocene marker in the KSSD No. 3 well. The siliceous microfossil assemblage is similar to that of the overlying interval, with the addition of the diatoms Actinocyclus divisus, Actinocyclus ochotensis, Biddulphia aurita, Coscinodiscus sp., Coscinodiscus asteromphalus, Coscinodiscus lineatus, Navicula optima, Porosira glacialis, Rhabdonema sp., Thalassiosira excentrica, and Thalassionema nitzschioides. Also occurring in this section is the silicoflagellate Distephanus speculum and the radiolarian Spongodiscus sp. Reworked older siliceous elements include the diatoms Coscinodiscus marginatus fossilis, Denticulopsis kantschatica, Stephanopyxis horridus, Thalassiosira decipiens, and the ebridian Ebriopsis antiqua.

The calcareous nannofossil assemblage contains Coccolithus doronicoides, Coccolithus pelagicus, Cricolithus sp., Gephyrocapsa sp., and reworked Dictyococcites bisectus.

Additions to the dinocyst assemblage include Operculodinium centrocarpum, Selenopemphix nephroides, Spiniferites spp., and Spiniferites mirabilis. The assemblage also includes reworked Eocene Areosphaeridium diktyoplokus and Jurassic Gonyaulacysta jurassica. The pollen and spore assemblage is similar to that of the overlying interval, but also contains additional long-ranging taxa such as Chenopodiaceae, Compositae (Helianthus sp.), Laevigatosporites ovatus, Malvaceae, and Osmundacidites claytonites, along with probable reworked specimens of Faguspollenites sp., Tiliaepollenites sp., and Tsugaepollenites igniculus.

The foraminiferal assemblage is similar to that of the overlying section, with the addition of Cassidulina islandica, Cassidulina limbata, Cassidulina translucens, Cibicides lobatulus, Cibicides mckannai, Dentalina spp., Epistominella exigua, Nodosaria spp., Oolina spp., Oolina williamsoni, Polymorphina sp., Quinqueloculina akneriana, Uvigerina cushmani, and Uvigerina cf. U. peregrina. Also appearing near the base of this interval are Eilohedra levicula, Fissurina lucida, Pullenia salisburyi, Uvigerina cf. U. juncea, and rare Virgulina cf. V. fusiformis. Planktonic foraminifera occurring in the interval are Globigerina quinqueloba and sinistrally coiled Neogloboquadrina pachyderma. Molluscan shell fragments are frequent to common throughout the

interval, and sponge spicules and echinoid fragments are consistently present.

Environment. Paleoenvironments in this interval are middle to outer neritic from 1,850 to 2,000 feet, and outer neritic to upper bathyal from 2,000 to 2,360 feet. From 2,360 feet, the environments of deposition are considered to be outer neritic to upper bathyal down to the base of the interval at 2,660 feet (fig. 73, p. 165). Although the paleoclimate according to the pollen was cool-temperate, the presence of Coccolithus pelagicus and sinistral Neogloboquadrina pachyderma indicate water temperatures that were cold. Wise and Wind (1976) indicate that modern forms of Coccolithus pelagicus have a temperature range of 6° to 14° C. Coccolithus pelagicus is limited to cold water and high latitudes in its distribution (Haq, 1980).

Early Pleistocene

From 2,660 to 3,110 feet, the section is early Pleistocene in age. No strictly age-diagnostic microfossils were found. The age was inferred from the stratigraphic position of the section and evidence of climatic moderation and environmental change related to deeper water as reflected by foraminifera occurrences. Evidence of warmer water, indicating probable early Pleistocene conditions, includes sporadic occurrences of dextrally coiled Neogloboquadrina pachyderma, consistent occurrences of common to abundant Epistominella pacifica, the first downhole occurrences of Melonis pompilioides (frequent), Virgulina cf. V. fusiformis (frequent to common), and consistent appearances of Pullenia salisburyi. The remainder of the foraminiferal assemblage is similar to that of the overlying interval, with the addition of Cassidulina cf. C. cushmani, Dentalina soluta, Fissurina spp., Karrerella baccata, Lenticulina sp., Melonis cf. M. barleeianum, Uvigerina sp., and Uvigerina peregrina. Additional planktonic species include Globigerinita uvula and Globigerina woodi var. Other biotic constituents present include molluscan shell fragments, echinoid fragments, and sponge spicules.

The calcareous nannofossil assemblage is similar to that of the overlying section, with the addition of Braarudosphaera bigelowi and Cyclococcolithina leptopora.

No new siliceous microfossil species appeared in this interval.

The dinocyst assemblage includes the additional species ?Operculodinium sp. and Filisphaera filifera. The pollen and spore assemblage is similar to that of the overlying section, with the addition of Caryapollenites simplex, Compositae (Taraxacum sp.), Cyathidites/Deltoidospora spp., Epilobium sp., Lycopodiumsporites annotinioides, Polemoniaceae, Polypodiidites favus, Salixpollenites sp., Selaginellaites selaginoides, Sphagnumsporites antiquasporites, and Taxodiaceapollenites hiatus.

Environment. Depositional environments in the interval were middle to lower bathyal with cool-temperate climatic conditions (fig. 73, p. 165).

Pliocene

The Pliocene section of the well is subdivided into late Pliocene (3,110 to 3,560 feet) and early Pliocene (3,550 to 4,880 feet) on the basis of diatom, silicoflagellate, and foraminiferal data.

Late Pliocene

The interval from 3,110 to 3,560 feet is late Pliocene in age based on the occurrence of the silicoflagellate Ammodoichium rectangulare and the diatoms Thalassiosira cf. antiqua (at 3,110 feet), and Stephanopyxis horridus and Thalassiosira antiqua (at 3,200 feet). This assemblage is similar to that of the Pliocene interval of the KSST No. 2, KSST No. 3, and KSSD No. 3 wells. The lower boundary of the interval is based on the lowest stratigraphic occurrences of Thalassiosira nidulus (at 3,380 feet) and Coscinodiscus excentricus and Thalassiosira gravis (at 3,560 feet). Additional siliceous species with highest occurrences in this interval are the diatoms Actinocyclus cf. A. ellipticus, Actinocyclus cf. A. ingens, Asterolampra marylandicus, Chaetoceros sp., Denticulopsis kamtschatica, Denticulopsis seminae fossilis, Stephanopyxis dimorpha, Thalassiosira lineatus, and reworked Cladogramma dubia. The Radiolaria Conosphaera sp., Sphaeropyle robusta, Xiphospira circularis, and an Acanthodesmid are also present.

The calcareous nannofossil assemblage is similar to that in the overlying section, with the addition of reworked Dictyococcites sp.

The foraminiferal assemblage is similar to that of the overlying section, with the addition of Bulimina subacuminata, Cassidulina yabei, Gaudryina laevigata, Glandulina laevigata, Globobulimina affinis, Globobulimina pacifica, Haplophragmoides spp., Nonionella pulchella, and Uvigerina hispidocostata. Virgulina cf. V. pertusa, recovered from a sidewall core at 3,542 feet, also occurred in the early part of the late Pliocene section of the St. George COST No. 1 and No. 2 wells (Turner and others, 1984a,b). The planktonic species Globorotalia cf. G. inflata also appears at 3,542 feet (swc), and supports a late Pliocene age (Stainforth and others, 1975; Boersma, 1978). The planktonic species Globigerina cf. G. quadrilatera is also present in the interval. Molluscan shell fragments are rare in the lower part of the section. Numerous fish fragments are present.

The dinocyst assemblage is similar to that of the overlying section, with the addition of the probable late Pliocene species Filisphaera pilosa and Impagidinium japonicum along with Achomosphaera ramulifera, Spiniferites membranaceus, Spiniferites ramosus ramosus, and Tectatodinium pellitum. Probable reworked

specimens of Reticulosphaera actinocoronata also appear. Additional pollen and spores of highest occurrence appearing in this interval are Betulaceoipollenites betuloides/infrequens, Carpinipites spackmaniana, Compositae (Artemesia), Ericipites antecursorioides, Gramineae, Onagraceae, and Selaginellaites sinuites. Also present are the algal cysts Leiosphaeridia sp. and Tasmanites globulus, the fungal spore Exesisporites spp., and reworked Diervillapollenites sp. and Momipites triorbicularis.

Environment. The paleodepths in this interval ranged from middle to lower bathyal (fig. 73, p. 165). The paleoclimate was cool-temperate.

Early Pliocene

The interval from 3,560 to 4,880 feet is probable early Pliocene in age, although it contains no definitive age-diagnostic microfossils. The age of the section is based primarily on stratigraphic position.

The dinocyst assemblage is similar to that of the overlying section, with the addition of ?Baltisphaeridium sp., Impagidinium patulum, Lejeunecysta sp., Tuberculodinium vancampoe, and reworked Cretaceous specimens of Luxadinium propatum and Odontochitina operculata. The pollen and spore assemblage is similar to that of the overlying interval, with the addition of Ericipites compactipolleniatus, Pachysandra spp., Pterocaryapollenites stellatus (= Polyatriopollenites stellatus), and reworked Triassic to Cretaceous Vitreisporites pallidus. Also present are cysts of the freshwater algae Pterospermopsis sp. and Pediastrum boryanum.

The siliceous microfossil assemblage is similar to that of the overlying interval, with the addition of the diatoms Cocconeis scutellum, Coscinodiscus pustulatus, and Thalassiosira sp.

The calcareous nannofossil assemblage is similar to that of the overlying interval, with the addition of Coccolithus pliopelagicus, Coccolithus productus, Gephyrocapsa cf. G. oceanica, and reworked ?Cyclicargolithus sp. and Dictyococcites cf. D. scrippsae.

The foraminiferal assemblage in this interval is similar to that of the overlying interval. Additional species include Bulimina ovula, Bulimina subcalva, Cyclammina cancellata, Cyclammina pacifica, Elphidium cf. E. acutum, Haplophragmoides deformes, Haplophragmoides trullissata, Nonionella digitata, Pullenia malkinae, Quinqueloculina cf. Q. frigida, Saccamina sp., Sphaeroidina cf. S. variabilis, Textularia cf. T. abbreviata, Textularia cf. T. flinti, and Uvigerina senticosa. Also present is the planktonic species Globorotalia pseudopima. According to Kennett and Srinivasan (1983), this species first appears at the N19/N20 zone boundary in the early Pliocene, supporting an early Pliocene age for this interval. Molluscan shell fragments are rare at the top of the interval, increasing to frequent below 4,100 feet.

Environment. Paleodepths were middle to lower bathyal throughout the interval (fig. 73, p. 165). Paleoclimatic conditions were cool-temperate.

Miocene

The Miocene section of the well is subdivided into middle to late Miocene (4,880 to 5,900 feet) and early? to middle Miocene (5,900 to 6,142 feet) on the basis of foraminifera and dinocyst occurrences.

Middle to Late Miocene

The interval from 4,880 to 5,900 feet is middle to late Miocene in age on the basis of foraminifera occurrences. Regionally useful species present in the interval include Ammonia aff. A. japonica (at 5,210 feet), which has appeared in the Miocene and Oligocene sections of several Bering Sea COST wells (Turner and others, 1983a,b, 1984a,b,c), Gyroidina altiformis (at 4,880 feet), Gyroidina rotundimargo (at 5,840 feet), and Gyroidina soldanii (at 5,510 feet). Species of Gyroidina, including Gyroidina soldanii, have not been noted in sediments younger than Miocene in the Gulf of Alaska (Lagoe, 1978, 1983; Rau and others, 1983). Also appearing in the interval are Bolivina cf. B. pacifica, Chilostomella sp., Eggerella sp., Haplophragmoides scutulium, Martinottiella communis, Planulina cf. P. wuellerstorfi, Plectofrondicularia californica, and Sigmomorphina sp.

The siliceous microfossil assemblage is similar to that of the overlying interval, with the addition of the Radiolaria Sphaeropyle sp. and Stylocentarium acuilonium. Frequent unidentified Radiolaria were also observed in foraminifera samples from 4,820 to 5,300 feet. Unaltered siliceous microfossils were not noted below 5,480 feet, although pyritized forms were observed in the foraminifera samples.

The calcareous nannofossil assemblage is similar to that of the overlying section, with the addition of Cyclococcolithina cf. C. macintyreii.

The dinocyst assemblage is similar to that of the overlying interval, with the addition of Lejeunecysta cf. L. fallax, the late Miocene or older Spiniferites frigidus, and the brackish to freshwater species Peridinium sp. A. Rare reworked specimens of Cordosphaeridium gracile, Cordosphaeridium cf. C. fibrospinosum, Lejeunecysta paratenella, Phthanoperidinium comatum, and Wetzeliella sp. are also present. The pollen and spore assemblage is similar to that of the overlying section, with the addition of Graminidites sp.

Environment. Depositional environments from 4,880 to 5,900 feet alternate between upper, middle, and lower bathyal throughout the interval, with a brief outer neritic to upper bathyal interval indicated between 5,720 and 5,810 feet (fig. 73, p. 165). The paleoclimate was probably cool-temperate.

Early? to Middle Miocene

The interval from 5,900 to 6,142 feet is early? to middle Miocene in age based on an occurrence of the dinoflagellate Systematophora ancyrea (at 5,900 feet). The Bujak Davies Group believes that this species indicates an early to middle Miocene age (Bujak Davies Group, oral commun., 1987). It is also present in the same stratigraphic position in the KSSD No. 2 well (at 6,720 feet) and KSSD No. 3 well (at 7,220 feet).

The palynomorph assemblage is similar to that of the overlying section, with the addition of Nuphar spp. and the fungal spore Pluricellaesporites spp. Reworked specimens of the Eocene dinocysts Glaphyrocysta exuberans and Wetzeliella cf. W. ovalis are also present.

The foraminiferal assemblage is very similar to that of the above interval, but it is relatively sparse. Globulina sp. is the only new species observed. With the exception of molluscan shell fragments, other biotic constituents are quite rare.

The calcareous nannofossil assemblage is similar to that of the overlying interval.

Environment. The environments of deposition in this interval were probably upper bathyal (fig. 73, p. 165). Pollen data tentatively suggest a cool-temperate climate.

Eocene

The Eocene section is subdivided into middle Eocene (6,142 to 7,370 feet) and early Eocene (7,370 to 8,540 feet), primarily on the basis of the dinocyst assemblage. The upper boundary at 6,142 feet denotes a regional unconformity that separates the overlying Neogene section from the underlying Paleogene section.

Middle Eocene

The interval from 6,142 to 7,370 feet is considered to be possible middle Eocene in age on the basis of the dinocysts Glaphyrocysta exuberans at the top of the interval, Cordosphaeridium gracile (at 6,170 feet), Deflandrea sagittula (at 6,200 feet), Deflandrea cf. D. wetzellii (at 6,380 feet), and the Eocene dinocyst Areosphaeridium diktyoplokus. The dinocysts Systematophora placacantha (at 6,230 feet) and Phthanoperidinium alectrolophum (at 6,410 feet) and the fungal spore Pesavis tagluensis (at 7,010 feet) also support an Eocene age. Other dinocysts occurring within this interval are Cordosphaeridium cf. C. fibrospinosum, Deflandrea sp., Deflandrea aff. D. diebeli, Glaphyrocysta sp., Impletosphaeridium insolitum, Lejeunecysta paratenella, Lentinia sp., Operculodinium centrocarpum, ?Phthanoperidinium amoenum, Phthanoperidinium comatum, Spiniferites sp., Spiniferites membranaceus, Spiniferites mirabilis, Spiniferites ramosus ramosus, Systematophora sp., Wetzeliella sp., Wetzeliella cf. W. ovalis, and unidentified chorate dinocyst

fragments, along with possibly reworked Lanternosphaeridium radiatum and Luxadinium propatulum.

The pollen and spore assemblage contains Alnipollenites spp. (= Polyvestibulopollenites verus), Betulaceoipollenites betuloides/infrequens, Carpinipites spackmaniana, Caryapollenites simplex, Cyathidites/Deltoidospora sp., Ericipites antecursorioides, Juglanspollenites sp., Laevigatosporites sp., Laevigatosporites ovatus, Lycopodiumsporites annotinioides, Osmundacidites claytonites, Piceaepollenites sp., Pinuspollenites sp., Pluricellaesporites sp., Polypodiaceae, Sphagnumsporites antiquasporites, Taxodiaceaeipollenites hiatus, Tiliaepollenites sp., Tsugaepollenites igniculus, undifferentiated bisaccate pollen, the fungal spore Microthyrites spp., the freshwater alga Pediastrum boryanum, the marine alga Tasmanites globulus, and the reworked Late Cretaceous pollen Wodehouseia spinata. Several of the species are also present in the overlying Miocene interval, reflecting a combination of the long range of some of the species and contamination due to the caving of younger forms (Filisphaera pilosa and Impagidinium japonicum).

A new foraminiferal assemblage appears in this interval, with a large proportion of agglutinated species, and a minor component of calcareous species. Species present include Ammobaculites spp., Ammodiscus sp., Ammosphaeroidina sp., Bathysiphon cf. B. alexanderi, Bathysiphon sanctaerucis, Cibicides cf. C. pseudowuellerstorfi, Cyclammina cf. C. cancellata, Cyclammina pacifica, Cyclammina spp., Denticulina spp., Eggerella spp., Gaudryina spp., Glomospira sp., Haplophragmoides cf. H. crassus, Haplophragmoides cf. H. deformes, Haplophragmoides cf. H. excavata, Haplophragmoides cf. H. indentatus, Haplophragmoides cf. H. obliquicameratus, Lenticulina sp., Nodosaria sp., Planorbulina sp., Quinqueloculina sp., Rheophax sp., Saccamina sp., Trochammina spp., and Virgulina sp. Echinoid and molluscan shell fragments and fragments of fecal pellets(?) are rare to frequent.

The calcareous nannofossil assemblage is similar to that in the overlying interval, reflecting a combination of the long range of Coccolithus pelagicus and ?Coccolithus cf. C. doronicoides and contamination due to caving. No calcareous nannofossils were found below 6,470 feet.

Environment. Paleodepth interpretations in this section (fig. 73, p. 165) are somewhat tenuous because of the sparsity of paleobathymetrically definitive calcareous foraminifera. The presence of the arenaceous species Cyclammina cf. C. cancellata and Cyclammina pacifica supports a bathyal depth, although this long-ranging genus appears to have also lived in somewhat shallower depths before late Pliocene times (Robinson, 1970). Other arenaceous genera present, such as Ammobaculites, Ammodiscus, Bathysiphon, Haplophragmoides, and Rheophax, along with the calcareous genera Lenticulina, Nodosaria, and Virgulina, also support a deep-water interpretation. The near absence of calcareous foraminifera in the interval could be due to deposition in deep water below the carbonate compensation depth, resulting in

dissolution of many of the calcareous forms. The age-equivalent Sitkalidak Formation on Kodiak Island contains what appear to be deep-water turbidite sequences (Nilsen and Moore, 1979), which also supports an interpretation of deep-water deposition for this interval in the well. Stewart (1976) and Moore and others (1983) argue on the basis of petrologic criteria that the Sitkalidak Formation on Kodiak Island is the proximal equivalent of Eocene-Oligocene turbidite deposits of the Zodiac Fan, penetrated by Deep Sea Drilling Project Hole 183, located about 160 miles south-southwest of the Shumagin Islands. These same authors suggest that in the Eocene the Zodiac Fan lay to the southeast of its present position, and that it has been displaced to the northwest by plate movement. Calcareous nannofossil data from the KSSD wells exhibit some similarities with the Eocene nannoflora at Site 183 (Worsley, 1973). Eight of the 25 species that occur in the Eocene section at Site 183 (Braarudosphaera bigelowi, Coccolithus eopelagicus, Coccolithus pelagicus, Cyclococcolithus sp., Cyclococcolithus formosa, Helicopontosphaera sp., Reticulofenestra sp., and Reticulosphaera umbilica) also occur in the Eocene of one or more of the Kodiak KSSD wells. A similar population is also found in the Paleogene section of Amlia Island and Atka Island in the Aleutian Islands (McLean and others, 1983; Hein and others, 1984). Also, Wolfe (1973) states that spore and pollen data from Site 183 are generally similar to beds of comparable age from the Alaska mainland. In addition, Evitt (1973) noted the presence of the dinoflagellate Areosphaeridium diktyoplokus, a species also present in the KSSD wells, in upper to middle Eocene sediments of Site 183. These data, while hardly conclusive, suggest that the Eocene sections of the KSSD wells might represent an intermediate facies between exposures of the upper fan deposits of the Eocene Sitkalidak Formation on Kodiak Island and the abyssal facies of the Zodiac Fan. This is not inconsistent with the very limited mineralogical data collected and analyzed from the KSSD wells (see Lithologic Summary chapter).

Comparisons of the Kodiak shelf COST wells with nearby coeval sedimentary sections to the east on the Yakutat block, in the Tenneco Middleton Island well (on the Prince William terrane), and at DSDP Site 183 (on the Pacific plate) are difficult because of a number of conflicting paleoclimate interpretations (Worsley, 1973; Wolfe, 1977; Stevenson and others, 1983; Keller and others, 1984; von Huene and others, 1985; Plafker, in press; among others). Some of the difficulties can be related to the fact that more than one tectonostratigraphic terrane is involved (see Seismic Stratigraphy and Tectonic Evolution of the Kodiak Shelf chapter), some are due to inconsistencies in and paucity of data, some are due to differing interpretations of different data, and some are due to differing interpretations of the same data. Keller and others (1984) and von Huene and others (1985), citing Worsley (1973), state that the Eocene nannofloras of Site 183 and the Middleton Island well are indicative of cool to cold water conditions, although the absence of warmer water calcareous nannofossils may not in itself be diagnostic of cool to cold climatic conditions, but rather a result of "selective preservation of solution-resistant forms" (Bukry, 1979, oral commun., cited in Stevenson and

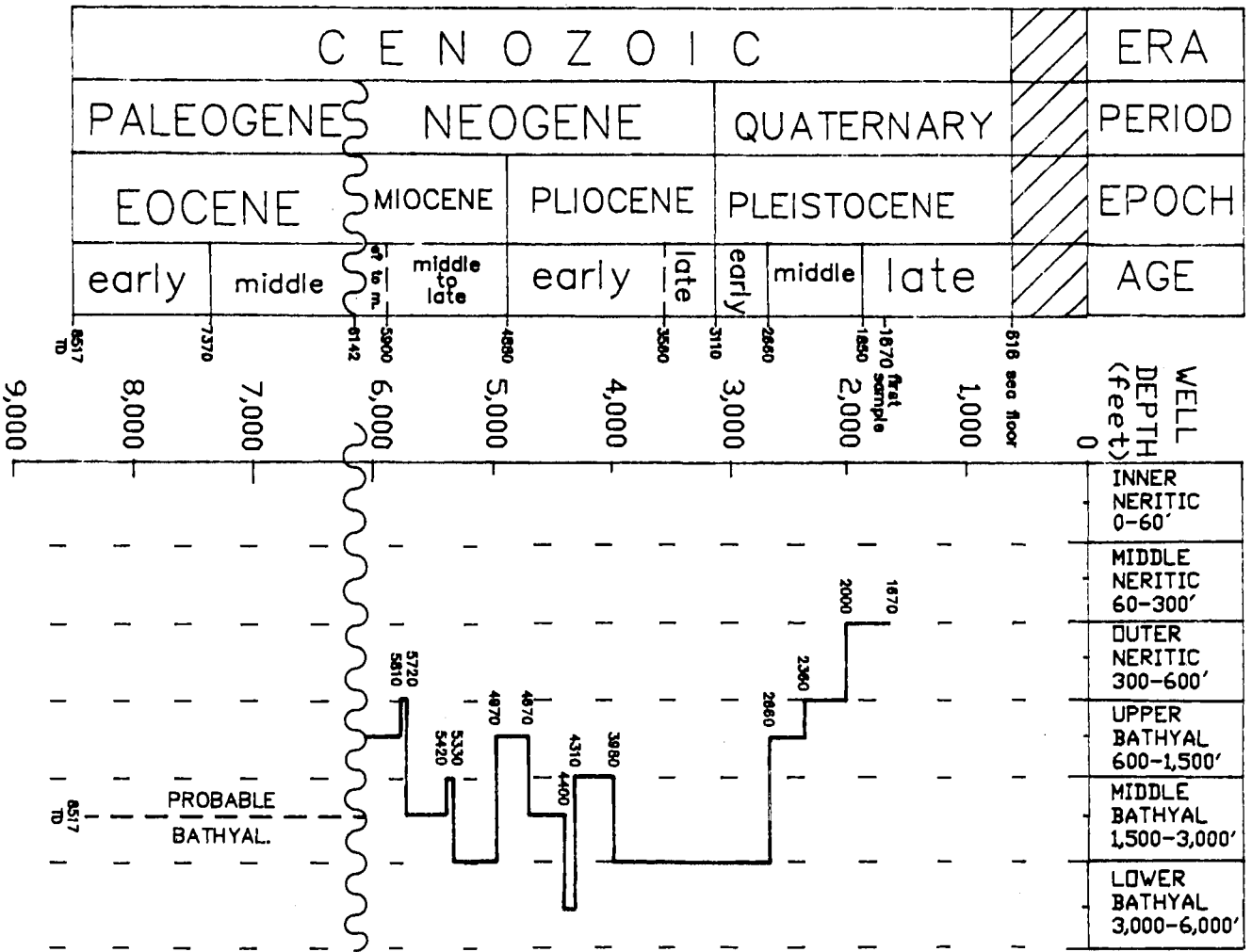


Figure 73. Biostratigraphy and paleobathymetry of the KSSD No. 1 well.

others, 1983). The same authors also cite a study by Wolfe (1977) on the paleoflora of the Katalla, Yakataga, and Malaspina districts of the eastern Gulf of Alaska as further evidence for cold (subarctic) conditions. Stevenson and others (1983), on the other hand, cite paleobotanical evidence from the same paper (Wolfe, 1977) to demonstrate that the climate of the middle to late Eocene was warm temperate to semitropical. Wolfe (1977, p. 35-36) does state that the climate of the late middle Eocene (early Ravenian) was paratropical; the early late Eocene (middle Ravenian) subtropical, and the late Eocene (late Ravenian) temperate. A similar conclusion regarding warm late Eocene conditions for south central British Columbia was reached by Rouse (1977) and for the eastern Gulf of Alaska by Wolfe and Poore (1982). However, Wolfe's (1977) study area was on or at the edge of an area now considered to be a part of the Yakutat block (Keller and others, 1984; von Huene and others, 1985). During the Eocene, this area may have lain 10° or more to the south of the Prince William terrane (von Huene and others, 1985), where the Kodiak COST wells are located, and might have experienced a slightly warmer climate. The presence of a fossil fish of the Jack family (Carangidae) in the late Paleogene rocks of Amlia Island in the Aleutian Islands (McLean and others, 1983) also argues for warmer paleoclimatic conditions. The present-day distribution of the Carangidae is dominantly tropical, although "jack mackerel" do range as far north as the southeastern part of Alaska. At present, there appears to be a case for the fossil data supporting either the warm or cool-cold paleoclimate scenario for the Eocene in the Kodiak shelf area, although the fish fossil from Amlia Island (McLean and others, 1983) hints at warmer water.

By and large, Eocene paleoclimatic indicators are lacking in the KSSD wells. The low-diversity calcareous nannoflora suggests deposition at high latitudes, although the absence of warmer water calcareous nannofossils may be due to dissolution or may be an indication of a barren or low-productivity water mass. The paleoclimate in the KSSD wells probably became cooler throughout the Eocene, ranging from tropical to cool temperate, in a succession similar to that described by Wolfe (1977), with the coolest temperatures in the latest Eocene.

Given the generally sparse data from the Eocene section of the Kodiak shelf COST wells, we cannot hope to reconcile all the differing interpretations of various researchers, although some of the data presented here (see particularly the discussion of reworked Eocene? Amphisteginas in the KSST No. 1 well) may suggest new avenues for further study.

Early Eocene

The interval from 7,370 to 8,540 feet (TD) is early Eocene in age based on the presence of the dinoflagellate Cordosphaeridium cf. C. biarmatum (at 7,370 feet). This age is supported by the presence of common Lanternosphaeridium radiatum (at 7,510 feet swc) and to a lesser degree by the presence of Dracodinium condylos (at 7,640 feet) and Dracodinium solidum (at 7,820 feet). Other, longer

ranging dinocysts include Cordosphaeridium sp., Cordosphaeridium inodes, Phthanoperidinium comatum var., and Trinovantedinium sp. A. A reworked specimen of the Late Cretaceous pollen Aquilapollenites sp. is also present.

The foraminiferal assemblage is similar to that of the overlying interval, with the addition of Ammodiscus spp., Cibicides spp., Elphidium cf. E. californicum, Elphidium sp., Martinottiella sp., Martinottiella cf. M. petrosa, Saracenaria sp., and Trochaminoides sp. Other biotic fragments are rare.

Environment. Paleodepths were probably outer neritic to lower bathyal, similar to the above interval (fig. 73). Species of the foraminifera Martinottiella bolster the interpretation of deep water in this interval. The paleoclimate is indeterminate.

KSSD NO. 2 WELL

Pleistocene

The Pleistocene section is subdivided into late Pleistocene (seafloor to 2,370 feet), middle Pleistocene (2,370 to 3,090 feet), and early Pleistocene (3,090 to 3,420 feet) on the basis of foraminifera, diatoms, silicoflagellates, and stratigraphic position.

Late Pleistocene

The unsampled interval from the seafloor to 1,470 feet is considered to be late Pleistocene (and Holocene) in age, in continuity with the sampled interval directly underlying it. The age of the sampled late Pleistocene section (1,470 to 2,370 feet) is based primarily on stratigraphic position, as it overlies a section of early to middle Pleistocene age. The microfossils present are generally long ranging or range into the Holocene. This section contains a wide variety of benthic foraminifera, including Bolivina decussata, Buccella frigida, Buccella tenerrima, Buliminella elegantissima, Cassidulina californica, Cassidulina islandica, Cassidulina minuta, Cassidulina norcrossi, Cassidulina subglobosa, Cassidulina teretis, Cassidulina yabei, Cibicides conoideus, Cibicides fletcheri, Cibicides lobatulus, Cibicides mckannai, Denticulina cf. D. soluta, Eilohedra levicula, Elphidiella arctica, Elphidiella hannai, Elphidiella oregonense, Elphidium bartletti, Elphidium clavatum, Elphidium discoideale, Elphidium frigidum, Epistominella exigua, Epistominella pacifica, Epistominella smithii, Eponides cf. E. isabelleanus, Fissurina lucida, Gaudryina arenaria, Karrerella baccata, Nodosaria spp., Nonionella auricula, Oolina apiopleura, Oolina melo, Polymorphina sp., Pullenia salisburyi, Pyrgo spp., Quinqueloculina spp., Rotalia columbiensis, Sigmomorphina sp., Trifarina angulosa, Trifarina fluens, and Uvigerina cushmani. Planktonic species present include Globigerina bulloides, Globigerina quinqueloba, and sinistrally coiled Neogloboquadrina pachyderma. Echinoid fragments, sponge

spicules, and molluscan shell fragments are present throughout the interval, along with rare ostracodes and bryozoan fragments.

The calcareous nanofossils present are Coccolithus carteri, Coccolithus doronicoides, Coccolithus pelagicus, Coccolithus pliipelagicus, Cyclococcolithina leptopora, Gephyrocapsa sp., and Gephyrocapsa cf. G. caribbeanica.

Diatoms species within this interval with age ranges that extend into the late Pleistocene are Actinocyclus divisus, Actinocyclus ehrenbergii, Actinocyclus ochotensis, Cocconeis scutellum, Coscinodiscus excentricus, Coscinodiscus lineatus, Coscinodiscus marginatus, Coscinodiscus marginatus cf. fossilis, Coscinodiscus oculus iridis, Denticulopsis seminae fossilis, Navicula optima, Rhabdonema sp., Rhizosolenia hebetata, Roperia cf. R. tessellata, Stephanopyxis dimorpha, Stephanopyxis turris, Thalassiosira decipiens, Thalassiosira lineatus, Thalassiosira gravida, Thalassiosira oestrupii, Thalassiothrix longissima, and Triceratium sp. Other siliceous microfossils present include the silicoflagellate Distephanus speculum and the radiolarians Artostrobium miralestense, Sphaeropyle langii, Spongodiscus sp., Spongotrochus glacialis, and an acanthodesmid form. Reworked siliceous species include the diatom Rhaphoneis cf. R. sachalinensis and the silicoflagellates Distephanus cf. D. octacanthus and Distephanus stauracanthus.

The dinocyst assemblage consists of Operculodinium sp., Operculodinium centrocarpum, Spiniferites sp., the brackish- to freshwater species Peridinium sp. A, and reworked Areosphaeridium diktyoplokus, Herendeenia pisciformis, and Phthanoperidinium amoenum. The pollen and spore assemblage consists of Alnipollenites spp. (= Polyvestibulopollenites verus), Betulaceoipollenites betuloides/infrequens, Compositae (Helianthus) sp., Cyathidites/Deltoidospora spp., Gleicheniidites senonicus, Graminidites sp., Juglanspollenites sp., Laevigatosporites ovatus, Lycopodiumsporites annotinioides, Onagraceae, Osmundacidites spp., Osmundacidites claytonites, Ovoidites spp., Piceaepollenites sp., Pinuspollenites sp., Polemoniaceae, Polypodiaceae sp., Pterocaryapollenites sp., Stereisporites antiquasporites, Taxodiaceaeapollenites sp., Tsugaepollenites igniculus, Ulmipollenites sp., undifferentiated bisaccate pollen, possibly reworked Boisduvalia sp., Ericipites antecursorioides, and Tiliaepollenites sp., along with reworked Aquilapollenites sp., Carpinipites spackmaniana, Caryapollenites simplex, Faguspollenites sp., Ilexpollenites margaritus, and Quercoidites microhenrica. Leiosphaeridia minor, a possible algal cyst, and the freshwater alga Pediastrum boryanum are also present.

Environment. The environments of deposition were outer neritic from 1,470 (first sample) to 2,190 feet, and outer neritic to upper bathyal from 2,190 to 2,370 feet (fig. 74, p. 175). The palynomorph assemblage suggests a cool-temperate climate. However, the presence of sinistrally coiled Neogloboquadrina pachyderma and Coccolithus pelagicus indicate cold water conditions. Wise and Wind (1976) indicate that modern forms of Coccolithus pelagicus

live in waters with temperatures ranging from 6° to 14° C, and Haq (1980) maintains that Coccolithus pelagicus is limited to cold water and high latitudes.

Early to Middle Pleistocene

The early to middle Pleistocene assignment (2,370 to 3,090 feet) is based on the highest stratigraphic occurrence of the diatom Thalassiosira nidulus (at 2,370 feet). This species was also used to define the top of the middle Pleistocene in the KSSD No. 1 and No. 3 wells and the KSST No. 3 well. The diatom assemblage is similar to that of the overlying interval, with the addition of Coscinodiscus sp., Coscinodiscus asteromphalus, Porosira glacialis, and Rhizosolenia styliformis. A species of the silicoflagellate Distephanus is also present. The radiolarian assemblage is similar to that of the overlying section.

The foraminiferal assemblage is similar to that of the overlying interval, with the addition of Buliminella subfusiformis, Cassidulina cf. C. limbata, Cassidulina tortuosa, Ellipsonodosaria verneuili, Planulina ornata, Quinqueloculina akneriana, and Rosalina ornatissima. Sporadic occurrences of frequent Epistominella pacifica occur below 2,760 feet. This species was abundant in the early Pleistocene section of the KSST No. 1 and KSSD No. 1 wells, and is consistently present in early Pleistocene and Pliocene intervals of the KSSD No. 3 well. Molluscan shell fragments, sponge spicules, and ostracodes are also present in this interval.

The dinocyst assemblage is similar to that of the overlying section. Additional palynomorphs include the pollen Gramineae and Nyassapollenites sp., and a marine alga assignable to the Tasmanaceae.

Samples from this interval contain a sparse calcareous nannofossil assemblage. Most of the taxa found in the overlying interval are absent and the only new taxon is Coccolithus cf. C. productus.

Environment. Paleoenvironments were outer neritic to upper bathyal from 2,370 to 3,090 feet, and upper bathyal from 3,090 to 3,420 feet (fig. 74, p. 175). On the basis of palynology, the paleoclimate was cool-temperate.

Early Pleistocene

The early Pleistocene (3,090 to 3,420 feet) is based on the highest stratigraphic occurrence of the silicoflagellates Dictyochoa cf. D. subarctios (at 3,090 feet) and Dictyochoa subarctios (at 3,180 feet). Dictyochoa subarctios is restricted to the early Pleistocene. The diatom assemblage is similar to that of the overlying interval, with the addition of Actinocyclus curvatulus, Denticulopsis cf. D. kamtschatica, and Denticulopsis cf. D. seminae. The radiolarian assemblage is similar to that of the early to middle Pleistocene.

The dinocyst assemblage is similar to that of the overlying interval, as is the pollen and spore assemblage, with the addition of Exesisporites spp. and Pterocaryapollenites stellatus (= Polyatriopollenites stellatus).

The foraminiferal assemblage is similar to that of the overlying interval, with the addition of Bolivina spissa, Karrerella sp., Marginulina(?) sp., Uvigerina peregrina, and the planktonic species Globigerinita uvula.

The calcareous nannofossil assemblage is similar to but less diverse than the sparse assemblage in the overlying interval. The only additional elements are reworked specimens of Watznaueria barnesae.

Environment. The paleoenvironment was upper bathyal (fig. 74, p. 175). Although the palynological data indicate a paleoclimate similar to that of the overlying interval (cool-temperate), the foraminiferal data suggest somewhat warmer conditions.

Pliocene

The age of the Pliocene section (3,420 to 4,590 feet) is based on the presence of the pollen Epilobium sp. (at 3,420 feet), which is characteristic of the Pliocene section in the St. George Basin and southern Bering Sea. The pollen Ericipites compactipolleniatus (at 3,900 feet), which is known from the early Pliocene and older rocks of the Alaska North Slope, is also considered to be diagnostic. Also present is the spore Rouseisporites sp. (at 3,420 feet), a taxon that occurs in other wells of the Kodiak area in Pliocene and older rocks. The remaining palynomorph assemblage is similar to that of the overlying interval, with the addition of Botrychium lanceolatum, Chenopodiaceae, Compositae (Artemisia sp.), Liquidambarpollenites sp., Quercoidites sp., and Selaginellaites selaginoides. The dinocyst assemblage is similar to that of the overlying section.

The siliceous microfossil assemblage is similar to that of the overlying middle to early Pleistocene section, with the addition of the diatoms Actinocyclus oculatus, Asterolampra marylandica, Coscinodiscus marginatus fossilis, Cocconeis costata, Denticulopsis seminae, Melosira sulcata, Rhizosolenia barboi, Rhizosolenia curvirostris, and Thalassiosira excentricus. Also present are the silicoflagellates Dictyocha cf. D. pseudofibula and Distephanus cf. D. boliviensis. The radiolarian assemblage is similar to that of the overlying interval, with the addition of Cenosphaera sp., Phacodiscus sp., Sphaeropyle cf. S. robusta, and reworked Stylatractus universus.

In addition to most of the foraminifera listed in the overlying sections, this interval contains Bathysiphon sp., Cassidulina translucens, Globobulimina pacifica, Melonis cf. M. barleeianum, Planularia sp., and Pullenia malkinae. Epistominella pacifica is consistently present. The planktonic species

Globigerina quadrilatera also appears. Echinoid fragments, molluscan shell fragments, and sponge spicules are present throughout the interval.

Most of the calcareous nannofossils recovered from this interval came from sidewall cores and were non-age-diagnostic. Additional species are Cricolithus jonesi, Discolithina anisotrema, Reticulofenestra pseudoumbilica, and reworked specimens of Dictyococcites bisectus.

Environment. Upper bathyal conditions characterize the section from 3,420 to 3,720 feet. From 3,720 to 4,020 feet, the depositional environment was outer neritic to upper bathyal. In the lower part of the interval, from 4,020 to 4,590 feet, the paleodepths were upper bathyal (fig. 74, p. 175). The paleoclimate may have been cool-temperate, similar to the overlying interval, although the presence of Quercoidites (oak) and Liquidambarpollenites (sweet gum) suggests the possibility of warmer conditions.

Miocene

The Miocene section is subdivided into middle to late Miocene (4,590 to 6,510 feet) and early? to middle Miocene (6,510 to 8,774 feet) on the basis of the dinoflagellate assemblage.

Middle to Late Miocene

The top of the middle to late Miocene interval (4,590 to 6,510 feet) is based on the occurrence of the dinocyst Impagidinium cornutum at 4,590 feet. The rest of the dinocyst assemblage is similar to that of the overlying interval, with the addition of ?Baltisphaeridium sp., Filisphaera pilosa, Impagidinium sp., Impagidinium japonicum, Spiniferites sp., Spiniferites membranaceus, and a reworked probable Eocene assemblage that includes Cordosphaeridium sp., Glaphyrocysta sp., Glaphyrocysta exuberans, Phthanoperidinium comatum, and Systematophora placacantha. The pollen and spore assemblage is similar to that of the Pliocene section, with the addition of Acerpollenites sp., Deltoidospora sp., Polyodiidites favus, and Taxodiaceapollenites hiatus, along with reworked Diervillapollenites sp. Also present were the fungal spore Pleuricellaesporites spp., and the marine alga Tasmanites globulus.

The siliceous microfossil assemblage is similar to that of the overlying interval, with the addition of the silicoflagellates Distephanus polyactis and reworked Dictyocha cf. D. fibula.

The foraminiferal assemblage is similar to that of the overlying Pliocene section. Additional species present include Bolivina cf. B. minuta, Bulimina exilis, Bulimina ovula, Bulimina subacuminata, Cassidulina limbata, Cibicides cf. C. spiralis, Elphidium acutum, Glandulina laevigata, Haplophragmoides deformes, and Oolina laevigata. The planktonic species Globigerina woodi

var. also appears in the interval. Molluscan shell fragments, sponge spicules, and rare echinoid fragments are present.

Calcareous nannofossil recovery was poor. The assemblage contained only Coccolithus carteri, Coccolithus pelagicus, and reworked Dictyococcites bisectus, Dictyococcites scrippsae, and Cyclococcolithina cf. C. formosa.

Environment. The depositional environment throughout this interval was upper bathyal (fig. 74, p. 175). The presence of scattered rare specimens of Globigerina woodi var. in this interval may indicate temperate paleoclimatic conditions.

Early? to Middle Miocene

An early? to middle Miocene age for the interval from 6,510 to 8,774 feet is based on the occurrences of the dinoflagellate Lingulodinium brevispinosum (at 6,510 feet). An early? to middle Miocene age for this section is also supported by the occurrence of Systematophora ancyrea (at 6,720 feet), a Miocene species that also occurred in the same relative position in the KSSD No. 1 and KSSD No. 3 wells. Other dinocysts present in this interval are Filisphaera filifera, Filisphaera pilosa, Operculodinium sp., Operculodinium centrocarpum, Reticulosphaera actinocoronata, Spiniferites ramosus ramosus, and reworked specimens of Areosphaeridium diktyoplokus, Cordosphaeridium funiculatum, ?Glaphyrocysta sp., Lejeunecysta hyalina, and Odontochitina operculata. Most published ranges of Filisphaera filifera and Filisphaera pilosa show occurrences of these species beginning directly above a mid-Miocene unconformity in the Bering Sea region. However, Bujak (personal commun., 1987) noted that Filisphaera sp. A, a form that extends downward at least to the early Miocene, may in fact be Filisphaera pilosa. Judging from this occurrence, and the fact that the other published lower range limits of Filisphaera spp. appear directly above a missing middle Miocene section, it is not implausible that Filisphaera filifera and Filisphaera pilosa might extend into the middle Miocene in uninterrupted sections, and that their occurrence would fit into the biostratigraphy described here for the KSSD No. 2 well. Additional pollen and spores in this section are Compositae, Malvaceae sp., and Selaginellaites selaginoides, along with reworked Cicatricosporites spp., Classopollis classoides, and Momipites sp.

Additional siliceous microfossils recovered from this interval include the diatom Actinocyclus ingens (at 7,410 feet) which, if in place, indicates sediments no older than early Miocene. There are no taxonomically identifiable siliceous microfossils below 7,590 feet.

Several additional benthic foraminifera appear in this interval. These include Bolivina vaughani, Bolivina sp., Bulimina subclava, Chilostomella? sp., Cyclammina cf. C. cancellata, Cyclammina pacifica, Eggerella sp., Glandulina spp., Globobulimina affinis, Haplophragmoides spp., Haplophragmoides trullisata, Lenticulina sp., Loxostomum sp., Miliammina? sp., Melonis

pompilioides, Nonionella digitata, and Uvigerina hispidocostata. Cassidulina translucens, Epistominella pacifica, and Uvigerina cushmani are all frequent to common. Molluscan shell fragments and rare echinoid fragments are also present throughout the interval. Sponge spicule abundance is low below 7,230 feet.

The calcareous nannofossil assemblage most closely resembles that of the late Pleistocene section from 1,470 to 2,370 feet and may be caved. Both the abundance and diversity are greater in this interval than in overlying intervals. New calcareous nannofossils in the assemblage are Braarudosphaera bigelowi, Coccolithina cf. C. macintyreii, Helicopontosphaera sp., and reworked Cyclicargolithus? sp. and Reticulofenestra sp.

Environment. The depositional environments were upper bathyal in the section from 6,510 to 7,368 feet and middle to lower bathyal from 7,368 to 8,774 feet (fig. 74, p. 175). There were insufficient data to define the paleoclimate.

Eocene

The Eocene is subdivided into late Eocene (8,774 to 10,284 feet) and middle? to late Eocene (10,284 to 10,410 feet, TD) on the basis of calcareous nannofossils. The upper boundary (at 8,774 feet) denotes a regional unconformity that separates the overlying Neogene section from the underlying Paleogene section.

Late Eocene

The late Eocene age for the interval below the unconformity, from 8,774 to 10,284 feet, is based on the occurrence of the calcareous nannofossil Reticulofenestra hillae in a sidewall core at 10,284 feet. This species indicates an age no younger than early Oligocene and no older than early late Eocene. Correlations with the KSSD No. 1 and No. 3 wells, however, indicate that the interval below the unconformity is probably no younger than Eocene, making a late Eocene age assignment the most logical one. The remaining calcareous nannofossil assemblage is similar to that of the overlying interval, with the addition of Coccolithus sp., ?Coccolithus cf. C. doronicoides, Coccolithus eopelagicus, Coccolithus pelagicus, Cyclicargolithus sp., Cyclicargolithus floridanus, Cyclococcolithina cf. C. formosa, Dictyococcites bisectus, Dictyococcites scrippsae, Discolithina sp., Helicopontosphaera sp., and Reticulofenestra sp. The assemblage contains elements similar to that of the overlying interval, reflecting the long ranges of several species.

Also present are dinocyst species no younger than late Eocene, such as Impagidinium velorum and Phthanoperidinium alectrolophum. Areosphaeridium diktyoplokus, Cordosphaeridium funiculatum, Cordosphaeridium gracile, and Systematophora placacantha also support a late Eocene age. Also present are Achomosphaera ramulifera, Baltispheridium sp., Cordosphaeridium sp., Cyclonephelium exuberans, Deflandrea sp., Deflandrea phosphoritica, Glaphyrocysta sp., Heteraulacysta leptalea, Lejeunecysta hyalina,

Operculodinium sp., Operculodinium centrocarpum, Phthanoperidinium comatum, Spiniferites sp., Spiniferites membranaceus, Spiniferites ramosus granosus, Spiniferites ramosus multibrevis, Spiniferites ramosus ramosus, Systematophora ancyrea, Wetzeliella articulata, and possibly caved Tuberculodinium vancampoae. Occurrences in cuttings of Apectodinium hypercanthum (at 9,780 feet) and Hafniasphaera septata (at 10,050 feet), if in place, indicate an early to middle Eocene age for the lower part of this interval. However, because this interval was otherwise defined by occurrences of calcareous nannofossils in sidewall-core samples, it is presumed that these dinoflagellates have been reworked from older sediments. The pollen and spore assemblage includes Alnipollenites spp. (= Polyvestibulopollenites verus), Betulaceoipollenites betuloides/infrequens, Carpinipites cf. C. spackmaniana, Caryapollenites simplex, Classopollis classoides, Compositae sp., Compositae (Helianthus sp.), Cyathidites/Deltoidospora spp., Diervillapollenites sp., Ericaceae (tetrad), Ericipites antecursorioides, Juglanspollenites sp., Laevigatosporites sp., Laevigatosporites ovatus, Lycopodiumsporites sp., Lycopodiumsporites annotinioides, Osmundacidites sp., Osmundacidites claytonites, Piceapollenites spp., Pinuspollenites spp., Polyodiidites favus, Pterocaryapollenites stellatus (= Polyatriopollenites stellatus), Selaginellaites selaginoides, Sphagnumsporites sp., Stereispollenites antiquasporites, Taxodiaceapollenites hiatus, Tiliaepollenites sp., Tsugaepollenites sp., Tsugaepollenites igniculus, Camarozonosporites sp., the fungal genera Microthyrites spp., Exesisporites spp., Pluricellaesporites spp., the algal spores Pediastrum boryanum and Tasmanites globulus, and the reworked Maastrichtian-Paleocene pollen Paraalnipollenites confusus.

The foraminiferal assemblage in this interval is sparse and consists primarily of arenaceous forms, along with a minor component of calcareous species. This assemblage is similar to that described from the Eocene section of the KSSD No. 1 well. The principle species present are Ammodiscus sp., Cyclammina sp., Eggerella sp., Reophax? sp., Saccamina sp., and the calcareous species Nodogenerina spp., Nodogenerina lepidula, Nodogenerina koina, and Virgulina sp. There are also rare fragments of mollusc shells and echinoids present.

Environment. The paleobathymetry of this section is difficult to determine owing to the sparsity of the fauna. The microfossil assemblage consists principally of arenaceous foraminifera. Several of these, including Ammodiscus sp., Cyclammina sp., and Reophax sp., suggest that conditions were probably bathyal (fig. 74), although Cyclammina has been shown to have ranged into shallower depths before the late Pliocene (Robinson, 1970) and should be interpreted with care in older sediments. However, a deep-water interpretation is also supported by the presence of species of Nodogenerina sp. and Virgulina sp. Nilsen and Moore (1979) point out that the age-equivalent Sitkalidak Formation onshore on Kodiak Island includes sequences of what appear to be deep-water turbidites, which lends support to an interpretation of bathyal depths for this interval (see KSSD No. 1 well, middle

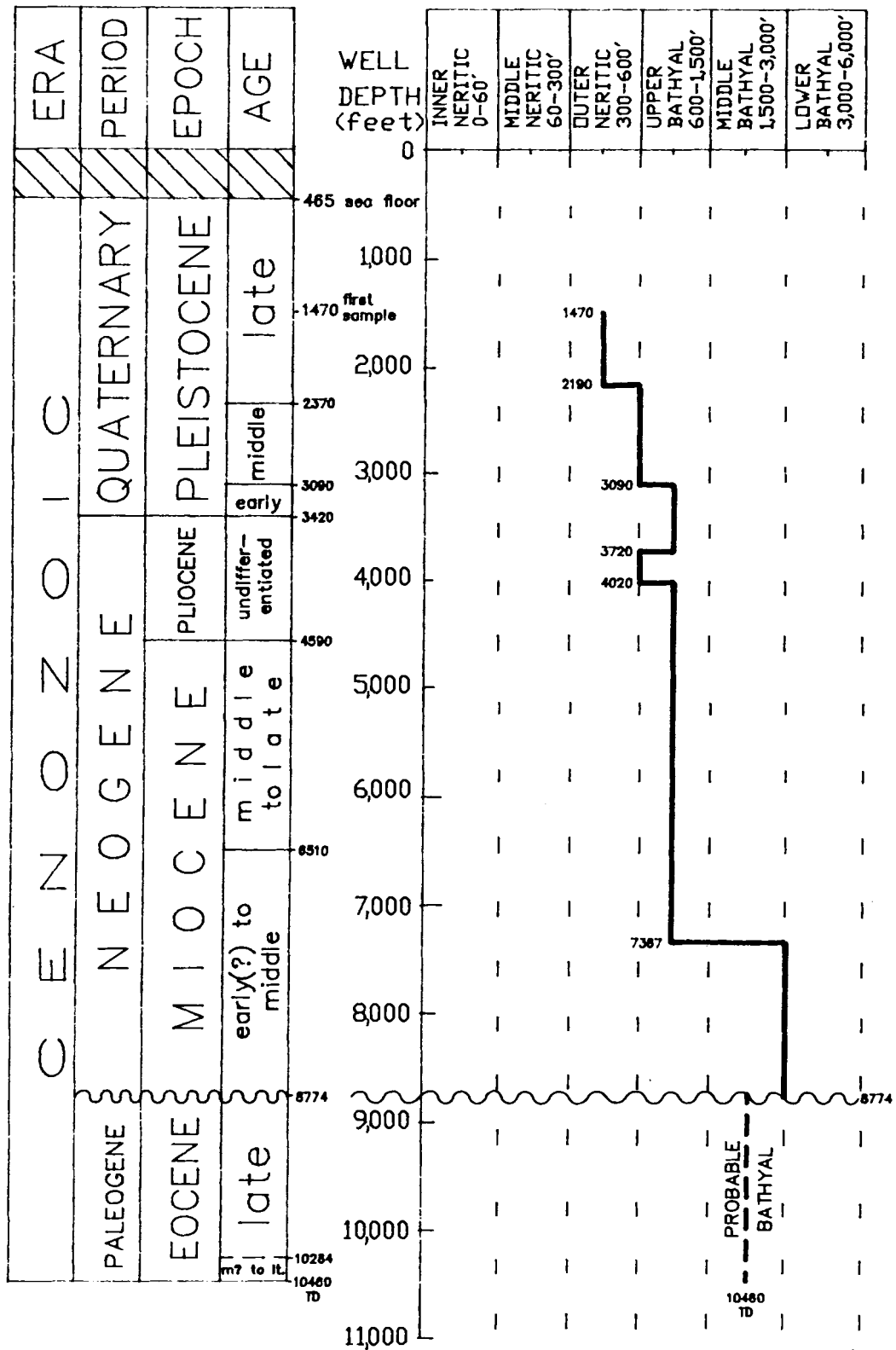


Figure 74. Biostratigraphy and paleobathymetry of the KSSD No. 2 well.

Eocene environment section). In addition, it can be argued that the near absence of calcareous foraminifera in this and the underlying middle to late Eocene section might be due to deposition in deep water, below the carbonate compensation depth, resulting in the dissolution of many of the calcareous forms. The paleoclimate for this interval was poorly defined (see the KSSD No. 1 well, middle Eocene environment section, for a more detailed discussion).

Middle? to Late Eocene

The middle? to late Eocene interval (10,284 to 10,410 feet, TD) is based on the occurrence of the calcareous nannofossil Reticulofenestra umbilica (at 10,410 feet, swc), which occurs in sediments no older than middle Eocene. The rest of the calcareous nannofossil assemblage is similar to that of the overlying interval, with the addition of Cricolithus? sp.

The dinocyst assemblage is similar to that of the late Eocene section, with the addition of Cordosphaeridium inodes and Spiniferites ramosus var. A. There are no pollen or spores new to this section.

The foraminiferal assemblage in this interval is essentially the same as that of the late Eocene, with the addition of Haplophragmoides cf. H. indentatus, Uvigerina cf. U. modeloensis, and Uvigerina cf. U. peregrina (possibly caved). No planktonic species were found. Molluscan shell fragments and rare echinoid fragments are present.

Environment. The environment of deposition was probably bathyal, similar to that of the overlying section (fig. 74). There were insufficient data to define the paleoclimate.

KSSD NO. 3 WELL

Pleistocene

The Pleistocene section of the KSSD No. 3 well is subdivided into late Pleistocene (seafloor to 1,500 feet), middle Pleistocene (1,500 to 2,835 feet), and early Pleistocene (2,835 to 3,350 feet) on the basis of diatom and dinoflagellate distributions and stratigraphic position.

Late Pleistocene

The unsampled interval from the sea floor to 1,370 feet is considered to be late Pleistocene (and Holocene) in age in continuity with the sampled interval directly underlying it. The age of the sampled late Pleistocene section (1,370 to 1,500 feet) is based primarily on stratigraphic position in that it overlies an interval containing microfossils of middle Pleistocene (and older) age.

Diatoms occurring in this interval with ages ranging into the late Pleistocene are Coscinodiscus excentricus, Coscinodiscus marginatus, Coscinodiscus oculus iridis, Stephanopyxis turris, Thalassiosira excentricus, Thalassiosira gravida, and Thalassiosira oestrupii.

Pollen and spores occurring in this interval include Alnipollenites spp. (= Polyvestibulopollenites verus), Osmundacidites sp., and Pinuspollenites sp. The only dinoflagellates recovered were Operculodinium centrocarpum and the reworked Early Cretaceous species Aptea polymorpha.

No calcareous nanofossils or Radiolaria were found.

The foraminiferal assemblage includes Cassidulina californica, Cassidulina islandica, Cassidulina norcrossi, Cassidulina subglobosa, Cassidulina teretis, Cassidulina yabei, Cibicides lobatulus, Elphidiella hannai, Elphidium bartletti, Elphidium clavatum, Elphidium cf. E. discoideale, Karrerella baccata, Nonionella auricula, and Quinqueloculina akneriana.

Environment. The environment of deposition was middle neritic (fig. 75, p. 185). Paleoclimatic data were inconclusive.

Middle Pleistocene

The middle Pleistocene section (1,500 to 2,835 feet) is based on the highest stratigraphic occurrence of the silicoflagellate Distephanus octonarius, the diatoms Rhizosolenia curvirostris and Thalassiosira nidulus (at 1,500 feet), and the radiolarian Lamprocyrtis haysi at 2,407 feet (swc). The highest stratigraphic occurrence of Thalassiosira nidulus was also used to define the top of the middle Pleistocene in the KSSD No. 1 and KSSD No. 2 wells, and Distephanus octonarius was found at the top of the middle Pleistocene in the KSSD No. 1 well. Long-ranging siliceous microfossils with highest occurrences in this interval include the diatoms Actinocyclus divisus, Actinocyclus ochotensis, Actinocyclus undulatus, Biddulphia aurita, Chaetoceros sp., Cocconeis costata, Cocconeis scutellum, Coscinodiscus asteromphalus, Coscinodiscus lineatus, Denticulopsis seminae, Denticulopsis seminae fossilis, Navicula optima, Porosira glacialis, Rhabdonema sp., Rhizosolenia bergonii, Rhizosolenia hebetata, Rhizosolenia styliformis, Stephanopyxis dimorpha, Thalassionema nitzschioides, Thalassiosira decipiens, and Thalassiothrix longissima, the silicoflagellate Distephanus speculum, the radiolarians Cenosphaera sp., Spongodiscus sp., Spongodiscus glacialis, and an unidentified acanthodesmid radiolarian.

Long-ranging dinocysts with highest occurrences in this interval are Spiniferites sp., Spiniferites membranaceous, and Spiniferites mirabilis, along with an extensive reworked assemblage from Jurassic, Early Cretaceous, Late Cretaceous-Paleocene, and Eocene age sediments (these include Areosphaeridium diktyoplokus?, Astrocyta cretacea, Ceratiopsis diebelii, Gonyaulacysta ambigua,

Gonyaulacysta cf. G. cladophora, Gonyaulacysta jurassica, Odontochitina operculata, Oligosphaeridium anthophorum, and Pareodinia ceratophora). Also present are the pollen and spores Betulaceoipollenites betuloides/infrequens, Chenopodiaceae, Cyathidites/Deltoidospora sp., Gramineae, Juglanspollenites sp., Laevigatosporites ovatus, Liquidambarpollenites sp., Lycopodiumsporites annotinioides, Onagraceae, Osmundacidites claytonites, Piceaepollenites sp., Polemoniaceae, Pterocaryapollenites stellatus (= Polyatriopollenites stellatus), Polyodiaceae (including Polyodiites favus), Polygonum sp., Quercoidites spp., Sphagnumsporites sp., Taxodiaceaeipollenites sp., Tsugaepollenites igniculus, Ulmipollenites sp., undifferentiated bisaccate pollen, possibly reworked Carpinipites spackmaniana and Caryapollenites simplex, and reworked Cicatricosisporites spp. and Rouseisporites sp. Also present are the freshwater algae Leiosphaeridia minor and Pediastrum boryanum, the fresh- to brackish-water dinoflagellate Peridinium sp. A, the alga Tasmaneeae (including Tasmanites globulus), the prasinophycean alga Pterospermopsis sp., and the fungal spore Exesisporites sp.

Calcareous nannofossils with highest occurrences in this interval are Coccolithus carteri, Coccolithus daronicoides, Coccolithus pelagicus, Cyclococcolithina sp., Gephyrocapsa sp., Gephyrocapsa caribbeanica, and Gephyrocapsa oceanica.

The foraminiferal assemblage is similar that of the overlying interval, with the addition of Bolivina decussata, Buccella frigida, Buccella tenerrima, Buliminella elegantissima, Cassidulina limbata, Cassidulina minuta, Cassidulina cf. C. translucens, Cibicides conoideus, Cibicides fletcheri, Cibicides cf. C. perlucidus, Cibicides cf. C. suppressus, Dentalina decepta, Dentalina cf. D. soluta, Discorbis spp., Elphidiella alaskense, Elphidielella cf. E. siberica, Elphidium cf. E. acutum, Elphidium frigidum, Epistominella exigua, Epistominella pacifica (rare), Fissurina sp., Gaudryina arenaria, Glandulina laevigata, Lagena spp., Lenticulina sp., Marginulina sp., Melonis aff. M. barleeianum, Oolina sp., Oolina apiopleura, Polymorphina charlottensis, Polymorphina kincaidi, Protoelphidium orbiculare, Pseudopolymorphina spp., Pyrgo spp., Rotalia columbiensis, Triloculina sp., Trifarina cf. T. fluens, and Uvigerina cushmani. Eilohedra levicula, a species noted in the middle to late Pleistocene section of the KSSD No. 1 well and in the late Pleistocene section of the KSSD No. 2 well, was noted in this interval as well. Planktonic species present include Globigerina bulloides, Globigerina quadrilatera, Globigerina quinqueloba, and sinistrally coiled Neogloboquadrina pachyderma. Echinoid fragments, ostracodes, and sponge spicules are present, and molluscan shell fragments are frequent to common throughout most of this interval.

Environment. The foraminiferal assemblage indicates that the environments of deposition were middle neritic from 1,500 to 2,060 feet and middle to outer neritic from 2,060 to 2,835 feet (fig. 75, p. 185). Although the miospores indicate a cool-temperate climate for this interval, the presence of Coccolithus

pelagicus, Protoelphidium orbiculare, and sinistrally coiled Neogloboquadrina pachyderma indicates water temperatures that were cold. Wise and Wind (1976) indicate that modern forms of Coccolithus pelagicus have a water temperature range of 6 to 14 °C, and Haq (1980) states that the species is dominantly cold water and high latitude in its distribution.

Early Pleistocene

The interval from 2,835 to 3,350 feet is defined as early Pleistocene on the basis of diatoms and stratigraphic position. Although the age of the interval is based on the highest stratigraphic occurrence of Actinocyclus cf. A. oculatus (in the sample interval of 2,810 to 2,900 feet), the "top" of the section was picked at a change in the dipmeter log pattern at 2,835 feet that is indicative of a change from a glacio-marine shelf sequence to a deeper water, probable turbidite sequence (see Well Log Interpretation chapter). The highest stratigraphic occurrence of Actinocyclus oculatus was also found in the correlative section of in the KSSD No. 1 and KSSD No. 2 wells. Other siliceous microfossils with highest occurrences in the interval are the diatoms Actinocyclus ehrenbergii and Rhaphoneis cf. R. sachalinensis, and the radiolarian Phacodiscus sp.

The calcareous nannofossil assemblage is similar to that of the overlying interval, with the addition of Braarudosphaera bigelowii and reworked Cyclicargolithus sp. and Cyclococcolithina cf. C. neogammation.

The dinocyst assemblage is similar to that of the overlying interval, with the addition of Spiniferites ramosus ramosus. The pollen and spore assemblage is similar to that of the overlying interval, with the addition of Compositae (Helianthus sp.), Ericipites sp., and Ilexpollenites sp., along with possibly reworked Boisduvalia sp. and Tiliaepollenites sp., and reworked Cicatricosisporites sp. and Vitreisporites pallidus.

The foraminiferal assemblage is similar to the assemblage in the overlying interval. Species with highest occurrences in this interval are Nonionella labradorica, Quinqueloculina stalkerii, and the planktonic species Globigerina woodi var. and Globigerinita uvula. In addition, Epistominella pacifica and Glandulina laevigata are more consistently present in this interval. Analysis of the abundance of Epistominella pacifica appears to be helpful in identifying intervals of this age, at least locally, as it is also common in the early Pleistocene and late Pliocene of the KSST No. 1 and No. 4A wells, the KSSD No. 1 and No. 2 wells, and in the late Pliocene of the KSST No. 2 well. Other species that may have potential for correlation in this interval include Pullenia malkinae, which is consistently present below 2,900 feet in this well and was also present in the Pliocene section of the KSSD No. 2 well, and Pullenia salisburyi, which is consistently present below 2,990 feet here and in the early Pleistocene section of the KSSD No. 1 well. Molluscan fragments and sponge spicules are present throughout the interval.

Environment. Environments of deposition were outer neritic to upper bathyal (fig. 75, p. 185). The paleoclimate was cool-temperate, perhaps warmer than the overlying interval.

Pliocene

The age and boundaries of the Pliocene section (3,350 to 5,060 feet) are based on siliceous microfossils and stratigraphic position. There were insufficient data to subdivide the section.

Diatoms present with highest stratigraphic occurrences in the late Pliocene are Coscinodiscus marginatus cf. fossilis (at 3,370 feet, swc), Coscinodiscus marginatus fossilis (at 4,000 feet, swc), Coscinodiscus cf. C. pustulatus (at 3,620 feet), Coscinodiscus pustulatus (at 4,730 feet), Stephanopyxis cf. S. horridus (at 3,889 feet, swc), Stephanopyxis horridus (at 4,400 feet swc), Thalassiosira cf. T. antiqua (at 3,620 feet), Thalassiosira antiqua (at 3,889 feet swc), and the silicoflagellate Ammodochium rectangulare (at 3,370 feet, swc). The remainder of the siliceous microfossil assemblage is similar to that of the overlying interval, with the addition of the diatom Nitzschia sp. and the silicoflagellate Distephanus boliviensis.

The dinoflagellate assemblage is similar to that of the overlying interval, with the appearance of Filisphaera pilosa supporting a Pliocene age. Other species appearing in the interval include Filisphaera filifera and Operculodinium centrocarpum. Extensive reworked elements include Cyclonephelium distinctum, Phthanoperidinium comatum, Wetzeliella articulata, and Isabelidinium acuminatum. Pollen and spores with highest occurrences in this interval include Faguspollenites sp., Malvaceae, Pachysandra sp., Taxodiaceapollenites hiatus, and possibly reworked Diervillapollenites sp. The fungal spore Pluricellaesporites spp. is also present.

The calcareous nannofossil assemblage is similar to that of the overlying interval, with the addition of non-age-diagnostic Coccolithus pliopelagicus, Cyclococcolithina leptopora, Cyclococcolithina cf. C. macintyreii, and reworked Dictyococcites scrippsae and Reticulofenestra sp.

The foraminiferal assemblage is similar to that of the overlying interval, with the addition of Bathysiphon sp., Cyclammina cf. C. cancellata, Cyclammina pacifica, Fissurina lucida, Guttulina sp., Virgulina sp., and Haplophragmoides deformes. Epistominella pacifica is consistently present, becoming somewhat more frequent below 4,070 feet. Molluscan shell fragments, sponge spicules, rare echinoid fragments, and ostracodes are also present.

Large, well-preserved fragments of the bryozoans Myriozoum subgracile and Myriozoum coarctatum are present in the KSSD No. 3 well between 3,920 and 4,310 feet. These specimens are essentially identical to modern forms collected by bottom sampling of the Kodiak shelf, where they are a conspicuous component of an

extensive coquinoïd veneer and are the most abundant and widespread taxa of the bryozoan fauna (Cuffey and Turner, 1987). These circumpolar species have been recorded from water depths of 5 to 1,700 feet, but on the modern Kodiak shelf they are most common between 130 and 345 feet. The rigid, erect, branched, cylindrical colonial form (vinculariiform zoarium) is far more common in deeper water below effective wave base, although robust forms can withstand moderate hydrodynamic stress. Vinculariiform zoaria are by far the most common colonial type on the modern Kodiak shelf, particularly at middle neritic depths. This same pattern probably existed in the past. The fossil record of these species is obscure, but Myrionozoum subgracile may have been described from the Tertiary of France (d'Orbigny, 1852).

Environment. Outer neritic to upper bathyal conditions were present from 3,350 to 3,920 feet, and the section from 3,920 to 5,060 feet was predominantly upper bathyal (fig. 75, p. 185). The paleoclimate was probably cool-temperate, similar to that of the overlying interval, although the angiosperm pollen data suggest slightly warmer conditions.

Miocene

The Miocene section is subdivided into probable late Miocene (5,060 to 6,890 feet) and middle Miocene (6,890 to 7,805 feet) on the basis of dinoflagellate and calcareous nannofossil data, stratigraphic position, and changes in the patterns of the dipmeter well log.

Probable Late Miocene

The "top" of the probable late Miocene section (5,060 to 6,890 feet) is based on a change in sediment source indicated by an approximate 90-degree shift in overall dip direction (from approximately southwest to approximately southeast) observed on the dipmeter log.

The presence of the dinoflagellatae Nematosphaeropsis cf. N. balcombiana in this interval supports a Miocene age. Other dinoflagellates with highest occurrences in this interval are Reticulosphaera actinocoronata, Tectatodinium pellitum, Tuberculodinium vancampoae, reworked Cordosphaeridium sp., Deflandrea sagittula, Glaphyrocysta exuberans, and probably reworked Systematophora ancyrea. Pollen and spores with highest occurrences in this interval are Botrychium lanceolatum, Compositae, Ericipites compactipolleniatus, Nyassapollenites sp., Selaginellaites selaginoides, possibly reworked Ericipites antecursorioides, and reworked Aquilapollenites sp.

The siliceous microfossil assemblage is similar to that of the overlying interval, with the addition of the diatoms Actinocyclus sp., Actinocyclus ingens, Nitzschia sp., Rhaphoneis ampiceros, Thalassiosira convexa, and Thalassiosira zabellinae, the silicoflagellate Distephanus speculum, and the radiolarians

Sphaeropyle robusta, Pterocanium sp., and Sphaeropyle cf. S. langii.

The calcareous nannofossil assemblage is similar to that of the overlying interval, with the addition of reworked Dictyococcites bisectus.

The foraminiferal assemblage is similar to that of the overlying Pliocene section, with the addition of Ammosphaeroidina sp., Bulimina ovula, Dentalina soluta, Discorbis sp., Glandulina sp., Globulina sp., Haplophragmoides trullissata, Haplophragmoides spp., Karrerella sp., and Nonionella miocenica. Gyroidina altiformis, which has not been noted in sediments younger than Miocene in the Gulf of Alaska (Lagoe, 1978, 1983; Rau and others, 1983), is also present in this interval (at 5,396 feet, swc). This species was noted in the middle to late Miocene section of the KSSD No. 1 well. Molluscan shell fragments and sponge spicules are also present.

Environment. The depositional environment was upper bathyal from 5,060 to 6,170 feet and outer neritic to upper bathyal from 6,170 to 6,890 feet (fig. 75, p. 185). The miospore assemblage suggests a slightly cooler climate than that of the overlying cool-temperate interval.

Middle Miocene

The upper part of the middle Miocene section (6,890 to 7,807 feet) contains no age-diagnostic microfossils. The upper boundary was somewhat arbitrarily picked on the basis of lithologic and/or diagenetic changes (or possible overcompaction of the sediments) suggested by well log curves. The middle Miocene age for this section is based on the dinoflagellates Spiniferites crassipellis (at 7,706 feet, swc) and Systematophora ancyrea (at 7,220 feet), and the calcareous nannofossil Cyclicargolithus floridanus (at 7,800 feet, swc).

No additional palynomorphs appear in this interval.

Other calcareous nannofossils with highest occurrences in this interval are ?Dictyococcites sp., Helicopontosphaera cf. H. compacta, ?Isthmolithus recurvus, Transversopontis cf. T. pulcher, and reworked Discolithina cf. D. plana and ?Dictyococcites cf. D. bisectus.

The siliceous microfossil assemblage is similar to that of the overlying interval, with the addition of the diatom Actinocyclus cf. A. ingens and the Radiolaria ?Phacodiscus sp. and Stylocypridium acquilonium.

The foraminiferal assemblage is similar to that of the overlying interval, with additional rare occurrences of several new forms, including Bathysiphon sp., Cibicides mckannai, Cyclammina sp., Eggerella sp., Nodogenerina lepidula, Nonionella digitata, Rosalina sp., Saccammina sp., and Uvigerina cf. C. hootsi.

Nodogenerina lepidula and two other species of Nodogenerina were also noted in the KSSD No. 2 well, but only in the Eocene section, so it is possible that this species is reworked in the KSSD No. 3 well. Molluscan and echinoid fragments are also present in the interval.

Environment. Paleodepths in this section were upper to middle bathyal (fig. 75, p. 185). The climate was probably cool-temperate.

Middle? to Late Eocene

The interval from 7,805 to 9,355 feet (TD) is middle? to late Eocene in age based on the calcareous nannofossil Dictyococcites cf. D. scrippsae, which is no older than late middle Eocene, and the dinoflagellate Areosphaeridium diktyoplokus. The upper boundary at 7,805 feet denotes a regional unconformity that separates the overlying middle Miocene section from the underlying Paleogene section.

Other calcareous nannofossils with highest occurrences in the interval are Braarudosphaera sp., ?Coccolithus cf. C. doricoides, Coccolithus cf. C. pelagicus, Cyclicargolithus sp., ?Dictyococcites sp., Dictyococcites bisectus, Helicopontosphaera cf. H. compacta, Reticulofenestra sp., Transversopontis cf. T. pulcher, and (probably caved) Discolithina sp.

The dinoflagellate assemblage contains numerous specimens caved from the overlying interval. Additional in situ species in the interval include Cordosphaeridium sp., Cordosphaeridium fibrospinosum, Glaphyrocysta exuberans, Operculodinium centrocarpum, Palaeoperidinium basilium, Paralecaniella indentata, Phthanoperidinium comatum, Spiniferites spp., Spiniferites crassipellis, and Spiniferites ramosus ramosus. Reworked forms include Ceratiopsis diebellii. Possibly reworked forms include Hafniasphaera cryptovesiculata (at 9,080 feet) and Hafniasphaera septata (at 8,030 feet). If these two species are in place and not reworked, they may indicate an early, rather than middle? to late, Eocene age for the interval. Also present are the pollen and spores Alnipollenites spp. (= Polyvestibulopollenites verus), Betulaceoipollenites betuloides/infrequens, Botrychium lanceolatum, Carpinipites cf. C. spackmaniana, Caryapollenites simplex, Cicatricosisporites sp., Cyathidites/Deltoidospora spp., Diervillapollenites sp., Juglanspollenites sp., Laevigatosporites spp., Laevigatosporites ovatus, Lycopodiumsporites annotinioides, Osmundacidites spp., Osmundacidites claytonites, Piceapollenites sp., Pinuspollenites sp., Pterocaryapollenites stellatus (= Polyatriopollenites stellatus, Polypodiaceae (including Polypodiidites favus), Sphagnumsporites sp., Sphagnumsporites igniculus, Taxodiaceae (including Taxodiaceapollenites hiatus), Tsugaepollenites sp., undifferentiated bisaccate pollen, the fungal spores Brachysporites spp., Microthyrites spp., and Pluricellaesporites spp., algae assignable to the Tasmanaceae (including Tasmanites globulus), and reworked Vitreisporites pallidus.

The siliceous microfossil assemblage is similar to that of the overlying interval, with the addition of the Radiolaria Pterocanium korotnevi and Xiphospira circularis. No in situ siliceous microfossils were found below 8,060 feet.

A new assemblage of foraminifera consisting mainly of arenaceous forms appears in this interval. Species present include Ammobaculites sp., Ammodiscus sp., Bathysiphon cf. B. alexanderi, Bathysiphon sp., Cibicides cf. C. spiropunctatus, Cyclammina sp., Dentalina sp., Eggerella sp., Elphidium cf. E. acutum, Glomospira sp., Haplophragmoides cf. H. crassus, Haplophragmoides cf. H. deformes, Haplophragmoides desertorum, Haplophragmoides cf. H. excavata, Haplophragmoides cf. H. translucens, Martinottiella? sp., Martinottiella communis, Proteonina sp., Spiroplectammina sp., Textularia sp., Trochammina sp., Trochamminoides sp., and Verneuilina sp. Also present are Haplophragmoides cf. H. indentatus, which was also observed in the Eocene section of the KSSD No. 1 and No. 2 wells, and Bathysiphon santaecrucis, which appeared in the Eocene section of the KSSD No. 1 well. No planktonic foraminifera were observed in this interval. Molluscan fragments, rare barnacle plates, and fecal pellets(?) are present.

Environment. The predominantly arenaceous foraminiferal assemblage indicates paleoenvironments that were probably bathyal (fig. 75), based on the presence of such deeper water genera as Ammobaculites, Ammodiscus, Bathysiphon, Cyclammina, Haplophragmoides, and Martinottiella. Bathymetric interpretations must be made with care, however, because some genera such as Cyclammina have been shown to have ranged into somewhat shallower depths before the late Pliocene (Robinson, 1970). However, a deep-water interpretation is also supported by the observations of Nilsen and Moore (1979) indicating that the age-equivalent Sitkalidak Formation onshore on Kodiak Island contains turbidite sequences of apparent deep-water origin (see KSSD No. 1 well, early Eocene environment section). In addition, the near-absence of calcareous foraminifera could be due to deposition in deep water, below the carbonate compensation depth, resulting in the dissolution or non-preservation of calcareous forms. Thin sections from 9,051 and 9,060 feet were described by Core Laboratories (appendix 1) as micrite and laminated algal boundstones with possible desiccation fractures, all of which suggest warm, very shallow water. On the basis of all other lines of evidence, this does not seem to represent the actual lithology or depositional environment of this interval. However, close investigation of the cuttings (MMS personnel were not able to examine the cores or thin sections held by either Corelab or Sun Oil Company) revealed the presence of minor amounts of brown micrite in the dominantly deep-water clastic sediments. The best explanation of this is that the micrite represents shallow-water material displaced downslope in turbidite flows. That algal mat depositional environments were possible in this region at the time is supported by observations of rare, small algal heads in age-equivalent outcrop sections on the Alaska Peninsula (James E. Case, USGS, personal commun., 1987) and the recovery of (somewhat older?) shallow-water limestones from the

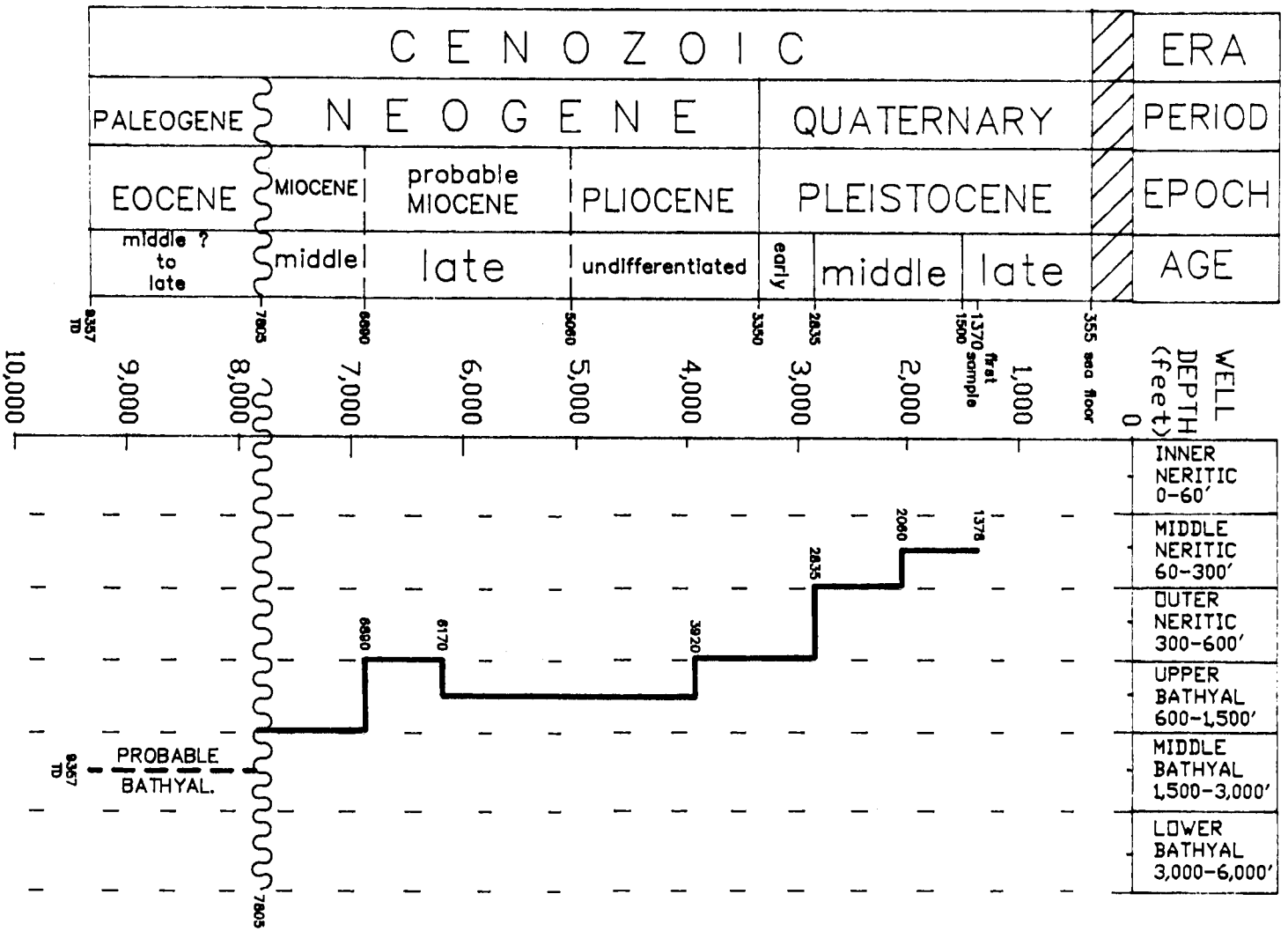


Figure 75. Biostratigraphy and paleobathymetry of the KSSD No. 3 well.

Gulf of Alaska continental slope (Plafker, in press). There were insufficient data to define the paleoclimate (see KSSD No. 1 well, middle Eocene environment section, for a more detailed discussion).

CORRELATION OF KODIAK SHELF STRATIGRAPHIC TEST WELLS

Correlations between the six stratigraphic test wells on the Kodiak shelf are, for the most part, based on biostratigraphy rather than lithology or seismic stratigraphy. The biostratigraphy, however, is complicated by a scarcity of age-diagnostic species, the developmental nature of high-latitude correlation zonations, and by extensive reworking and redeposition of the sediments. In most of the wells, boundaries between stratigraphic sections could not be unequivocally established owing to the sparse nature of the data. Seismic marker horizons could not be followed between the wells or between subbasins because of structural complexity, and are generally not useful in supporting the biostratigraphic correlations. The "Miocene unconformity" (base of Miocene, top of Eocene), however, appears to be a correlatable horizon of regional extent.

The microfossil species used to define the biostratigraphic correlations in this section are discussed individually, well by well, with the wells in the order of their geographic locations from the southwest to the northeast: the KSST No. 1 well, the KSSD No. 3 well, the KSST No. 2 well, the KSSD No. 1 well, the KSST No. 4A well, and the KSSD No. 2 well (fig. 76).

Late Pleistocene

The late Pleistocene age section contained no strictly age-diagnostic microfossils. The age of the section was generally established from its stratigraphic position relative to the underlying middle Pleistocene. The unsampled intervals from the seafloor to the first samples in all the wells were assumed to be late Pleistocene (and Holocene) in age, except for the KSST No. 1 well, where a late Pliocene to early Pleistocene age section was encountered in the first sample, just below the seafloor. Strata of late Pleistocene age at the KSST 4A well site were apparently uplifted and eroded or not deposited.

Middle Pleistocene

Sediments of middle Pleistocene age were noted in all of the KSSD wells, and early to middle Pleistocene age sediments are present in the KSST No. 2 and KSST No. 4A wells. The age determinations are based on occurrences of the diatoms Rhizosolenia curvirostris in the KSSD No. 3 well and the KSST No. 2 well, Thalassiosira nidulus in the KSSD No. 3 well, the KSST No. 2 well, the KSSD No. 1 well, and the KSSD No. 2 well; the silicoflagellate Distephanus octonarius in the KSSD No. 3 well and the KSSD No. 1 well; and the radiolarian Lamprocyrtis haysi in the KSSD No. 3 well. The benthic foraminifera Eilohedra levicula in the KSSD

No. 3 well and the KSSD No. 1 well, Pullenia malkinae in the KSST No. 2 well and the KSST No. 4A wells, and the sinistrally coiled planktonic foraminifera Neogloboquadrina pachyderma in the KSST No. 2 well were also useful in correlation and age determination. Age-diagnostic dinoflagellates that were useful included Impagidinium japonicum in the KSST No. 2 well, and the generally Pleistocene species Spiniferites membranaceus and Spiniferites mirabilis in the KSST No. 2 well.

Early Pleistocene

Early Pleistocene strata are present in all of the KSSD wells and probably in the KSST No. 1 well, and an early to middle Pleistocene section is present in the KSST No. 2 and KSST No. 4A wells. Ages are defined on the basis of occurrences of the following microfossils: the diatom Actinocyclus oculatus in the KSSD No. 3 well; the silicoflagellate Dictyocha subarctios in the KSSD No. 2 well; dextrally coiled populations of the planktonic foraminifera Neogloboquadrina pachyderma (late Pliocene to early Pleistocene) in the KSST No. 1 well, the KSSD No. 1 well, and the KSST No. 4A well; the benthic foraminifera Pullenia malkinae in the KSSD No. 3 well, and Melonis pompilioides, Pullenia salisburyi, and Virgulina fusiformis in the KSSD No. 1 well.

Late Pliocene

Definite late Pliocene strata are present in all of the wells except the KSSD No. 3 and No. 2 wells, where the Pliocene section could not be subdivided. Ages are defined on the basis of occurrences of several microfossils, including the diatoms Coscinodiscus marginatus fossilis in the KSSD No. 3 well; Coscinodiscus pustulatus in the KSSD No. 3 well, the KSST No. 2 well, and the KSST No. 4A well; Stephanopyxis horridus in the KSSD No. 3 well, the KSST No. 2 well, the KSSD No. 1 well, and the KSST No. 4A well; Thalassiosira antiqua in the KSST No. 1 well, the KSSD No. 3 well, the KSSD No. 1 well, and the KSST No. 4A well; Thalassiosira decipiens in the KSST No. 2 well; Thalassiosira usatschevii in the KSST No. 2 well; Coscinodiscus excentricus (lowest stratigraphic occurrence) in the KSSD No. 1 well; Thalassiosira gravida (lowest stratigraphic occurrence) in the KSSD No. 1 well; and Thalassiosira nidulus (lowest stratigraphic occurrence) in the KSSD No. 1 well. The silicoflagellate Ammodochium rectangulare was useful in the KSSD No. 3 well, the KSST No. 2 well, and the KSSD No. 1 well. Also important were the benthic foraminifera Epistominella pacifica in the KSST No. 2 well and the KSSD No. 2 well, Virgulina cf. V. pertusa in the KSSD No. 1 well, and deep-water arenaceous foraminifera in the KSST No. 1 well. The planktonic foraminifera Globorotalia cf. G. inflata in the KSSD No. 1 well also helped define the late Pliocene, along with dextrally coiled populations of Neogloboquadrina pachyderma in the KSST No. 2 well and the KSST No. 4A well. The pollen Epilobium compactipollenites in the KSSD No. 2 well and the spore Rouseisporites sp. in the KSSD No. 2 well were also important.

Early Pliocene

An early Pliocene section was discernible in the KSSD No. 1 well only. It was defined by its stratigraphic position relative to the overlying and underlying sections.

Late Miocene

Probable late or middle to late Miocene strata are present in all three KSSD wells. The section is defined on the basis of occurrences of the following microfossils: the foraminifera Ammonia aff. A. japonica in the KSSD No. 1 well, Gyroidina altiformis in the KSSD No. 3 well and the KSSD No. 1 well, Gyroidina rotundimargo and Gyroidina soldanii in the KSSD No. 1 well; and the dinoflagellate Impagidinium cornutum in the KSSD No. 2 well.

Middle (or Early? to Middle) Miocene

Middle (or early? to middle) Miocene age strata are present in all three KSSD wells. The following microfossils were used to define the section: the dinoflagellates Lingulodinium brevispinosum and Reticulosphaera actinocoronata in the KSSD No. 2 well, Spiniferites crassipellis in the KSSD No. 3 well, Systematophora ancyrea in the KSSD No. 3 well, the KSSD No. 1 well, and the KSSD No. 2 well; and the calcareous nannofossil Cyclicargolithus floridanus in the KSSD No. 3 well.

Late Eocene

Late and middle? to late Eocene strata are present in the KSSD No. 3 and No. 2 wells. The upper boundary denotes a regional unconformity that separates the overlying Neogene section from the underlying Paleogene section. This unconformity truncates the middle Eocene section in the KSSD No. 1 well. The late Eocene interval was defined on the basis of occurrences of the calcareous nannofossils Dictyococcites cf. D. scrippsae in the KSSD No. 3 well and Reticulofenestra hillae in the KSSD No. 2 well, and the dinoflagellates Impagidinium velorum and Phthanoperidinium alectrolophum in the KSSD No. 2 well. A late Eocene age for the interval is also supported by the arenaceous foraminifera Bathysiphon sanctaerucis in the KSSD No. 3 and KSSD No. 1 wells, and Haplophragmoides cf. H. indentatus in all three KSSD wells.

Middle Eocene

Middle Eocene strata are present in the KSSD No. 1 well and are indicated by occurrences of the following microfossils: the dinoflagellates Cordosphaeridium gracile, Deflandrea sagittula, Deflandrea cf. D. wetzelii and Glaphyrocysta exuberans in the KSSD No. 1 well; and the lowest occurrence of the calcareous nannofossil Reticulofenestra umbilica in the KSSD No. 2 well.

Early Eocene

The early Eocene interval is defined only in the KSSD No. 1 well. This age is based on occurrences of the dinoflagellates Cordosphaeridium cf. C. biarmatum, Dracodinium condylos, and Lanternosphaeridium radiatum.

8. ORGANIC GEOCHEMISTRY

INTRODUCTION

Six COST wells were drilled on the Kodiak shelf for the purpose of evaluating the petroleum potential of the sediments in a Cenozoic accretion belt which occurs between the Aleutian volcanic arc and the Aleutian trench. They extended from the southwest to the northeast in the following order: KSST No. 1, KSSD No. 3, KSST No. 2, KSSD No. 1, KSST No. 4A, and KSSD No. 2 wells (fig. 2, p. 4). The three KSSD wells were drilled to depths of 8,000 to 11,000 feet and are of the greatest significance because of the thickness of the stratigraphic section which they penetrate. The three KSST wells were drilled to depths of less than 5,000 feet, and did not sample a significant section of mature sediments. Because of this, only the KSSD wells are discussed in detail, although a synopsis of the petroleum potential and some data for the shallow KSST wells are provided (Appendix 6). All depths given in this section of the report are measured from the Kelly bushings of the respective wells.

Hunt (1979) believes that cuttings are generally preferable to sidewall cores for hydrocarbon surveys because the sidewall cores have been exposed to the high pressure of drilling muds and are, therefore, more likely to be contaminated by pipe dope, mud additives, or circulated indigenous organic materials if they are present. Data included in this report have been obtained mostly from cuttings samples, but other samples did not produce contradictory data, nor would an interpretation based on sidewall cores and drilling-mud data differ significantly from the interpretation presented here.

KSSD NO. 1 WELL

The KSSD No. 1 well was drilled by Sun Oil Company on the western flank of the west half of the Stevenson Basin. The elevation of the Kelly bushing was 90 feet above mean sea level and the water depth at the well site is 526 feet. Two hundred forty-five cuttings samples were collected at 30-foot intervals and sent to GeoChem Laboratories, Inc. (GeoChem Labs), of Houston, Texas, for analysis. Seventeen sidewall cores and four conventional core samples were also analyzed. The samples were analyzed for total organic carbon content (TOC), kerogen type and alteration, C₁-C₇ light gas and gasoline fractions, and C₁₅+ extractable hydrocarbons (Bayliss, 1977). Twenty-six composite samples derived from cuttings samples held by

the Minerals Management Service were also sent to the Bujak Davies Group (Bujak Davies) of Calgary, Alberta, for palynological analysis (Bujak Davies Group, 1987). The kerogen content was estimated and an evaluation of the thermal alteration index (TAI) was made on 22 of these samples.

Total organic carbon content has been used for about three decades to screen potential source rocks (Ronov, 1958). A minimum organic carbon content of 0.5 percent is generally considered to be necessary for the generation of oil (Hunt, 1979; Tissot and Welte, 1978). According to Hunt, an average shale contains about 1 percent organic carbon, and most hydrocarbon-source-quality shales contain from 1 to 2 percent organic carbon and several hundred parts per million (ppm) C₁₅+ hydrocarbon. Very rich source rocks often contain considerably more organic carbon.

GeoChem Labs measured the TOC from finely ground, acid-washed samples by combustion in a Leco carbon analyzer. Soxhlet extraction was performed on 100 gram samples using a benzene-methanol solvent to dissolve bitumen. The pentane-soluble fraction was then dissolved from the bitumen in pentane, leaving the insoluble asphaltenes. Finally, the pentane-soluble fraction was separated into saturates, aromatics, and nitrogen-sulfur-oxygen (NSO) compounds by adsorption chromatography on a silica gel-alumina column. The content and molecular composition of the heavy C₁₅+ saturated hydrocarbons were then determined by gas chromatography.

Figure 77 provides a summary of organic carbon analyses for the KSSD No. 1 well. Only eight cuttings samples yielded TOC values greater than 0.5 percent. The highest observed TOC value, 0.60 percent, came from a sample representing the interval from 3,470 to 3,500 feet. Only six samples yielded C₁₅+ extractable hydrocarbons in measurable amounts (fig. 77). The highest value was 92 ppm from a cuttings sample collected from the interval between 7,340 and 7,370 feet. Most of the C₁₅+ extract was composed of asphaltenes (non-hydrocarbons).

The organic material in the KSSD No. 1 well was examined in transmitted light by GeoChem Labs and by Bujak Davies. GeoChem Labs indicated that the kerogen was composed predominantly of herbaceous-spore/cuticle material. Lesser amounts of woody materials and trace amounts of opaque (coaly) materials were present (fig. 77). The Bujak Davies Group were substantially in agreement with GeoChem Labs, but felt that herbaceous and woody kerogens occurred in roughly equal parts throughout the post-Eocene section (surface to 6,142 feet). Herbaceous kerogen was reported to be more common in the Eocene section (6,142 to 8,517 feet, TD). Bujak Davies referred to opaque materials as inertinite and noted that trace amounts were present. The Bujak Davies data are listed in Appendix 2. True coals were not observed nor were they indicated by TOC values in this well.

Light hydrocarbons (C₁ to C₇ headspace gas from blended cuttings) are used as indicators of kerogen quality, thermal maturity, and hydrocarbon generation. Significant amounts of the C₂

to C₇ fraction are found in oil and thermally mature sediments, but not in plants, animals, or thermally immature sediments (Tissot and Welte, 1984; Hunt, 1979). This suggests that C₂-C₇ hydrocarbons are products of catagenesis, the process by which organic material is altered due to the effects of increasing temperature (Hunt, 1979). Modest amounts of light hydrocarbon gas occur throughout the KSSD

No. 1 well. Both wetness $\left(\frac{C_2 + C_3 + C_4}{C_1 + C_2 + C_3 + C_4} \times 100 \right)$ and the C₅-C₇

fraction appear to increase below the unconformity at 6,142 feet, but neither increases sufficiently to indicate that catagenesis has occurred (fig. 78).

Hunt (1979) notes that young, immature oils contain more isoalkanes, whereas old, mature oils contain a greater proportion of normal alkane homologs. Consequently, the iso- to normal butane ratio (iC₄/nC₄) decreases with depth, demonstrating isomeric equilibrium as a function of thermodynamic maturity (Reznikof, 1967). In the predominantly Neogene sediments at depths of less than 6,400 feet, the iC₄/nC₄ ratio is relatively high and varies erratically (fig. 78). Below this depth, in the Paleogene section, the iC₄/nC₄ ratio remains between approximately 1 and 2. This supports the hypothesis that there is little change in thermal maturity of the light hydrocarbons from sediments above the unconformity at 6,142 feet, but that below the unconformity, where temperatures are higher and the time increments represented by intervals of sediment are greater, levels of thermal maturity may be very slightly greater.

Total C₁₅+ hydrocarbon extracts from this well are low (fig. 77), making interpretation of gas chromatograms and hydrocarbon ratios derived from them equivocal. However, table 9 shows naphthene to paraffin ratios (n/p), paraffin-naphthene to aromatic ratios (p-n/a), and the carbon preference indices (CPI) for this well.

$$\text{CPI} = 1/2 \left(\frac{C_{25} + C_{27} + C_{29} + C_{31}}{C_{26} + C_{28} + C_{30} + C_{32}} + \frac{C_{25} + C_{27} + C_{29} + C_{31}}{C_{24} + C_{26} + C_{28} + C_{30}} \right)$$

Figure 79 shows four representative gas chromatograms of extracted C₁₅+ hydrocarbons. The chromatograms from samples at 6,020 and 6,350 feet bracket the "Miocene" unconformity. Free-energy data from naphthenes (n) and paraffins (p) indicate that the paraffins are more likely to be stable at higher temperatures, which means that the naphthene to paraffin ratio (n/p) should decrease with increasing depth (increasing age and temperature) of the sediments from which the hydrocarbons have been extracted. The change in the n/p ratio has been observed to be logarithmic with a linear increase in depth through the Mesozoic. This generalization has not been observed to hold for older Paleozoic rocks (Hunt, 1979).

TABLE 9. Naphthene/paraffin ratios, paraffin-naphthene/aromatics ratios, and carbon preference indices, KSSD No. 1 well.

	Depth (feet)	n/p	(p-n)/a	CPI
	1,700	44		
	2,060	12		
	2,390	24		
	2,750	10		1.70
	3,140	9		1.82
	3,500	7	1.41	1.32
	3,830	8		1.36
Post-Eocene Sediments	4,220	9		1.49
	4,580	12	1.15	1.63
	4,940	14		
	5,300	14		
	5,660	18	1.50	1.95
	5,824	16		
	6,020	14		1.94
-----U-N-C-O-N-F-O-R-M-I-T-Y-----				
	6,350	5		1.54
	6,650	5	0.69	1.54
Eocene Sediments	7,010	3	0.82	1.60
	7,370	3	1.04	1.62
	7,730	4		1.59
	8,090	4		1.57
	8,450	4		1.51
	8,525	3		1.51

Naphthene backgrounds are generally lower below the unconformity (table 9), suggesting that $C_{15}+$ extracts may be slightly more mature. Low (p-n)/a ratios (less than about 1.0) are generally associated with immature sediment (Bayliss and Smith, 1980). In the interval from 6,350 to 8,525 feet, the CPI ranges between 1.62 and 1.51. The lower maximum CPI value, combined with the reduced range of CPI values beneath the unconformity, may also suggest a slight increase in the maturity of the generally immature $C_{15}+$ extracts.

The thermal alteration index (TAI) shown on figure 77 was proposed by Staplin (1969). It has been used for nearly two decades to describe the level of thermal alteration reached by organic material in sediments as the sediments are exposed to increasing temperatures with depth of burial. The technique is highly subjective in that the observer must assign a number to a color he perceives. Staplin (1982) has provided a list of the precautions he believes should be observed in order to obtain valid, reproducible results.

TAI profiles plotted from data produced by GeoChem Labs and by Bujak Davies are given on figure 77, along with several mean random vitrinite reflectance (R_o) values observed by Bujak Davies. Appendix 5 contains a table that correlates TAI values used by Bujak Davies

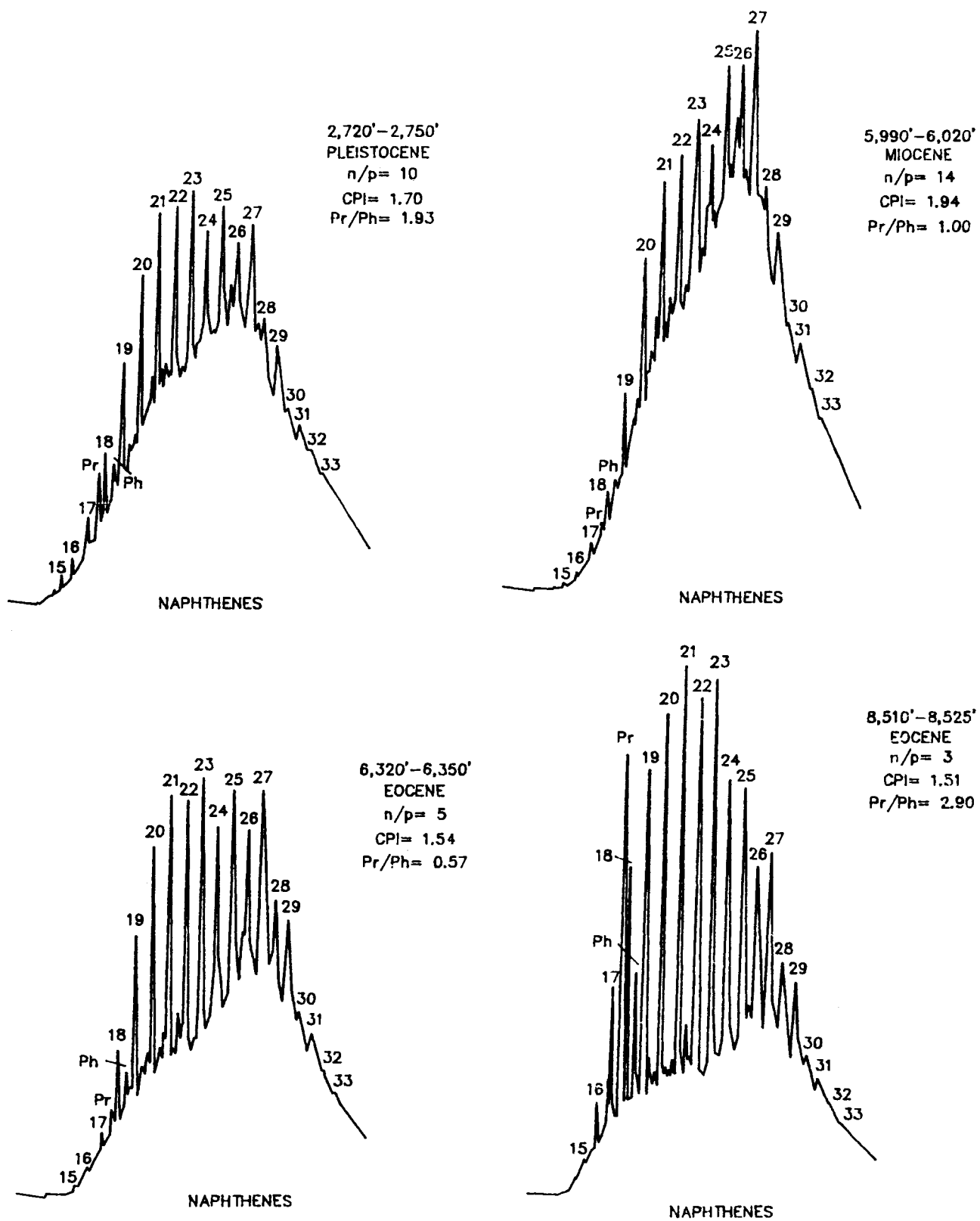


Figure 79. Representative C₁₅+ gas chromatograms from cuttings samples, KSSD No. 1 well.

and GeoChem Labs with R_o values and with a numerical scale used by GeoChem Labs to decimalize integer TAI values that are modified by positive or negative signs. Observed TAI values have been converted to the numerical scale to facilitate plotting the values on the profiles. All of the R_o values derived from Bujak Davies data are recorded in Appendix 2. These averages represent the dominant populations and were derived from the modes on histograms that are believed to represent unrecycled organic matter. They are plotted on figures 77, 80, and 83.

Bujak Davies states that the onset of thermal maturity for herbaceous woody kerogen occurs at TAI values of 2 to 2^+ (2.40 on the numerical scale on fig. 77) and approaches optimum generative maturity at a TAI of about 2^+ to 3^- (2.80 on the numerical scale, fig. 77). GeoChem Labs suggests that moderate maturity of kerogen occurs when TAI values reach 2 (2.20 on their numerical scale) and that they are near their optimum value for hydrocarbon generation at a TAI value of 3^- (3.00 on their numerical scale).

The Bujak Davies TAI data on figure 77 suggest that catagenesis occurs from about 5,000 feet to total depth in this well, although this is in contrast to most other available data. GeoChem Labs TAI values imply that the kerogen is thermally immature throughout the section penetrated by this well. Wetness of the headspace gas is only beginning to increase near the bottom of the well (fig. 78), the heavy hydrocarbon content is still skewed toward the odd-chain paraffins in the C_{21} - C_{23} range, and naphthenes are still the predominant saturated hydrocarbons (fig. 79), which indicates that the extract present in the sediment is at about the same level of thermal maturity as the kerogen TAI values observed by GeoChem Labs.

Four cuttings samples were sent to Bujak Davies for evaluation of mean random vitrinite reflectance (R_o). The data produced multimodal histograms that appear to agree favorably with most other indications of thermal maturity if a profile is projected through the populations on histograms with minimal R_o values to the surface, where unaltered organic material usually exhibits R_o values of 0.18 to 0.2 percent (Hunt, 1979). This R_o profile projects to 0.6 percent at 8,500 or 9,000 feet at the KSSD No. 1 well location. An R_o of 0.6 percent is considered by most authorities to represent the onset of catagenesis in humic kerogens (Hunt, 1979; Tissot and Welte, 1984). The multimodal histograms suggest that reworked sediments are present throughout the well. If this is correct, it is necessary to regard all of these analyses with a degree of caution.

KSSD NO. 1 WELL SUMMARY

The sediments penetrated by the KSSD No. 1 well are thermally immature, contain predominately herbaceous-woody kerogen with very little organic carbon, and do not appear to contain significant amounts of hydrocarbons other than methane. It is possible that methane from a biogenic or a low-temperature source could occur in

these sediments, but geochemistry performed on samples obtained from this well do not provide any indication that this has occurred.

KSSD NO. 2 WELL

The KSSD No. 2 well was drilled on the southeast flank of the east half of the Stevenson Basin. The elevation of the Kelly bushing was 90 feet above mean sea level and the water depth, at this location, is 375 feet. One hundred forty-eight cuttings samples were collected representing 30-foot intervals and sent to GeoChem Labs for analysis (Bayliss, 1977). Thirty sidewall cores and six mud samples were also analyzed. Fifty-one composite cuttings samples held by the MMS were sent to the Bujak Davies Group for palynological analysis. Kerogen identification and TAI evaluation were performed on 29 of these samples (Bujak Davies Group, 1987).

Profiles of the organic carbon content of the KSSD No. 2 well are shown in figure 80. No samples contained more than 0.5 percent TOC. The maximum observed TOC value was 0.49 percent. Seven cuttings samples contained C₁₅₊ hydrocarbons (fig. 80) in excess of 100 ppm; of these, only one contained more than 200 ppm C₁₅₊ hydrocarbons and is, therefore, considered by GeoChem Labs to be a good anomaly (Bayliss and Smith, 1980). This cuttings sample represents the interval between 5,910 and 5,940 feet and contained 302 ppm total C₁₅₊ hydrocarbons. The sample from which this extract was derived was composed mostly of slightly calcareous claystone containing only 0.37 percent TOC. Most of the C₁₅₊ extract obtained from cuttings samples was made up of asphaltenes (non-hydrocarbons), as was the case in the KSSD No. 1 well.

Organic material from the KSSD No. 2 well was examined in transmitted light by both GeoChem Labs and Bujak Davies. GeoChem Labs observed mostly herbaceous-spore/cuticle material in this well, as in the KSSD No. 1 well. Again, minor amounts of black inertinite-related (coaly) debris were present in trace amounts. Bujak Davies also reported herbaceous, woody and coaly kerogen, with woody kerogen being slightly more common in some sections (Appendix 3). Small amounts of amorphous material, possibly degraded herbaceous kerogen, was observed by both laboratories.

The content of light hydrocarbons (C₁-C₇) is indicated graphically on figure 81. Modest amounts of light hydrocarbons occur throughout the well, but the total amounts of light hydrocarbons are not particularly impressive and there is no apparent progressive increase in the heavier hydrocarbons with depth. From about 8,000 to 10,460 feet (TD), there is an increase in C₂-C₄ and C₅-C₇ hydrocarbons in the headspace gas. The abruptness of the increase suggests that it is more probably related to changes in lithology than to increasing maturity of the sediments. The iso- to normal butane ratio (iC₄/nC₄) exhibits very little change throughout the section penetrated by the KSSD No. 2 well, which suggests that no significant change in thermal maturity has occurred.

Total C₁₅+ extracts are shown in figure 80. As in the KSSD No. 1 well, the hydrocarbon content of these extracts is low. Naphthene to paraffin ratios, paraffin-naphthene to aromatics ratios, and the carbon preference indices for cuttings samples from the KSSD No. 2 well are given in table 10. Four representative gas chromatograms are shown in figure 82. The chromatograms from 8,640 to 8,670 feet straddle the Paleogene-Neogene unconformity.

There are no significant changes in the hydrocarbon ratios listed in table 10, nor do the representative chromatograms indicate any apparent increase in thermal maturity with depth. The high naphthene backgrounds and significant contents of heavy, long-chain paraffins are consistent with values derived from immature extracts.

One feature that does stand out in figure 80 is the increase in total C₁₅+ extract (largely asphaltenes) that occurs in samples representing the interval below 5,310 feet. An overconsolidated zone occurs from approximately 5,490 to 5,690 feet that may have inhibited the upward migration of bitumen at this location. Alternatively, a fault intersecting the wellbore at about 5,590 feet may have confined the bitumen to the deeper sediments.

The organic matter from the sediments penetrated by KSSD No. 2 well were studied in transmitted light by both GeoChem Labs and Bujak Davies. Four samples were also examined by Bujak Davies in reflected light for R_o values. The Bujak Davies data were nearly one TAI unit greater than the GeoChem Labs data (figure 80). As with the data from the KSSD No. 1 well, the low wetness of the C₁ to C₄ headspace gas, a predominance of long-chain paraffins and naphthenes in C₁₅+ extracts, and the limited available R_o data, all tend to suggest that reworked material may have yielded somewhat high TAI values for Bujak Davies palynologists. Vitrinite group kerogens were not particularly abundant in the samples submitted from this well for analysis, and, as a consequence, the R_o values were a bit more erratic than in the other wells. The R_o values project to 0.6 percent, the threshold for catagenesis of humic kerogens (Hunt, 1979; Tissot and Welte, 1984), at about 11,500 feet. As in the KSSD No. 1 well, this interpretation of the R_o values is based upon the assumption that the population with the lowest values represents indigenous kerogen.

KSSD NO. 2 WELL SUMMARY

The sediments sampled in the KSSD No. 2 well appear to be thermally immature, contain predominately herbaceous-woody kerogen with very little organic carbon, and do not appear to possess significant amounts of hydrocarbons other than methane. Dry gas (methane) occurs in Eocene rocks below the unconformity at 8,774 feet and near the surface in recent sediments. The deeper gas contains traces of gasoline-range hydrocarbons (C₅ to C₇) and may be of thermogenic origin, but such hydrocarbons would probably not have been generated at 8,000 to 10,000 feet at this site. The shallow gas is almost completely composed of methane and is believed to be of biogenic origin. Because of the low organic carbon content and the

predominance of herbaceous and woody organic material in the sedimentary section penetrated, as well as the low levels of thermal maturity shown by most indicators, it seems unlikely that economically significant quantities of petroleum have been generated

TABLE 10. Naphthene/paraffin ratios, paraffin-naphthene/aromatics, and carbon preference indices, KSSD No. 2 well.

	Depth (feet)	n/p	(p-n)/a	CPI
	1,470-1,500	30	2.00	1.41
	1,536-1,537	9		
	1,710-1,740	10		1.71
	2,010-2,040	7		
	2,213-2,214	10		
	2,310-2,340	6		
	2,468-2,469	11		
	2,610-2,640	13 ¹		1.62
	2,776-2,778	12		
	2,910-2,940	8		
	3,210-3,240	7	0.75	
	3,119-3,120	10		
	3,520-3,521	11		
	3,769-3,770	14		
	3,810-3,840	17	2.11	1.42
	4,035-4,036	10		
	4,110-4,140	12		1.56
	4,316-4,317	12		
	4,380-4,410	17	2.17	1.43
Post-Eocene Sediments	4,439-4,440	12		
	4,710-4,740	17		
	5,010-5,040	12		
	5,310-5,340	18	1.44	
	5,610-5,640	14		
	5,910-5,940	21	1.88	
	6,210-6,240	12		
	6,510-6,540	17	1.28	1.40
	6,810-6,840	12		
	7,110-7,140	16	0.83	1.50
	-7,362	6	0.62	1.86
	7,380-7,410	17	1.56	1.68
	7,680-7,710	10	0.59	1.54
	7,980-8,010	9	0.60	1.56
	8,280-8,310	7	0.71	1.55
	8,580-8,610	9		1.53
	8,640-8,670	12	1.05	1.60
-----U-N-C-O-N-F-O-R-M-I-T-Y-----				
	8,880-8,910	9	1.26	1.68
	9,180-9,210	10		2.32
Eocene Sediments	9,480-9,510	27	2.97	1.87
	9,780-9,810	10	1.15	2.44
	10,080-10,110	9	1.22	2.08
	10,440-10,460	16	1.54	2.27

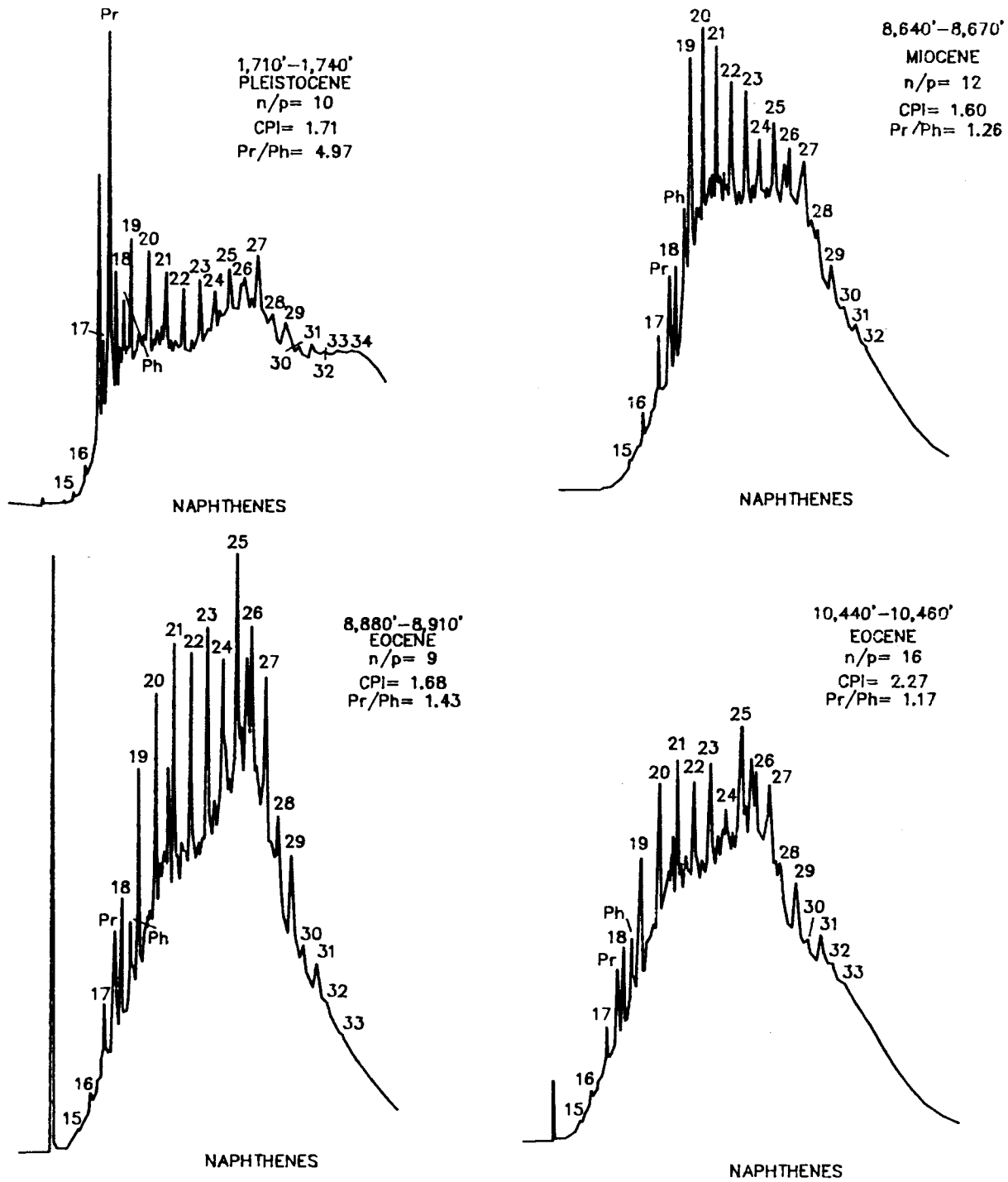


Figure 82. Representative C₁₅+ gas chromatograms from cuttings samples, KSSD No. 2 well.

at this location. If petroleum were to be generated at this site it would probably form at depths greater than approximately 11,500 feet.

KSSD NO. 3 WELL

The KSSD No. 3 well was drilled in a local depression north-east of the Albatross Basin. The elevation of the Kelly bushing was 90 feet above mean sea level and the water depth is 265 feet. Two hundred sixty-four canned cuttings samples representing 30-foot intervals were collected from this well. Thirty-nine sidewall core samples, 2 conventional core samples, and 22 canned mud samples were also collected. The samples were sent to GeoChem Labs for analysis (Cernock, 1977). Twenty-five composite cuttings samples held by the MMS were also sent to the Bujak Davies Group for palynological analysis. Kerogen identification and TAI evaluation were made on 22 of these samples (Bujak Davies Group, 1987).

Organic carbon content profiles of the KSSD No. 3 well appear on figure 83. The TOC values did not generally exceed 0.51 percent. However, at 2,304, 2,930, 5,099, 7,800, 8,100, 9,000, and 9,300 feet, conventional core samples produced the following respective TOC values: 0.61, 0.54, 0.61, 0.56, 0.59, 0.55, and 0.64 percent. All of these values are actually somewhat below the average values for shales (Hunt, 1979). Only four cuttings samples produced any C₁₅+ extractable hydrocarbons. Two samples representing the intervals from 1,370 to 1,400 feet and 5,000 to 5,090 feet produced more than 200 ppm C₁₅+ hydrocarbons and would, therefore, be considered as good anomalies by GeoChem Laboratories (Bayliss and Smith, 1980). The total extractable C₁₅+ hydrocarbons were 350 ppm and 233 ppm, respectively. The first sample contained only 0.38 percent TOC and was thought to be contaminated by mud additives or pipe dope. The second, deeper sample contained 0.51 percent TOC and might represent a potential source rock if a sufficient volume were present.

Organic material from the KSSD No. 3 well was examined in transmitted light by both GeoChem Labs and by Bujak Davies. GeoChem Labs observed only gas-prone herbaceous and woody kerogen throughout the section (fig. 83). Bujak Davies described predominantly herbaceous, woody and coaly (inertinitic) material with small amounts of resinous and amorphous material from approximately 2,660 to 3,170 feet and at approximately 4,850 feet (Appendix 4).

Light hydrocarbons (C₁-C₇) are reported on figure 84. Fairly impressive levels of light hydrocarbons, mostly methane, are present from the surface to the unconformity at 7,805 feet. In the sample representing the interval from 7,760 to 7,990 feet, the wetness ratio and content of the gasoline-fraction (C₅-C₇) hydrocarbons increase sharply and remain high to total depth (9,357 feet). The iC₄/nC₄ ratio does not change significantly throughout the well, but the values obtained from below the unconformity are less variable than those obtained from depths of less than about 7,800 feet. The abruptness of the change in C₂-C₇ values and the failure of the iC₄/nC₄ ratio to change suggest that the light-hydrocarbon content of

the sediments is responding to a change in lithology and may be related to the unconformity rather than to a gradual and progressive change in the thermal maturity.

Figures 83 and 85 show the composition of C₁₅+ extracts from the KSSD No. 3 well. The extracts are composed mostly of asphaltenes. Table 11 shows the n/p ratios, (p-n)/a, and the CPI values for this well.

TABLE 11. Naphthene/paraffin ratios, paraffin-naphthene/aromatics, and carbon preference indices, KSSD No. 3 well.

	Depth (feet)	n/p	(p-n)/a	CPI
	1,370-1,400	22	1.85	1.67
	1,730-1,760	12		1.35
	2,090-2,120	18		1.43
	2,450-2,480	10		1.29
Post-Eocene Sediments	2,810-2,840	7		1.19
	3,170-3,200	19		
	3,530-3,560	13	1.67	1.45
	3,830-3,920	12		1.59
	4,250-4,280	6		1.41
	4,580-4,670	16		1.74
	5,000-5,090	21	2.26	1.62
	5,300-5,390	5		1.39
	5,660-5,810	8		1.87
	6,080-6,170	32	1.38	
	6,380-6,470	10		2.17
	6,740-6,830	8		1.94
	7,100-7,190	6		0.95
	7,460-7,550	8		1.65
-----U-N-C-O-N-F-O-R-M-I-T-Y-----				
	7,880-7,910	3		
Eocene Sediments	8,240-8,270	10		1.77
	8,540-8,630	3		
	8,960-8,990	3		

There are no very apparent changes or trends in the values listed in table 11. However, a reduction in the n/p ratio occurs in the vicinity of the unconformity (approximately 7,800 feet). This change shows up fairly graphically on the representative chromatograms on figure 85. This may reflect a slight increase in maturity of the C₁₅+ extracts below the unconformity. However, all of the chromatograms exhibit molecular distribution of normal paraffins skewed towards a higher molecular weight range that is characteristic of immaturity in C₁₅+ hydrocarbons. The steranes and terpanes identified on the deepest sample (8,960 to 8,990 feet) are generally considered to be indicators of thermal immaturity (Waples, 1981; Tissot and Welte, 1984).

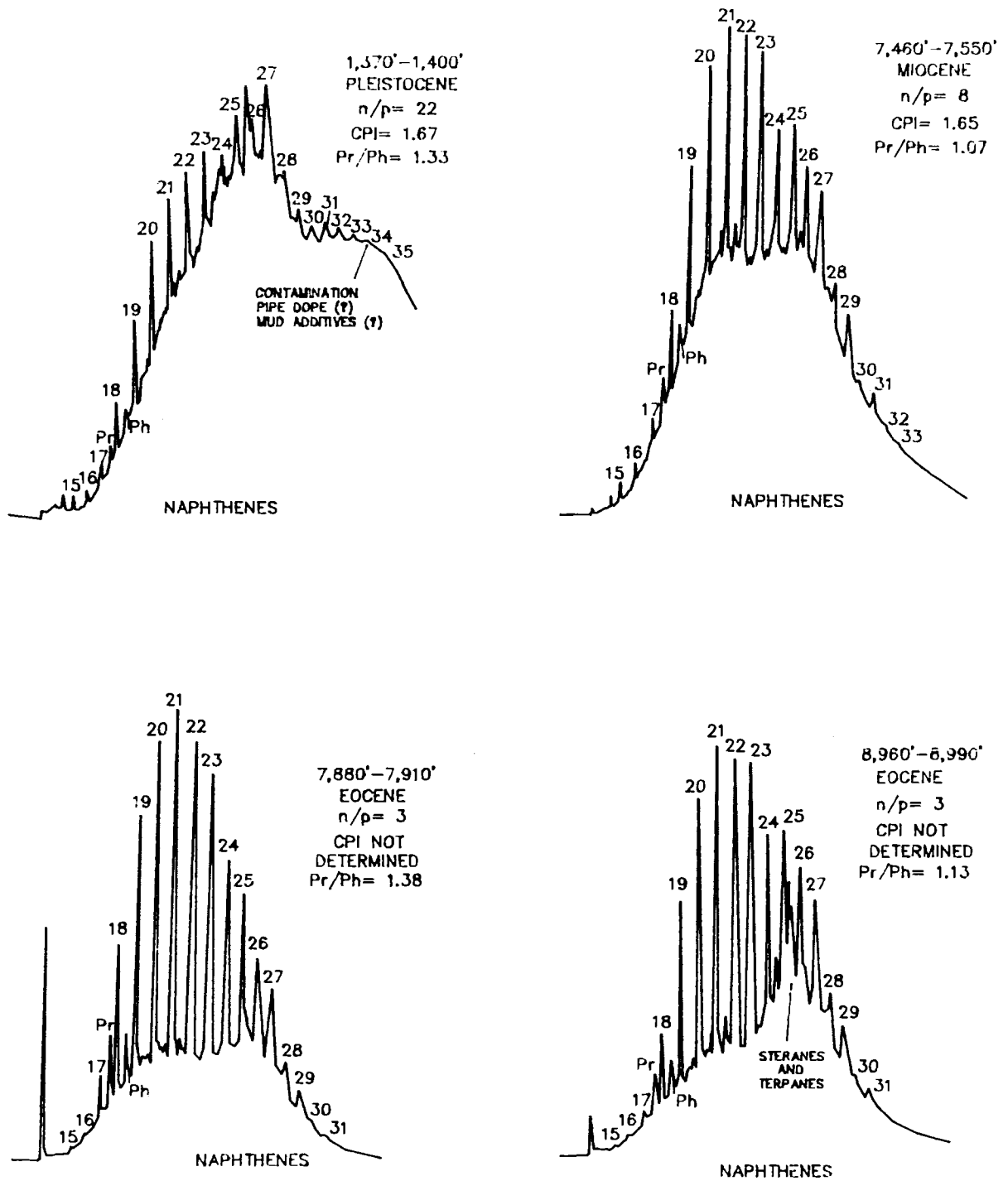


Figure 85. Representative $C_{15}+$ gas chromatograms from cuttings samples, KSSD No. 3 well.

Organic matter from sediments penetrated by the KSSD No. 3 well were studied in transmitted light by GeoChem Labs and Bujak Davies. Four cuttings samples held by MMS were also sent to Bujak Davies for re-evaluation in reflected light. The results of these analyses are shown on figure 83. GeoChem Labs TAI values appear to be in better agreement with the various hydrocarbon analyses, particularly the distribution of C₁₅+ extracted hydrocarbons. From 7,100 to 9,200 feet there is a change in the rate of increase in the TAI values for the GeoChem Labs data. However, the R₀ values do not anywhere exceed 0.5 percent (Appendix 4). Additionally, steranes and terpanes are present in C₁₅+ extracts from these depths (fig. 85), which indicates thermal immaturity. Significant amounts of reworked kerogen may have biased the TAI interpretation within this interval. A projection of R₀ values from the surface (fig. 83) suggests that catagenesis of humic kerogen probably occurs at a depth of about 11,500 feet at this location.

TOC and R₀ values for samples from the Eocene Sitkalidak Formation from the southeast coast of Kodiak Island have been published by Armentrout and Anderson (1980). Neither specific sample locations nor descriptions of the samples were given. TOC values ranged from 0.01 to 2.38 percent and R₀ values from 0.54 to 0.92 percent. The authors concluded from these analyses and from the poor reservoir character of the sandstones that the Sitkadilak Formation has a low potential for hydrocarbon production.

KSSD NO. 3 WELL SUMMARY

The sediments penetrated by the KSSD No. 3 well are thermally immature, contain predominantly herbaceous, woody and coaly material with very low amounts of organic carbon. Reworked sediments are believed to have contributed some kerogen that appears to have undergone catagenesis. The autochthonous kerogen is immature. Although Eocene sediments from beneath the unconformity at 7,805 feet contain some "wet gas," these hydrocarbons do not appear to have been generated by the sediments sampled in this well. It may be that they formed from small amounts of organic matter disseminated throughout large volumes of sediment deeper in the basin.

KSST NO. 1 WELL

The KSST No. 1 well was drilled on the south flank of the Albatross Basin to a total depth of 4,225 feet. The elevation of the Kelly bushing was 52 feet above mean sea level. The sea floor depth at the well site is 162 feet. Sixty-four canned cuttings samples representing 30-foot intervals, 20 samples of sidewall cores, and 9 drilling fluid samples were collected from this well and sent to GeoChem Labs for analysis (Carlisle, 1976a). Bujak Davies examined 9 cuttings samples held by the MMS for TAI level and identification of kerogen (Bujak Davies Group, 1987). Because this well and the two other KSST wells penetrated only Pleistocene and Pliocene sediments, only a brief synopsis of the geochemical data is given below.

The organic carbon content in the KSST No. 1 well is generally low; individual samples did not exceed 0.49 percent TOC. Two cuttings samples produced total C₁₅+ extractable hydrocarbon levels of 408 ppm from sample intervals of 3,630 to 3,660 feet and 3,930 to 3,960 feet. A shallow sample (630 to 660 feet) yielded 331 ppm C₁₅+ extractable hydrocarbons and contained 0.48 percent TOC. Both Bujak Davies and GeoChem Labs palynologists identified predominantly woody and coaly kerogen with lesser amounts of herbaceous material. Bujak Davies found herbaceous material somewhat more common from about 2,970 feet to total depth. The kerogen is considered to be gas prone.

Fairly large amounts of methane (up to 16,423 ppm) were present in headspace gas obtained from cuttings samples down to about 1,500 feet. These gases are most probably of biogenic origin. Levels of methane from 1,500 to 4,225 feet (TD) are somewhat lower but are generally below a few thousand ppm. Wetness throughout the well is low (generally less than 2 percent). The C₁₅+ extracts tend to contain relatively high amounts of asphaltenes (14 to 65 percent), and the chromatograms show high naphthene backgrounds. The paraffin distribution includes long chain homologs of up to 27, 29, and 31 carbon atoms. The CPI values range from 1.63 to 2.68, with the highest value from the deepest sample (4,200 to 4,225). This suggests that the extracts are thermally immature and contain a significant amount of terrestrially derived (waxy?) debris. If these extracts were derived from reworked sediments, the original CPI values for the unaltered sediments would most probably have been higher.

Bujak Davies reported levels of thermal alteration that increased from a TAI value of 2⁻ to 2 (an R_o equivalent of about 0.5 percent) at 450 feet, to 2 (an R_o equivalent of about 0.6 percent) at 3,900 feet. GeoChem Labs TAI values ranged from 1⁺ to 2⁻ at 660, 900, and 1,200 feet (the underlined 2⁻ indicates that the distribution of TAI values in the dominant population was skewed to the 2⁻ end). This is approximately equivalent to an R_o value of 0.43 percent (Bayliss and Smith, 1980). The deepest samples (from 4,120 and 4,225 feet) exhibited exactly the same TAI values (1⁺ to 2⁻). Between 1,300 and 4,000 feet, the GeoChem Labs TAI distribution is somewhat erratic. Dominant populations ranged as high as 2 to 2⁺ (equivalent to an R_o of 0.7 percent; Bayliss and Smith, 1980) at 1,316, 1,470, and 2,200 feet. The fact that the Bujak Davies values for very shallow sediments are relatively high, combined with the erratic nature of the GeoChem Labs data, implies that samples sent to the laboratories probably contained significant amounts of reworked material, and that sample contamination may also have been a problem.

KSST NO. 1 WELL SUMMARY

The sedimentary section penetrated by the KSST No. 1 well is thermally immature. Organic material that appears to be near to or within the zone of catagenesis has most likely been reworked and may have also have been contaminated. The kerogen is composed

predominantly of woody and coaly macerals with some herbaceous material, particularly in the deeper parts of the well, and contains minimal amounts of organic carbon. Organic material of this nature is derived from a terrestrial source and is usually gas prone when petroleum is present.

KSST NO. 2 WELL

The KSST No. 2 well was drilled to a depth of 4,307 feet. The well is located less than 10 miles northeast of the KSSD No. 3 well and penetrated a similar Neogene section. The elevation of the Kelly bushing was 52 feet above mean sea level. Sea depth at this location is 237 feet. Seventy-six canned cuttings samples representing 30-foot intervals, 13 sidewall core samples, and 11 drilling fluid samples were collected for analysis by GeoChem Labs (Carlisle, 1976b). The Bujak Davies Group studied 7 cuttings samples held by the MMS for kerogen content and TAI level (Bujak Davies Group, 1987).

The organic carbon content of the sediments sampled by this well is generally low, 0.5 percent or less. However, cuttings samples to depths of 3,420, 3,600, and 3,660 feet contained 1.67, 1.08 and 1.08 percent TOC, respectively. These samples were made up of 60 to 90 percent soft claystone which contained "possible partial drilling mud." Total C₁₅+ extractable hydrocarbon ranged as high as 344 ppm between 2,310 and 2,340 feet, but the TOC for this sample was only 0.39 percent, which would not be regarded as potential source rock by most authorities (Hunt, 1979; Tissot and Welte, 1984). This sample was composed of 50 percent clay which, according to GeoChem Labs, may have been largely drilling mud.

Bujak Davies and GeoChem Labs both listed woody kerogen as the predominant kerogen type, with lesser amounts of herbaceous material. According to GeoChem Labs, a considerable number of the samples also contained drilling mud additives composed of bark or walnut hulls.

Substantial amounts of methane were present in headspace gas to a depth of about 3,400 feet (up to 34,318 ppm at 2,910 to 2,940 feet), but significant amounts of C₂ - C₇ were not present and the wetness ratio did not exceed 0.7 percent except for the shallowest sample (2.9 percent at 450 to 480 feet).

C₁₅+ extracts from this well generally contain high amounts of asphaltenes (39 to 80 percent of the extract). The gas chromatograms exhibit high naphthene backgrounds, and the paraffin distribution contains long chain homologs of up to 27, 29, and 31 carbon atoms. CPI values range from 1.50 to 2.26 with one exception. Sample descriptions indicate that reworked material was present in the sediments. Extracts derived from reworked material would probably produce CPI values slightly lower than those derived from unaltered sediments. The walnut shells appear to have been excluded from samples before analyses were performed because the chromatograms do

not resemble those of walnut shells from the St. George Basin COST No. 1 well and because the TOC values are relatively low.

Bujak Davies found that the level of thermal alteration increased from a TAI value of 2⁻ to 2 at 600 feet, to about 2 at 3,300 feet. This is equivalent to an R_o range of about 0.5 to 0.6 percent. GeoChem Labs assigned TAI values of 1⁺ to 2⁻ for sediments both near the surface (1,320, 1,430, and 1,530 feet) and at total depth (4,080, 4,233, and 4,307 feet). The equivalent R_o would be about 0.4 percent (Bayliss and Smith, 1980). From 1,680 to 3,798 feet, GeoChem Labs TAI values are somewhat erratic but tend to vary around the 1⁺ to 2⁻ level. This may reflect an alternating influx of sediment containing reworked material or it might be caused by contaminants. In general, the sediments appear to be thermally immature in spite of the presence of reworked organic material.

KSST NO. 2 WELL SUMMARY

The sedimentary section penetrated by the KSST No. 2 well contains predominantly woody kerogen with lesser amounts of herbaceous material and low amounts of organic carbon. The sediments are immature and contain some reworked material. Methane, probably of biogenic origin, is present throughout most of the section penetrated by this well.

KSST NO. 4A WELL

The KSST No. 4A well was drilled to a depth of 1,391 feet at a location about 16 miles northeast of the KSSD No. 1 well, on the flank of the Portlock Anticline. The elevation of the Kelly bushing was 52 feet above mean sea level and the water depth was 307 feet. Eighteen canned cuttings samples representing 30-foot intervals, four sidewall core samples, and two drilling fluid samples were collected and sent to GeoChem Labs for analysis (Carlisle, 1976c). Two cuttings samples held by the MMS were examined in transmitted light by the Bujak Davies Group for kerogen identification and TAI level (Bujak Davies Group, 1987).

TOC values reported by GeoChem Labs are all less than 0.5 percent except for two samples from 1,020 and 1,040 feet which yielded values of 0.75 and 0.65 percent, respectively. Only one sample from the interval from 530 to 560 feet produced measurable amounts of C₁₅+ extractable hydrocarbons (131 ppm). Bujak Davies and GeoChem Labs palynologists observed mostly woody kerogen with lesser amounts of coaly and herbaceous material.

Methane levels in headspace gas ranged from about 1,000 to 39,000 ppm. "Wetness" of the gas was generally less than 1.0 percent, but was highest (6.7 percent) in the shallowest sample (479 to 500 feet).

The C₁₅+ extracts were composed mostly of asphaltenes (63 to 74 percent). Only the sample from 530 to 560 feet contained measurable quantities of C₁₅+ hydrocarbons. Gas chromatograms of all samples show high naphthene backgrounds, the presence of long-chain paraffins (C₂₇, C₂₉, C₃₁), and CPI values of around 2.

Bujak Davies recorded a TAI level of 2⁻ to 2 for cuttings samples representing both the intervals from 530 to 560 and 1,370 to 1,400 feet (an R_o equivalent of about 0.5 percent). Cuttings from 560, 625, 800, and 818 feet examined by GeoChem Labs exhibited TAI values of 3⁻ to 3, an R_o equivalent of 1.2 or 1.3 percent (Bayliss and Smith, 1980). Samples from 1,020 and 1,400 feet contained dominant TAI populations in the 1⁺ to 2⁻ range, or an R_o equivalent of about 0.43 percent (Bayliss and Smith, 1980). It is almost certain that a good deal of reworked material was present in the dominantly glaciomarine sediments that were sampled.

KSST NO. 4A WELL SUMMARY

The sedimentary section penetrated by the KSST No. 4A well contained predominantly woody kerogen with low levels of organic carbon, much of it probably reworked. The sediments contain organic material that could be characterized as either thermally immature or mature depending upon how much reworked material is contained in a sample. The extracted bitumens are immature. The methane in the sediments was probably derived from biogenic rather than thermogenic sources.

SUMMARY AND CONCLUSIONS

Sediments sampled by these six stratigraphic test wells contain mostly humic to woody kerogen, which is generally considered to be gas prone. The levels of organic carbon present as solid kerogen and as C₁₅+ extractable hydrocarbons are not impressive. The TOC values tend to be less than 0.6 percent. The only samples that contained more than 1.0 percent organic carbon were obtained at about 3,500 feet from the KSST No. 2 well and are suspected of having been contaminated by drilling additives. Although some of the organic matter analyzed may have undergone catagenesis, it is probable that these sediments have been reworked. Projections of a limited number of R_o measurements from the deeper KSSD wells suggest that catagenesis may be occurring in rocks that are at least of Eocene age and have been buried to depths of 8,500 to 11,500 feet.

Methane is present in all of the wells, particularly in surface sediments. In the KSSD No. 3 well, the presence of gasoline-range hydrocarbons and an abrupt increase in the C₂ to C₄ paraffins appears to be associated with Eocene rocks beneath a regional unconformity, but these wet gases do not appear to have been generated in situ. In general, the hydrocarbon content of the sedimentary sections penetrated by the wells on the Kodiak shelf is low, and there appears

to be insufficient organic matter to generate significant amounts of hydrocarbons.

9. GEOTHERMAL GRADIENT

A temperature gradient for Kodiak shelf was computed from data obtained from the KSSD No. 1 well. Because adequate drilling histories were unavailable, no temperature gradients were calculated for the KSSD No. 2 nor the KSSD No. 3 wells. The maximum observed bottom hole temperatures for these wells were 134 °F (from the compensated formation density log at 10,443 feet below KB) and 124 °F (from a proximity log at 9,355 feet below KB), respectively.

"True" formation temperatures were estimated for each of the two logging runs completed in the KSSD No. 1 well by extrapolating bottom hole temperature (BHT) measurements obtained from successive log suites to a corrected static formation temperature as suggested by Fertl and Wichmann (1977). This analytical extrapolation is accomplished by applying a linear regression to BHT observations versus the logarithm of the expression:

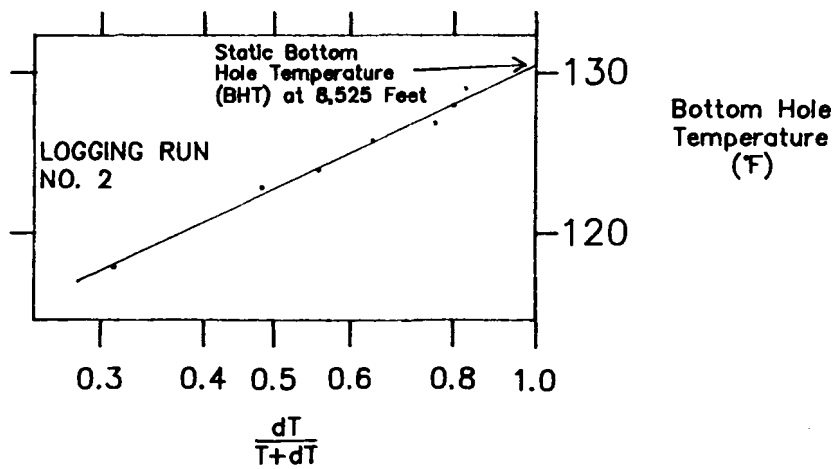
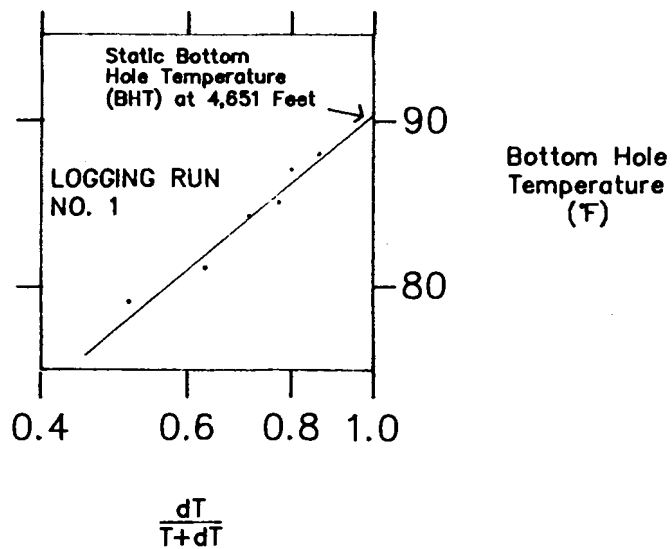
$$\frac{dt}{t + dt}$$

Where for each measurement, dt = time (in hours) after mud circulation ceased and t = mud circulation time (in hours) at the logging point prior to logging. The corrected static BHT was estimated by projecting the line extrapolated from this ratio to:

$$\frac{dt}{t + dt} = 1$$

The technique is based on the observation that the temperature rise, after mud circulation has stopped, is similar to static pressure buildup and may, therefore, be analyzed in a similar manner (Fertl and Wichmann, 1977). The procedure is illustrated in figure 86 for the two logging runs. These extrapolations yield corrected static BHT values of 90 °F at 4,651 feet and 130 °F at 8,525 feet below KB.

An average temperature gradient was computed using corrected BHT values from the two logging runs (fig. 87) by means of a least squares regression. The linear function derived from these points produces an average temperature gradient of 1.03 °F per 100 feet (18.8 °C per kilometer).



T equals circulating time in hours and dT equals elapsed time after circulation stopped.

Figure 86. Graph showing the extrapolation of bottom hole temperatures (BHT) to determine static BHT for KSSD No. 1 well.

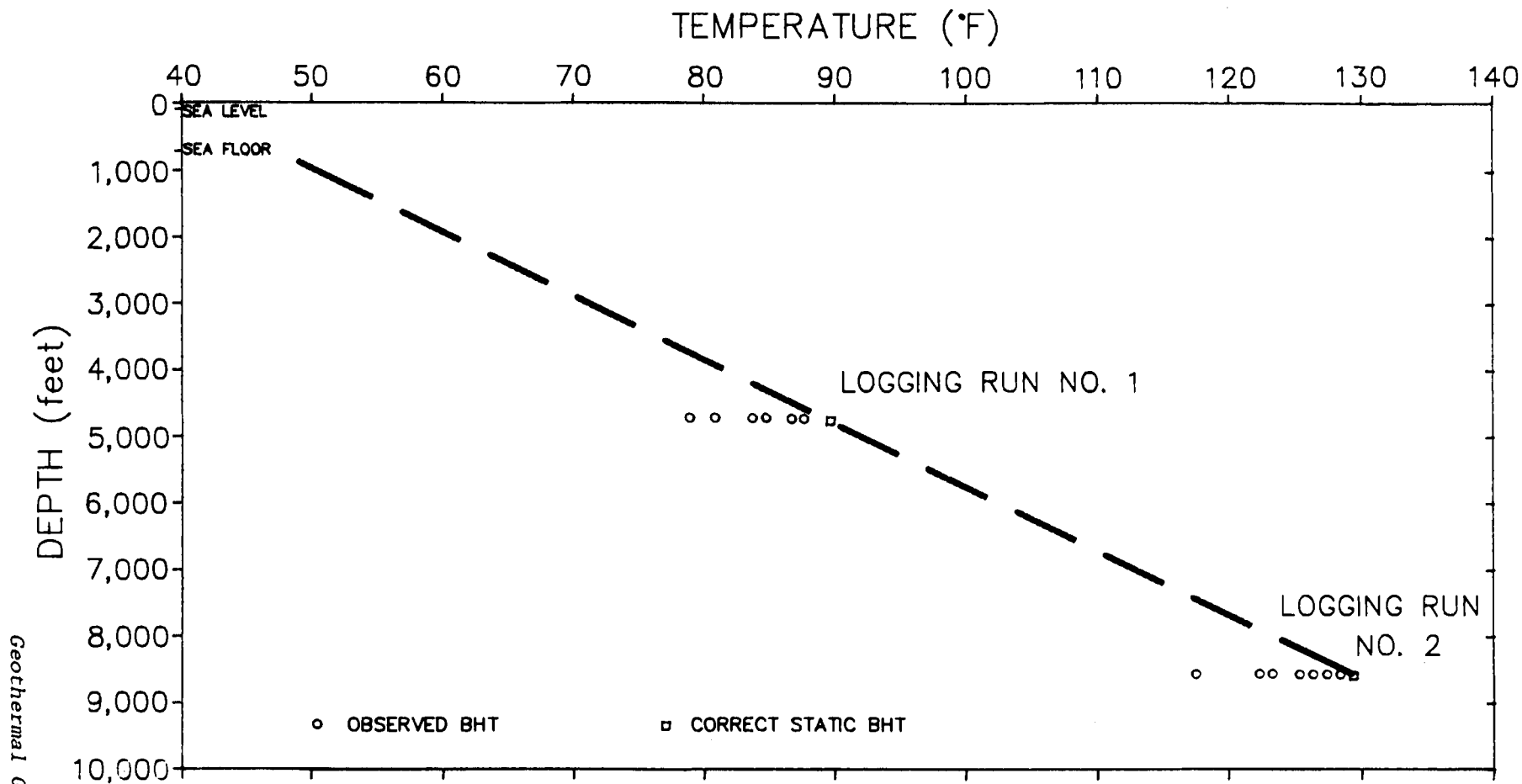


Figure 87. Temperature gradient from KSSD No. 1 well.

Preliminary Lopatin modeling (Lopatin, 1971; Waples, 1985) suggests that these temperatures will not generate the relatively low levels of thermal maturity predicted by microscopic and geochemical analyses (see Organic Geochemistry chapter). It is probable that the complex tectonics of the subduction zone and/or the high rate of recent sedimentation have complicated the geothermal history of this region. The thermal maturity of Eocene sediments at this location bear no relationship to the current thermal gradient.

10. ABNORMAL FORMATION PRESSURE

INTRODUCTION

In the course of the Kodiak shelf stratigraphic evaluation program, a total of six wells were drilled (fig. 88). Three of these wells were drilled to relatively shallow depths ranging from 1,390 to 4,303 feet. The remaining three wells were drilled to depths ranging from 8,525 to 10,460 feet and sampled the entire sequence between the surface and the top of basement in addition to making significant penetrations of the basement complex. At all three well sites, the top of the basement complex corresponds to the top of "acoustic basement" as identified in seismic data.

From an operational standpoint, the drilling of these wells was largely uneventful. However, the KSSD No. 2 well experienced some gas flow at approximately 7,000 feet which decreased the mud weight and required the addition of solids to the drilling mud in order to mitigate the flow. Minor gas influx persisted to the bottom of the well. In response, the mud weight was raised incrementally at depths below the first encounter with gas, and, by the time drilling was completed, the mud weight had been raised to 13.6 pounds per gallon (ppg). Drilling performance data gathered at the well site also suggested the presence of abnormal formation pressure at depth in this well. Because of these observations, the KSSD No. 2 well and the other wells in the Kodiak shelf stratigraphic test program were specifically analyzed for the presence of abnormal formation pressure. The purpose of this work was to identify the areal distribution, and perhaps the mechanism, of the overpressure phenomenon and to provide a practical framework for engineering considerations for future drilling programs on the Kodiak and Gulf of Alaska shelf.

The analysis concludes that only the KSSD No. 2 well encountered abnormal formation pressure. The remaining five wells encountered normal formation pressures, suggesting that overpressure is confined to certain parts of the Kodiak shelf. The study suggests that the occurrence of abnormal formation pressure is controlled by structural setting and processes of tectonic dewatering in the accretionary complex beneath the Kodiak shelf. The area of overpressure may be tectonically allied to the Gulf of Alaska shelf, where abnormal formation pressure is widespread (Hottmann and others, 1979).

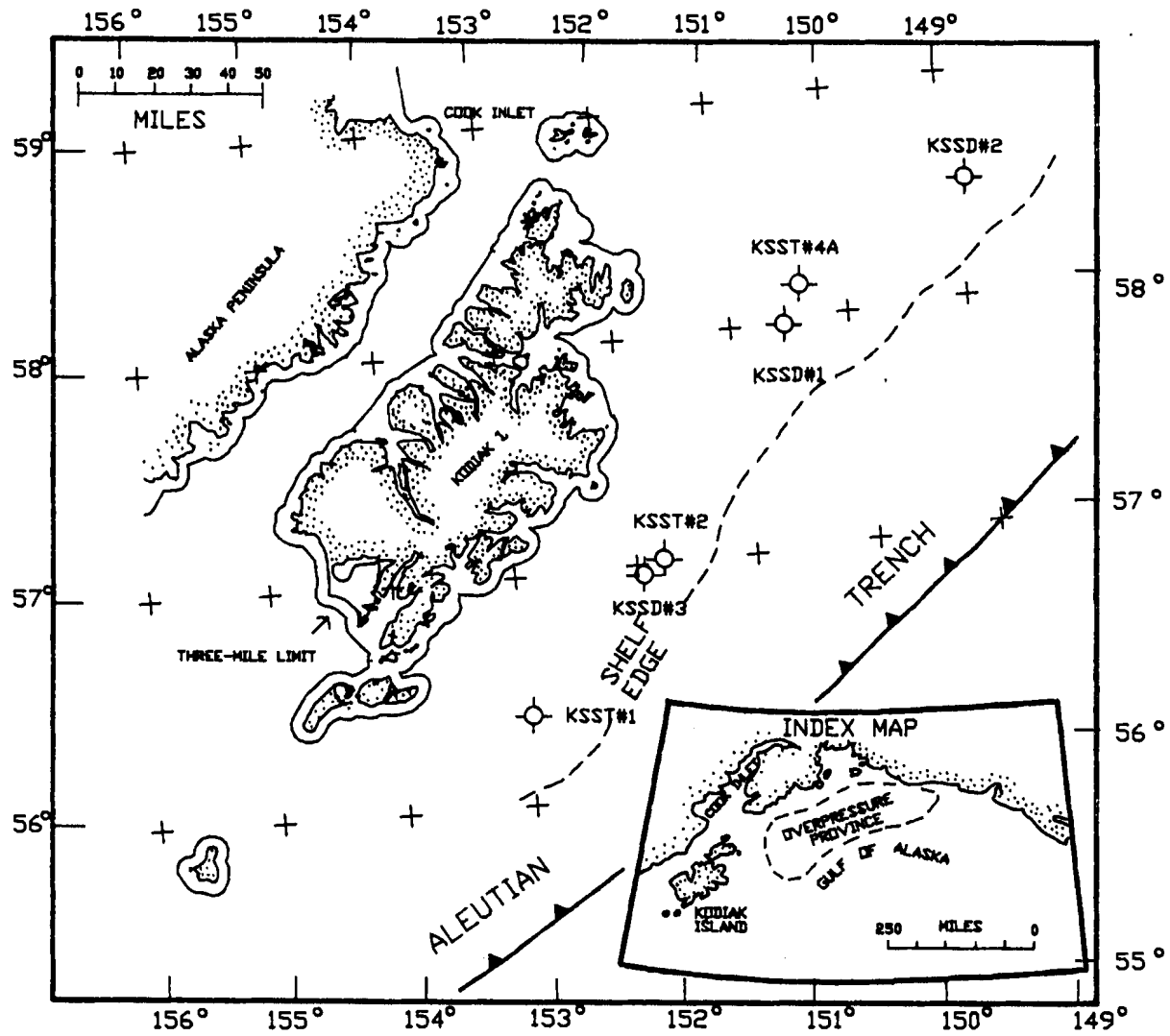


Figure 88. Index map showing locations of Kodiak Shelf Stratigraphic Test wells.

METHODS OF INVESTIGATION

No drill stem tests (which directly measure formation fluid pressure) were conducted in any of the wells drilled on the Kodiak shelf. Repeat formation (RFT) tests were attempted as a means of obtaining pressure data in the KSSD No. 2 and the KSSD No. 3 wells. In the KSSD No. 2 well, 13 RFT measurements were attempted; all were unsuccessful due to poor seal or impermeable formation. In the KSSD No. 3 well, 10 RFT measurements were attempted. Of these tests, 6 obtained usable pressure measurements which indicated normal hydrostatic gradients; the remainder were unsuccessful because of poor seals or the presence of impermeable formation.

In the absence of direct measurements of formation pressure, wireline well logs which measure physical properties such as electrical conductivity, acoustic velocity, and density may be employed to obtain estimates of formation pore pressure. It is a common empirical observation that the resistivity (inverse of electrical conductivity), acoustic velocity, and density of sediments rise progressively with depth of burial (Hottmann and Johnson, 1965). These physical changes reflect the loss of porosity and greater interparticle bonding that result from closer grain packing and the introduction of diagenetic cements into the pore system. The natural consequence of these processes is the expulsion of pore fluids, or "dewatering." Abnormal formation pressure ensues where these processes are reversed or arrested because of the confinement and retention of pore fluids. Excess (that is, greater than hydrostatic) pore pressure preserves or increases porosity and reduces formation shear strength (Hubbert and Rubey, 1959), resulting in a condition termed "undercompaction." The anomalous physical properties of rocks in overpressured zones are reflected in the measurements obtained by wireline logs. In depth profiles of resistivity, interval velocity, and density, abnormal formation pressure is manifested by a reversal or deviation from the normal (positive) compaction trend observed in superincumbent, normally pressured strata. These physical changes are observed to occur to some degree in most sedimentary rocks, but vary most systematically with pore pressure in shales. Because of this systematic relationship, shale is the lithology most often analyzed in wireline log studies of pore pressure phenomena.

Empirical studies, such as the pioneering paper by Hottmann and Johnson (1965), have conclusively demonstrated that the anomalous physical properties of overpressured shales can be quantitatively related to pore fluid pressures. The present study utilized a set of shale evaluation curves published by McClure (1977). Empirical curves for pressure evaluation have also been published by Hottmann and Johnson (1965), MacGregor (1965), Wallace (1965) and Ham (1966). Pennebaker (1968a; 1968b) has published studies which show that overpressured zones can be identified by acoustic velocities obtained from seismic reflection data.

In the three deep test wells (KSSD No. 1, KSSD No. 2, and KSSD No. 3) on the Kodiak shelf, NL Baroid continuously monitored formation pore pressure through iterative calculation of a parameter

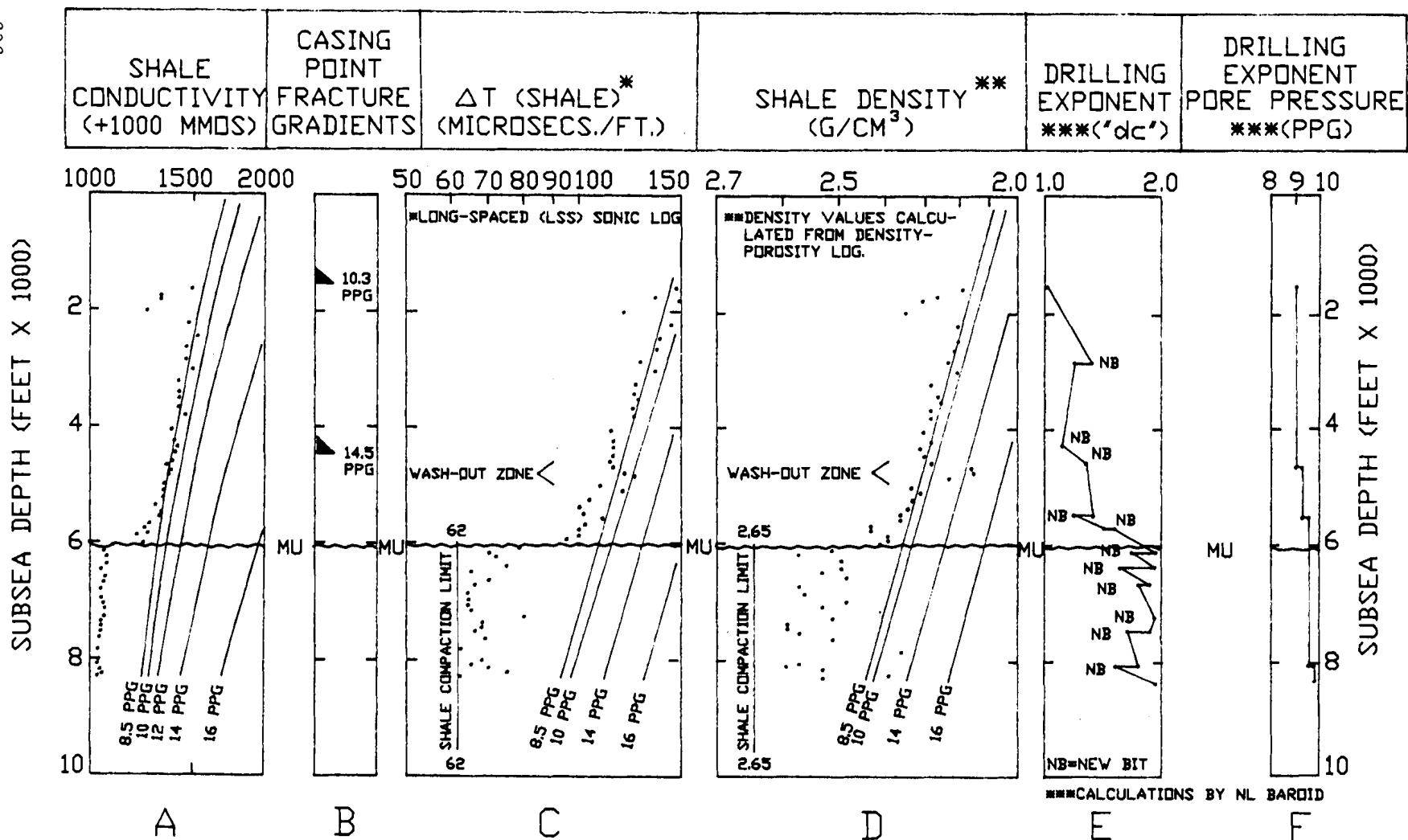


Figure 89. Sun Oil KSSD No. 1 well. Synopsis of drilling data and wireline log data for shales. Normal compaction trends occur above the Miocene unconformity (MU). Highly deformed strata below the unconformity are overconsolidated. No overpressured intervals appear to be present.

termed "dc" or "corrected drilling exponent." NL Baroid also calculated pore pressure gradients from drilling data at regular depth increments for advisory purposes in maintenance of drilling fluid density, or "mud weight." The fundamental assumption underlying the "drilling exponent" method of pressure evaluation is that the rate of penetration varies in a positive manner with the differential pressure at the rock surface contacted by the drill bit. A high differential pressure (formation fluid pressure exceeds mud column pressure, or an "underbalanced" condition) aids the drilling process because the shear strength of the rock is lowered and the percussive impact of the teeth of the drill bit detaches greater quantities of rock chips from the drill face. Penetration rates commonly increase dramatically when overpressured zones are entered because the increasing pore pressure increases the differential between formation fluid pressure and the opposing pressure exerted by the column of drilling mud. A rapid increase in penetration rate on a dulling bit in a lithologically monotonous sequence is often one of the earliest warnings that an overpressured zone has been entered.

However, lithology and several variables associated with drilling operations (for example, mud weight, mud viscosity, bit weight, bit condition, rotation rate, hole size, downhole drill assembly, etc.) can also markedly affect penetration rate. Calculation of pore pressures from dc data attempts to account for changes in these variables in order to calculate a theoretical "normalized" rate against which the actual penetration rate may be compared. Drill rates in excess of the normalized rate are considered anomalous and may indicate the presence of an overpressured zone. To a certain extent, the drill rate "anomaly" may be quantitatively related to formation pressure. Drilling exponent data are typically plotted in depth profiles along with pore pressure estimates. An increase in drilling exponent with depth on the same bit is normal and reflects progressive dulling of the bit. This is termed a positive drilling exponent trend. Conversely, a decrease in drilling exponent with depth on an individual bit, termed a negative drilling exponent trend, is anomalous and can be indicative of rising pore pressure. An excellent summary of the basic method of interpretation of drilling data can be found in Jordan and Shirley (1966).

SUN OIL KSSD NO. 1 WELL

The KSSD No. 1 well was drilled on the southwest flank of Stevenson Basin, along the northeast flank of the Portlock anticline. The well penetrated a relatively undisturbed sequence of Miocene and younger strata that rest unconformably upon rocks of Eocene age. Based upon data presented elsewhere in this report, and following the usage proposed by Fisher and von Huene (1980), the unconformity which separates these two major sequences is termed the "Miocene unconformity." The Miocene unconformity is posted as the "MU" in figure 89. Wireline log data for shales penetrated by the KSSD No. 1 well are presented in figure 89 along with drilling exponent data obtained by NL Baroid. Electrical conductivity, velocity, and

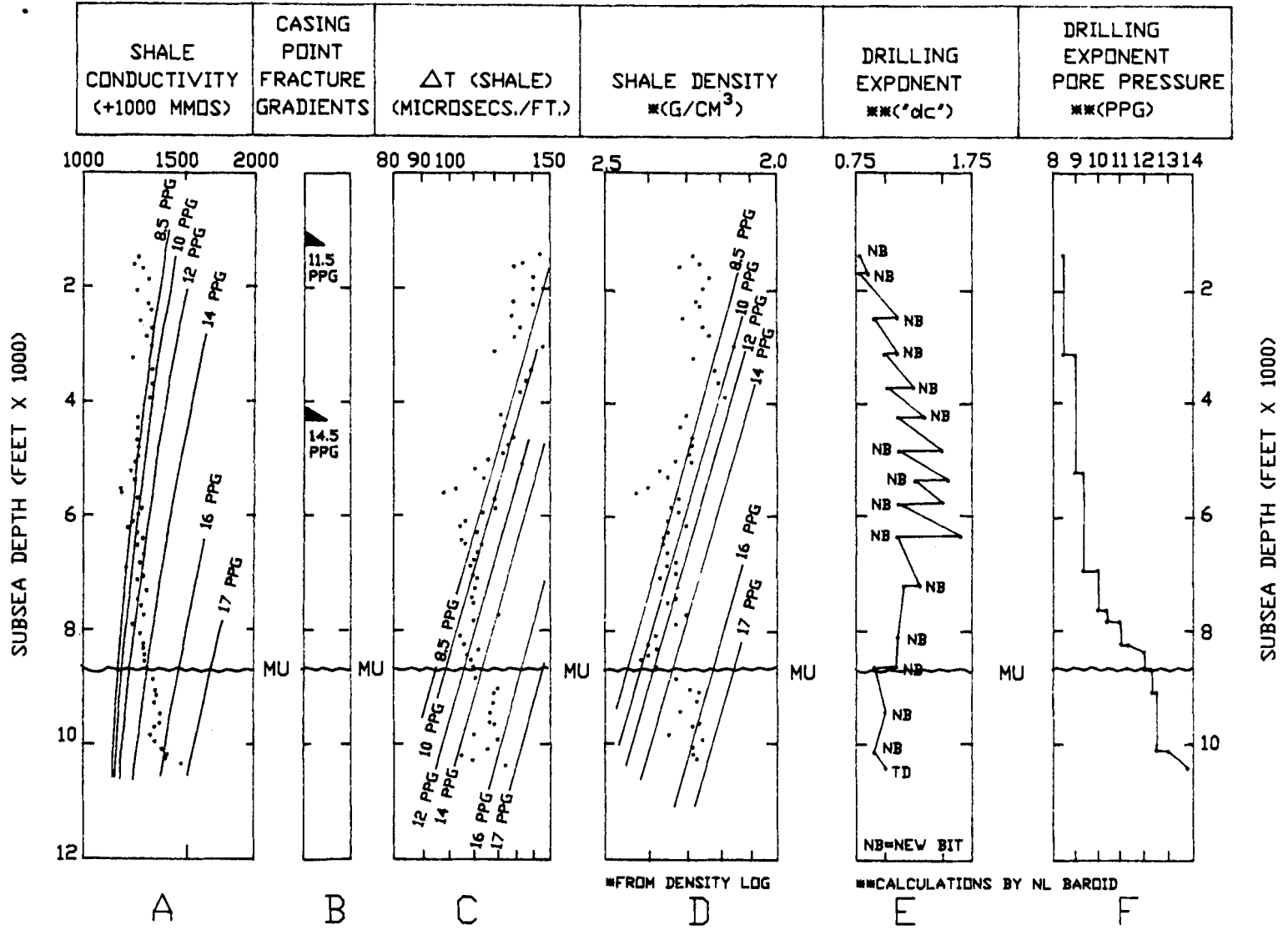


Figure 90. Sun Oil KSSD No. 2 well. Synopsis of drilling data and wireline log data for shales. Normal compaction trends can be identified in the interval from 3,400 to 6,500 feet. Strata below 6,500 feet appear to be overpressured.

density data for shales in the sequence above the Miocene unconformity (MU) clearly show a strong development of a normal compaction trend, which has been matched to the 8.5-ppg line in McClure's (1977) pressure evaluation curves (posted in figure 89). The data reveal no significant reversals which are attributable to abnormal formation pressure. The incursion toward lower velocities and densities in the interval from 4,600 to 5,000 feet (fig. 89c, d) is a consequence of an enlarged hole condition ("washout zone") just beneath the casing shoe at 4,494 feet (subsea).

Below the Miocene unconformity (MU), the resistivities (inverse of conductivity), velocities (inverse of travel time), and densities of shales all rise abruptly, and velocities and densities approach the compaction limit for shales (posted in fig. 89c, d). Dipmeter data for this sequence show steep, erratic dips which suggest severe deformation and extreme structural complexity. No compaction trend can be discerned in the data in figure 89 for the subunconformity sequence, in part because these rocks are steeply inclined, but also because they were not compacted by normal burial processes but rather by structural strain related to tectonism. If the sequences above and below the unconformity were both undisturbed, the shift in the data at the unconformity could be interpreted to indicate that at least 8,000 feet of pre-existing overburden had been stripped at the unconformity. However, because the state of consolidation of the subunconformity sequence at this well site is related to tectonism rather than burial, this figure is essentially meaningless.

Drilling data are synopsisized in diagrams 89e and 89f. Drilling exponent trends are largely positive and no fluid pressure gradients greater than 9.7 ppg were obtained. Drilling operations were uneventful. The wireline log data and the analysis of the drilling data collectively suggest that no overpressured strata were encountered by the KSSD No. 1 well.

SUN OIL KSSD NO. 2 WELL

The KSSD No. 2 well is the northeasternmost of the stratigraphic test wells and was drilled in the northeast part of Stevenson Basin. The well encountered a relatively undisturbed sequence of Miocene and younger strata that rest unconformably at the Miocene unconformity upon strata of Eocene age. Dipmeter data show that strata within the subunconformity sequence are homoclinally tilted 20 to 40 degrees to the north-northwest. The consistency of the dipmeter measurements in the subunconformity sequence suggests that it has not experienced the intense deformation observed in coeval rocks at the KSSD No. 1 well. The Miocene unconformity, which corresponds to the top of "acoustic basement" as identified in seismic data, is posted as "MU" in figure 90. Wireline log data for shales penetrated by the KSSD No. 2 well are shown in figure 90 along with drilling exponent data obtained at the well site by NL Baroid.

The drilling exponent data identified two major compaction sequences in the well. The depth interval between 1,500 and 6,400

feet is characterized by strongly positive dc trends (fig. 90e), whereas below 6,400 feet, dc trends abruptly become less positive and then reverse and are largely neutral or negative throughout the lower part of the well. In this lower interval, NL Baroid calculated rapidly increasing pore pressure gradients which continued to rise to the bottom of the well (fig. 90f). A maximum pore pressure gradient of 14 ppg was estimated at total depth.

Wireline log data appear to identify three major compaction sequences within the KSSD No. 2 well. The uppermost sequence ranges across the depth interval from 1,500 to 3,400 feet (subsea) and is characterized by high data scatter (fig. 90a, c, d). The second sequence lies in the depth interval from 3,400 to 6,500 feet and is characterized by moderate data scatter and a normal compaction trend. The third interval extends from 6,500 feet to the base of the well and is characterized by a reversed compaction trend. This latter interval is clearly undercompacted and overpressured.

The uppermost interval contains abundant gravels above 2,100 feet and is largely Pleistocene in age. The "mudstones" in this interval are typically very silty and probably are composed largely of clay-size unweathered rock and mineral fragments of glacial derivation (rock flour). Similar lithologic attributes for coeval sediments have been reported for the Gulf of Alaska shelf by Plafker and Addicott (1976) and Hottmann and others (1979, p. 1478). The high data scatter and atypical values found in these shallow sediments are considered to reflect the unusual compositions of these periglacial sediments. For this reason, the uppermost sequence was considered nonrepresentative and was disregarded in fitting the evaluation curves to the data.

In the normally compacted sequence in the depth interval from 3,400 to 6,500 feet, the least graphical scatter is found in the electrical conductivity data, and by visual inspection, the normal compaction line (8.5 ppg) was matched to the conductivity data in this interval. Velocity and density data were evaluated in a similar fashion. Data scatter in this interval is attributed to lithologic variation, primarily silt content, among "mudstones."

All of the wireline log data sets appear to identify an overconsolidated interval between 5,400 and 5,600 feet. This zone is characterized by low conductivity, low acoustic travel times, and high density. Seals or "caprocks" above overpressured zones typically are somewhat cemented and exhibit this kind of anomalous overconsolidation. However, the data suggest that this zone lies nearly 1,000 feet above the top of the overpressured zone, which does not appear to be associated with a typical caprock. Dipmeter data suggest that a fault intersects the wellbore at 5,500 feet (subsea). Strata in the vicinity of this fault may have been fractured by fault movements and subsequently mineralized by fluids migrating along the fault, resulting in the lithification anomaly observed in the interval from 5,400 to 5,600 feet in figure 90.

The interpretations of wireline log data in figure 90 suggest that fluid pressure gradients begin to depart from normal (8.5 ppg) at a depth of 6,500 feet (subsea). At the Miocene unconformity (MU), fluid pressure gradients abruptly rise to values greater than 14 ppg. This contrasts distinctly with the abrupt increase in consolidation which occurs below the Miocene unconformity in the other Kodiak shelf wells. Instead, in the 300-foot interval immediately below the Miocene unconformity in the KSSD No. 2 well, there is an abrupt shift toward less consolidation. Below the Miocene unconformity, pore pressures continue to progressively rise toward the bottom of the well, where the wireline log analysis finds pore pressure gradients of approximately 17 ppg. These observations suggest that the excess pore fluids are being driven upward from a source within the basement complex and that the Miocene unconformity forms a seal which impedes, but does not block, the upward migration of fluids. Superincumbent strata are apparently dynamically supercharged by these high-pressure fluids. Speculative projection of the "undercompaction" trend within the basement complex below the base of the well suggests that lithostatic fluid pressures (19.5 ppg) could be achieved at depths as shallow as 12,000 feet.

The pressure evaluation indicates that underbalanced conditions existed throughout the drilling of the lower part of the well. The integrity of the formation exposed to the open hole just below the 13 3/8-inch casing shoe at 4,341 feet (subsea) was pressure tested at 14.5 ppg (fig. 90b). At the approximate depth of the Miocene unconformity (MU), the well began to enter an environment where formation pore pressure gradients exceeded 14.5 ppg. If significant incursion of formation fluids into the wellbore had occurred from a fracture zone or porous bed in the interval below the Miocene unconformity, control of the flow might have required mud weights in excess of the integrity of the formation at the top of the open hole. Fluid loss into an induced fracture at the top of the open hole would have severely compromised control of the flow condition. In fact, when the well penetrated the Miocene unconformity, the mud weight was 12.2 ppg. Influx of gas from a sandy interval just beneath the unconformity was controlled by raising the mud weight to 13.4 ppg. Fortunately, weights in excess of 14.5 ppg were not required, probably owing to the low permeability or limited extent of the sands.

Future drilling in the area of the KSSD No. 2 well can anticipate this kind of problem by designing casing programs such that the base of the casing is set within or closer to the top of the overpressure zone. The higher integrity naturally incurred at greater depths would provide a larger safety margin for the open hole and would allow greater operational flexibility in the event that very dense mud is required to control a flow condition.

SUN OIL KSSD NO. 3 WELL

The KSSD No. 3 well was drilled on the central shelf uplift between the Albatross and Stevenson Basins. The well penetrated a

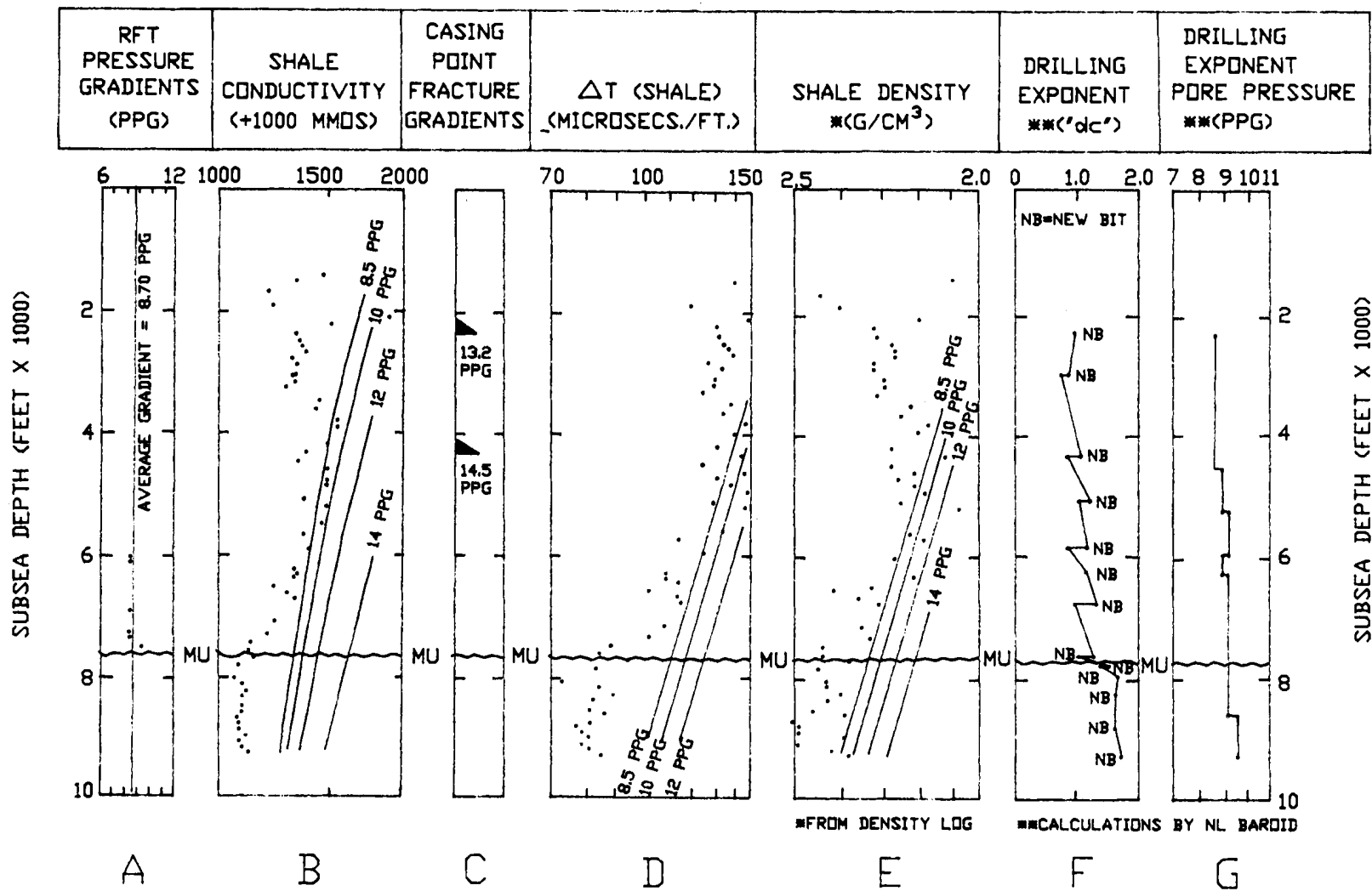


Figure 91. Sun Oil KSSD No. 3 well. Synopsis of pressure data, drilling data, and wireline log data for shales. Normal compaction trends occur above the Miocene unconformity (MU) in the interval between 3,500 and 6,800 feet. Highly deformed strata below the unconformity are overconsolidated. No overpressured intervals appear to be present.

relatively undisturbed sequence of Miocene and younger rocks which rest unconformably upon steeply dipping strata of Eocene age. These two major sequences are separated by the regional Miocene unconformity identified in the other deep tests on the Kodiak shelf (posted as "MU" on figure 91).

The KSSD No. 3 well is the only well on the Kodiak shelf in which direct measurements of formation fluid pressure were successfully obtained. A total of 10 repeat formation (RFT) tests were attempted; 6 tests were successful. The results of these tests are tabulated below:

TABLE 12. KSSD No. 3 well, Repeat Formation Test data.

	<u>MD=TVD</u>	<u>SSD</u>	<u>PSI</u>	<u>PSI/FOOT</u>	<u>EFD</u>
1.	6,138	6,048	2,671	0.442	8.52
2.	6,210	6,120	2,715	0.444	8.56
3.	7,064	6,974	3,099	0.444	8.56
4.	7,448	7,358	3,266	0.444	8.56
5.	7,491	7,401	3,300	0.446	8.60
6.	7,674	7,584	3,689	0.486	9.37

Where: MD= Measured Depth (feet).
 TVD= True Vertical Depth (feet).
 SSD= Subsea Depth (feet).
 PSI= Formation Pressure, in
 Pounds per Square Inch.
 PSI/FOOT= Pressure Gradient, in
 Pounds per Square Inch per
 Foot.
 EFD= Equivalent Fluid Density, in
 Pounds per Gallon.

All of the measured pressure gradients are considered normal hydrostatic gradients, well within the range of 0.433 to 0.493 psi/foot for common brines as published by McClure (1977, p.AP-2). The average of the six measurements is 0.451 psi/foot (8.70 ppg). The RFT data are plotted versus depth in figure 91a.

Wireline log data for shales penetrated by the KSSD No. 3 well are presented along with drilling exponent data in figure 91. The wireline log data identify four major compaction sequences in the well. The uppermost sequence, from 1,400 to 3,500 feet (subsea), is characterized by low coherence of all data sets and scattered anomalous values which outwardly suggest overcompaction (fig. 91b, d, e). The second sequence extends from 3,500 to 6,800 feet, and, despite high scatter in some data sets, appears to be normally compacted. The third sequence extends from 6,800 feet down to the Miocene unconformity at 7,715 feet (subsea) and appears to be somewhat overconsolidated. The fourth sequence extends from the Miocene unconformity down to the total depth of the well and is

characterized by overconsolidation and relatively invariant shale properties.

The uppermost sequence contains abundant gravels above 3,200 feet and is Pleistocene in age. It is primarily of glaciomarine origin. The "clays" in this interval are very silty and sandy, and probably contain abundant clay-sized unweathered rock and mineral fragments (rock flour). The high content of non-clay materials may be responsible for the data scatter and locally high densities and velocities of "shales" in this interval. Anomalously low conductivities may reflect a low proportion of clay minerals or the presence of fresh pore fluids in these shallow sediments. For these reasons, the uppermost sequence was considered nonrepresentative and was excluded from the analysis.

All data sets suggest that a normal compaction trend is developed in the second compaction sequence from 3,500 to 6,800 feet. In this interval, the electrical conductivity data exhibit the least graphical scatter (fig. 91b). The McClure (1977) evaluation curves were fit by inspection to the conductivity data by centering the normal compaction line (8.5 ppg) within the trend of the data points within this interval. Despite the high degree of scatter, shale density and travel-time data also clearly exhibit normal compaction trends (fig. 91d, e). Although somewhat more subjective, evaluation curves have been fit to these data sets in the same manner, but guided by the evaluation of the conductivity data. The high data scatter in this interval is tentatively attributed to variation in the silt content of the "claystones." The claystones are variously described as silty to very silty, grading into siltstone, and ranging from soft to firm.

The third compaction sequence, from 6,800 to 7,715 feet, appears to be overconsolidated (data points plot to the left of the 8.5-ppg curve). However, this sequence is lithologically distinguished from the overlying sequence by a relative abundance of sandstones and conglomerates. Claystones in this interval are very silty and the presence of this lithologic component may account for the apparent overconsolidation of "shales" within this interval. No unconformity is recognized at the top of this interval.

The fourth compaction sequence corresponds to the highly deformed and steeply dipping Eocene rocks below the Miocene unconformity. Electrical conductivities for shales in this sequence do not appear to vary with depth. The data sets for shale velocity and density are highly scattered. No compaction trend can be discerned in the subunconformity sequence, probably because the state of consolidation of these rocks is not a function of burial depth but rather of structural deformation related to tectonism.

Drilling exponent ("dc") trends are largely positive above the Miocene unconformity (MU) and become weakly positive to neutral in the subunconformity sequence (fig. 91f). The poor development of positive trends in the subunconformity sequence is probably a consequence of the effect of steeply dipping to vertical beds on

drilling performance, rather than a manifestation of abnormal formation pressure. No pore pressure gradients greater than 9.7 ppg were calculated anywhere in the well (fig. 91g). Drilling operations were uneventful. The pressure tests, wireline logs, and drilling data collectively suggest that no overpressured strata were encountered by the KSSD No. 3 well.

EXPLORATION SERVICES KSST NO. 1 WELL

The KSST No. 1 well, the southwesternmost of the Kodiak shelf stratigraphic test wells (fig. 88), was drilled to a depth of 4,225 feet on the southeast flank of the Albatross Basin (northwest flank of Albatross Bank uplift) and encountered strata of Pliocene and Pleistocene age. The Miocene unconformity was not penetrated. Strata in the KSST No. 1 well are inclined 30 degrees to the north-northwest from the bottom of the well up to the shallowest logged depth (approximately 400 feet).

Neither well site pressure evaluation studies (e.g., drilling exponent) nor any formation pressure measurements were conducted. The well was drilled with normally weighted (9.0 ppg) drilling muds and drilling operations were uneventful.

Wireline log data for shales penetrated by the KSST No. 1 well are presented in figure 92. Electrical conductivity measurements (fig. 92a) are largely constant throughout the well. Shale densities (fig. 92c), probably because of their greater sensitivity to lithologic variations, exhibit a high degree of scatter and are not interpretable. Shale velocity data (fig. 92b), though somewhat scattered, clearly define an interpretable compaction trend. The velocities of the shales penetrated by this well are anomalously high with respect to their present burial depths. Comparison of shale velocity data from this well to shale velocity data from the nearest deep test (KSSD No. 3) 54 miles to the northeast suggests that 4,000 to 5,000 feet of overlying strata have been erosionally removed at the present seafloor surface at the KSST No. 1 well site. A similar comparison to the more coherent velocity data obtained from the KSSD No. 1 well (140 miles northeast) suggests that at least 3,000 feet of uplift and erosion has occurred at the KSST No. 1 well site. Farther southeast, on the Albatross Bank uplift, Fisher and von Huene (1980) suggested from seismic data that at least 3,000 meters (9,800 feet) of uplift has occurred.

Electrical conductivity and velocity data (fig. 92a, b) suggest the presence of a highly consolidated zone in the interval from 1,600 to 1,900 feet (subsea). The dipmeter data suggest that the wellbore is intersected by faults at 1,720 and 1,925 feet. Mineralization of host rocks by fluids migrating along these faults may have produced this local zone of well-indurated strata. However, it is also possible that the overcompacted zone represents a relict caprock which formed at the top of an overpressure zone since destroyed by uplift and breaching of the affected strata at the seafloor.

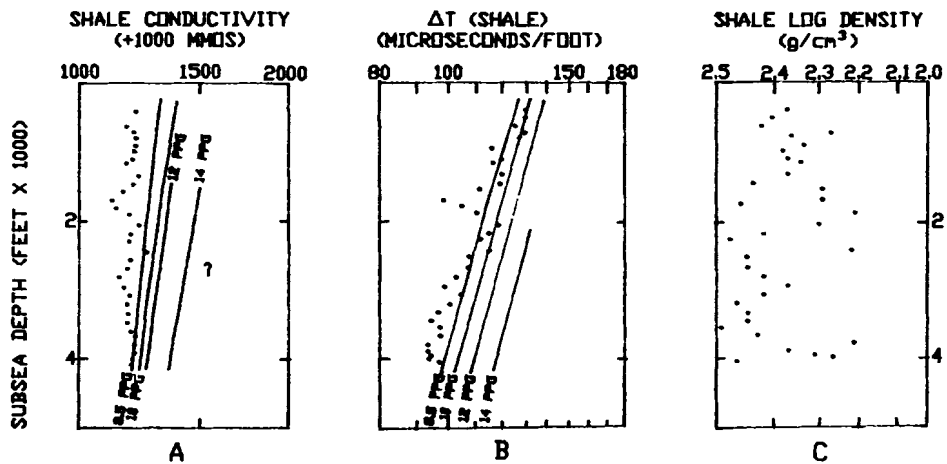


FIGURE 92. Exploration Services KSST No. 1 well. Synopsis of wireline log data for shales.

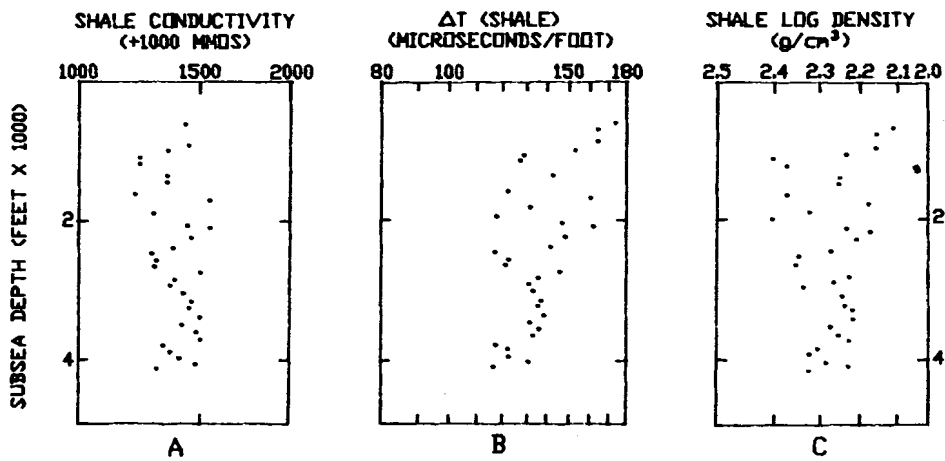


FIGURE 93. Exploration Services KSST No. 2 well. Synopsis of wireline log data for shales.

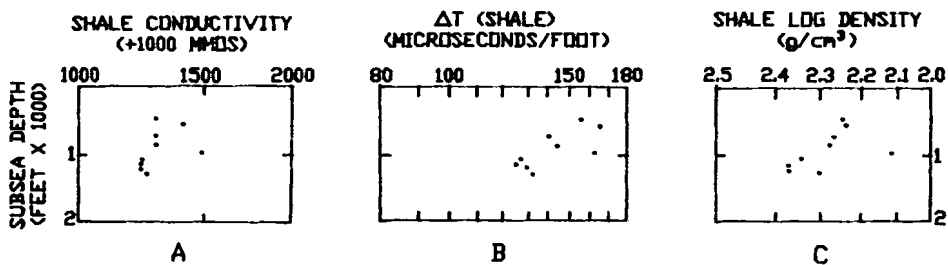


FIGURE 94. Exploration Services KSST No. 4A well. Synopsis of wireline log data for shales.

The available data do not reveal any anomalies in the KSST No. 1 well that can be related to the modern presence of abnormal formation pressure. It is concluded that no overpressured strata were encountered. However, the possible occurrence of overpressure at greater depths or elsewhere within the Albatross Basin cannot be ruled out on the basis of this well.

EXPLORATION SERVICES KSST NO. 2 WELL

The KSST No. 2 well was drilled to a depth of 4,303 feet and sampled an undisturbed sequence of late Pliocene and younger strata. The KSST No. 2 well was drilled 9 miles northeast of the KSSD No. 3 well (fig. 88). The KSSD No. 3 well, evaluated in an earlier section, essentially resampled the same shallow sequence of strata. No well site pressure studies (e.g., drilling exponent, direct measurements) were conducted in the KSST No. 2 well. The well was drilled with normal (9.0 ppg) drilling fluids and drilling operations were uneventful.

Wireline log data for mudstones penetrated by the KSST No. 2 well are presented in figure 93. All data sets exhibit a high degree of scatter and no compaction trends can be identified. Similar data scatter in this interval was also observed in the KSSD No. 3 well (fig. 91), where the scatter was attributed to lithologic effects.

EXPLORATION SERVICES KSST NO. 4A WELL

The KSST No. 4A well was drilled to a depth of 1,391 feet and sampled a sequence of late Pliocene and Pleistocene strata. This well is located only 16 miles northeast of the KSSD No. 1 well (fig. 88), which essentially resampled the same shallow sequence. No well site pressure data were gathered at the KSST No. 4A well. The well was drilled with normal muds and operations were uneventful.

Wireline log data for muds and clays penetrated by the KSST No. 4A well are presented in figure 94. All data sets exhibit the same high degree of scatter observed in the shallow parts of other nearby Kodiak shelf wells. No interpretable compaction trends can be identified.

DISCUSSION

The results of the three deep wells drilled on the Kodiak shelf allow the shelf to be divided, for discussion purposes, into two provinces. The central and southwestern parts of the shelf, sampled by the KSSD No. 1 and KSSD No. 3 wells, respectively, contain relatively undisturbed strata of Miocene and younger age which unconformably overlie a tectonized basement complex which contains rocks at least as young as Eocene. The subunconformity complex here is steeply dipping and highly consolidated and was tectonically dewatered prior to the development of the Miocene unconformity.

Abnormal formation pressure does not appear to be present in any of the wells drilled in this part of the shelf.

The northeastern part of the shelf, sampled by the KSSD No. 2 well, contains relatively undisturbed strata of Miocene and younger age which unconformably overlie, with modest angular discordance, a tilted sequence of rocks at least as young as Eocene. Well data indicate that, in contrast to the southwest part of the Kodiak shelf, the subunconformity sequence is not highly deformed and is in fact highly undercompacted. Abnormal formation pressures are first noted high in the post-unconformity sequence, and increase very gradually down to the Miocene unconformity. Pore pressure gradients rise abruptly below the unconformity, suggesting that the unconformity forms an imperfect seal which impedes, but does not prevent, the upward migration of fluids expressed from sources at depth.

The source for the excess pore fluids in the subunconformity sequence at the KSSD No. 2 well is unknown. Potential sources include: 1) rapid sedimentary loading of "acoustic basement" by Miocene and younger deposits; 2) rapid uplift and nonequilibration of pressured strata; 3) thermally controlled illitization of smectites (Bruce, 1984); 4) structural collapse of diagenetically weakened framework grains in response to overburden pressure; 5) "aquathermal pressuring," or thermal expansion of confined pore fluids (Barker, 1972); and 6) tectonic dewatering of uncompacted rocks at depth.

Rapid sedimentary loading might induce excess pore pressures in the basement rocks, but this mechanism does not account for the highly structured and overconsolidated state of the basement at other well sites, where it is overlain by comparable thicknesses of Miocene and younger strata. A mechanism involving rapid recent uplift is not supported by the stratigraphy of the post-unconformity sequence at the KSSD No. 2 well site. Illitization of smectites forms an unlikely in situ source for excess pore fluids because the maximum temperature recorded in the well was 134 °F, far below the 198 to 232 °F accepted as the common temperature range (although Bruce (1984) reports extremes of 160 to 300 °F) for the onset of smectite destabilization (Burst, 1969). In the Gulf Coast the onset of smectite illitization is commonly observed to coincide closely with the tops of zones of abnormal formation pressure (Bruce, 1984; Berg and Habeck, 1982). Sherwood (1984) reported similar findings in the Navarin Basin COST No. 1 well. Based on temperature data from the KSSD No. 2 well and an assumed activation temperature of 200 °F, the onset of smectite illitization should begin at depths below 21,000 feet, far beneath the top of the overpressured zone at 6,500 feet.

A mechanism involving collapse of framework grains which have been softened by diagenesis is not favored because sandstone is a relatively sparse lithology in the well. The process of "aquathermal pressuring" could contribute to the elevated pore pressures encountered in the KSSD No. 2 well. However, because of the low geothermal gradient on the Kodiak shelf, the aquathermal effect alone can only account for 32 percent of the excess pore pressure observed at total depth in this well, a conclusion drawn from calculations by

the author based upon data published by Barker (1972). Tectonic dewatering forms a plausible source for the excess pore fluids, and some aspects of this interesting mechanism are reviewed below.

Severely elevated formation pressures (in excess of 17 ppg) were encountered in all wells on the continental shelf in the eastern Gulf of Alaska (Hottmann and others, 1979). Abnormal formation pressures as high as 17 ppg (author, unpub. data) were also encountered in the Tenneco Middleton Island No. 1 well, near the shelf edge in the central Gulf of Alaska. In the eastern Gulf of Alaska, Hottmann and others (1979) correlated the depth of onset (ranging from 6,000 to 10,700 feet) of abnormal formation pressure with depths where lateral compressive stresses begin to exceed overburden stresses. The authors identified this transition on seismic panels as the level where extensional faulting at shallower depths grades downward into a zone dominated by thrust faulting. However, examination of seismic reflection data in the vicinity of the KSSD No. 2 well fails to reveal an analogous vertical transformation of structural style. Compressional folds of relatively young age (early Pleistocene?) occur toward the shelf edge within a few miles of the KSSD No. 2 well. Some of these features are illustrated on the map and cross section of figure 95. Thrust faults are inferred to core these folds and appear to dip northwest beneath the well. However, a simplistic correlation between compressional environment and abnormal formation pressure does not satisfactorily explain the absence of overpressured strata at the other Kodiak shelf well sites. These wells are also located in areas which contain young compressional features. Perhaps another explanation, other than general setting in a compressional environment, is required to explain the distribution of abnormal formation pressure on the Kodiak shelf.

All of the Kodiak test wells are located on the outer continental shelf near the Aleutian trench (fig. 88), where the Pacific oceanic plate underthrusts the Kodiak shelf at a present rate of 6.6 centimeters per year (Minster and Jordan, 1978). Von Huene and Lee (1983) have emphasized the role of elevated fluid pressures in the subduction process and conclude that it may be essential to the widespread decoupling and underplating observed in subduction-related tectonism. Moore, Biju-Duval, and others (1982, p. 1072) in fact report encountering near-lithostatic fluid pressures at DSDP site 542 at 240 meters (790 feet) below the seafloor in a frontal detachment in the Barbados subduction zone. Similar findings have also been reported from the Guatemalan subduction zone (Aubouin, von Huene, and others, 1982). This confirms that elevated pore pressures at least locally characterize the subduction process at shallow crustal levels. Near-lithostatic pore pressures in the frontal detachment zone in the Aleutian trench have been inferred from fault geometries by Davis and von Huene (1987). Cloos (1984) has proposed that some landward-dipping reflectors observed in seismic reflection data in the overriding plate near the continental slope along convergent margins represent conduits filled with high-pressure fluids derived from dewatering of underthrust sediments. Bray and Karig (1985) presented porosity studies which suggest that high rates of dewatering and porosity loss in accretionary complexes

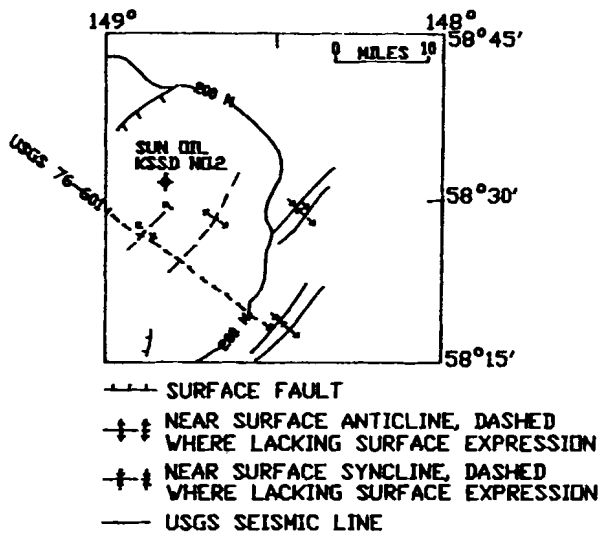
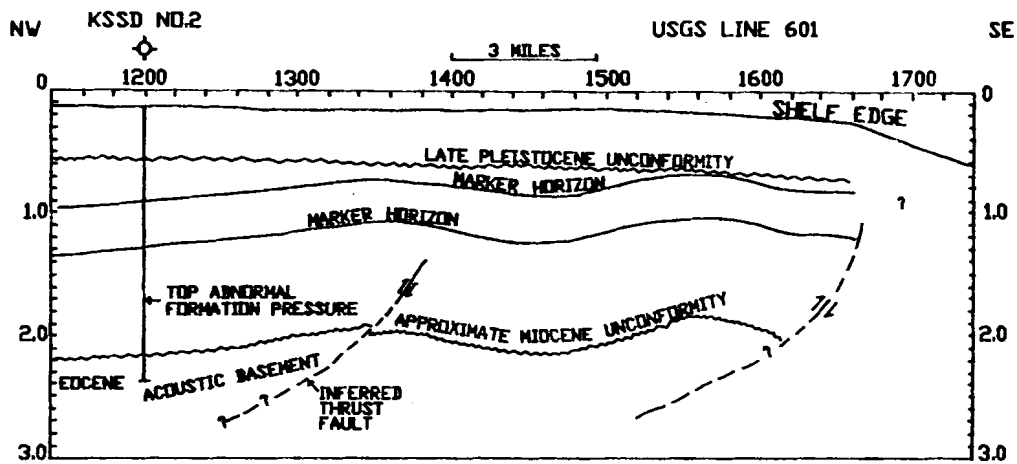


Figure 95. Sketch of seismic panel and map showing locations of near-surface structures in the vicinity of the Sun Oil KSSD No. 2 well. Map modified after von Huene and others (1980b).

result from the intense penetrative and discrete shear which characterizes these tectonic settings. From geobarometric determinations on fluid inclusions in syntectonic veins in outcrop specimens from the Kodiak accretionary complex, Vrolijk (1987) concluded that near-lithostatic fluid pressures were achieved prior to dewatering. Ritger and others (1987) have suggested from isotopic data that modern carbonate cementation of surficial slope sediments along the Oregon-Washington convergent margin occurs where fluids structurally dewatered from the accretionary prism are vented at the seafloor. From this brief survey, it is evident that convergent margins are logically and widely regarded as sites of unusually rapid rates of dewatering and the potential development of abnormal formation pressures.

The KSSD No. 2 well differs from the other wells on the Kodiak shelf in two ways: 1) it alone encountered abnormal formation pressure, and the overpressured zone extends across a depth range which includes virtually undisturbed basinal strata and the underlying acoustic basement; and 2) the basement complex in the KSSD No. 2 well is undercompacted and appears to be homoclinally tilted northward, whereas coeval strata in wells to the southwest are steeply dipping, highly deformed, and overconsolidated. This areal contrast in the structural history of the basement suite is difficult to reconcile with the outward similarity of the tectonic setting of all of these wells near the shelf edge (fig. 88) on the Kodiak convergent margin.

Pulpan and Kienle (1979) and Davies and others (1981) published the results of earthquake studies which suggest tectonic segmentation of the Aleutian arc, especially as it bears upon seismic risks associated with the Shumagin seismic gap, southwest of Kodiak Island. Using geologic data, Fisher and others (1981) assessed two features termed "transverse boundaries" that cross the Kodiak shelf at approximately right angles to the trend of the Aleutian arc-trench system. The locations of these features are shown in figure 96. The northern boundary, which they termed the "Kodiak-Kenai transverse boundary", separates the KSSD No. 2 well from the other Kodiak shelf wells. The evidence marshalled by these authors for the existence of a major transverse structure along the Kodiak-Kenai feature includes: 1) a discontinuity in the trends of Quaternary volcanoes on the Aleutian arc; 2) an alignment of Oligocene(?) volcanic centers along the boundary; 3) the existence of structural arches and anticlines which parallel the boundary and are therefore discordant to the overall structural fabric of the arc; and 4) differences in morphology and structural style on the continental slope on either side of the junction between the slope and the boundary (Fisher and others, 1981, p. 15). Fisher, von Huene, Smith, and Bruns (1983) identified deep events unique to reflection seismic data collected over the Kodiak-Kenai transverse boundary. Fisher, von Huene, Smith, and Bruns (1983) initially attributed these events to two possible sources: 1) a linear diffractor (fault edge?) oriented transverse to the arc; or 2) overpressured (low velocity) sediments in the major detachment between upper and lower plates in the Aleutian subduction zone. In a subsequent paper, Fisher and others (1987) presented new

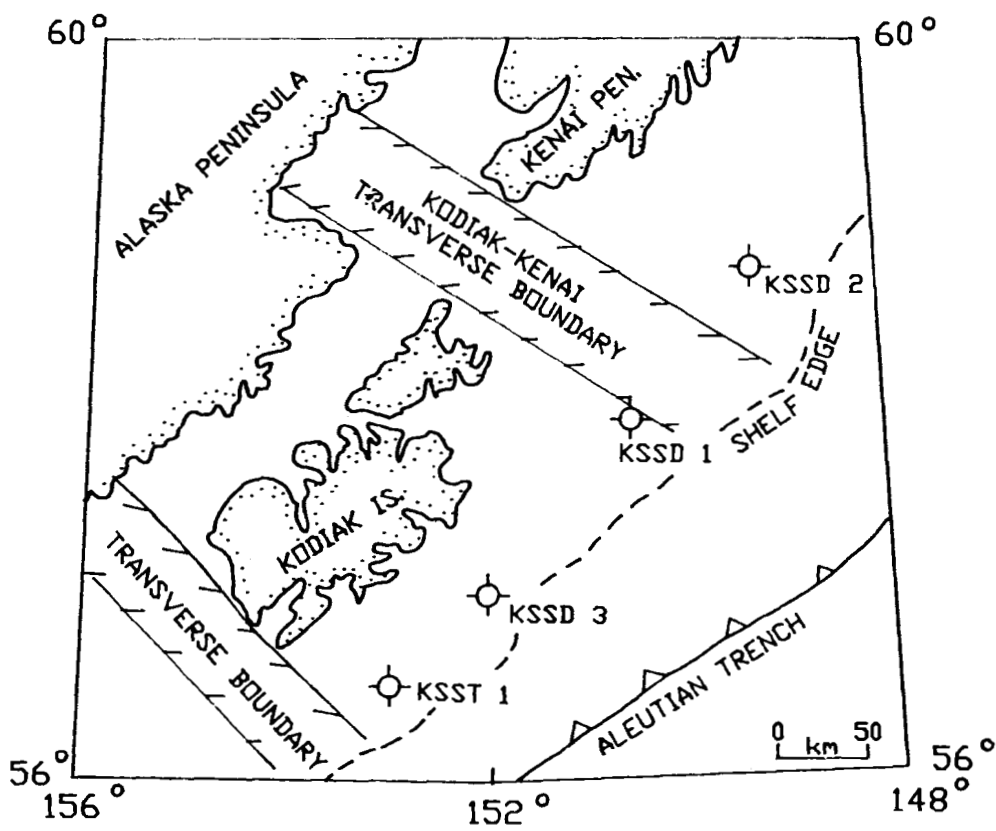


Figure 96. Transverse tectonic boundaries which bound the Kodiak Island block as identified by Fisher and others (1981, fig. 1).

data which suggests that these reflections instead originate from arched underplated rocks in the subduction complex at depths greater than 8 kilometers (26,300 feet). This arch is oriented north-south, oblique to the overall structural grain of the arc, and may be related in some way to movement on the Kodiak-Kenai transverse boundary (Fisher and others, 1987, p. 7911).

No significant strike-slip movement has occurred at shallow crustal levels along the Kodiak-Kenai transverse boundary, as major arc-parallel geologic features (such as the Border Ranges fault) are not offset at the boundary. Fisher and others (1981, p.15) suggested that the boundary may have formed in response to unspecified structural discontinuities in the underlying Wadati-Benioff zone or subducting oceanic plate. In fact, Pulpan and Frohlich (1985, p.807) have more recently published an interpretation of earthquake hypocentral data which suggests the presence of a "tear," or rupture, in the subducted plate beneath the Kodiak-Kenai transverse boundary. Although areally coincident and therefore possibly genetically related, the mechanical relationship between the discontinuities in the upper and lower plates in the area of the transverse boundary remains obscure.

Fisher and others (1981, p.15) indicate that uplift along the Kodiak-Kenai boundary occurred at least as early as late Miocene to Pliocene time. However, as noted above, the most striking contrast between the KSSD No. 2 and the other Kodiak shelf wells is the degree of deformation and state of consolidation of the Eocene rocks within the basement complex. Therefore, it is possible that the Kodiak-Kenai transverse boundary may have been active as a tectonic element on the Kodiak shelf at the time of deformation of the complex. Well data indicate that this deformation occurred between late Eocene and early Miocene time (this report). Data from the Kodiak Islands indicate an age range of early Eocene to late Oligocene for the deformation (Moore and Allwardt, 1980; Byrne, 1986). Collectively, these data sets suggest that the deformation occurred between late Eocene and late Oligocene time.

The maturation level of basement rocks in the wells southwest of the Kodiak-Kenai transverse boundary is relatively low (immature, or pregeneration). This suggests that the strong deformation and dewatering of the basement suite there occurred at quite shallow depths, probably no deeper than the depths at which they lie at present. The "basement" sequence below the Miocene unconformity in the KSSD No. 2 well is also thermally immature, suggesting that it has not previously undergone deeper burial and exhumation.

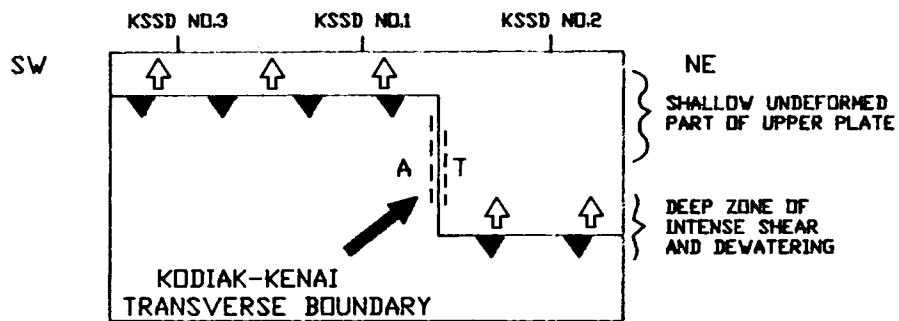
It may be possible to reconcile all of these observations within a model which analogizes the mechanical role of the Kodiak-Kenai transverse boundary to that of the "transverse ramp" in thrust systems. The transverse ramp is an inclined tear fault which transfers thrusts or detachments to a different structural level laterally along the strike of the thrust sheet. This may occur without rupture or deformation of the overriding sheet above the transverse ramp if the thrust transport azimuth parallels the strike

of the ramp. Any movement oblique to the ramp will cause interaction between the lower and upper blocks at the ramp and will result in the development of transverse structures in the upper sheet (Dahlstrom, 1970, fig. 48). However, the key feature of the transverse ramp analog for the purposes of the present argument is that it offers a mechanism whereby shear between upper and lower plates could occur simultaneously at different structural levels along the trend of the convergent margin. The intense shear and resulting deformation within the upper plate may be confined, as in some thrust systems, to fairly discrete zones that are enclosed by rocks which have not experienced significant penetrative deformation.

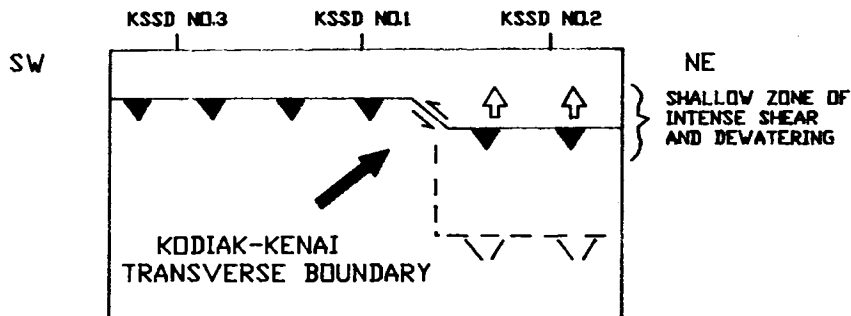
From the observations presented above, I speculate that the differences observed in the severity of deformation of basement rocks on opposite sides of the Kodiak-Kenai transverse boundary could be the result of coeval structural interaction between upper and lower plates taking place at very different structural levels laterally within the accretionary complex. The deformation of the basement protolith southwest of the transverse boundary occurred, as noted above, at shallow crustal levels. To the northeast, the zone of shear and dewatering during this deformational event may have been transferred to much deeper structural levels by a tear fault or transverse ramp at the transverse boundary. If the level of intense deformation in this area was much deeper, rocks at shallow structural levels could have escaped the intense deformation and dewatering experienced by coeval sequences to the southwest. Following the pre-late Oligocene deformational event, the zone of decoupling and intense deformation in the block northeast of the transverse boundary may have migrated upward to much shallower structural levels. It is not known why this might have occurred. The re-structuring of the transverse boundary, however, may have resulted from a change in azimuth of plate convergence at the Kodiak margin resulting from a reorganization of northeast Pacific plates (subduction of the Kula plate; Grow and Atwater, 1970). This change may coincide with Miocene and younger uplift along the Kodiak-Kenai transverse boundary (Fisher and others, 1981). Subsequent (possibly ongoing; fig. 95) deformation at a new, shallower level northeast of the transverse boundary led to intense dewatering of the shallow strata which were previously passively carried in the upper plate above the older, deeper "thrust" zone. If the fluids expressed from these tectonized rocks are unable to migrate upward through overlying strata at the same rate as that at which they are generated, a dynamic condition of abnormal formation pressure would develop. The basic elements of this two-stage model are illustrated in the schematic cross sections of figure 97.

SUMMARY

Analysis of shale properties as measured by wireline logs has identified one major zone of abnormal formation pressure in the KSSD No. 2 well. No evidence of abnormal formation pressure was found in the other five wells on the Kodiak shelf. In the KSSD No. 2 well, the overpressured zone extends from 6,500 feet (subsea) to beyond the



OLIGOCENE (?) DEFORMATIONAL EVENT



MIOCENE (?) TO HOLOCENE DEFORMATION

Figure 97. Schematic cross section illustrating hypothetical model for transfer of level of intense shear and dewatering within accretionary complex at Kodiak-Kenai transverse boundary. Small arrows denote movements of fluids dewatered from zones of intense deformation near detachments. Teeth on detachments point toward underthrust block. "A" and "T" in upper diagram signify relative movement of blocks away or toward the viewer. Re-structuring of transverse boundary may be due to change in azimuth of convergence of Pacific plate and Aleutian arc.

base of the well at 10,370 feet (subsea). Eocene strata of the basement complex and superincumbent strata of Miocene age are both included within the zone of abnormal formation pressure.

No direct measurements of fluid pressure were obtained within the overpressured zone in the KSSD No. 2 well. Analysis of shale properties using empirical pressure evaluation curves suggests that hydrostatic gradients as high as 0.88 psi/foot (17.0 ppg equivalent fluid density) exist within the part of the overpressured zone penetrated by the well. Although mud weight was progressively increased while drilling below the top of the overpressured zone, virtually the entire zone was drilled in an underbalanced condition. However, because of the low permeability of strata within the overpressured zone, no significant incursion of formation fluid or gas into the wellbore occurred during drilling operations.

Within the KSSD No. 2 well, the severity of overpressure increases abruptly below the Miocene unconformity and continues to increase steadily to the base of the well. Hypothetical projection of "undercompaction" trends below the base of the well suggests that lithostatic fluid pressures could be achieved at depths as shallow as 12,000 feet. These observations suggest that the excess pore fluids in the overpressured interval are migrating upward from a source within the basement complex. Because of the inadequacies of alternative mechanisms, and because the well penetrated an accretionary complex which overlies an active subduction zone, the preferred hypothesis for the source of the excess pore fluid is tectonic dewatering in active shear zones within the accretionary complex.

The KSSD No. 2 well is separated from the other Kodiak shelf wells by the Kodiak-Kenai transverse boundary mapped by Fisher and others (1981). The rocks that make up the basement complex in the wells southwest of this transverse structure were strongly deformed and dewatered at low temperatures (shallow depths) prior to development of the Miocene unconformity. Coeval rocks in the KSSD No. 2 well escaped this dewatering event and appear to be the present source for the excess pore fluids in that well. This contrast in the structural histories of "basement" rocks in blocks northeast and southwest of the transverse boundary may be explained with a model wherein deformation in the two adjacent blocks occurred at different structural levels. The role of the transverse boundary in this model is suggested to be similar to that of the "transverse ramp" of thrust terranes, in that it mechanically linked coplanar "thrusts," or shear zones, which localized deformation at different structural levels at different times in the blocks northeast and southwest of the boundary.

11. SHALLOW GEOLOGY AND GEOLOGIC HAZARDS

SHALLOW GEOLOGY

Physiography and Bathymetry

The Kodiak shelf geologic province extends approximately 400 miles along the southern continental margin of Alaska. The width of the shelf, as defined by the 300-foot bathymetric contour, ranges between 50 and 100 miles (fig. 98). The principal physiographic features that make up the shelf are four relatively flat submarine banks, ranging in depth from 150 to 300 feet, which are separated by troughs up to 650 feet deep (fig. 99). The physiography is closely related to major structural features that underlie the shelf and to modification by Quaternary glaciers.

Large areas of the shelf, particularly the banks (fig. 99), are free of unconsolidated sediment, and strata of Plio-Pleistocene and undifferentiated Tertiary age crop out at the sea floor (Thrasher, 1979). Thrasher (1979) identified several ridges and sea-floor lineations across the banks. These features, some with as much as 15 feet of relief, represent bedrock hogbacks. Von Huene and others (1980b) identified a variety of other second-order physiographic features including fault scarps, sand waves, and a discontinuous series of arches along the shelf break. These arches are the sea-floor expressions of anticlines that underlie the shelf edge.

Surficial Sediment and Bedrock Outcrops

On the basis of seismic reflection characteristics and 217 sea-floor sediment samples, Thrasher (1979) mapped 10 shallow stratigraphic units comprising bedrock and unconsolidated sea-floor sediment (table 13, fig. 100). Thrasher (1979) inferred the depositional facies of some of these units on the basis of their seismic characteristics and stratigraphic positions. He also differentiated the Holocene sediment on the basis of the presence or absence of bedforms. The Holocene sediment without bedforms is mostly gray-green, ash-rich silt and clay with accessory sand, gravel, shell fragments, and glass shards. This sediment type lines the bottoms of local sea-floor depressions and major valleys such as the Kiliuda, Chiniak, and Stevenson Troughs. The Holocene sediment displaying bedforms is clean, well-sorted sand that occurs as isolated deposits that range in areal extent from 20 to 60 square miles. These deposits are present on sloping rather than horizontal sea floor.

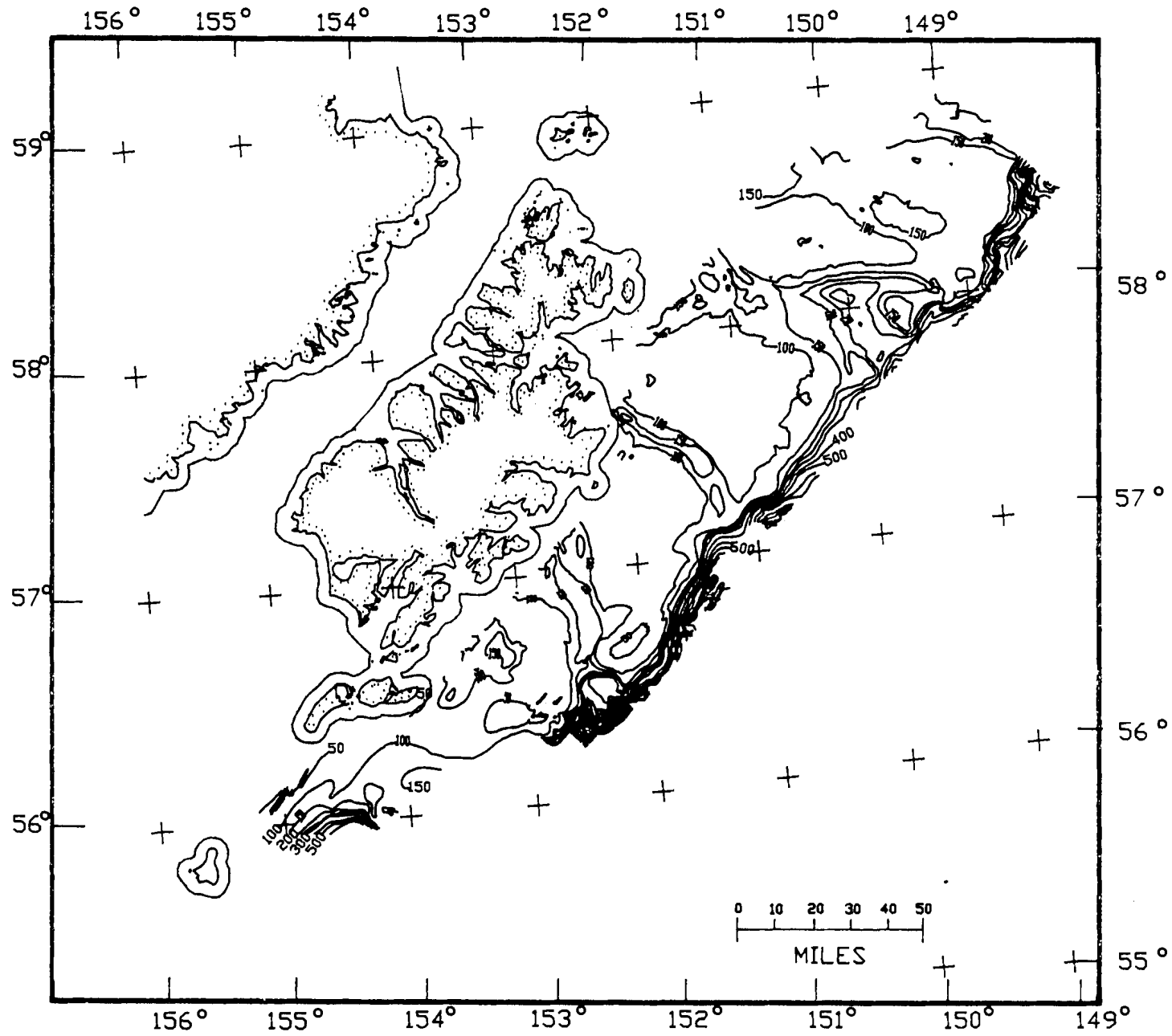


Figure 98. Bathymetry of the Kodiak shelf (after Turner and others, 1979). Depths are in meters.

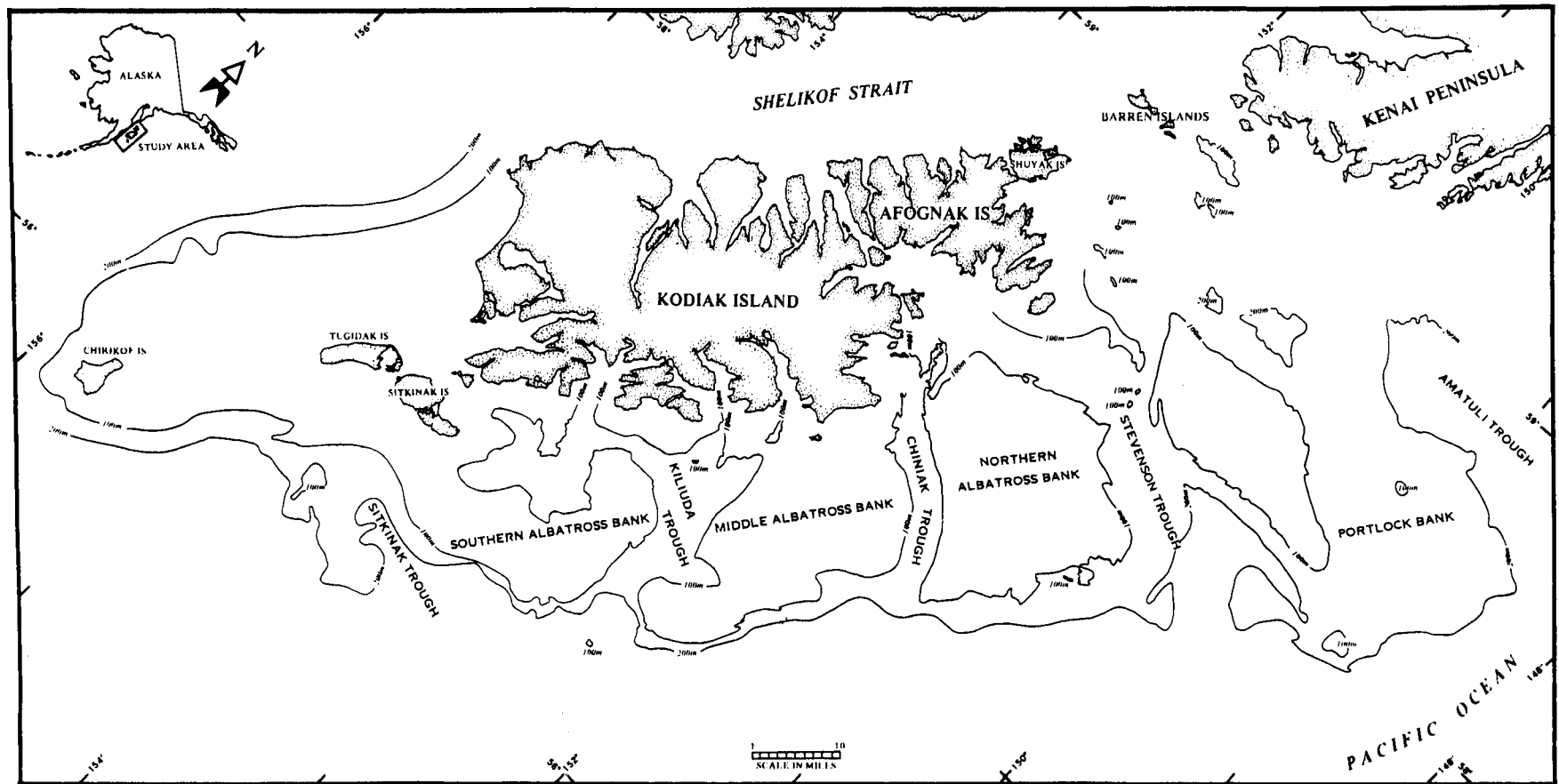


Figure 99. Physiography of the Kodiak shelf.

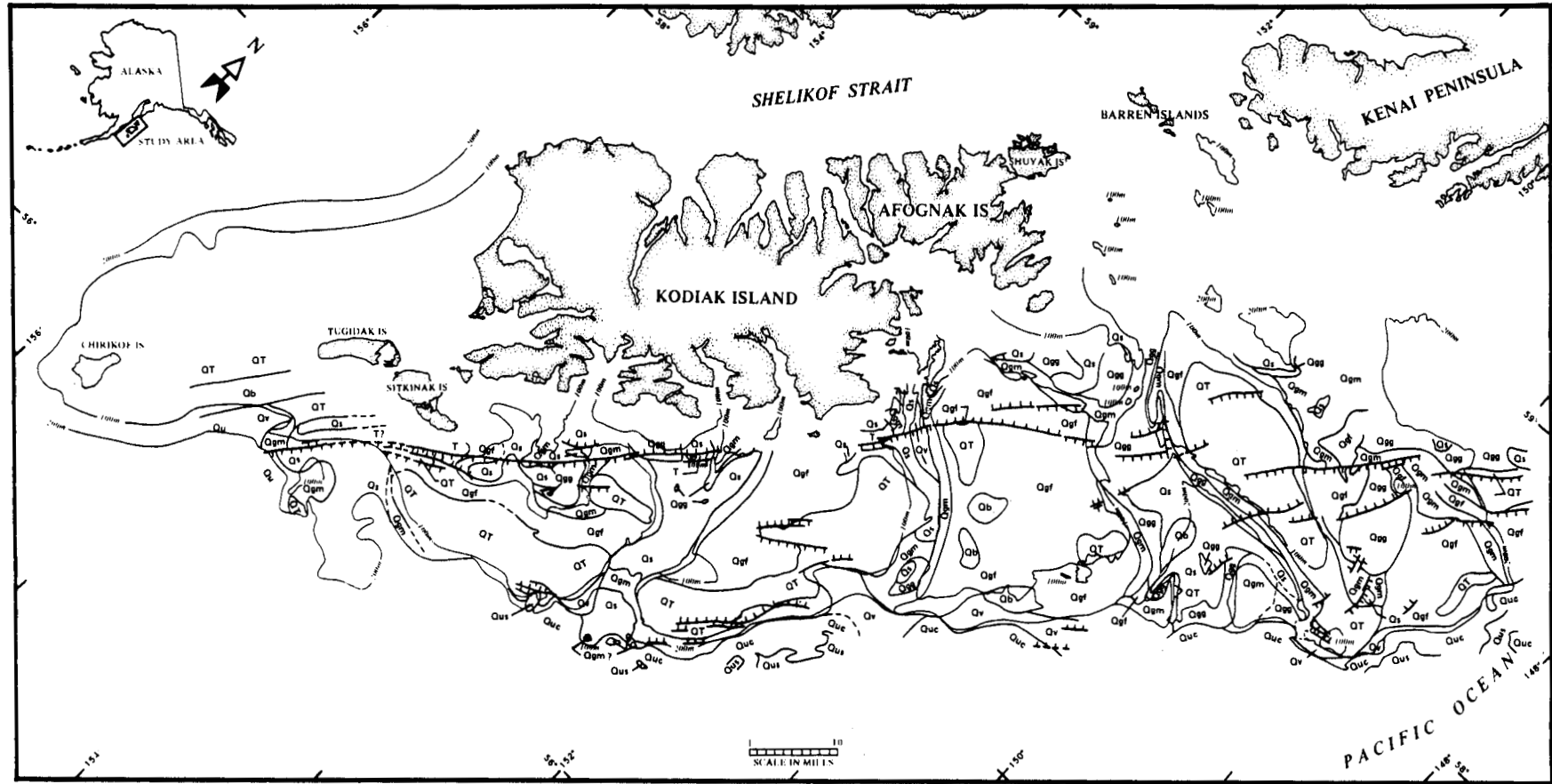


Figure 100. Geologic map of the Kodiak shelf showing bedrock outcrops and surficial sedimentary units (after Thrasher, 1979). See table 13 for descriptions.

Recent sediments on the Kodiak shelf are composed mostly of reworked detritus. This conclusion is supported by the extensive outcrops of bedrock across the shelf, the patchy and distinctly current-controlled deposits of Holocene sediment, and the general absence of major rivers draining the adjacent landmass which could introduce terrigenous sediment onto the shelf. The 1912 eruption of Katmai volcano on the Alaska Peninsula deposited considerable volcanic ash onto the shelf (Hampton and others, 1979). As with the other Holocene sediments, the ash was preferentially deposited in troughs and depressions and not on the banks (von Huene and others, 1980b). The marked absence of ash on the flat-topped banks suggests the presence of a current competent to winnow and rework the shelf sediments. This current, which has been detected by moored current meters, surface drift cards, satellite-tracked drift buoys, and Dopplershift radar (Muench and Schumacher, 1980), is part of the southwestward-flowing Alaska Stream.

Thrasher (1979) differentiated four types of Pleistocene sediment (table 13, fig. 100). These sediment types represent various glacial moraine and outwash deposits that occur as extensive deposits that blanket approximately 40 percent of the shelf.

Plio-Pleistocene rocks that crop out at the sea floor are composed of lithified and semi-lithified sandstone and siltstone. Rocks of this unit are moderately deformed, containing numerous folds and faults, and its upper surface is angularly discordant with the sea floor. On the southwestern part of the shelf, Thrasher (1979) tentatively correlated these rocks with the Pliocene Tugidak Formation; where they crop out on the northeastern part of the shelf, he correlated them with the late Tertiary and Quaternary Yakataga Formation. Thrasher (1979) also tentatively correlated sea-floor bedrock outcrops near Kodiak Island with either the Eocene-Oligocene Sitkalidak or the Eocene Ghost Rocks Formations that crop out along strike on nearby islands.

TABLE 13. Description of sedimentary units (after Thrasher, 1979). Refer to figure 100.

Qs: Holocene Soft Sediments. These units are thin deposits of Holocene sediments that, on high-resolution seismic profiles, exhibit well-defined, laterally continuous, horizontal reflections. The sea-floor sediment is mostly gray-green, ash-rich silt and clay with variable amounts of sand and pebbles, and common glass shards and shell fragments.

Qb: Holocene Bedforms and Sand-Fields. These units are mappable deposits that are characterized by sea-floor bedforms. The sea-floor sediment is clean, well-sorted sand.

Qu: Holocene and Pleistocene Undifferentiated Deposits. On high-resolution seismic profiles, these deposits exhibit well-developed, non-horizontal, parallel layering with occasional indications of internal deformation. The composition of the sea-floor sediment ranges from green, muddy ash to gravelly sand.

Qgm: Pleistocene Glacial Lateral and Terminal Moraines. These deposits have fairly linear morphologies and are located mostly along the sides and across the mouths of the sea valleys. On high-resolution seismic profiles, these deposits are characterized by poor acoustic penetration with very little or no internal structure evident. The sea-floor sediment is mostly gravelly sand with rare occurrences of volcanic ash and stiff gray mud.

Qgg: Pleistocene Glacial Ground Moraine. On high-resolution seismic profiles, these deposits are characterized by hummocky upper surfaces, poor acoustic penetration, and no acoustic stratification. The composition of the sea-floor sediment is predominantly muddy sand or sandy mud with accessory volcanic ash, glass shards, shell fragments, and pebbles. This sediment type commonly lines troughs.

Qgf: Pleistocene Glacial-Fluvial and Glacial-Marine Deposits. This unit occurs as thick deposits which, on high-resolution seismic profiles, are characterized by reflections that are discontinuous, non-parallel, and non-horizontal. The sea-floor sediment is composed of sand, shell debris, pebbles, gravel, volcanic ash, and mud. This sediment type commonly occurs on the banks between sea valleys.

QT: Plio-Pleistocene Sedimentary Rock. This unit is composed of gently dipping sedimentary rocks that exhibit well-developed, parallel internal reflections on seismic profiles. The upper surface of this unit is a regional angular unconformity. Most samples from this unit are claystone or siltstone.

T: Tertiary Sedimentary Rocks. This unit is characterized by the absence of any seismically resolvable internal structure. It occurs only in small outcrops along the landward edge of the shelf.

Quc: Quaternary Undifferentiated Continental Slope Deposits. The large vertical exaggeration of the seismic data and the steep inclination of the continental slope preclude inferences regarding the structure or stratification of this unit.

Qus: Quaternary Undifferentiated Sediment Basins on the Upper Continental Slope. This unit is made up of ponded sediment deposits that exhibit well-defined, near-horizontal, continuous reflections on seismic profiles.

Shallow Structures

Using high-resolution seismic data, Thrasher (1979) and von Huene and others (1980b) mapped shallow faults and folds on the Kodiak shelf (fig. 101). These faults strike generally northeast-southwest, parallel to the axis of subduction. The fold axes also trend generally northeast-southwest, but tend to show more variation in strike than do the faults. Most of the variation in fold axis trends occurs in two narrow, northwest-southeast zones that transect the shelf. These two zones, which are located at either end of Kodiak Island, represent transverse tectonic boundaries that separate the Kodiak tectonic block from the Shumagin tectonic block to the southwest and the Kenai tectonic block to the northeast (Pulpan and Kienle, 1979; Davies and others, 1981; Fisher and others, 1981).

The presence of these transverse tectonic boundaries is also apparent in the COST well data. Dipmeter log data from the KSSD No. 1 well, which was drilled within the more northern transverse tectonic boundary, indicate that the strata penetrated by

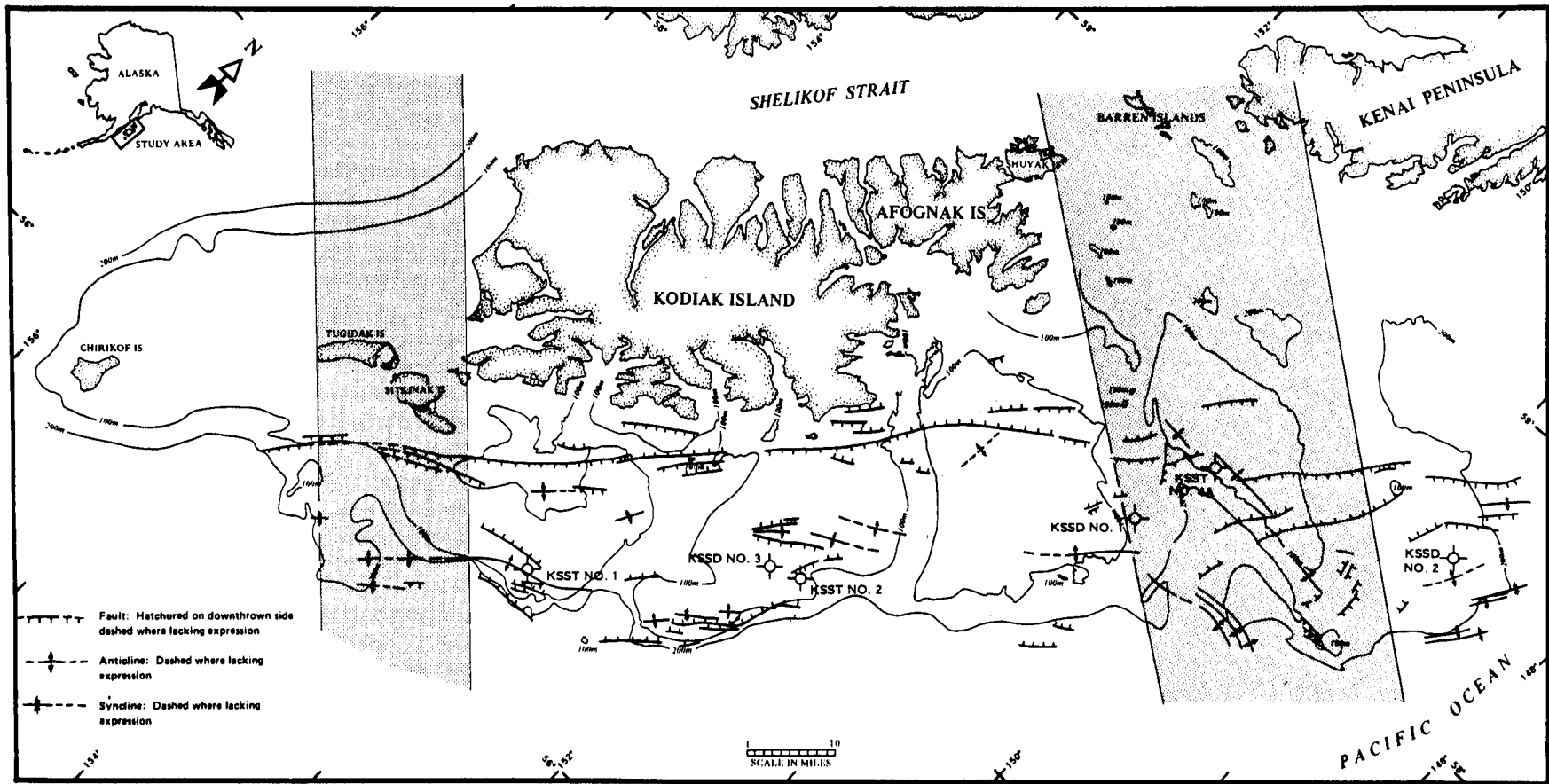


Figure 101. Shallow folds and faults underlying the Kodiak shelf (after Thrasher, 1979, and von Huene and others, 1980b). The locations of the KSSD and KSST wells are indicated. The approximate extents of the transverse tectonic zones are indicated by the shaded regions (after Fisher and others, 1981).

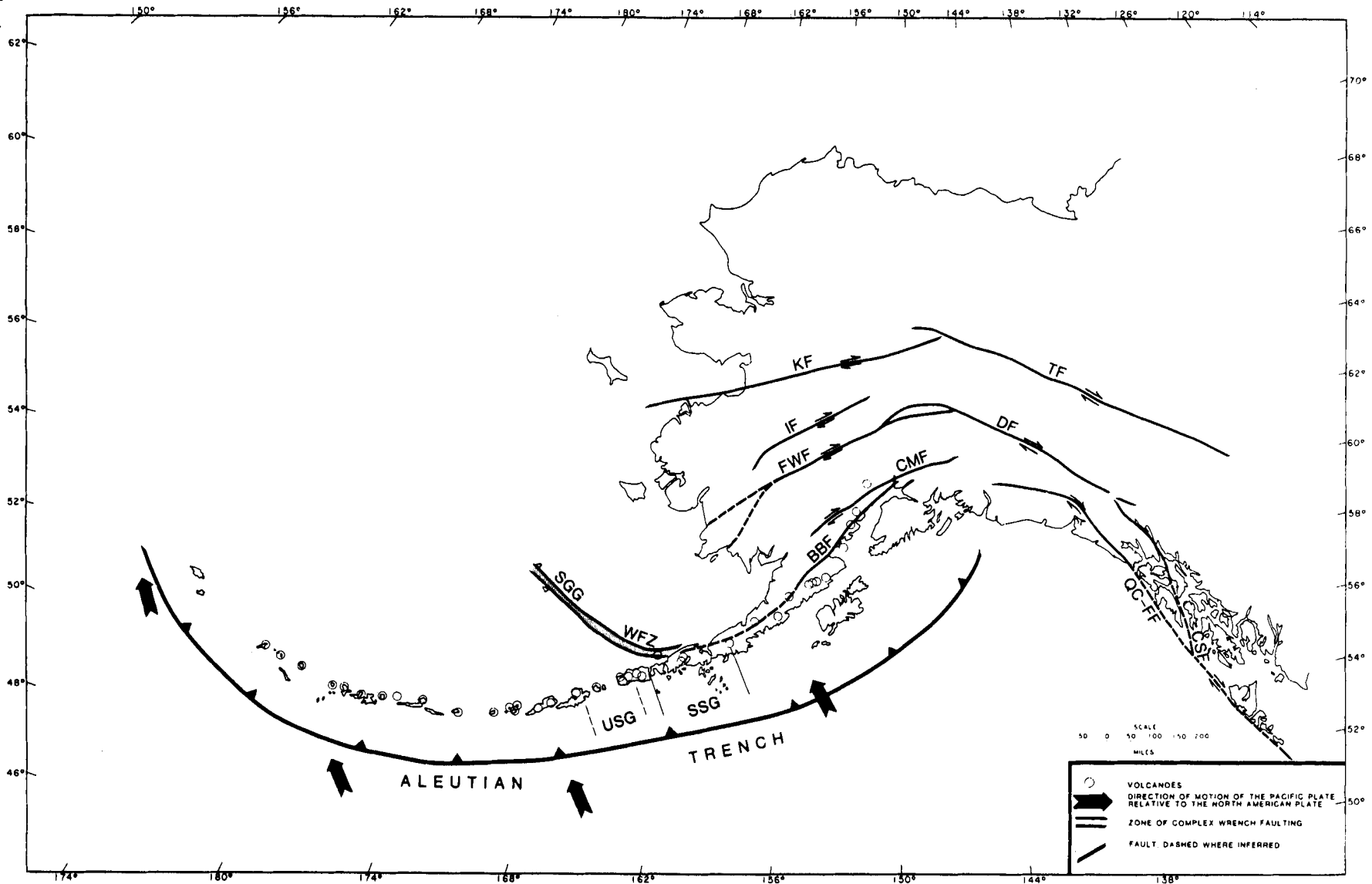


Figure 102. Major strike-slip faults (after King, 1969), historically active volcanoes (Simkin and others, 1981), and convergence directions between the Pacific and the North American lithospheric plates (Chase, 1978; Minster and Jordan, 1978). Inferred trend of the Bruin Bay fault after Bruhn and Pavlis (1981). Trend of the St. George graben after Comer and others (1987). Trend of the Bering Sea shelf wrench fault zone after Hoose (1987). Locations of the Shumagin and Unalaska seismic gaps after McCann and others (1980) and House and others (1981), respectively. Abbreviations: WFZ - Bering Sea shelf wrench fault zone, SGG - St. George graben, KF - Kaltag fault, TF - Tintina fault, IF - Iditarod fault, FWF - Farewell fault, DF - Denali fault, CMF - Castle Mountain fault, BBF - Bruin Bay fault, QC-FF - Queen Charlotte-Fairweather fault, CSF - Chatam Strait fault, USG - Unalaska seismic gap, and SSG - Shumagin seismic gap.

the well are more steeply dipping than in the other wells (see Well Log Interpretation chapter). An analysis of the physical properties of the shales penetrated by the KSSD No. 1 well confirms that they have been both deformed and dewatered (see Abnormal Formation Pressure chapter). Kerogen maturity data, however, indicate that the deformation and dewatering was not caused by burial (see Organic Geochemistry and Abnormal Formation Pressure chapters). Thus the deformation apparent in both the dipmeter data and in the physical properties of the shale is here interpreted as reflecting the deformation taking place within this transverse zone as the adjacent tectonic blocks move relative to each other.

Through a comparison of bathymetric data collected before and after the March 27, 1964, earthquake (magnitude (M_w) 9.2) von Huene and others (1972) were able to document that the Middle Albatross Bank (fig. 99) was uplifted by as much as 22 feet by that event. Von Huene and Fisher (1984) further noted that the sea floor landward of the Albatross Basin is offset by normal faults. Those investigators suggested that the extensional tectonics reflected by those faults occurred in response to crustal relaxation at the landward edge of the Albatross forearc basin following the 1964 earthquake. These observations indicate that shallow structures are still actively forming. The relationship between shallow structures and regional tectonics is also supported by the formation of faults on Montague Island during the 1964 earthquake (Plafker, 1965; Malloy and Merrill, 1972) and the presence of other sea-floor fault scarps on the Kodiak shelf (Thrasher, 1979).

GEOLOGIC HAZARDS

Seismicity

The Alaska-Aleutian arc is one of the world's most active seismic belts in terms of both the number of events and the amount of energy released annually. This belt is part of a nearly continuous zone of seismicity, volcanic activity, and crustal deformation that rings the Pacific Ocean and reflects the interactions between mobile lithospheric plates. Along the Kodiak shelf, this seismicity is a manifestation of the subduction of the Pacific plate beneath the North American plate along the Aleutian trench (fig. 102).

Minster and Jordan (1978) and Chase (1978) calculated that the long-term average rate of plate convergence along the Aleutian subduction zone is 7.7 centimeters per year. Most of the accumulated elastic strain associated with this convergence is relieved during great earthquakes with surface wave magnitudes (M_s) greater than 7.8 on the Richter scale (McCann and others, 1980). Studies of the aftershock zones of large earthquakes (Sykes, 1971; Pulpan and Kienle, 1979; Sykes and others, 1980) and of regional and local geologic trends (Fisher and others, 1981) revealed that the tectonic margin of southern Alaska is segmented into discrete blocks that respond individually to subduction-related tectonics. These tectonic

blocks are separated by the transverse tectonic boundaries discussed above.

The repeat time for large earthquakes within a given tectonic block is a function of the average rate of plate convergence and the net amount of slip across a spatially complex deformation zone involved in the earthquake (McCann and others, 1980). Studies indicate that the Kodiak tectonic block was involved in the rupture zone of the March 27, 1964, earthquake and that the southwestern end of the rupture zone coincided with the transverse tectonic boundary southwest of Kodiak Island (Sykes and Ewing, 1965; Nishenko and McCann, 1979; Pulpan and Kienle, 1979). Plafker (1972) estimated that the net amount of slip associated with the 1964 great Alaskan earthquake was 65 feet. Using seismic moment and published plate convergence rates, McCann and others (1980) estimated that the repeat time for an earthquake comparable to the 1964 event located in the same segment of the arc would be 220 years. Estimates of recurrence intervals in other tectonic segments along the arc range from 800 years (based on long-term geologic evidence (Plafker and Rubin, 1967)) to 30 years (based on historic records (Sykes, 1971)).

An arc segment that is relatively aseismic or that has not experienced a large earthquake within a probable repeat time is termed a seismic gap and represents a likely site for a future large earthquake (Sykes, 1971). The Shumagin seismic gap, located southwest of the Kodiak Shelf Planning Area (fig. 102), has not experienced a large earthquake since the turn of the century (Sykes, 1971). Because of its proximity and high potential for rupture, the seismic potential of the adjacent Shumagin tectonic block must be considered when assessing the seismic risk on the Kodiak shelf. When the Shumagin gap ruptures, the Kodiak shelf will probably experience substantial ground motion.

Earthquakes smaller than great events (less than magnitude 7.8 on the Richter scale) are also capable of causing severe destruction. Since 1902, at least 95 potentially destructive events of magnitude 6 or greater have occurred on or near the Kodiak shelf (von Huene and others, 1980a). Many of these events were precursors to or aftershocks of great earthquakes. Some events near the mouth of Kiliuda Trough and on the southern and middle Albatross Banks were probably related to the tectonics of the adjacent transverse tectonic boundary (von Huene and others, 1980a; Fisher and others, 1981).

Sediment Slides

Bedrock crops out across much of the Kodiak shelf, and elsewhere the unconsolidated sediment veneer is generally thin. Only one sediment slide has been observed in water depths of less than 500 feet on the Kodiak shelf. Hampton and Bouma (1977) identified that feature on one of the steepest walls in the Stevenson Trough (fig. 103). In that area the surficial sediment is composed of volcanic ash and terrigenous sand and mud, and the occurrence of the slide is probably related to the relatively high water content and correspondingly low shear strength of that sediment type. On the

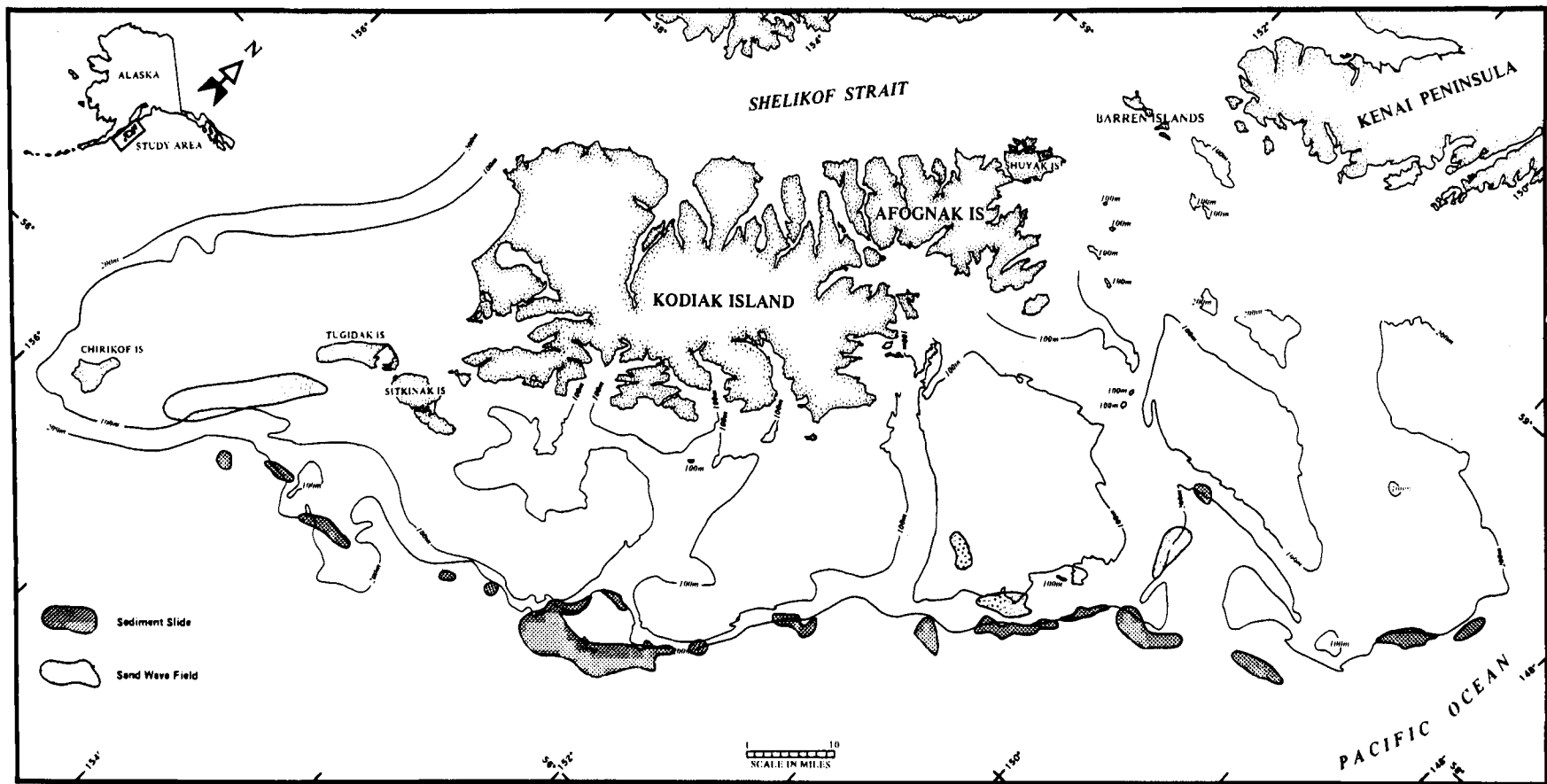


Figure 103. Locations of sediment slides and sand wave fields (after Fisher and others, 1984, and Thrasher, unpublished MMS interpretation).

basis of geotechnical analysis, Hampton (1983) also identified an area of potential instability in Sitkinak Trough. Elsewhere on the shelf, von Huene and others (1980a) associated the weakest sediment with evidence of gas-charging. However, those investigators did not consider the areas of gas-charged sediment to be susceptible to failure because they were found primarily in areas where the sea floor was flat rather than inclined. Von Huene and others (1980a) also pointed out that other possible types of instability are liquefaction and consolidation subsidence.

In contrast with the shelf, several sediment slides have occurred on the upper slope (Hampton and Bouma, 1977). Those slides occurred in water depths greater than 500 feet and do not pose a threat to oil exploration and production on the shelf (fig. 103). Fisher and others (1984) point out that those parts of the upper slope that have evidence of mass movement also have evidence of modern tectonic activity such as the growth of near-surface folds, tilting of the sea floor, and seismicity.

Shallow Gas

On the basis of acoustic anomalies apparent on high-resolution seismic data, Fisher (1980), Hampton and Kvenvolden (1981), and Thrasher (unpublished interpretation) identified several localities where shallow gas-charged sediments are present (fig. 104). In some areas of the shelf, gas generation is great enough to produce gas seeps which show up on high-resolution seismic profiles as water-column anomalies. Interstitial gas has also been sampled in sediment cores from the Kodiak shelf (Fisher, 1980; Hampton and Kvenvolden, 1981). On the basis of the high methane to ethane plus propane ratios ($C_1:[C_2+C_3]$, average 12,000) and $\delta^{13}C$ values that average as low as -79 o/oo PDB, those investigators attributed the gas to microbial activity rather than thermal generation, although Hampton and Kvenvolden (1981) suggested that one fault-associated gas seep may be venting from a deeper, thermogenic source.

The presence of gas-charged sediment is significant because on continental shelves elsewhere it has been associated with sea-floor instability, overpressuring, and low sediment shear strength (Whelan and others, 1976; Nelson and others, 1978). Fisher and others (1984) saw no gas-produced sea-floor craters on Kodiak shelf such as have been observed in Norton Sound (Nelson and others, 1979). However, Thrasher (1979) noted "indistinct scattered dimples or blemishes, 5-10 meters in diameter" on sea floor underlain by soft Holocene sediment. Fisher and others (1984) caution that although evidence for naturally triggered, gas-related, sea-floor failure is lacking, engineering activities or seismicity might provide an artificial trigger for such failure.

Volcanic Activity

Most of Alaska's active and dormant volcanoes occur along an arcuate belt that extends over 2,500 miles from Mt. Spurr near Anchorage to the tip of the Aleutian archipelago (fig. 102). This

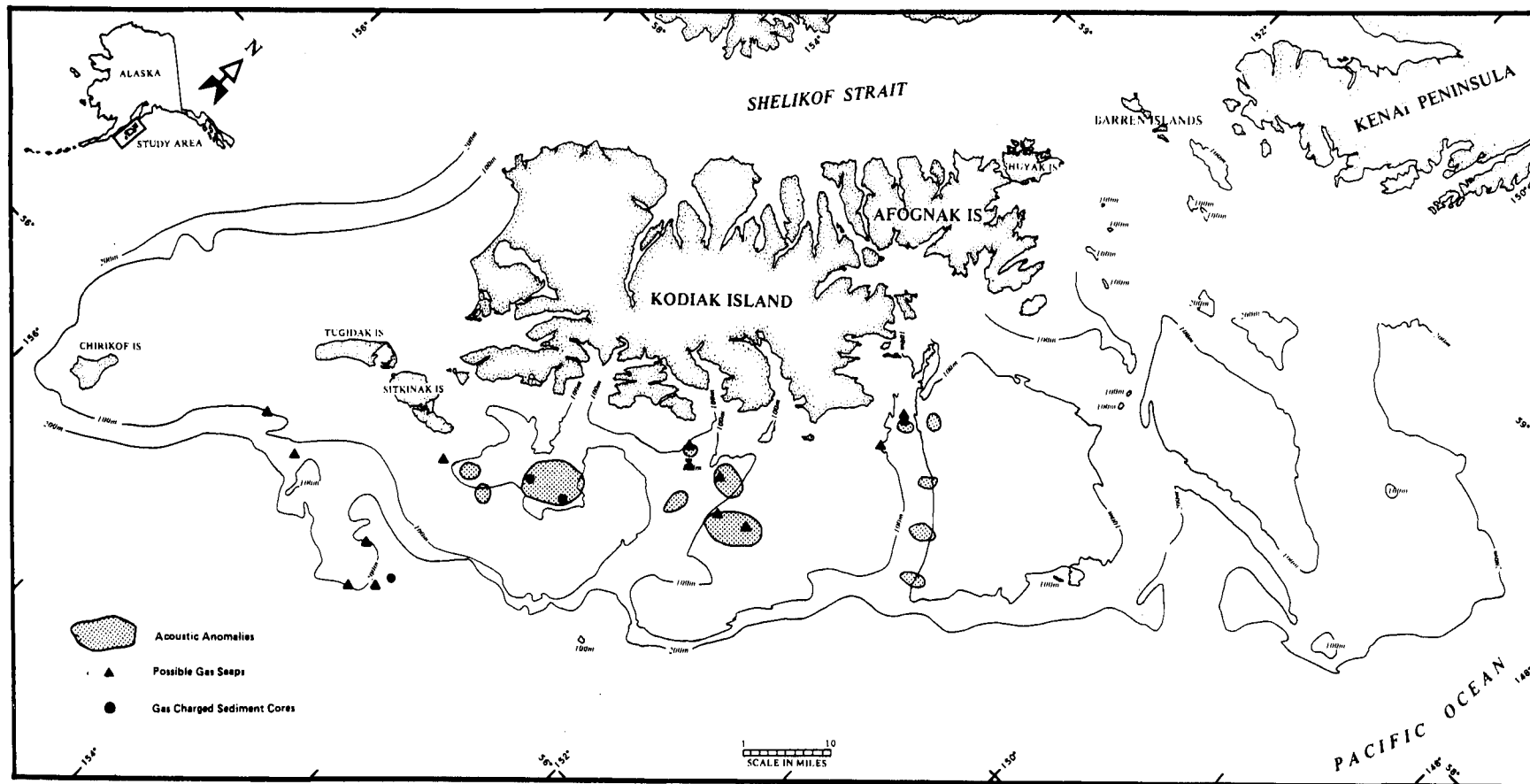


Figure 104. Locations of indicators of possible gas.

belt, which is characterized by modern seismicity as well as volcanic activity, is the manifestation of the subduction of the Pacific plate beneath the North American plate along the Aleutian trench. Within this belt, 32 active or dormant volcanic centers are located within 250 miles of the Kodiak Shelf Planning Area (table 14), with the closest volcanoes situated within 40 miles of Kodiak Island. Of these 32 volcanic centers, 21 have been active within the last 200 years.

TABLE 14. Volcanic activity along the Alaska Peninsula (Simkin and others, 1981).

<u>Name</u>	<u>Latitude</u>	<u>Longitude</u>	<u>Type (Elev. feet)</u>	<u>Last Eruption</u>
Frosty	55.07 N	162.82 W	Strato-volcano (5,783)	Holocene
Emmons	55.33 N	162.07 W	Caldera (4,349)	historic (fumarolic)
Pavlof	55.42 N	161.90 W	Strato-volcano (8,259)	1987
Pavlof Sister	55.45 N	161.87 W	Strato-volcano (7,026)	1786
Dana	55.62 N	161.22 W	Strato-volcano (4,198)	Holocene
Kupreanof	56.02 N	159.80 W	Strato-volcano (5,159)	historic (solfataric)
Veniaminof	56.17 N	159.38 W	Strato-volcano (8,223)	1984
Black Peak	56.57 N	158.80 W	Strato-volcano (3,132)	Holocene
Aniakchak	56.88 N	158.15 W	Caldera (4,448)	1942
Yantarni	57.02 N	157.18 W	Strato-volcano (4,100)	Holocene
Chiginagak	57.13 N	157.00 W	Strato-volcano (7,003)	1972
Kialagvik	57.20 N	156.70 W	Strato-volcano (5,576)	Holocene
Peulik	57.75 N	156.35 W	Strato-volcano (4,835)	1852
Ukinrek Maars	57.83 N	156.61 W	Maar (312)	1977
Martin	58.15 N	155.38 W	Strato-volcano (6,048)	1953
Mageik	58.20 N	155.25 W	Strato-volcano (7,249)	1946
Novarupta	58.27 N	155.16 W	Lava dome (2,758)	1950
Griggs	58.35 N	155.12 W	Strato-volcano (7,429)	historic (fumarolic)
Trident	58.23 N	155.12 W	Strato-volcano (6,790)	1975
Katmai	58.27 N	154.98 W	Strato-volcano (6,714)	1931
Snowy	58.33 N	154.73 W	Strato-volcano (7,088)	uncertain
Denison	58.42 N	154.45 W	Strato-volcano (7,603)	Holocene
Steller	58.43 N	154.40 W	Strato-volcano (7,452)	Holocene
Kukak	58.47 N	154.35 W	Strato-volcano (6,691)	historic (fumarolic)
Devils Desk	58.48 N	154.30 W	Strato-volcano (6,409)	uncertain

(Table 14 cont.)

<u>Name</u>	<u>Latitude</u>	<u>Longitude</u>	<u>Type (Elev. feet)</u>	<u>Last Eruption</u>
Kaguyak	58.62 N	154.08 W	Strato-volcano (2,955)	Holocene
Fourpeaked	58.77 N	153.68 W	Strato-volcano (6,901)	uncertain
Douglas	58.87 N	153.55 W	Strato-volcano (7,003)	historic (fumarolic)
Augustine	59.37 N	153.42 W	Strato-volcano (4,025)	1986
Iliamna	60.03 N	153.08 W	Strato-volcano (10,014)	1978(?)
Redoubt	60.48 N	152.75 W	Strato-volcano (10,194)	1968
Spurr	61.30 N	152.25 W	Strato-volcano (11,067)	1954

Volcanic activity is capable of producing a variety of phenomena that could pose hazards to oil exploration and production facilities. Due to the relatively large distances separating the volcanoes from the planning area, hazards posed by localized phenomena such as lava flows, mud slides, bombs, floods, and nuee ardente are not considered to be significant. However, volcanic phenomena that could pose a hazard over extended distances are ash fall, tsunamis, and radio interference. Volcanic eruptions can produce large volumes of ash that could blanket the region downwind of the volcano. The 1912 eruption of Katmai volcano generated a considerable volume of ash (Wilcox, 1959) that caused significant damage to some communities due to the abrasive action of the volcanic particles and the corrosiveness of the ash-produced acid (Arctic Environmental Information and Data Center, 1974). The potential threat of ashfall to the Kodiak shelf is corroborated by the significant component of ash found in unconsolidated sediment on the shelf (Thrasher, 1979; Hampton and others, 1979).

12. ENVIRONMENTAL CONSIDERATIONS

The following is a history of the permitting process that culminated in the drilling of six Deep Stratigraphic Test (DST) wells on the Kodiak shelf on the east side of Kodiak Island. The data sources are the Environmental Analysis (EA) prepared for the proposal, data submittals required by the office of the Oil and Gas Supervisor, Alaska Area (now Regional Supervisor, Field Operations, Alaska OCS Region), and the files of correspondence.

Exploration Services Co., Inc. (ESCI), as operator for itself and other participants, submitted a letter to the Conservation Division of the U.S. Geological Survey (now Minerals Management Service) dated January 7, 1975, for permission to drill up to 20 core holes in the western Gulf of Alaska. Each hole was to be cored, sampled, and logged. The maximum proposed depth was 2,000 feet. The letter proposed a timetable, a drilling program, a science program, and methods that would comply with Outer Continental Shelf (OCS) orders and the Code of Federal Regulations (30 CFR Parts 250 and 251). The permit application for the drilling of these DST wells was designated OCS Permit 75-87. ESCI later submitted a letter dated November 18, 1975, amending their original application and requesting a maximum depth of 4,000 feet and asking for a permit to drill 10 of the 20 holes in 1976. The new permit application was designated OCS Permit 76-35. The three wells drilled were subsequently referred to as the Kodiak Shelf Stratigraphic Test (KSST) wells by the operator and industry.

Sun Oil Company, as operator for itself and other participants, submitted a letter dated March 31, 1977, to the Conservation Division for drilling three additional DST wells in the western Gulf of Alaska. Documents initially submitted in support of this proposal included a Drilling Plan and an Application for Permit to Drill (APD) for each potential site. Site-specific surveys (cultural, biological, and shallow hazards) were required to investigate and document environmental conditions at each well location before drilling was allowed to begin. Four potential well locations, numbers 1, 2, 2a, and 3, were identified in the Drilling Plan. The applicant followed the requirements of 30 CFR 251 in obtaining a Geological and Geophysical (G&G) Permit for these wells. The permit was designated OCS Permit 77-1. These wells were subsequently referred to as the Kodiak Shelf Deep Stratigraphic (KSSD) wells.

A DST well, commonly referred to as a COST well by industry, is drilled for the acquisition of geological and engineering data to determine the potential for hydrocarbon generation and retention within a proposed lease area, not to locate hydrocarbon accumulations. The regulations in place at the time of the proposal required COST wells to be drilled off-structure. The information gathered from these test wells was used to evaluate the hydrocarbon potential of the Sale 46 portion of the Kodiak Shelf Planning Area.

As part of the permit application review process, Environmental Analyses (EA's) were prepared to include the environmental setting, an assessment of potential effects of the proposal on the described environment, alternatives, unavoidable adverse effects, mitigating measures, conclusions, and a National Environmental Policy Act (NEPA) determination. An addendum was prepared for the Amendment to Permit 75-87. The amendment was not recirculated to other Federal and State agencies, as it was determined that the drilling of an additional 2,000 feet at the 10 proposed locations would not materially increase the environmental effects beyond those addressed in the original plan.

Because it was determined that the original EA for Permit 77-1 discussed the drilling of only one well, an addendum was prepared that discussed the drilling of two additional wells. Both EA's and the addendums concluded that an Environmental Impact Statement (EIS) did not need to be prepared.

ENVIRONMENTAL SETTING

The western Gulf of Alaska is in a maritime climatic zone. The weather in this area is characterized by moderately heavy precipitation, high fog and cloud frequency, and cool temperatures with little freezing weather. The area has high humidity and small temperature variation, with a mean annual temperature of 41 °F. Gulf water temperatures range from 36 °F in the winter to 54 °F in the summer.

Storm winds are predominant in the western Gulf. Sustained wind speeds range from 50 to 75 knots, with gusts as high as 100 knots. Unusually intense storms can have sustained winds of 100 knots. An average of one sustained 100-knot wind may occur annually. Gale-force (greater than 34-knot) winds are infrequent in the summer months. A 100-year storm in the Gulf is defined as having 56-knot winds with 101-knot gusts, 51-foot wave heights (with a 102-foot maximum), and 3-knot currents.

Tides in the Gulf of Alaska are of mixed form, with diurnal inequality superimposed on the semidiurnal tide. Tidal amplitudes are usually in the range of 6.5 to 13 feet. Current velocities are on the order of 3 knots. Trochoidal sea waves predominate over the shelf and tend to be irregular in shape, height, and period. Offshore circulation is dominated by the Alaska Stream (0.5 to 3.5 feet per second) and is driven by both geostrophic and wind-stress

conditions. Bottom morphology and tidal currents superimpose on the Alaska Stream to form a complex circulation system. Tsunamis, "tidal" waves generated by earthquakes, are not uncommon in the area. Their magnitude is controlled by water depth in the area of origin and the efficiency of energy transfer.

During the spring and summer months, tremendous numbers of pelagic birds move into offshore areas of the western Gulf, although the Kodiak Archipelago generally lies outside the main bird-migration routes of Alaska and extensive staging areas are not evident in the Kodiak area. Two endangered species of birds, the short-tailed albatross and the Aleutian Canada goose, are found in the western Gulf of Alaska.

Approximately 22 species of marine mammals occur in the area. The most abundant marine mammals are the northern sea lion, harbor seal, northern fur seal, sea otter, Dall and harbor porpoises, and the gray whale. Seven whale species listed as endangered are found in the western Gulf, the blue whale (Balaeonoptera musculus), fin whale (Balaeonoptera physalus), sei whale (Balaeonoptera borealis), right whale (Balaeonoptera glacialis), gray whale (Eschrichtius robustus), humpback whale (Megaptera norvaeangliae), and the sperm whale (Physeter macrocephalus).

The Kodiak region is dependant on fishing and seafood processing for more than one-third of all employment. The shelf waters in the western Gulf have a high order of biological productivity and support a major fishing industry with stocks of king crab, Tanner crab, shrimp, and groundfish. The area provides essential rearing habitats for the Kodiak and Lower Cook Inlet anadromous fish stocks. The area also supports halibut, Pacific ocean perch, Pacific cod, turbot, pollock, rockfish, sablefish, sole, flounder, and scallops.

Archaeological research in the Kodiak Island area has revealed an extensive prehistoric occupation extending nearly 6,000 years before the present. This archaeological sequence represents a succession of maritime hunting and gathering cultures. Lower sea levels at earlier times may have allowed occupation of the shelf area out as far as the 100-meter bathymetric contour.

ENVIRONMENTAL EFFECTS OF THE PROPOSED DRILLING

The anchor pattern of the drilling vessel and the water depth resulted in a total enclosed area of seafloor of about 0.46 square miles (1.2 square kilometers). The actual seafloor contact was restricted to the anchor emplacements and drilling-base plate.

No significant deterioration of air quality in the vicinity of the drilling site was anticipated from exhaust and combustion products from primary electricity generation, helicopters, or auxiliary and supply boat diesel engines. Near-surface air circulation, the isolation of the installation, and the types of

emissions expected produced only minor and transitory air-contamination effects.

The geophysical operation consisted of running acoustic profiles through each site perpendicular to existing geophysical lines in order to provide final confirmation of the safety of the hole. These techniques utilized nonexplosive, very low-energy seismic sources.

Drilling-mud discharges resulted in only a short-term local increase in water turbidity. Production of formation waters was not anticipated. Management of oily wastes, human sewage, solid wastes, and wash water was in accordance with OCS operating orders and other applicable Federal regulations. The operator provided an estimate of the waste mud to be discharged to the ocean along with information on the Median Tolerance Limits (TLM), which represents the concentration of the material tested that causes fatalities in 50 percent of the test organisms (Mollienisias latipinna, the Sailfin Molly) for a specific period of time. The operator advised that a one-to-one dilution with seawater would dilute the chemical additives below their 96-hour TLM levels. A one-to-one dilution should take place in a short period of time after dumping. The operator stated that a total of 1,327 barrels (bbls) of mud would be discharged from each hole. The water depth at the well sites varies from 126 to 486 feet. Assuming a point-source discharge at the surface and a bottom-settling diameter of 300 feet (a cone with a base of 300 feet), a dilution ratio of 398-to-1 would be achieved in 486 feet of water. The drilled volume of a 2,000-foot well is 24 cubic yards, and of a 4,000-foot well, 96 cubic yards. The potential effects of bottom-covering by mud and drill cuttings or of seawater contamination appeared minor considering the relatively small volumes of waste materials and the dilution and dispersion action at the proposed well sites. No significant affect on the biological community was expected or encountered.

It was possible, though unlikely, that unexpected oil or gas might be encountered in the core-drilling operation. The possibility of causing an uncontrolled oil spill or encountering a significant volume of oil was rendered extremely unlikely by using the best available technology to investigate the locations and requiring the use of the same blowout-prevention and spill equipment required for wildcat operations. No oil spills occurred.

The Bureau of Land Management (BLM) proximity analyses used the rule of thumb that any platform within 20 miles of shore had the potential for aesthetic impact. Due to the distance from the nearest human community, no significant aesthetic effect was anticipated from the drilling operations. Although there was a localized increase in noise from the associated marine and helicopter traffic, because of its short duration and the distance from shore the net effects were inconsequential.

CONDITIONS OF APPROVAL

No alternatives to the proposals were recommended or considered. Unavoidable adverse effects were deemed mitigated by regulatory compliance. Both Permit Applications were submitted to State and Federal agencies for comment. No comments were received identifying effects not adequately discussed in the EA's and no alternatives or attachments to the permits were proposed. The Permits were conditionally approved requiring additional procedures, plans, and data. An emergency-operating-procedures plan that included requirements for safety meetings and drills was required. The safety meetings were to occur weekly with all hands and each crew was to participate in weekly drills. A multi-sensored acoustic and geophysical survey was required at each site to determine water depth, overburden thickness, shallow structural detail, and sites, structures, or objects of historical or archaeological significance. An oil-spill-contingency plan was required that detailed the containment, cleanup, and disposal methods for spilled oil. The plan described the equipment to be used and the sea and weather conditions for the equipment. A biological survey was required at each site to determine if any additional requirements were to be imposed for the protection of marine resources. All plans, procedures, and data were required to be reviewed and approved before drilling could commence. A report for each well was submitted and MMS personnel performed an independent analysis of submitted and other data for each location.

WELL SITES

KSST No. 1 Well Site

The KSST No. 1 well location is on the northwest flank of a breached, northeast-trending positive feature with strata dipping north-northwest at 10° to 15° into the adjacent syncline. The bedding appears to be continuous and unbroken updip to seafloor outcrops which are reflected by small hogbacks correlatable from profile to profile along the outcrop trend. No hazardous conditions appeared to be present and it was unlikely that any would occur in this structural setting. The water bottom is flat and clear at the location.

KSST No. 2 Well Site

The location is on the northwest nose of a broad, breached positive feature with truncated strata that crop out on the seafloor. High-resolution seismic data show no evidence of shallow faulting or seeps. Data quality is too poor to allow identification of shallow gas accumulations, but the structural configuration should preclude this possibility. The water bottom appears to be rough and hard and could pose anchoring difficulties.

KSST No. 4 Well Site

Location 4 is on the southern flank of an east-west-trending positive feature. Data quality beneath the regional unconformity is generally poor, but because strong evidence exists that combination traps may occur beneath the unconformity it did not seem prudent to permit drilling to a depth greater than 4,000 feet.

The data submitted were largely inconclusive due to extremely poor quality, apparently a result of indurated rock at the sea floor. The shallow subbottom section may be locally fractured or may contain local boulder/gravel accumulations. No evidence of shallow gas was observed. The structural configuration suggests that no shallow trapping mechanism exists.

KSSD No. 1 Well Site

The site lies on the south flank of the Stevenson Trough, which is between Portlock and Northern Albatross Banks. The maximum average slope at the site is 0.25° . The undulating slope surface is apparently not slump related. There are no indications of slumping, surface faulting, or seeps. An overburden of coarse sand and shell debris overlies a glacially scoured surface. A fault indicated on the anomaly map does not extend through the well site. There are no indications of closure or shallow gas. A review of marine CDP seismic data at and near the site confirms that the location is sufficiently off structure to minimize the probability of hydrocarbon entrapment.

KSSD No. 2 Well Site

The bottom is nearly flat. Some gentle undulations occur with a relief of 5 to 8 feet over distances of several thousand feet. Sidescan sonar shows patchy (probably slaty) outcrops on the highs and smooth (probably sandy) sediment in the lows. There are no indications of slumping, faulting, or seeps. Site-specific data is inadequate to define the lower limit of unconsolidated overburden. Regional data suggest that the material from the surface to approximately 200 feet is probably quite hard, although bottom sampling recovered largely sand-sized unconsolidated material from a 10 to 25-foot thick unconsolidated sediment veneer. There are no indications of faulting or closure. Regional reflectors across Portlock Bank at approximately 50 and 100 milliseconds are locally attenuated in patches in and around the KSSD No. 2 well site. Although this attenuation may be due to depositional features, such as a local gravel bar or boulder field, the presence of gas could cause a similar acoustic response. The feature is not mappable across the survey area largely because of the noisy outgoing pulse on the sparker. No seeps occur in the area even where these reflectors are broken by faults. A local-amplitude anomaly (200 feet below mud line) at the proposed location may represent shallow gas and/or local porosity development in a beach sand or barrier bar. The latter seems more likely in the absence of other indicators of gas and the

lack of structural closure. Relocation of the site approximately 656 feet to the southwest was proposed to mitigate this possible problem.

KSSD No. 2A Well Site

The location is on the slope from Portlock Bank into Amatuli Trough. The angle of slope ranges from 1.5° to 2.2° at the edge of the bank, to 0.5° at the well location, and 0.2° farther downslope. The seafloor is generally smooth from the upper slope down to the well location, where the seafloor then becomes hummocky downslope. Possible slump deposits are present at the well location and farther downslope. The hummocky seafloor does not appear to be covered by current-generated features. It is possible that slumps originate at the bank edge and flow down the higher-angle slope until they reach the lower-angle slope where they lose momentum and settle. There is at least 10 to 15 milliseconds (25 to 40 feet) of overburden displayed on the profiler, although the regional data show up to 80 milliseconds (200 feet) of possible overburden present in the area. There are no indications of faulting, closure, seeps, or shallow gas. The possible slump features may actually be longitudinal current indicators, but in any case represent no hazard to drilling operations conducted from a floating platform.

KSSD No. 3 Well Site

The well site is essentially flat, with surface undulations having 16 feet of relief within 1.2 miles of the location. The maximum local slope is 1 percent. Sand waves with a wave length of approximately 3 feet are present in irregular patches. There are no indications of slumping or faulting. The sediment thickness varies between 164 and 328 feet, with the thickest areas over buried channels. The proposed well site does not overlie a channel. Faulting was not observed within 0.6 miles of the location, although probable small faults lie northeast, west, and south of the location. A small closure exists 0.7 miles southeast of the location. No evidence of shallow gas is present in the site-specific survey data, but regional data indicate possible shallow gas in the vicinity. Water-column anomalies were observed. These anomalies were probably fish, although there is some possibility that they are gas. No potential hazards were observed at the proposed location, although channel features east and west of the location could provide opportunities for gas entrapment should porosity barriers exist.

BIOLOGICAL SURVEY

An oceanographic and marine biological survey associated with the four KSSD well locations was conducted during April and May of 1977. The bottom sediments collected consisted largely of silty sands containing scattered pebbles and shell debris. Copepods and euphausiids (shrimp-like crustaceans) were the two most abundant zooplankton. Crab larvae collected included Dungeness, Tanner, King, and an unknown species, probably an oregoniid. The three most abundant families of larval fishes were stichaeids (prickleback),

pleuronectids (sole), and macrourids (natfish). Grab sampling averaged 16 species per grab sample and 1,095 individuals per square mile. Polychaetes (bristle worms) were the most common group (90 species that represented 64 percent of the organisms collected). The polychaete Myriochele heeri comprised 33 percent of all invertebrates. Mollusks accounted for 55 species that made up 14 percent of all the organisms collected. Two commercially important invertebrates collected by trawling were pink shrimp (Pandalus borealis) and Tanner crabs (Chionoectes bairdi). A total of 593 fish representing 14 species was collected. The three most abundant flatfish included the flathead sole (Hippoglossoides elassodon), Pacific halibut (Hippoglossus stenolepis), and the rex sole (Glyptocephalus zachirus). The two most abundant roundfish were the walleye pollock (Theragra chalcogramma) and the northern rockfish (Sebastes polyspinus). Gravid (pregnant) females of three species were collected: flathead sole, rex sole, and northern rockfish.

The sooty shearwater (Puffinus griseus) was the most abundant of the 13 bird species observed. Dolphins, fur seals, and sea lions were also observed in the study areas. Television monitoring and bottom photography indicated that the dominant epibenthic organism was a sea pen (?Virgularia).

REGULATORY COMPLIANCE

KSST Wells

ESCI submitted an Oil-Spill-Contingency Plan (OSCP) that included reporting procedures, water-pollution control, the pollution-control materials on hand within the oil industry and commercially available, marine equipment available, air-transportation capabilities, and communication capabilities within the industry. The G&G permit application was conditionally approved May 27, 1976. On June 29, 1976, the USGS, BLM, and FWS representatives met to discuss the preliminary results of the site-specific biological surveys. No objections were raised or recommendations made to amend the proposal. No additional environmental protection measures were attached in approving APD's submitted subsequent to the G&G Permit approval.

KSSD Wells

An Emergency Response Organization and OSCP was submitted on April 1, 1977. The plan included an organizational chart for Sun Oil Company, job descriptions for the Emergency Response Organization, Oil-Spill-Alert Procedures, a directory of Federal, State, and company agencies, and a description of oil-spill containment and cleanup equipment available onsite and at onshore support locations. The G&G application was conditionally approved on May 24, 1977. No additional environmental protection measures were attached in approving the APD subsequent to the G&G Permit approval. The EA's, amendments, and supporting documents are available for review in the

public file at Minerals Management Service, Alaska OCS Region,
Library, Room 502, 949 East 36th Avenue, Anchorage, Alaska 99508.

REFERENCES

- Allison, B. C., 1976, Late Oligocene through Pleistocene molluscan faunas in the Gulf of Alaska region, *in* Saito, T., and Ujiie, H., (eds.), Proceedings of the First International Congress on Pacific Neogene Stratigraphy: International Union of Geological Sciences, Commission on Stratigraphy, Regional Committee on Pacific Neogene Stratigraphy, Science Council of Japan, Geological Society of Japan, p. 313-316.
- Anderson, Warren, and Associates, 1977a, 1977 Kodiak stratigraphic program, Corehole No. 1, Kodiak Shelf, Gulf of Alaska: San Diego, 64 p.
- Anderson, Warren, and Associates, 1977b, 1977 Kodiak stratigraphic program, Corehole No. 2, Kodiak Shelf, Gulf of Alaska: San Diego, 97 p.
- Anderson, Warren, and Associates, 1977c, 1977 Kodiak stratigraphic program, Corehole No. 3, Kodiak Shelf, Gulf of Alaska: San Diego, 90 p.
- Arctic Environmental Information and Data Center and Institute of Social, Economic, Government Research, University of Alaska, 1974, The western Gulf of Alaska, a summary of available knowledge: Marine Minerals Division, Bureau of Land Management, U.S. Department of the Interior, Washington, D.C., 559 p.
- Armentrout, J. M., and Anderson, G. A., 1980, Hydrocarbon potential of the Sitkalidak Formation, Eocene submarine fan complex, Kodiak Island Archipelago, Alaska: AAPG Bulletin (Association Round Table), v. 64, p. 671.
- Asquith, G. E., and Gibson, C. G., 1982, Basic well log analysis for geologists: American Association of Petroleum Geologists, Tulsa, 216 p.
- Aubouin, J., von Huene, R. E., and others, 1982, Leg 84 of the Deep Sea Drilling Project, subduction without accretion, Middle America Trench off Guatemala: Nature, v. 297, p. 458-460.

- Bandy, O. L., 1960, The geologic significance of coiling ratios in the foraminifer Globigerina pachyderma (Ehrenberg): Journal of Paleontology, v. 34, no. 4, p. 671-681.
- Bandy, O. L., Frerichs, W. E., and Vincent, E., 1969, Origin, development, and geologic significance of Neogloboquadrina Bandy, Frerichs and Vincent, Gen. Nov.: Contributions from the Cushman Foundation for Foraminiferal Research, v. 18, Part 4, October 1967, p. 152-157.
- Barker, C., 1972, Aquathermal pressuring, role of temperature in development of abnormal pressure zones: AAPG Bulletin, v. 56, no. 10, p. 2068-2071.
- Barnes, F. F., 1962, Geologic map of lower Matanuska Valley, Alaska: U.S. Geological Survey Miscellaneous Geological Investigations Map I-359, three oversized sheets, scale 1:63,360.
- Barnes, F. F., and Payne, T. G., 1956, Wishbone Hill district, Matanuska Coal field, Alaska: U.S. Geological Survey Bulletin 1016, 88 p.
- Barron, J. A., 1980, Lower Miocene to Quaternary diatom biostratigraphy of Leg 57, off northeastern Japan, Deep Sea Drilling Project, in Initial Reports of the Deep Sea Drilling Project, Volume 56, 57, part 2: Washington, D. C., (National Science Foundation), 1,417 p., p. 641-685.
- Barron, J. A., 1985, Miocene to Holocene planktic diatoms, in Bolli, H. M., Saunders, J. B., and Perch-Nielsen, K., (eds.), Plankton Stratigraphy: Cambridge University Press, 1032 p., p. 763-809.
- Bayliss, G. S., 1977, Hydrocarbon source facies analysis Sunmark 1977 Kodiak shelf program stratigraphic test wells no. 1 and 2 (KSSD-1 and KSSD-2): Houston, Texas, GeoChem Laboratories, Inc., 76 p. [prepared for Sunmark Exploration Co. of Houston].
- Bayliss, G. S., and Smith, M. R., 1980, Source rock evaluation reference manual: Houston, Texas, GeoChem Laboratories, 80 p.
- Berg, H. C., Jones, D. L., and Richter, D. H., 1972, Gravina-Nutzotin belt - tectonic significance of an upper Mesozoic sedimentary and volcanic sequence in southern and southeastern Alaska, in Geological Survey Research 1972, U.S. Geological Survey Professional Paper 800-D, p. D1-D24.
- Berg, R. R., and Habeck, M. F., 1982, Abnormal pressures in the lower Vicksburg McAllen Ranch Field, south Texas: Gulf Coast Association of Geological Societies Transactions, v. 32, p. 247-253.

- Blondeau, W. A., and Brabb, E. E., 1983, Large foraminifers of Eocene age from the coast ranges of California, *in* E. E. Brabb, (ed.), *Studies in Tertiary Stratigraphy of the California Coast Ranges: U.S. Geological Survey Professional Paper 1213*, 93 p., p. 41-48.
- Boersma, A., 1978, Foraminifera, *in* Haq, B. U., and Boersma, A., (eds.), *Introduction to Marine Micropaleontology: Elsevier*, 376 p., p. 19-77.
- Bray, E. E., and Evans, E. D., 1961, Distribution of n-paraffins as a clue to recognition of source beds: *Geochimica et Cosmochimica Acta*, v. 22, p. 2-15.
- Bray, E. E., and Evans, E. D., 1965, Hydrocarbons in non-reservoir-rock source beds: *AAPG Bulletin*, v. 49, no. 3, p. 248-257.
- Bray, C. J., and Karig, D. E., 1985, Porosity of sediments in accretionary prisms and some implications for dewatering processes: *Journal of Geophysical Research*, v. 90, p. 768-778.
- Brockway, R., Alexander, B., Day, P., Lyle, W., Hiles, R., Decker, W., Polski, W., and Reed, B., 1975, Bristol Bay region, stratigraphic correlation section, southwest Alaska: *Alaska Geological Society*, Anchorage, 1 oversized sheet.
- Bruce, C. H., 1984, Smectite dehydration--its relation to structural development and hydrocarbon accumulation in northern Gulf of Mexico Basin: *AAPG Bulletin*, v. 68, no. 6, p. 673-683.
- Bruhn, R. L., and Pavlis, T. L., 1981, Late Cenozoic deformation in the Matanuska Valley, Alaska: three-dimensional strain in a forearc region: *Geological Society of America Bulletin*, Part 1, v. 92, no. 5, p. 282-293.
- Bujak, J., 1984, Cenozoic dinoflagellate cysts and acritarchs from the Bering Sea and western North Pacific, Leg 19: *Micropaleontology*, v. 30, no. 2, p. 180-212.
- Bujak Davies Group, 1987, Palynological subdivision and correlation of six subsurface sections, Gulf of Alaska: Calgary, Alberta, 45 p. [A report prepared for the Minerals Management Service].
- Bukry, D., 1973, Low-latitude coccolith biostratigraphic zonation, *in* Edgar, N. T., Saunders, J. B., and others, *Initial Reports of the Deep Sea Drilling Project, Volume 15: Washington, (U.S. Government Printing Office)*, 1,137 p., p. 685-703.

- Bukry, D., 1975, Coccolith and silicoflagellate stratigraphy, northwestern Pacific Ocean, Deep Sea Drilling Project, Leg 32, in Larson, R. L., Moberly, R., and others, Initial Reports of the Deep Sea Drilling Project, Volume 32: Washington (U. S. Government Printing Office), 980 p., p. 677-702.
- Burk, C. A., 1965, Geology of the Alaska Peninsula - Island Arc and Continental Margin: Geological Society of America Memoir 99, 250 p.
- Burst, J. F., 1969, Diagenesis of Gulf Coast clayey sediments and its possible relation to petroleum migration: AAPG Bulletin, v. 53, no. 1, p. 73-93.
- Byrne, T., 1986, Eocene underplating along the Kodiak shelf, Alaska: implications and regional correlations: Tectonics, v. 5, no. 3, p. 403-421.
- Carlisle, C. T., 1976a, 1976 Kodiak shelf core hole program, core hole no. 1, geochemical data report (KSST-1): Houston, Texas, Geochemical Laboratories, Inc., 30 p. [Prepared for a consortium whose membership is unspecified].
- Carlisle, C. T., 1976b, 1976 Kodiak shelf core hole program, core hole no. 2, geochemical data report (KSST-2): Houston, Texas, GeoChem Laboratories, Inc., 28 p. [Prepared for a consortium whose membership is unspecified].
- Carlisle, C. T., 1976c, 1976 Kodiak shelf core hole program, core hole no. 4A, geochemical data report (KSST-4A): Houston, Texas, GeoChem Laboratories, Inc., 16 p. [Prepared for a consortium whose membership is unspecified].
- Cernock, P. J., 1977, Hydrocarbon source rock evaluation study Kodiak shelf strat test no. 3, Gulf of Alaska (KSSD-3): Houston, Texas, GeoChem Laboratories, Inc., 48 p. [Prepared for Sunmark Exploration Co., Dallas].
- Chase, C. G., 1978, Plate kinematics: the Americas, East Africa, and the rest of the world: Earth and Planetary Science Letters, v. 37, p. 355-368.
- Clark, S. H. B., 1972, Reconnaissance bedrock geologic map of the Chugach Mountains near Anchorage, Alaska: U.S. Geological Survey Miscellaneous Geological Investigations Map MF-350, 1 sheet, scale 1:250,000.
- Clark, S. H. B., 1973, The McHugh Complex of south-central Alaska: U.S. Geological Survey Bulletin 1372-D, p. D1-D11.
- Cloos, M., 1984, Landward-dipping reflectors in accretionary wedges: active dewatering conduits? Geology, v. 12, p. 519-522.

- Comer, C. D., Herman, B. M., and Zerwick, S. A., 1987, Geologic report for the St. George Basin Planning Area, Bering Sea, Alaska: U.S. Minerals Management Service OCS Report MMS 87-0030, 84 p.
- Coney, P. J., Jones, D. L., and Monger, J. W. H., 1980, Cordilleran suspect terranes: *Nature*, v. 288, p. 329-333.
- Connelly, W., 1978, Uyak complex, Kodiak Islands, Alaska: A Cretaceous subduction complex: *Geological Society of America Bulletin*, v. 89, no. 5, p. 755-769.
- Core Laboratories Inc., 1976a, Core analysis report for Exploration Services Co., KSST No. 1 stratigraphic test, Kodiak Shelf, Alaska: Dallas.
- Core Laboratories Inc., 1976b, Core analysis report for Exploration Services Co., KSST No. 2 stratigraphic test, Kodiak Shelf, Alaska: Dallas.
- Core Laboratories, Inc., 1977a, Special core analysis study for Sunmark Exploration Co., KSSD No. 1 well, Kodiak Island, Alaska: Dallas, 48 p.
- Core Laboratories Inc., 1977b, Special core analysis study for Sunmark Exploration Co., KSSD No. 2 stratigraphic test, Kodiak Shelf, Alaska: Dallas, 18 p.
- Core Laboratories Inc., 1978, Special core analysis study for Sunmark Exploration Co., KSSD No. 3 stratigraphic test, Kodiak Shelf, Alaska: Dallas, 33 p.
- Crouch, R. W., and Poag, C. W., 1979, Amphistegina gibbosa d'Orbigny from the California borderlands: the Caribbean connection: *Journal of Foraminiferal Research*, v. 9, no. 2, p. 85-106.
- Cuffey, R. J., and Turner, R. F., 1987, Modern Bryozoans on the Kodiak Shelf, Southern Alaska: in Ross, J. R. P., (ed.), *Bryozoa: Present and Past*: Western Washington University, Bellingham, 333 p.
- Cushman, J. A., and Hanna, M. A., 1927, Foraminifera from the Eocene near San Diego, California: *San Diego Society Natural History Transactions*, v. 5, p. 45-64.
- Cushman, J. A., and McMasters, J. H., 1936, Middle Eocene foraminifera from the Llajas Formation, Ventura County, California: *Journal of Paleontology*, v. 10, no. 6, p. 497-517.
- Dahlstrom, C. D. A., 1970, Structural geology in the eastern margin of the Canadian Rocky Mountains: *Bulletin of Canadian Petroleum Geology*, v. 18, no. 3, p. 332-406.

- Davies, E. H., 1985, The Anemiacean, Schizaeacean and related spores: An index to genera and species: Dartmouth, Canada, Bedford Institute of Oceanography, Canadian Technical Report of Hydrography and Ocean Studies No. 67, 217 p.
- Davies, J., Sykes, L., House, L., and Jacob, K., 1981, Shumagin seismic gap, Alaska Peninsula: History of great earthquakes, tectonic setting, and evidence for high seismic potential: *Journal of Geophysical Research*, v. 86, no. B5, p. 3821-3855.
- Davis, D. M., and von Huene, R., 1987, Inferences on sediment strength and fault friction from structures at the Aleutian trench: *Geology*, v. 15, p. 517-522.
- DeLong, S. E., Fox, P. J., and McDowell, F. W., 1978, Subduction of the Kula ridge at the Aleutian Trench: *Geological Society of America Bulletin*, v. 89, no. 1, p. 83-95.
- DeLong, S. E., Fox, P. J., and McDowell, F. W., 1980, Subduction of the Kula Ridge at the Aleutian Trench: Reply to the Discussion by Farrar, E., and Dixon, J. M.: *Geological Society of America Bulletin*, v. 90, no. 7, p. 700-702.
- DeLong, S. E., and McDowell, F. W., 1975, K-Ar ages from the Near Islands, western Aleutian Islands, Alaska: Indication of a mid-Oligocene thermal event: *Geology*, v. 3, no. 12, p. 691-694.
- Detterman, R. L., 1986, Glaciation of the Alaska Peninsula, *in* Hamilton, T. D., Reed, K. M., and Thorson, R. M., (eds.), *Glaciation in Alaska, the Geologic Record*: Alaska Geological Society, Anchorage, 265 p., p. 151-170.
- Dickinson, W. R., and Suczak, C. A., 1979, Plate tectonics and sandstone compositions: *AAPG Bulletin*, v. 63, no. 12, p. 2164-2182.
- Dix, C. H., 1955, Seismic velocities from surface measurements: *Geophysics*, v. 20, p. 68-86.
- Dresser Atlas, 1979, Log interpretation charts: Houston, Dresser Industries, Inc., 107 p.
- Ericson, D. B., 1959, Coiling direction of *Globigerina pachyderma* as a climatic index: *Science*, v. 130, July 24, p. 219-220.
- Evitt, W. R., 1973, Dinoflagellates from Leg 19, Sites 183 and 192, Deep Sea Drilling Project, *in* Creager, J. S., Scholl, D. W., and others, *Initial Reports of the Deep Sea Drilling Project, Volume 19*: Washington (U. S. Government Printing Office), 913 p., p. 737-738.
- Fertl, W. H., and Wichmann, P. A., 1977, How to determine static BHT from well log data: *World Oil*, v. 184, p. 105-106.

- Fisher, M. A., 1980, Petroleum geology of the Kodiak Shelf, Alaska: AAPG Bulletin, v. 64, no. 8, p. 1140-1157.
- Fisher, M. A., Bruns, T. R., and von Huene, R., 1981, Transverse tectonic boundaries near Kodiak Island, Alaska: Geological Society of America Bulletin, Part 1, v. 92, no. 1, p. 10-18.
- Fisher, M. A., and Holmes, M. L., 1980, Large-scale structure of deep strata beneath Kodiak shelf, Alaska: Geological Society of America Bulletin, Part 1, v. 91, no. 4, p. 218-224.
- Fisher, M. A., and Magoon, L. B., 1978, Framework geology of Lower Cook Inlet, Alaska: AAPG Bulletin, v. 62, no. 3, p. 373-402.
- Fisher, M. A., and von Huene, R., 1980, Structure of upper Cenozoic strata beneath Kodiak shelf, Alaska: AAPG Bulletin, v. 64, no. 7, p. 1014-1033.
- Fisher, M. A., von Huene, R., and Hampton, M. A., 1984, Summary geologic report for petroleum Lease Sale No. 100, Kodiak shelf, Alaska: U.S. Geological Survey Open-File Report 84-24, 46 p.
- Fisher, M. A., von Huene, R. E., and Smith, G. L., 1987, Reflections from midcrustal rocks within the Mesozoic subduction complex near the eastern Aleutian trench: Journal of Geophysical Research, v. 92, no. B8, p. 7907-7915.
- Fisher, M. A., von Huene, R. E., Smith, G. L., and Bruns, T. R., 1983, Possible seismic reflections from the downgoing Pacific plate, 275 kilometers arcward from the eastern Aleutian trench: Journal of Geophysical Research, v. 88, no. B7, p. 5835-5849.
- Foreman, H. P., 1975, Radiolaria from the North Pacific, Deep Sea Drilling Project, Leg 32, *in* Larson, R. L., Moberly, R., and others, Initial Reports of the Deep Sea Drilling Project, Volume 32: Washington (U. S. Government Printing Office), 980 p., p. 579-676.
- Gates, O., and Gibson, W., 1956, Interpretation of the configuration of the Aleutian ridge: Geological Society of America Bulletin, v. 67, no. 2, p. 127-146.
- GeoChem Laboratories, Inc. For reports published by GeoChem, see Bayliss, 1977; Carlisle, 1976a, b, c; and Cernock, 1977.
- Goetz, J. F., Prins, W. J., and Logar, J. F., 1977, Reservoir delineation by wireline techniques: paper presented at the Sixth Annual Convention of the Indonesian Petroleum Association, Jakarta, *in* Dipmeter Interpretation Seminar, Anchorage, Alaska, Oct. 2, 1985, Schlumberger, Inc.

- Grow, J. A., and Atwater, T., 1970, Mid-Tertiary tectonic transition in the Aleutian arc: Geological Society of America Bulletin, v. 81, no. 12, p. 3715-3722.
- Ham, H. H., 1966, New charts help estimate formation pressure: Oil and Gas Journal, v. 64, p. 58-63.
- Hampton, M. A., 1983, Geotechnical framework study of the Kodiak Shelf, Alaska: U.S. Geological Survey Open-File Report 83-171, 86 p.
- Hampton, M. A., and Bouma, A. H., 1977, Slope instability near the shelf break, western Gulf of Alaska: Marine Geotechnology, v. 1, p. 309-331.
- Hampton, M. A., Bouma, A. H., Pulpan, H., and von Huene, R. E., 1979, Geoenvironmental potential assessment of the Kodiak Shelf, western Gulf of Alaska: Proceedings 11th Offshore Technology Conference, Houston Texas, v. I, p. 365-376.
- Hampton, M. A., and Kvenvolden, K. A., 1981, Geology and geochemistry of gas-charged sediment on Kodiak shelf, Alaska: Geo-Marine Letters, v. 1, p. 141-147.
- Haq, B. U., 1980, Biogeographic history of Miocene calcareous nannoplankton and paleoceanography of the Atlantic Ocean: Micropaleontology, v. 26, p. 414-432, *in* Haq, B. U., (ed.), 1983, Benchmark papers in geology, v. 79, Calcareous nannoplankton: Stroudsburg, Pa., Hutchinson Ross, 338 p., p. 207-227.
- Hein, J. R., McLean, H., and Vallier, T., 1984, Reconnaissance Geology of Southern Atka Island, Aleutian Islands, Alaska: U.S. Geological Survey Bulletin 1609, Washington, 69 p.
- Helby, R. J., Kidson, E. J., Stover, L. E., Williams, G. L., and Hart, G. F., 1984, Survey of dinoflagellate biostratigraphy, short course notes, Sept. 17-21, at Louisiana State University, Baton Rouge, Louisiana, HARTAX.
- Holmes, M. L., Meeder, C. A., and Creager, K. C., 1978, Sonobuoy refraction data near Kodiak, Alaska: U.S. Geological Survey Open-File Report 78-368.
- Hoose, P. J., 1987, Wrench-fault tectonics: S.E. Bering Sea shelf: EOS, v. 68, no. 16, p.423.
- Hoose, P. J., Horowitz, W. L., and Sherwood K. W., 1984, Geological report for the Kodiak OCS Planning Area, Kodiak Shelf, Alaska: U.S. Minerals Management Service unpublished OCS report, 67 p.
- Hottmann, C. E., and Johnson, R. K., 1965, Estimation of formation pressures from log-derived shale properties: Journal of Petroleum Technology, v. 17, no. 6, p. 717-722.

- Hottmann, C. E., Smith, J. H., and Purcell, W. R., 1979, Relationship among earth stresses, pore pressure, and drilling problems offshore Gulf of Alaska: *Journal of Petroleum Technology*, v. 31, p. 1477-1484.
- House, L. S., Sykes, L. R., Davies, J. N., and Jacob, K. H., 1981, Identification of a possible seismic gap near Unalaska Island, eastern Aleutians, Alaska: *in* Simpson, D. W., and Richards, P. G., (eds.), *Earthquake Prediction, an International Review*: American Geophysical Union, Washington, D.C., p. 81-92.
- Hubbert, M. K., and Rubey, W. W., 1959, Role of fluid pressure in mechanics of overthrust faulting: *Geological Society of America Bulletin*, v. 70, p. 115-166.
- Hunt, J. M., 1979, *Petroleum geochemistry and geology*: San Francisco, California, W. H. Freeman, 614 p.
- Ingle, J. C., Jr., 1967, Foraminiferal biofacies variation and the Miocene-Pliocene boundary in southern California: *Bulletin of American Paleontology*, v. 52, no. 236, 394 p.
- Jarrard, R. D., 1986, Terrane motion by strike-slip faulting of forearc slivers: *Geology*, v. 14, no. 9, p. 780-783.
- Jones, D. L., Blake, M. C., Jr., Bailey, E. H., and McLaughlin, R. J., 1978, Distribution and character of upper Mesozoic subduction complexes along the west coast of North America: *Tectonophysics*, v. 47, no. 2, p. 207-222.
- Jones, D. L., and Silberling, N. J., 1979, Mesozoic stratigraphy - the key to tectonic analysis of southern and central Alaska: U.S. Geological Survey Open-File Report 79-1200, 41 p.
- Jones, D. L., Silberling, N. J., Berg, H. C., and Plafker, G., 1981, Map showing tectonostratigraphic terranes of Alaska, columnar sections, and summary descriptions of terranes: U.S. Geological Survey Open-File Report 81-792, 20 p. and 2 oversized sheets, scale 1:250,000.
- Jordan, J. R., and Shirley, O. J., 1966, Application of drilling performance data to overpressure detection: *Journal of Petroleum Technology*, v. 18, p. 1387-1394.
- Karlstrom, T. N. V., 1964, Quaternary Geology of the Kenai Lowland and glacial history of the Cook Inlet region, Alaska: U.S. Geological Survey Professional Paper 443, Washington, 69 p.
- Karlstrom, T. N. V., and Ball, G. E., 1969, The Kodiak Island refugium: Its geology, flora, fauna, and history: The Boreal Institute of Alberta, Ryerson Press, 262 p.

- Keller, G., von Huene, R., McDougall, K., and Bruns, T. R., 1984, Paleoclimatic evidence for Cenozoic migration of Alaskan terranes: *Tectonics*, v. 3, no. 4, p. 473-495.
- Kennett, J. P., and Srinivasan, M. S., 1983, Neogene planktonic foraminifera: A phylogenetic atlas: Stroudsburg, Pa., Hutchinson Ross, 265 p.
- King, P. B., 1969, Tectonic map of North America: U.S. Geological Survey, scale 1:5,000,000, 2 oversized sheets.
- Kirschner, C. E., and Lyon, C. A., 1973, Stratigraphic and tectonic development of Cook Inlet petroleum province, *in* Pitcher, M. G., (ed.), *Arctic Geology*, American Association of Petroleum Geologists Memoir 19, p. 396-407.
- Kluge, G. A., 1962, Bryozoa of the northern seas of the USSR, No. 76: Akademiya Nauk, SSR, Moscow [translated from the Russian in 1975 for the Smithsonian Institution and National Science Foundation, Washington, D. C. by B. R. Sharma], Amerind Publishing, No. TT-72-SZ010, New Delhi, 712 p.
- Kulm, L. D., von Huene, R. E., and others, 1973, Initial Reports of the Deep Sea Drilling Project, v. 18, Washington, (U.S. Government Printing Office), p. 297-513.
- Lagoë, M. B., 1978, Foraminifera from the uppermost Poul Creek and lowermost Yakataga Formations, Yakataga District, Alaska; *in* Ikebe, N., (ed.), *Correlation of tropical through high latitude marine Neogene deposits of the Pacific Basin: International Correlation Programme, Project 114; Biostratigraphic Datum-planes of the Pacific Neogene, Third Working Group Meeting, Sponsored by the International Union of Geological Sciences; Stanford University Publication, Geol. Sci.*, 14, p. 34-35.
- Lagoë, M. B., 1983, Oligocene through Pliocene foraminifera from the Yakataga Reef section, Gulf of Alaska Tertiary Province, Alaska: *Micropaleontology*, v. 29, no. 2, p. 202-222.
- Larsen, A. R., 1976, Studies of recent Amphistegina: Taxonomy and some aspects: *Israel Journal of Earth Sciences*, v. 25, p. 1-26.
- Larsen, A. R., 1978, Phylogenetic and paleobiogeographical trends in the foraminiferal genus Amphistegina: *Revista Espanola de Micropaleontologia*, v. 10, no. 2, p. 217-243.
- Lentin, J. K., and Williams, G. L., 1985, Fossil Dinoflagellates: Index to Genera and Species, 1985 Edition, Bedford Institute of Oceanography, Canadian Technical Report of Hydrography and Ocean Sciences No. 60: Dartmouth, Canada, 451 p.

- Loney, R. A., Brew, D. A., Muffler, L. J. P., and Pomeroy, J. S., 1975, Reconnaissance geology of Chichagof, Baranof, and Kruzof Islands, southeastern Alaska: U.S. Geological Survey Professional Paper 792, 105 p.
- Lopatin, N. V., 1971, Temperature and geologic time as factors in coalification (in Russian): *Izvestiya Akademii Nauk USSR, Seriya Geologicheskaya*, No. 3, p. 95-106.
- MacGregor, J. R., 1965, Quantitative determination of reservoir pressures from conductivity log: *AAPG Bulletin*, v. 49, no. 9, p. 1502-1511.
- Malloy, R. J., and Merrill, G. F., 1972, Vertical crustal movement on the sea floor, in *The Great Alaska Earthquake of 1964, Oceanography and Coastal Engineering: National Research Council, National Academy of Sciences, Washington, D.C.*, p. 252-265.
- Martin, G. C., 1921, Preliminary report on petroleum in Alaska: U.S. Geological Survey Bulletin 719, 85 p.
- McCann, W. R., Perez, O. J., and Sykes, L. R., 1980, Yakataga gap, Alaska: seismic history and earthquake potential: *Science*, v. 207, p. 1309-1314.
- McClellan, P. H., Arnal, R. E., Barron, J. A., von Huene, R. E., Fisher, M. A., and Moore, G. W., 1980, Biostratigraphic results of dart-coring in the western Gulf of Alaska, and their tectonic implications: U.S. Geological Survey Open-File Report 80-63.
- McClure, L. J., 1977, Drill abnormal pressure safely, a short course manual by L. J. McClure: Houston, Texas, 114 p.
- McIntyre, A., 1967, Coccoliths as paleoclimatic indicators of Pleistocene glaciation: originally published in *Science*, v. 158, p. 1314-1317; reprinted in Haq, B. U., (ed.), 1983, *Benchmark papers in geology*, v. 79, Nannofossil biostratigraphy, Stroudsburg, Pa., Hutchinson Ross, 338 p., p. 186-189.
- McLean, H., Hein, J. R., and Vallier, T. L., 1983, Reconnaissance geology of Amlia Island, Aleutian Islands, Alaska: *Geological Society of America Bulletin*, v. 94, no. 8, p. 1020-1027.
- Miller, D. J., Payne, T. G., and Gryc, G., 1959, Geology of possible petroleum provinces in Alaska with an annotated bibliography by Edward J. Cobb: U.S. Geological Survey Bulletin 1049, 131 p.
- Minster, J. B., and Jordan, T. H., 1978, Present-day plate motions: *Journal of Geophysical Research*, v. 83, p. 5331-5354.

- Mitchell, J. M., 1958, The weather and climate of Alaska: Weatherwise, v. 11, p. 151-160.
- Molnia, B. F., 1979, Glacially derived sediments in the northern Gulf of Alaska - geology and engineering characteristics: Proceedings 11th Offshore Technology Conference, Houston, Texas, v. I, p. 647-655.
- Moore, G. W., 1969, New formations on Kodiak and adjacent islands, Alaska: U.S. Geological Survey Bulletin 1274-A, p. A27-35.
- Moore, J. C., 1972, Uplifted trench sediments: Southwestern Alaska-Bering Sea edge: Science, v. 175, p. 1103-1105.
- Moore, J. C., 1974, Geologic and structural map of part of the outer Shumagin Islands, southwestern Alaska: U.S. Geological Survey Miscellaneous Investigations Series Map I-815, 1 sheet, scale 1:63,360.
- Moore, J. C., and Allwardt, A., 1980, Progressive deformation of a Tertiary trench slope, Kodiak Islands, Alaska: Journal of Geophysical Research, v. 85, no. B9, p. 4741-4756.
- Moore, J. C., Biju-Duval, B., and others, 1982, Offscraping and underthrusting of sediment at the deformation front of the Barbados Ridge; Deep Sea Drilling Project Leg 78A: Geological Society of America Bulletin, v. 93, p. 1065-1077.
- Moore, J. C., Byrne, T., Plumley, P. W., Reid, M., Gibbons, H., and Coe, R. S., 1983, Paleogene evolution of the Kodiak Islands, Alaska: consequences of ridge-trench interaction in a more southerly latitude: Tectonics, v. 2, no. 3, p. 265-293.
- Moore, J. C., and Connelly, W., 1976, Subduction, arc volcanism, and forearc sedimentation during the early Mesozoic, SW Alaska: Geological Society of America Abstracts with Programs, v. 8, p. 397-398.
- Muench, R. D., and Schumacher, J. D., 1980, Physical oceanographic and meteorological conditions in the northwest Gulf of Alaska: NOAA Technical Memorandum ERL PMEL-22, Pacific Marine Environmental Laboratory, Seattle, Washington, 147 p.
- Nelson, C. H., Kvenvolden, K. A., and Clukey, E. C., 1978, Thermogenic gases in near-surface sediments of Norton Sound, Alaska: Proceedings 10th Offshore Technology Conference, Houston, Texas, v. IV, p. 2623-2633.
- Nelson, C. H., and Nilsen, T. H., 1984, Modern and ancient deep-sea fan sedimentation: Society of Economic Paleontologists and Mineralogists lecture notes for Short Course No. 14, 404 p.

- Nelson, C. H., Thor, D. R., Sandstrom, M. W., and Kvenvolden, K. A., 1979, Modern biogenic gas-generated craters (sea-floor "pockmarks") on the Bering shelf, Alaska: Geological Society of America Bulletin, Part 1, v. 90, no. 12, p. 1144-1152.
- Nilsen, T. H., and Moore, G. W., 1979, Reconnaissance study of Upper Cretaceous to Miocene stratigraphic units and sedimentary facies, Kodiak and adjacent islands, Alaska, with a section on sedimentary petrology by G. R. Winkler: U.S. Geological Survey Professional Paper 1093, 34 p.
- Nishenko, S., and McCann, W., 1979, Large thrust earthquakes and tsunamis: implications for the development of fore arc basins: Journal of Geophysical Research, v. 84, no. B2, p. 573-584.
- Normark, W. R., 1978, Fan valleys, channels, and depositional lobes on modern submarine fans--characters for recognition of sandy turbidite environments: AAPG Bulletin, v. 62, p. 912-931.
- d'Orbigny, A. D., 1852, Paleontologie francaise; description des animaux invertebres; terrain Cretace: Tome 5, Bryozoaires, Mason, Paris, 1192 p.
- Osborn, R. C., 1950, Bryozoa of the Pacific Coast of America; Part 1, Cheilostomata-Anasca: Allan Hancock Pacific Expedition, v. 14, p. 1-269, University of Southern California, Los Angeles, CA.
- Osborn, R. C., 1952, Bryozoa of the Pacific Coast of America; Part 2, Cheilostomata-Ascophora: Allan Hancock Pacific Expedition, v. 14, p. 271-611, University of Southern California, Los Angeles, CA.
- Pennebaker, E. S., Jr., 1968a, An engineering interpretation of seismic data: Society of Petroleum Engineers of AIME, Special Paper no. 2165, 43rd AIME Fall Meeting, Houston, Texas, p. 1-12.
- Pennebaker, E. S., Jr., 1968b, Detection of abnormal-pressure formations from seismic field data: American Petroleum Institute, paper no. 926-13-C, p. 184-191.
- Perch-Nielsen, K., 1985, Cenozoic calcareous nannofossils, in Bolli, H. M., Saunders, J. B., and Perch-Nielsen, K., (eds.), Plankton Stratigraphy: Cambridge University Press, 1032 p., p. 427-554.
- Plafker, G., 1965, Tectonic deformation associated with the 1964 Alaska earthquake: Science, v. 148, p. 1675-1687.
- Plafker, G., 1972, Tectonics, in The Great Alaska Earthquake of 1964, Geology: National Research Council, National Academy of Sciences, Washington, D.C., p. 42-122.

- Plafker, G., (in press), Regional geology and petroleum potential of the northern Gulf of Alaska continental margin, in Scholl, D., Grantz, A., and Bedder, J. G., (eds.), *Geology and Resource Potential of the Continental Margin of Western North America and Adjacent Ocean Basins--Beaufort Sea to Baja California: Circum-Pacific Council for Energy and Mineral Research, Earth Science Series, Houston, Texas.*
- Plafker, G., and Addicott, W. O., 1976, Glaciomarine deposits of Miocene through Holocene age in the Yakataga Formation along the Gulf of Alaska margin: in Miller, T. P., (ed.), *Recent and Ancient Sedimentary Environments in Alaska, Alaska Geological Society, Anchorage, p. Q1-Q23.*
- Plafker, G., Jones, D. L., Hudson, T., and Berg, H. C., 1976, The Border Ranges fault system in the Saint Elias Mountains and Alexander Archipelago: U.S. Geological Survey Circular 722, p. 14-16.
- Plafker, G., Jones, D. L., and Pessagno, E. A., Jr., 1977, A Cretaceous accretionary flysch and melange terrane along the Gulf of Alaska margin, in Blean, K.M., (ed.), *The United States Geological Survey in Alaska: Accomplishments During 1976: U.S. Geological Survey Circular 751-B, p. B41-B43.*
- Plafker, G., and Rubin, M., 1967, Vertical tectonic displacements in southcentral Alaska during and prior to the great 1964 earthquake: *Journal of Geoscience, Osaka City University, p. 53-72.*
- Plumley, P. W., Coe, R. S., Byrne, T., Reid, M. R., and Moore, J. C., 1982, Paleomagnetism of volcanic rocks of the Kodiak Islands indicates northward latitudinal displacement: *Nature, v. 300, no. 5887, p. 50-52.*
- Powell, T. G., and McKirdy, D. M., 1975, The effect of source material, rock type and diagenesis on the n-alkane content of sediments: *Geochimica et Cosmochimica Acta, v. 37, p. 623-633.*
- Pulpan, H., and Frohlich, C., 1985, Geometry of the subducted plate near Kodiak Island and Lower Cook Inlet, Alaska, determined from relocated earthquake hypocenters: *Bulletin of the Seismological Society of America, v. 75, no. 3, p. 791-810.*
- Pulpan, H., and Kienle, F., 1979, Western Gulf of Alaska seismic risk: *Proceedings 11th Offshore Technology Conference, Houston, Texas, v. IV, p. 2209-2218.*
- Rau, W. W., Plafker, G., and Winkler, G. R., 1983, Foraminiferal biostratigraphy and correlations in the Gulf of Alaska Tertiary province: U.S. Geological Survey Oil and Gas Investigations Chart OC-120, 11 p., 3 plates.

- Reed, B. L., and Lanphere, M. A., 1973, Alaska-Aleutian Range batholith: geochronology, chemistry, and relation to circum-Pacific plutonism: Geological Society of America Bulletin, v. 84, no. 8, p. 2583-2610.
- Reznikof, A. N., 1967, The geochemical conversion of oils and condensates in the zone of catagenesis: Geologi a Neftin i Gaza, no. 5: pp. 24-28.
- Ritger, S., Carson, B., and Suess, E., 1987, Methane-derived authigenic carbonates formed by subduction-induced pore-water expulsion along the Oregon/Washington margin: Geological Society of America Bulletin, v. 98, p. 147-156.
- Robinson, G. S., 1970, Change of the bathymetric distribution of the genus Cyclammina: Transactions of the Gulf Coast Association of Geological Societies, v. 20, p. 201-209.
- Ronov, A. B., 1958, Organic carbon in sedimentary rocks (in relation to presence of petroleum): translation in Geochemistry, no. 5, p. 510-536.
- Rouse, G. E., 1977, Paleogene palynomorph ranges in western and northern Canada, in Elsik, W. C., (ed.), Contributions of Stratigraphic Palynology (with emphasis on North America), v. 1, Cenozoic palynology, American Association of Stratigraphic Palynologists Contribution Series no. 5A, 166 p., p. 48-65.
- Sanfilippo, A., and Riedel, W. R., 1985, Cretaceous Radiolaria: in Bolli, H. M., Saunders, J. B., and Perch-Nielsen, K., (ed.), Plankton stratigraphy: Cambridge University Press, 1032 p., p. 573-660.
- Sanfilippo, A., Westberg-Smith, M. J., and Riedel, W. R., 1985, Cenozoic Radiolaria: in Bolli, H. M., Saunders, J. B., and Perch-Nielsen, K., (ed.), Plankton stratigraphy: Cambridge University Press, 1032 p., p. 631-712.
- Scholl, D. W., and Creager, J. S., 1973, Geologic synthesis of Leg 19 (DSDP) results; far North Pacific, and Aleutian Ridge, and Bering Sea, in Creager, J. S., Scholl, D. W., and others, Initial Reports of the Deep Sea Drilling Project, Volume 19: Washington (U. S. Government Printing Office), p. 897-913.
- Scholle, P. A., and Spearing, D. R., (ed.), 1982, Sandstone depositional environments: AAPG, Tulsa, 410 p.
- Seely, D. R., 1977, The significance of landward vergence and oblique structural trends on trench inner slopes, in Talwani, M., and Pitman III, W. C., (eds.), Island Arcs, Deep Sea Trenches, and Back Arc Basins: American Geophysical Union, Washington, D.C., p. 187-198.

- Seely, D. R., Vail, P. R., and Walton, G. G., 1974, Trench slope model, in Burk, C. A., and Drake, C. L., (eds.), *Geology of Continental Margins*: Springer Verlag, New York, p. 249-260.
- Selley, R. C., 1978, Concepts and methods of subsurface facies analysis: AAPG Education Course Note Series No. 9, 86 p.
- Selley, R. C., 1979, Dipmeter and log motifs in North Sea submarine-fan sands: AAPG Bulletin v. 63, p. 905-917.
- Sherwood, K. W., 1984, Abnormal formation pressure, in Turner, R. F., (ed.), *Geological and operational summary, Navarin Basin COST No.1 well, Bering Sea, Alaska*: U.S. Minerals Management Service, OCS Report MMS 84-0031, p. 167-192.
- Simkin, T., Siebert, L., McClelland, L., Bridge, D., Newhall, C., and Latter, J. H., 1981, *Volcanoes of the World*: Hutchinson Ross Publishing Co., Stroudsburg, Pennsylvania, 232 p.
- Soffer, Z., 1984, Stable carbon isotope compositions of crude oils: Application to source depositional environments and petroleum alteration: AAPG Bulletin, v. 68, no. 1, p. 31-49.
- Stainforth, R. M., Lamb, J. L., Luterbacher, H., Beard, J. H., and Jeffords, R. M., 1975, Cenozoic planktonic foraminiferal zonation and characteristics of index forms: *University of Kansas Paleontological Contributions, Article 62*: University of Kansas Paleontological Institute, Lawrence, Kansas, 425 p.
- Staplin, F. L., 1969, Sedimentary organic matter, organic metamorphism and oil and gas occurrence: *Canadian Petroleum Geological Bulletin*, v. 17, no. 1, p. 47-66.
- Staplin, F. L., 1982, Determination of thermal alteration index from color of exinite (pollen, spores) in SEPM short course no. 7, How to assess maturation and paleotemperatures: Tulsa, Oklahoma, Society of Economic Paleontologists and Mineralogists, p. 7-11.
- Stevenson, A. J., Scholl, D. W., and Vallier, T. L., 1983, Tectonic and geologic implications of the Zodiac fan, Aleutian Abyssal Plain, northeast Pacific: *Geological Society of America Bulletin*, v. 94, no. 2, p. 259-273.
- Stewart, R. J., 1976, Turbidites of the Aleutian abyssal plain: Mineralogy, provenance, and constraints for Cenozoic motion of the Pacific plate: *Geological Society of America Bulletin*, v. 87, no. 5, p. 793-808.
- Stoneley, R., 1967, The structural development of the Gulf of Alaska sedimentary province in southern Alaska: *Quarterly Journal of the Geological Society of London*, v. 123, p. 25-57.

- Sykes, L. R., 1971, Aftershock zones of great earthquakes, seismicity gaps, earthquake prediction for Alaska and the Aleutians: *Journal of Geophysical Research*, v. 76, no. 32, p. 8021-8041.
- Sykes, L. R., and Ewing, M., 1965, The seismicity of the Caribbean region: *Journal of Geophysical Research*, v. 70, p. 5065-5074.
- Sykes, L. R., Kisslinger, J. B., House, L., Davies, J. N., and Jacob, J. H., 1980, Rupture zones of great earthquakes in the Alaska-Aleutian arc 1784-1980: *Science*, v. 210, p. 1343-1345.
- Thrasher, G. P., 1979, Geologic map of the Kodiak outer continental shelf, western Gulf of Alaska: U.S. Geological Survey Open-File Report 79-1267, 2 oversized sheets, scale 1:250,000.
- Tissot, B. P., and Welte, D. H., 1978 and 1984, Petroleum formation and occurrence, editions 1 and 2: New York, Springer-Verlag, 699 p.
- Todd, R., 1976, Some observations about Amphistegina (foraminifera), in Takayanagi, Y., and Saito, T., (eds.), *Progress in Micropaleontology Special Publication*, Micropaleontology Press: The American Museum of Natural History, New York, p. 382-394.
- Turner, B. W., Thrasher, G. P., Shearer, G. B., and Holden, K. D., 1979, Bathymetric maps of the Kodiak outer continental shelf, western Gulf of Alaska: U.S. Geological Survey Open-File Report 79-263, 13 sheets, scale 1:250,000.
- Turner, R. F., 1976, Paleontology Report: Kodiak Shelf Stratigraphic Test Wells 1, 2, 4A. Exploration Services, Inc., OCS Permit 76-35: Anchorage (U. S. Department of the Interior, Minerals Management Service), 91 p., 2 fig., 3 tables [unpublished report].
- Turner, R. F., 1978, Paleontology Report: Atlantic Richfield Company, Salome Prospect, OCS-Y-0007 No. 1 Well, OCS Permit No. 72-1: Anchorage (U. S. Department of the Interior, Minerals Management Service), 102 p. [unpublished report].
- Turner, R. F., Bolm, J. G., McCarthy, C. M., Steffy, D. A., Lowry, P., and Flett, T. O., 1983a, Geological and operational summary, Norton Sound COST No. 1 well, Norton Sound, Alaska: U.S. Geological Survey Open File Report 83-124: Anchorage (U.S. Department of the Interior, Minerals Management Service), 170 p.

- Turner, R. F., Bolm, J. G., McCarthy, C. M., Steffy, D. A., Lowry, P., Flett, T. O., and Blunt, D., 1983b, Geological and operational summary, Norton Sound COST No. 2 well, Norton Sound, Alaska: U.S. Geological Survey Open-File Report 83-557: Anchorage (U.S. Department of the Interior, Minerals Management Service), 161 p.
- Turner, R. F., McCarthy, C. M., Comer, C. D., Larson, J. A., Bolm, J. G., Banet, A. C., and Adams, A. J., 1984a, Geological and operational summary, St. George Basin COST No. 1 well, Bering Sea, Alaska: OCS Report MMS 84-0016: Anchorage (U.S. Department of the Interior, Minerals Management Service), 109 p.
- Turner, R. F., McCarthy, C. M., Comer, C. D., Larson, J. A., Bolm, J. G., Flett, T. O., and Adams, A. J., 1984b, Geological and operational summary, St. George Basin COST No. 2 well, Bering Sea, Alaska: OCS Report MMS 84-0018: Anchorage (U.S. Department of the Interior, Minerals Management Service), 104 p.
- Turner, R. F., McCarthy, C. M., Steffy, D. A., Lynch, M. B., Martin, G. C., Sherwood, K. W., Flett, T. O., and Adams, A. J., 1984c, Geological and operational summary, Navarin Basin COST No. 1 well, Bering Sea, Alaska: OCS Report MMS 84-0031: Anchorage (U.S. Department of the Interior, Minerals Management Service), 252 p.
- Turner, R. F., Martin, G. M., Flett, T. O., and Steffy, D. A., 1985, Geologic Report for the Navarin Basin planning area, Bering Sea, Alaska: OCS Report MMS 85-0045: Anchorage (U.S. Department of the Interior, Minerals Management Service), 156 p.
- Turner, R. F., Martin, G. C., Risley, D. E., Steffy, D. A., Flett, T. O., and Lynch, M. B., 1986, Geologic Report for the Norton Basin planning area, Bering Sea, Alaska: OCS Report MMS 86-0033: Anchorage (U.S. Department of the Interior, Minerals Management Service), 179 p.
- Turner, R. F., and others, (in press), Geologic report for the North Aleutian Basin planning area, Bering Sea, Alaska, OCS Report MMS _____: Anchorage (U.S. Department of the Interior, Minerals Management Service).
- Turner, R. F., and others, (in press), Geological and operational summary, North Aleutian Basin COST No. 1 well, Bering Sea, Alaska, OCS Report MMS _____: Anchorage (U.S. Department of the Interior, Minerals Management Service).
- von Huene, R. E., and Fisher, M. A., 1984, Recent deformation on the Kodiak Shelf: Seismological Society of America, Annual Meeting Abstracts, p. 18.

- von Huene, R., Fisher, M. A., Hampton, M. A., and Lynch, M., 1980a, Petroleum potential, environmental geology, and the technology for exploration and development of the Kodiak Lease Sale Area No. 61: U.S. Geological Survey Open-File Report 80-1082, 70 p.
- von Huene, R., Hampton, M. A., Fisher, M. A., Varchol, D. J., and Cochrane, G. R., 1980b, Map showing near-surface geologic structures of Kodiak shelf, Alaska: U.S. Geological Survey Miscellaneous Field Studies Map MF-1200, 1 sheet, scale 1:500,000
- von Huene, R., Keller, G., Bruns, T. R., and McDougall, K., 1985, Cenozoic migration of Alaskan terranes indicated by paleontologic study, *in* Howell, D. G., (ed.), Tectonostratigraphic terranes of the circum-Pacific region: Houston, Circum-Pacific Council for Energy and Mineral Resources, Earth Science Series No. 1, p. 121-136.
- von Huene, R. E., and Lee, H., 1983, The possible significance of pore fluid pressures in subduction zones: AAPG Memoir 34, p. 781-791.
- von Huene, R., Shor, G. G., and Malloy, R. J., 1972, Offshore tectonic features in the affected region, *in* The Great Alaska Earthquake of 1964, Oceanography and Coastal Engineering: National Research Council, National Academy of Sciences, Washington, D.C., p. 266-289.
- Vrolijk, P., 1987, Tectonically driven fluid flow in the Kodiak accretionary complex, Alaska: *Geology*, v. 15, p. 466-469.
- Walker, R. G., 1978, Deep-water sandstone facies and ancient submarine fans: models for exploration for stratigraphic traps: AAPG Bulletin, v. 62, no. 6, p. 932-966.
- Wallace, W. E., 1965, Application of electric-log-measured pressures to drilling problems and a new simplified chart for well site pressure computation: *Log Analyst*, v. 6, p. 26-28.
- Waples, D. W., 1981, Organic geochemistry for exploration geologists: Minneapolis, Burgess Publishing Company, 151 p.
- Waples, D. W., 1985, Geochemistry in Petroleum Exploration: Boston, International Human Resources Development Corporation, 232 p.
- Whelan, T., Coleman, J. M., Roberts, H. A., and Suhayda, J. N., 1976, The occurrence of methane in recent deltaic sediments and its effect on soil stability: *International Association of Engineering Geologists Bulletin*, v. 14, p. 55-64.

- Wilcox, R. E., 1959, Some effects of recent volcanic ash falls, with especial reference to Alaska: U.S. Geological Survey Bulletin 1028-N, p. 409-476.
- Williams, G. L., and Bujak, J. P., 1977, Cenozoic palynostratigraphy of offshore eastern Canada, in Elsik, W. C., (ed.), Contributions of Stratigraphic Palynology (with emphasis on North America), v. 1, Cenozoic Palynology: American Association of Stratigraphic Palynologists Contribution Series, no. 5A, 166 p., p. 14-47.
- Williams, G. L. and Bujak, J. P., 1985, Mesozoic and Cenozoic Dinoflagellates: in Bolli, H. M., Saunders, J. B., and Perch-Nielsen, K., (eds.), Plankton stratigraphy: Cambridge University Press, 1032 p., p. 847-964.
- Wise, S. W., Jr. and Wind, F. H., 1976, Mesozoic and Cenozoic calcareous nannofossils recovered by DSDP Leg 36 drilling on the Falkland Plateau, southwest Atlantic sector of the Southern Ocean, in Barker, P. F., Dalziel, I. W. D., and others, Initial Reports of the Deep Sea Drilling Project, Volume 36: Washington (U. S. Government Printing Office), 1080 p., p. 269-492.
- Wolfe, J. A., 1973, Reconnaissance spore and pollen examination, early Tertiary turbidite beds, Aleutian abyssal plain, Site 183, in Creager, J. S., Scholl, D. W., and others, Initial Reports of the Deep Sea Drilling Project, Volume 19: Washington (U. S. Government Printing Office), 913p., p. 739.
- Wolfe, J. A., 1977, Paleogene floras from the Gulf of Alaska Region: U.S. Geological Survey Professional Paper 977, 108 p.
- Wolfe, J. A., and Poore, R. Z., 1982, Tertiary marine and nonmarine climatic trends, in Climate in Earth History, U. S. National Research Council Study Committee, Berger, W. H., and Crowell, J. C., panel cochairmen: National Academic Press, Washington, 198 p., p. 154-158.
- Worsley, T. R., 1973, Calcareous nannofossils: Leg 19 of the Deep Sea Drilling Project, in Creager, J. S., Scholl, D. W., and others, Initial Reports of the Deep Sea Drilling Project, Volume 19: Washington (U. S. Government Printing Office), 913 p., p. 741-750.
- Wyllie, M. R. J., and Rose, W. D., 1950, Some theoretical considerations related to the quantitative evaluations of the physical characteristics of reservoir rock from electric log data: Journal of Petroleum Technology, v. 189, p. 105-110.

APPENDIX 1

KSSD No. 1 well

Permeabilities, porosities, and grain densities of conventional core samples (from Core Laboratories data).

<u>Sample number</u>	<u>Depth (feet)</u>	<u>Permeability (Millidarcies)</u>	<u>Porosity (Percent)</u>	<u>Grain Density (gm/cc)</u>
Core 1				
39	5,784.5	.79	15.5	2.67
Core 2				
1	5,794.0	8.4	14.7	2.65
2	5,815.0	fractured	13.7	2.64
Core 3				
3	6,496.0	.55	0.2	2.60
4	6,501.0	.01	3.7	2.65
5	6,503.0	.01	1.9	2.62
Core 4				
6	6,508.0	.01	3.2	2.64
Core 5				
7	8,140.5	.03	6.3	2.63
8	8,141.0	.03	5.9	2.63
9	8,141.5	.02	5.0	2.64
10	8,142.0	.03	5.8	2.63
11	8,142.5	.02	0.1	2.63
12	8,143.5	.01	2.4	2.64
13	8,144.5	.31	5.8	2.63
14	8,145.0	.05	6.3	2.64
15	8,145.5	.05	5.3	2.63
16	8,146.0	.05	4.5	2.63
17	8,146.5	.02	3.7	2.63
18	8,147.0	.04	5.6	2.63
19	8,147.5	.04	5.5	2.63
20	8,148.0	.04	5.4	2.63
21	8,148.5	.05	5.8	2.63
22	8,149.0	.05	5.5	2.63
23	8,149.5	.05	6.3	2.64
Core 6				
24	8,155.5	.03	5.6	2.64
25	8,156.0	.04	6.0	2.64
26	8,156.5	.06	6.4	2.65
27	8,157.0	.04	6.6	2.65
28	8,157.5	.03	6.2	2.65
29	8,158.0	.04	6.2	2.65
30	8,158.5	.03	5.4	2.65
31	8,159.0	.02	5.2	2.65
32	8,161.0	.02	2.4	2.67
33	8,162.5	.02	4.2	2.65
34	8,163.0	.01	3.7	2.67
35	8,166.0	.03	4.5	2.65
36	8,168.5	.02	3.5	2.65
37	8,173.5	.01	0.5	2.64
38	8,177.0	.01	1.9	2.64

(KSSD No. 1 well cont.)

X-ray diffraction percentage determinations of selected minerals in conventional core samples (from Core Laboratories data).

Sample Number	Depth (feet)	Quartz	Feldspars	Chlorite	Illite Mica	Pyrite	Kaolinite Chlorite	Calcite
Percent of Total Sample								
Core 1								
39	5,784.5	43	32	19	6			
Core 2								
1	5,794.0	46	28	21	5			
2	5,815.0	40	35	21	4			
Core 3								
3	6,496.0	31	26	33	9	1		
4	6,501.0	50	28	18	2	2		
5	6,503.0	54	29	16	1			
Core 4								
6	6,508.0	45	33	20				2
Core 5								
7	8,140.5	60	28		1		12	
13	8,144.5	52	37		1		10	
16	8,146.0	55	29		2		9	5
20	8,148.0	50	40		1		9	
21	8,148.5	39	46				15	
23	8,149.5	53	37		1		9	
Core 6								
24	8,155.5	41	50		1		8	
29	8,158.0	36	52		1		11	
32	8,161.0	31	25	34	10			
33	8,162.5	32	26	32	10			
34	8,163.0	29	34	27	10			
35	8,166.0	65	25	8	1			1
36	8,168.5	62	24	13				1
37	8,173.5	27	23	42	8			
38	8,177.0	40	24	24	6			6

CORE DESCRIPTIONS

Core 1 (5,775 to 5,783 feet)

This core consists of dark-gray, firm, plastic, slightly calcareous, slightly micaceous claystone containing scattered pyrite crystals.

Core 2 (5,785 to 5,824 feet)

This core is made up of dark-gray, massive, silty, slightly calcareous, claystone that contains scattered pebbles. The core appears massive from 5,785 to 5,795 feet, broken from 5,795 to 5,811 feet, and massive and more silty from 5,811 to 5,824 feet.

Core 3 (6,496 to 6,504 feet)

This core consists of gray and black laminated, indurated brittle shale that is slightly to very silty, and contains small pieces (1/16 in. square) of carbonaceous material. The laminations are approximately 1 in. thick, reflecting changes in the silt content of the shale. The apparent dip is about 45 degrees. Secondary calcite occurs along bedding planes.

Core 4 (6,508 to 6,512 feet)

Core 4 is shale similar to that described above but with an apparent dip of about 10 degrees.

Core 5 (8,140 to 8,153 feet)

The upper 2.5 feet of this core is hard, massive, light gray, very fine-grained sandstone. The grains are predominantly subrounded and subangular quartz with abundant feldspar that is partly altered to kaolinite. No visible porosity or permeability is apparent. The next 2.5 feet is dark-gray, hard, massive, vertically fractured claystone with fine-grained sandstone interbeds up to 1 inch thick. The sharp contacts between sandstone and claystone layers suggest scour and fill deposition. The next 7 feet of the core is fine- and very fine-grained sandstone similar to that at the top of the core. The bottom 1 foot of the core consists of fragments of claystone and sandstone similar to the top 12 feet of the core.

Core 6 (8,155 to 8,177 feet)

Core 6 is dark-gray and brown claystone with thin interbeds of light-gray to white, silty, very fine-grained sandstone containing subangular and subrounded grains. The core is cut by nearly vertical, slickensided, hackly fractures filled with secondary calcite cement. There is no visible porosity or permeability.

Petrographic Thin Section Analysis of Cores
(from Core Laboratories data)

Core 1

Depth 5,784.5 feet

Silty, very fine-grained sandstone: immature, chloritic subarkose

This sample consists of poorly-sorted grains ranging in size from very fine sand to very fine silt in a chloritic, clay-organic matrix. The grains are angular and vary in shape. Monocrystalline quartz is the dominant mineral, with about 20 percent feldspar. Micas, usually chloritized biotite, are also very common along with rounded, very pure clay clasts. The matrix is a mixture of clays, chlorite, altered mica, and very fine silica. Minute glauconite pellets and dark brown opaque organics are scattered throughout in trace amounts. The sample appears to be very soft and poorly consolidated.

Core 2

Depth 5,794 feet

Silty, very fine-grained sandstone: immature, chloritic subarkose

Similar to above sample.

Depth 5,815 feet

Silty, fine-grained sandstone: chloritic, micaceous subarkose

This sample consists of poorly-sorted grains ranging in size from medium sand (a few grains) to very fine silt in a chloritic, micaceous, siliceous clay-organic matrix. The grains are generally angular. Quartz is the dominant mineral, with about 20 percent feldspar. Micas, both muscovite and chloritized biotite, are also very common. The matrix is a mixture of fine micas, chlorite, very fine silica and, to a lesser degree, well-dispersed clays. Minute isolated patches of anhedral calcite represent recrystallized fossil remains. A slight tendency toward orientation is demonstrated by poorly-defined partings with higher percentages of clays and micas. Fine fractures follow several of these partings.

Core 3

Depth 6,496 feet

Coarse silt: immature, chloritic clayey subarkose

This sample consists of silt-sized grains in a clayey, chloritic matrix. The angular, equant grains are predominantly

monocrystalline quartz with about 30 percent feldspar. Fine mica, primarily muscovite, is present in minor amounts. The matrix is a mixture of chlorite, clay minerals, and clay-sized quartz. The grains are distributed evenly throughout the matrix, giving the sample a very homogeneous appearance. The clay minerals are also well-dispersed, but are sometimes concentrated in scattered, silt-sized, rounded clasts. Very fine fragments of black or dark brown, opaque organic material and microcrystalline pyrite are present in minor amounts.

Depth 6,501 feet

Medium-grained sandstone: submature, chloritic subarkose

This sample consists of moderately well-sorted grains which are tightly packed and cemented by calcite and clay-siliceous matrix. The equant grains are subrounded to angular and vary in size from medium sand to coarse silt. Mono- and polycrystalline quartz with straight or slightly undulose extinction dominate the grain fraction with about 30 percent feldspars also present. A wide range of alteration is observed in the feldspars, with microcline the least affected. Detrital chert, volcanic rock fragments, and fine clumps of microcrystalline pyrite are common. Secondary silica, chert, and syntaxial quartz overgrowths represent the first cementation stage, together with chlorite and clay minerals. Sparry calcite represents a later stage of cementation. Traces of hornblende are scattered throughout.

Depth 6,503 feet

Fine-grained sandstone: mature, siliceous subarkose

This sample is similar to the one at 6,508 feet, described below.

Core 4

Depth 6,508 feet

Fine-grained sandstone: mature, siliceous subarkose

This sample consists of well-sorted, fine sand-sized grains closely packed and cemented with secondary silica. The grains vary from angular to subrounded and are generally equant. Monocrystalline quartz dominates the sample with 10 to 15 percent feldspar present. Chert is more common in the matrix than as detrital grains. Biotite, with minor muscovite and sericite, represents the micas. Volcanic fragments are present in minor amounts along with trace amounts of zircon and hornblende. Syntaxial quartz overgrowths and precipitated, cherty silica are the most important cementing agents. Clay and chlorite altered from biotite are minor constituents. An irregular fracture varying in thickness from hairline to 0.5 mm cuts through the sample and is healed with blocky dolomite.

Core 5

Depth 8,140.5 feet

Medium-grained sandstone: mature, chert-cemented subarkose

This sample consists of well-sorted, closely packed grains cemented by silica. The grains are angular and equant. Monocrystalline quartz and feldspar are the dominant minerals. The quartz is primarily monocrystalline with straight extinction. Syntaxial overgrowths are responsible for the angularity and sutured boundaries between grains. A range of alteration is displayed by the feldspar grains, from fresh to cloudy. Chert is also a substantial component, both as detrital grains and as a cementing precipitate. Minute isolated patches of sparry calcite and chlorite are local cementing agents. Minor amounts of volcanic rock fragments are present. Small clusters of pyrite and black opaque organics are present in trace amounts.

Depth 8,141 feet

Medium-grained sandstone: mature, chert-cemented subarkose

This sample is similar to the one described above at 8,140.5 feet.

Depth 8,141.5 feet

Medium-grained sandstone: mature, siliceous subarkose

This sample is similar to the one described above at 8,140.5 feet.

Depth 8,142 feet

Medium-grained sandstone: mature, siliceous subarkose

This sample consists of well-sorted subrounded, equant grains ranging from medium- to fine-sand size. Sutured boundaries related to secondary overgrowths are common. Monocrystalline and polycrystalline quartz with generally straight extinction is the major constituent. Feldspar exhibiting a wide range of alteration is also very common, as are detrital chert and volcanic rock fragments. Mica, with chloritized biotite predominating over muscovite, is present in minor amounts. Precipitated silica is the dominant cementing agent, with chert being the most common form. Chlorite and clay minerals, usually the product of feldspar decay, are minor cementing agents along with a few isolated, dolomitized patches of calcite. Well-dispersed traces of opaque organics with associated microcrystalline pyrite are scattered through the sample.

Depth 8,142.5 feet

Coarse-grained siltstone: laminated, clayey subarkose

This sample represents a coarse-grained silt interlaminated with an organically-rich silty mudstone. The individual laminae vary in thickness and several are disturbed by burrows. A 15 mm lenticular body of well-sorted medium-grained sandstone was deposited while the sediment was still unconsolidated. The silty laminae are dominated by quartz grains with only minor amounts of mica and feldspar. The grains are closely packed and cemented with silica, and to a lesser degree, with clay minerals and chlorite. The mudstone laminae have a much lower silt content. Clay minerals, altered and hydrated mica, and opaque organics are all important components in the mudstone. Clusters of microcrystalline pyrite are associated with the organics, along with trace amounts of calcite.

Depth 8,143.5 feet

Medium-grained sandstone: clayey subarkose

This sample is a well-sorted sandstone. The grains are closely packed, subangular, and equant. Monocrystalline quartz is the dominant mineral. Feldspar, chert, and mica are common. The mica consists of highly-altered and chloritized biotite with only a few flakes of muscovite. The chert is primarily detrital, with only a small portion in the matrix. A few of the chert grains are chalcedonic. Well-dispersed clay and precipitated silica are the main cementing agents. The sutured boundaries between some of the grains strongly suggest secondary syntaxial overgrowths. A tendency toward orientation is indicated by fine, black organic partings, associated with microcrystalline pyrite and higher percentages of clays and micas. Badly-preserved, small foraminifera are present.

Depth 8,144.5 feet

Medium-grained sandstone: mature, siliceous subarkose

This sample closely resembles the one at 8,145 feet, described below.

Depth 8,145 feet

Medium-grained sandstone: mature, siliceous subarkose

This sample consists of well-sorted, closely-packed grains cemented with silica. The grains are angular to subangular, and often have sutured boundaries. Monocrystalline quartz is the most common mineral but does not dominate the sample. Feldspar, detrital chert, and volcanic rock fragments are all present in substantial

amounts. The feldspars are generally in an advanced state of alteration, exhibiting coatings of fine clays or containing fine clay flakes within the grains. The rock fragments are composed of fine feldspar laths and are also often masked by clays. The chert and fine polycrystalline quartz, often stretched, are occasionally difficult to distinguish from precipitated forms in the cement. Optically-continuous quartz overgrowths are a very important cementing agent. Chloritized biotite is present in minor amounts and sparry calcite occurs in isolated patches, often encroaching on quartz or feldspar grains.

Depth 8,145.5 feet

Medium-grained sandstone: mature, siliceous subarkose

This sample closely resembles the one at 8,145 feet, described above.

Depth 8,146 feet

Medium-grained sandstone: mature, siliceous subarkose

This sample is similar to the one at 8,145 feet, described above.

Depth 8,146.5 feet

Medium-grained sandstone: calcitic subarkose

This sample consists of well-sorted, closely-packed, subrounded to subangular, equant grains which are cemented by silica and calcite. The grains are medium sand-size and are composed of monocrystalline and polycrystalline quartz, feldspar, and chert. Chloritized biotite and volcanic rock fragments are present in much lesser quantities. The feldspars are often altered into clays, which sometimes mask an entire grain. Silica released through pressure solution was the initial, although weak, cementing agent. It was later supplemented by sparry calcite, which is now the primary cement. Calcite often replaces the feldspars and quartz. Chlorite and finely-dispersed clays are present in minor amounts as matrix.

Depth 8,147 feet

Medium-grained sandstone: mature, chert-cemented subarkose

This sample consists of well-sorted, closely packed, medium sand-sized, subangular and equant grains in a cherty matrix. Quartz (mono- and polycrystalline), chert, and feldspar are present in equal amounts. The quartz often contains bubbles and inclusions of rutile, and tourmaline. Some grains show the effects of pressure solution and the sutured boundaries suggest some secondary, optically continuous overgrowths. The feldspars are primarily orthoclase and plagioclase in various stages of alteration; a few

grains are masked by clay minerals. Chloritized biotite and volcanic rock fragments occur in minor amounts along with a few grains of myrmekite. Secondary chert is the primary cementing agent; sparry calcite appears only in minute isolated patches. Clay minerals and chlorite are rare. Hematite and opaque organics are present in trace amounts.

Depth 8,147.5 feet

Medium-grained sandstone: mature, chert-cemented subarkose

This sample is similar to the one at 8,147 feet, described above.

Depth 8,148 feet

Medium-grained sandstone: mature, chert-cemented subarkose

This sample is similar to the one at 8,147 feet, described above.

Depth 8,148.5 feet

Medium-grained sandstone: mature, chert-cemented subarkose

This sample is similar to the one at 8,147 feet, described above.

Depth 8,149 feet

Medium-grained sandstone: mature, chert-cemented subarkose

This sample is similar to the one at 8,147 feet, described above.

Depth 8,149.5 feet

Medium-grained sandstone: mature, siliceous subarkose

This sample consists of moderately well-sorted, very closely-packed, subangular and equant grains. Monocrystalline quartz with straight or slightly undulose extinction is the dominant mineral. Orthoclase and plagioclase feldspars, polycrystalline quartz, chert, and volcanic rock fragments are all common. A wide range of feldspar alteration is displayed, with some grains being completely masked by kaolinite. Some biotite is chloritized. Secondary quartz is the main cement, with precipitated chert, clays, and chlorite minor cementing agents. Isolated patches of fine micrite, sparry calcite, and dark brown, opaque organic material are scattered throughout. Trace amounts of zircon are present.

Core 6

Depth 8,155.5 feet

Medium-grained sandstone: mature, siliceous subarkose

This sample is similar to the one at 8,156 feet, described below.

Depth 8,156 feet

Medium-grained sandstone: mature, siliceous, chert-bearing arkose

This sample consists of well-sorted, very closely-packed, medium-sand-sized, angular grains. Sutured, interlocking boundaries, due to optically-continuous, secondary overgrowths, are very common. Monocrystalline quartz, feldspars, and chert are present in approximately equal amounts. The quartz is usually clear with only a few grains containing inclusions of rutile and bubbles. The chert commonly changes to polycrystalline quartz but a few chalcedonic grains are also present. Sericite, clay minerals, and chlorite are often present within the chert grains. Precipitated silica is the major cementing agent. The feldspars display all stages of alteration and some grains are masked by authigenic clays. Volcanic rock fragments are an important accessory component along with flakes of chloritized biotite which have been deformed by post-depositional compaction. Isolated, minute patches of sparry calcite are often associated with finely-dispersed organics. Myrmekite is present in trace amounts.

Depth 8,156.5 feet

Medium-grained sandstone: mature, siliceous subarkose

This sample is similar to the one at 8,156 feet, described above.

Depth 8,157 feet

Medium-grained sandstone: mature, siliceous, chert-bearing arkose

This sample consists of very closely-packed, moderately well-sorted, medium- to fine-sand-sized subangular grains. The original shape of the grains is difficult to determine due to pressure solution. The feldspars generally show high degrees of alteration; many grains are cloudy due to fine clays, and sericite flakes within some grains are common. Detrital chert is more common than secondary chert and both show a tendency to recrystallize into polycrystalline quartz. Volcanic rock fragments are an important constituent and resemble the feldspars in alteration. Mechanically-deformed and chloritized biotite flakes are dispersed throughout. Isolated patches of sparry calcite, often encroaching upon the clastic grains, are a minor cementing agent. Zircon and hornblende are present in trace amounts along with myrmekite.

Depth 8,157.5 feet

Medium-grained sandstone: mature, siliceous, chert-bearing arkose

This sample is similar to the one at 8,157 feet, described above.

Depth 8,158 feet

Medium-grained sandstone: mature, siliceous, chert-bearing arkose

This sample is similar to the one at 8,157 feet, described above.

Depth 8,158.5 feet

Medium-grained sandstone: mature, siliceous, chert-bearing arkose

This sample is similar to the one at 8,157 feet, described above.

Depth 8,159 feet

Medium-grained sandstone: mature, siliceous, chert-bearing arkose

This sample is similar to the one at 8,157 feet, described above.

Depth 8,161 feet

Silty, very fine-grained sandstone: laminated subarkose

This sample represents a well-sorted, closely-packed, very fine-grained sandstone interlaminated with silty mudstone. The sandstone consists of subangular grains of monocrystalline quartz with about 15 to 20 percent feldspar present. Mica, especially chloritized biotite, is also very common. The grains are cemented by a chlorite-clay matrix which occurs in patches supplemented by precipitated siliceous cement. Well-dispersed organic material is scattered throughout and shows a slight tendency to concentrate along poorly-defined, biotite-rich laminae. Microcrystalline pyrite is often associated with the organic-rich areas. Micro cross-bedding and pinching out of the laminae is common. Very clayey, chloritic siltstone that is rich in opaque material makes up part of the sample. The boundary between the siltstone and the sandstone is very sharp.

Depth 8,162.5 feet

Fine-grained sandstone: mature, siliceous subarkose

This sample is similar to the one at 8,166 feet, described below.

Depth 8,163 feet

Fine-grained sandstone: mature, siliceous subarkose

This sample is similar to the one at 8,166 feet, described below.

Depth 8,166 feet

Medium-grained sandstone: mature, siliceous subarkose

This sample consists of closely-packed, well-sorted, medium sand-sized, angular grains. Mono- and polycrystalline quartz are the major constituents. The angularity of the grains and the sutured, interlocking boundaries strongly suggest that optically continuous, secondary overgrowths are present. Detrital and precipitated chert is also a component, along with feldspar. The feldspar shows all stages of alteration; many grains are masked by clay minerals or include very fine flakes of sericite. Myrmekite occurs infrequently. Chloritized biotite and altered volcanic rock fragments are common. Secondary silica is the most important cementing agent. Minute, isolated patches of sparry calcite, often encroaching on the quartz or feldspars, are scattered throughout. Tourmaline and hematite are present in trace amounts along with well-dispersed organics.

Depth 8,173.5 feet

Silty, very fine-grained sandstone: laminated, chloritic subarkose

This sample consists of silty, chloritic, very fine-grained sandstone with faint, poorly defined laminae of silty mudstone. Normal packing of the angular to subangular and elongated sand grains is evident. Quartz dominates the sand fraction but feldspars are also present in substantial amounts. Chloritized biotite flakes are scattered throughout and are very common. The thin section is badly plucked because of the soft chloritic matrix. The matrix is mostly chlorite with some silica and a minor percentage of well-dispersed clay minerals derived from decaying feldspars. Well-dispersed brown, opaque organic material is common throughout the matrix along with randomly-oriented minute flakes of sericite.

Depth 8,177 feet

Silty, fine-grained sandstone: chloritic, subarkose and sandstone

This sample consists of moderately well-sorted fine sand- to fine silt-sized angular grains which are closely packed. Mono- and polycrystalline quartz are the major constituents. Often the polycrystalline variety seems to be recrystallized from chert which is also present in substantial amounts, both in detrital and precipitated forms. Stretched quartz is common; about 20 percent feldspar is present and shows all grades of alteration. Feldspathic rock fragments are common, and are often altered to clay minerals. Biotite flakes are commonly deformed by post-depositional compaction and are chloritized. Several poorly defined laminae rich in dark-brown organics, clay, chlorite, and a few clumps of pyrite are present. The matrix is a mixture of

(KSSD No. 1 well cont.)

secondary silica cement, chlorite, and a minor amount of well-dispersed clay minerals and patchy calcite. The very fine chloritic mudstone contains loose silt grains and is rich in opaque organics and very fine flakes of sericite.

KSSD No. 2 well

Permeabilities, porosities, and grain densities of core samples
(from Core Laboratories data).

<u>Sample number</u>	<u>Depth (feet)</u>	<u>Permeability (millidarcies)</u>	<u>Porosity (Percent)</u>	<u>Grain Density (gm/cc)</u>
Core 1				
1	7,354	fractured	20.1	2.70
2	7,357	fractured	21.3	2.72
3	7,361	.13	22.9	2.73
4	7,364	.09	21.2	2.72
5	7,367	.03	23.1	2.71
Core 2				
6	10,275	fractured	17.5	2.65
7	10,277	fractured	19.8	2.66
8	10,280.5	.06	19.9	2.65
9	10,282.5	.07	20.7	2.66
10	10,284	.03	21.3	2.67
11	10,286	.06	18.9	2.65
12	10,288	.17	24.1	2.66
13	10,290	52.00	25.9	2.65
14	10,292	21.00	25.3	2.69

X-ray diffraction percentage determinations of selected minerals
in core samples (from Core Laboratories data).

<u>Sample number</u>	<u>Depth (feet)</u>	<u>Quartz</u>	<u>Feldspar</u>	<u>Chlorite</u>	<u>Illite & Mica</u>	<u>Pyrite</u>	<u>Amphi-bole</u>	<u>Calcite Dolomite</u>	<u>Montmorillonite</u>
Percent of Total Sample									
Core 1									
1	7,354	29	33	25	10		3		
2	7,357	33	28	24	10		5		
3	7,361	27	28	24	11		10		
4	7,364	30	31	23	9		7		
5	7,367	25	33	18	7		12	5	
Core 2									
6	10,275	37	29	22	12				
7	10,277	36	28	28	8				
8	10,280	40	33	21	6				
9	10,282	30	30	18	7				15
10	10,284	33	40	17	7		3		
11	10,286	37	30	23	8			2	
12	10,288	53	31	10	4		2		
13	10,290	46	39	12	2			1	
14	10,292	45	32	11	3	1	6	2	

CORE DESCRIPTIONS

Core 1 (7,350 to 7,368 feet)

Core 1 consists of light-gray claystone that is silty to very silty, with sand-sized angular quartz grains scattered throughout. The core is massive and firm. Beds of siltstone are present, inclined 2 to 5 degrees from the horizontal. A slight hydrogen sulfide odor was detected.

Core 2 (10,274 to 10,293 feet)

Core 2 is made up of dark-gray, firm to hard claystone with slickensided fractures that are inclined approximately 26, 57, and 85 degrees from the horizontal. Less than 10 percent of the cored interval consists of fine- and very fine-grained, well indurated sandstone that occurs in thin (up to 1 inch thick) streaks and pods within the claystone. The sandstone layers and lenses contain subangular and subrounded grains of quartz, feldspar, and rock fragments.

Petrographic Thin Section Analysis of Cores
(from Core Laboratories data)

Core 1

Depth 7,354 feet

Silty mudstone

This sample consists of a clay and organic-rich matrix containing silt- to very fine sand-size quartz, feldspar, muscovite and biotite. Significant amounts of chlorite are indicated by large areas which have a distinct greenish cast. Finely-divided organic material gives the sample a dirty brown appearance, which is heightened by larger grains and stringers of opaque black and red-brown organics. The quartz and feldspar grains are generally angular to subangular, and often have a shard-like appearance. Numerous flakes of muscovite occur along with traces of hornblende. Rare crystals of sparry calcite are present along with scattered and disarticulated ostracod carapaces.

Depth 7,357 feet

Silty, chloritic shale

This sample represents a chlorite-rich shale containing substantial amounts of silt-sized quartz, feldspar, mica, and organics. The chlorite and clay minerals show a definite lineation under crossed nicols although the somewhat larger flakes of chlorite, muscovite and biotite are only subaligned. Angular to subangular grains range from

fine silt to very fine sand-size and consist predominantly of quartz and feldspar with abundant mica flakes and minor amounts of hornblende and epidote. A few larger sand grains are present among the silt grains. Scattered black and brown organics are present throughout the sample along with lesser amounts of pyrite. A system of irregular fractures is present.

Depth 7,361 feet

Silty, chloritic shale

This sample is similar to the one at 7,357 feet, described above.

Depth 7,364 feet

Silty, chloritic shale

This sample is similar to the one at 7,367 feet, described below.

Depth 7,367 feet

Silty, chloritic shale

This sample consists of a chlorite and clay-rich matrix containing substantial amounts of quartz, feldspar, opaque organics, and fine mica. The matrix displays a definite orientation of minerals. Subangular to subrounded grains range from silt to very fine sand-size, with a few up to fine sand-size. Most of the grains are subequant in shape. Quartz (monocrystalline and polycrystalline) and plagioclase feldspar are the dominant clastic minerals. Substantial amounts of muscovite and biotite also occur along with a significant amount of hornblende, minor epidote, and tourmaline. Abundant opaque organic material is present throughout along with pyrite and traces of glauconite. Irregular patches and crystals of calcite and some scattered foraminifera are also present. At least one foraminifera displays chambers filled with pyrite. Fractures occur locally.

Core 2

Depth 10,275 feet

Silty, fine-grained sandstone: immature, chloritic subarkose

This sample is similar to the one at 10,277 feet, described below.

Depth 10,277 feet

Silty, fine-grained sandstone: chloritic pelletoidal subarkose

This sample is an immature, poorly-sorted subarkose consisting of angular to subrounded grains of quartz and feldspar in a chloritic, organic-bearing matrix that contains numerous mica flakes, clay

lenses, and concentrations of pellets. The clay and organic-rich pellets range from .1 to .5 mm in length, generally have an elongate ovoid outline, and are usually clustered together. The larger clay lenses are more irregular in shape and occur throughout the sample. These show a definite alignment of clay minerals under crossed nicols. Abundant black and brown opaque organic material occurs throughout. Grains range from silt to medium sand-size and consist dominantly of monocrystalline quartz. Plagioclase is the most significant species of the feldspars. Numerous flakes of muscovite and biotite occur, along with traces of hornblende and epidote. A few scattered glauconite pellets are also present.

Depth 10,280.5 feet

Silty, chloritic mudstone

This sample consists of numerous silt- and fine sand-sized grains in a chloritic, organic-rich matrix. The abundant organic material, consisting of disseminated material, as well as opaque grains and stringers, contributes to the "junky" appearance of the sample. Fine flakes of mica, especially biotite, are scattered throughout the sample and show a tendency toward alignment. A few micritic and clayey peloids occur with rare glauconite pellets. The angular to subrounded grains range from fine silt- to very fine sand-size and are subequant to subelongate in shape. Monocrystalline quartz is dominant in the silt and sand-sized fraction, although substantial amounts of feldspar are also present. Traces of epidote are present.

Depth 10,282.5 feet

Silty, chloritic mudstone

This sample is a clayey, chloritic, organic-rich mudstone which contains numerous silt grains and mica flakes. Clayey lenses are interspersed throughout the siltier groundmass along with several uneven, silty laminae. Ellipsoidal pellets outlined by dark-brown organics and consisting of clay and organic material are often gathered together in lenticular masses that are concentrated in definite horizons. The grains are angular to subangular and range from very fine silt- to very fine sand-size. Quartz is dominant, with feldspar present in substantial amounts. Leached biotite is the major mica mineral. Only a few discrete chlorite flakes occur. Small, irregular and rounded patches of glauconite and some sparry calcite occur throughout the sample, along with minor amounts of pyrite.

Depth 10,284 feet

Silty, chloritic mudstone

This sample is similar to the one at 10,286 feet, described below.

Depth 10,286 feet

Silty, chloritic mudstone

This sample is a chlorite-rich mudstone containing abundant organic material and a significant silt component. The chlorite/clay matrix shows a general alignment of platy minerals. Opaque black and brown organics occur in streaks and clumps. Abundant fine flakes of mica, dominantly biotite, occur throughout the sample along with a few scattered clay-organic pellets. Fine silt- to very fine sand-size quartz and feldspar grains are evenly distributed across the section. Trace amounts of zircon, epidote, hornblende, and glauconite occur with minor pyrite and scattered oil patches. A laminae or pocket along one side of the section contains coarse silt- to fine sand-size grains of quartz, feldspar, chert, and mica in a clay-chlorite-organic matrix with some pyrite and patches of hydrocarbons. A sharp contact divides this area from the remainder of the sample.

Depth 10,288 feet

Sandy, coarse siltstone: chloritic subarkose

This sample consists of angular to subangular grains of quartz and feldspar along with numerous flakes of mica, organic debris, and lesser amounts of chert, hornblende, glauconite, epidote and clay peloids. Significant amounts of chlorite are present throughout the sample. Scattered clay peloids have an indistinct outline and may have a mixed carbonate composition. Abundant small pores remain open throughout the sample. Rare fossil fragments include whole and broken foraminifera tests. The quartz commonly contains bubbles and inclusions and is usually monocrystalline. Plagioclase is the most common feldspar. Leached biotite dominates the mica constituent, although significant discrete flakes of chlorite and some muscovite also occur.

Depth 10,290 feet

Clayey chloritic siltstone

This sample is similar to the one at 10,292 feet, described below.

Depth 10,292 feet

Silty, chloritic mudstone

This sample consists of a chloritic, clay-organic matrix containing numerous flakes of mica, predominantly biotite, and lenticular pockets of silt. The clay minerals and chlorite show a tendency toward alignment, but it is not well-defined enough to be called shaley. Much of the organic debris occurs in streaks and clumps and some pellets of clay-organic composition are evident throughout the sample. Scattered pockets of clay are also present, along with

(KSSD No. 2 well cont.)

numerous lenses and pockets of silt. Quartz and feldspar are the major clastic grains and generally have a subangular appearance. The grains are not confined to lenses, but occur throughout the sample. Irregular patches of dolomite are also fairly common. Hornblende, glauconite, and discrete flakes of chlorite are especially notable in the silt pockets.

KSSD No. 3 well

Permeabilities, porosities, and grain densities of conventional cores and sidewall core samples (from Core Laboratories data).

<u>Sample number</u>	<u>Depth (feet)</u>	<u>Permeability (millidarcies)</u>	<u>Porosity (percent)</u>	<u>Grain Density (gm/cc)</u>
Conventional Diamond Core Plugs				
1	6,271	0.04	3.5	2.70
2	7,604	5.0	10.1	2.67
3	7,615	1.0	8.7	2.66
4	8,178	32.0	15.2	2.63
5	8,181	0.56	7.6	2.67
7	9,051	12.0	23.9	2.64

Sidewall Core Plugs

1,453	<0.1	17.8
1,585	0.3	20.4
1,606	1.7	21.9
1,624	0.9	20.5
1,730	1.5	21.5
1,768	0.1	20.0
1,894	<0.1	20.3
1,906	0.9	21.0
1,926	1,000.0	31.5
2,178	0.2	21.7
2,212	<0.1	18.7
2,236	<0.1	18.3
2,252	<0.1	18.1
2,454	1,650.0	27.9
2,464	<0.1	19.1
2,468	<0.1	18.4
2,497	9.0	26.9
2,575	<0.1	17.9
2,713	<0.1	20.5
2,725	<0.1	22.8
2,735	6.1	23.5
2,753	<0.1	22.7
2,823	<0.1	21.7
2,833	<0.1	19.6
2,953	<0.1	18.8
2,969	<0.1	22.1
2,977	3.0	21.9
3,068	6.9	24.2
3,086	185.0	30.0
3,110	28.0	25.7
3,148	<0.1	19.2
3,230	2.3	21.1
3,244	9.0	24.2
3,385	1.8	21.3
3,404	0.2	19.8
3,424	610.0	29.3
3,448	0.7	19.6
3,498	3.9	22.7
3,502	73.0	25.9
3,515	2.4	23.8
3,672	5.4	21.4
3,678	<0.1	14.6
3,698	0.1	18.7
3,735	0.9	21.9
3,900	<0.1	22.0
3,925	<0.1	13.7
3,944	0.4	21.7
4,122	7.7	20.6

(KSSD No. 3 well cont.)

<u>Sample number</u>	<u>Depth (feet)</u>	<u>Permeability (millidarcies)</u>	<u>Porosity (percent)</u>	<u>Grain Density (gm/cc)</u>
4,124		1,250.0	32.8	
4,462		115.0	26.9	
4,506		0.1	19.8	
4,516		0.2	22.1	
4,526		100.0	30.1	
4,540		151.0	30.8	
4,554		587.0	33.4	
4,582		360.0	29.9	
4,704		<0.1	18.9	
4,713		<0.1	19.5	
4,725		125.0	29.1	
4,750		4.0	24.5	
4,921		<0.1	20.9	
5,066		<0.1	20.0	
5,074		1.7	22.1	
5,356		<0.1	19.0	
5,366		<0.1	17.1	
5,454		0.5	19.6	
5,502		<0.1	17.9	
5,704		<0.1	18.8	
5,736		0.8	20.5	
5,747		5.4	24.9	
5,760		4.5	26.7	
5,801		<0.1	18.7	
6,135		0.5	20.3	
6,152		<0.1	18.5	
6,212		386.0	32.9	
6,298		30.0	24.0	
6,503		1.2	20.5	
6,542		0.8	19.9	
6,894		<0.1	19.8	
6,910		<0.1	18.7	
6,914		165.0	29.5	
6,943		<0.1	21.7	
6,978		50.0	25.8	
7,006		5.5	20.1	
7,056		2.1	23.4	
7,066		110.0	27.4	
7,110		1.6	22.5	
7,274		75.0	26.0	
7,282		6.6	28.3	
7,337		1.8	22.8	
7,347		58.0	26.6	
7,355		0.2	18.4	
7,420		3.4	20.4	
7,438		<0.1	16.9	
7,500		<0.1	22.5	
7,580		1.2	20.8	
7,626		6.3	20.7	
7,681		0.6	22.7	

X-ray diffraction percentage determinations of selected minerals
in core samples (from Core Laboratories data).

Sample Depth (feet)	Quartz	Feldspar	Dolomite	Siderite	Pyrite	Chlorite	Illite Mica	Kaolinite
Percent of Total Sample								
6,271	58	27	2		1	11	2	
7,604	61	24			2	11	2	
7,615	68	20				10	2	
8,178	44	37	2		3	11	3	
8,181	37	40	1		3	14	5	
8,199	35	36			3	11	15	10
9,051	26	24		2	3	13	19	11
9,060	26	24			3	16	14	17

CORE DESCRIPTIONS

Core 1 (6,264 to 6,276 feet)

Core 1 consists of dark-gray, poorly-consolidated, soft, massive siltstone that locally contains very fine-grained sand.

Core 2 (7,601 to 7,617 feet)

Core 2 is made up of dark-gray, massive, friable siltstone containing megafossils and bioclastic debris, and rare coarse to pebbly, subrounded and rounded, dark-gray and black clasts.

Core 3 (8,175 to 8,201 feet)

The top 7.5 feet consists of dark bluish-gray, hard, massive siltstone that exhibits slickensided fractures inclined 20, 50, and 90 degrees from the horizontal. The lower 18.5 feet is hard, dark-brownish-gray shale and siltstone that is broken into 1- and 2-inch fragments. No dip is apparent.

Core 4 (9,044 to 9,063.5 feet)

Core 4 is made up of firm, dark-gray, micaceous shale that is friable, highly-fractured, and slickensided. It contains rare medium grain-sized subangular quartz and lithic fragments.

Petrographic Thin Section Analysis of Cores
(from Core Laboratories data)

Depth 1,906 feet (from a sidewall core)

Coarse-grained sandstone: feldspathic graywacke

This sample consists of poorly-sorted, medium- to coarse-grained sandstone composed of 40 percent quartz, 30 percent feldspar, lesser amounts of rock fragments and chert, and 15 percent matrix. The grains are rounded to subrounded, equant, and vary in size from 0.9 mm down to fine silt, which grades into matrix. The larger grains are generally chert or polycrystalline quartz. The quartz grains are primarily monocrystalline, inclusion free, and have straight extinction. The feldspars are about equally divided into plagioclase and orthoclase; both species are fresh and only a few grains show fine flakes of kaolinite on their surfaces. Volcanic and metamorphic rock fragments are present. Randomly-oriented, very fine feldspar laths in various stages of alteration distinguish the volcanic fragments from the well-oriented, mica-rich and clayey metamorphic fragments. The matrix is a mixture of clays and cherty silica and it includes fine silt-sized quartz and broken-down feldspars in a clayey groundmass which grades into very impure, cherty silica. Minor or accessory minerals present are chloritized biotite, epidote, hornblende, and calcite. The fine grains of neomorphic calcite, which are often associated with minute clusters of microcrystalline pyrite, represent recrystallized fossil fragments.

Depth 2,977 feet (from a sidewall core)

Coarse-grained sandstone: feldspathic graywacke

This sample consists of a moderately-sorted, medium- to coarse-grained sandstone composed of 40 percent quartz, 25 percent feldspar and lesser amounts of rock fragments and chert, and 20 percent matrix. Minor accessory minerals include epidote, hornblende, biotite, and calcite. The grains are subrounded, equant, and vary in size from 0.2 to 0.7 mm. The quartz grains are generally monocrystalline with straight or slightly undulose extinction. Plagioclase is the dominant species in the feldspar fraction. The potassium-rich feldspars appear to be more broken down and are well represented in the matrix. Chert grains often include chalcedony. The rock fragments are generally composed of fine, randomly-oriented feldspar laths in an advanced state of alteration into clay minerals. The matrix is a mixture of clayey and cherty groundmass with fine silt-sized grains of feldspars and quartz, often complemented by minute patches of micritic calcite associated with microcrystalline pyrite. The cementation is very irregular and large areas of the sample show as individual grains floating in the blue impregnating epoxy. Epidote, hornblende, and biotite are scattered throughout in trace amounts.

Depth 4,462 feet (from a sidewall core)

Medium-grained sandstone: feldspathic cherty graywacke

This sample consists of poorly-sorted, well-cemented sandstone composed of 30 percent quartz, 20 percent chert, 20 percent feldspar, and lesser amounts of rock fragments, chloritized biotite, calcite, and 15 percent matrix. The grains are subrounded, equant, and vary in size from very fine silt up to 0.5 mm, the latter being rare. The quartz grains are generally monocrystalline, inclusion-free, and have straight or slightly undulose extinction. The chert grains contain clayey impurities and many are crosscut with secondary quartz or chalcedony-healed fractures. Orthoclase and plagioclase are present in equal amounts. The rock fragments show well-developed orientation and are predominantly quartzitic with clayey streaks or laminae. Most are of metamorphic origin. The rather rare grains of calcite are recrystallized fossil remains. The matrix is a mixture of clays and cherty silicas.

Depth 5,736 feet (from a sidewall core)

Silty, medium-grained sandstone: feldspathic graywacke

This sample consists of silty, medium-grained sandstone with poorly-defined streaks of slightly different grain sizes. It is composed of 40 percent quartz, 20 percent feldspar, 15 percent chert, lesser amounts of rock fragments, mica flakes (chloritized biotite and very fine muscovite), and 15 percent matrix. The grains are subrounded, equant, and vary in size from fine silt to 0.4 mm. The quartz grains are primarily monocrystalline and inclusion-free with straight or slightly undulose extinction. The feldspar is generally fresh and about equally divided between orthoclase and plagioclase. The chert very often includes chalcedony and may be combined with polycrystalline quartz. Highly-altered, randomly-oriented, fine laths of feldspar are the main constituent of the rock fragments. The biotite flakes are usually chloritized and deformed by post-depositional compaction. Minute muscovite flakes are confined to small, clayey clasts present infrequently in the sample. Very poorly preserved small foraminifera, some with chambers infilled with microcrystalline pyrite, are scattered through the sample. The matrix is a mixture of clays and clayey, cherty silica with fine silt-sized feldspar and quartz. The sample is not uniformly cemented; portions are very poorly consolidated.

Depth 6,212 feet (from a sidewall core)

Fine-grained sandstone: arkosic arenite

This sample consists of well-sorted, fine-grained sandstone composed of 40 percent quartz, 20 percent feldspar, 15 percent chert, lesser amounts of rock fragments, and traces of epidote, glauconite, and hornblende. The grains are subrounded, equant, and average about

0.15 mm in size. Very rare rock fragments reach 0.6 mm. The quartz grains are generally monocrystalline with slightly undulose extinction and no inclusions. The feldspars are usually fresh and plagioclase predominates over orthoclase. The often clayey cherts occasionally include traces of chalcedony. Randomly-oriented, highly-altered, minute laths of feldspars are the major component of the rock fragments. The sample is very poorly consolidated. It has no matrix, but some of the grains have interlocking intergranular boundaries. Most grains appear to be floating in the blue impregnating epoxy.

Depth 6,271 feet (from conventional core 1)

Silty, fine-grained sandstone: feldspathic graywacke

This sample is a moderately well-sorted, fine-grained sandstone that consists of 50 percent quartz, 25 percent feldspar, lesser amounts of chert and rock fragments, and 15 percent matrix. Trace amounts of hornblende, epidote, organic fragments, glauconite, pyrite, and calcite are also present. The grains are subangular, equant, and range in size from 0.15 mm down to fine silt. The quartz grains are generally monocrystalline and inclusion-free, with slightly undulose extinction. The feldspars are about equally divided between plagioclase and orthoclase with a few microcline grains also present. The chert is often in very irregular shapes, deformed by post-depositional compaction. Fine laths of feldspar, often masked by clay minerals, are the main constituent in the rock fragments. The matrix is a mixture of chloritic clays and cherty silica. It is not homogeneous but occurs in patches of the sample which are very poorly-consolidated and show high intergranular porosities.

Depth 7,110 feet (from a sidewall core)

Medium-grained sandstone: feldspathic graywacke

This sample consists of moderately well-sorted medium-grained sandstone composed of 40 percent quartz, 25 percent feldspar, lesser amounts of chert, rock fragments, and 20 percent matrix. Calcite, glauconite, and epidote are minor accessories. The grains are subrounded, equant, and range in size from silt to 0.35 mm. The quartz grains are generally monocrystalline and inclusion-free with straight or slightly undulose extinction. The feldspars are about equally divided between orthoclase and plagioclase. Although some feldspar grains include fine flakes of clay minerals, most appear to be fresh. The chert grains contain chalcedony and clayey impurities. Randomly-oriented, altered, fine feldspar laths, cherty silica, and clays are the main components of the rock fragments. A very few poorly preserved foraminifers are scattered through the sample along with some neomorphic spar grains and micritic clasts of uncertain origin. Traces of myrmekite also occur. The matrix is a mixture of cherty silica, clay minerals, and finely-dispersed opaque, organic fragments and pyrite. The sample appears to be well-cemented.

Depth 7,282 feet (from a sidewall core)

Medium-grained sandstone: feldspathic cherty graywacke

The sample is a moderately well-sorted, medium-grained sandstone composed of 40 percent quartz, 15 percent chert, 10 percent feldspar, 10 percent rock fragments, minor amounts of calcite, and 15 percent matrix. Epidote is present in traces. The grains are subrounded, equant, and range in size from fine silt to 0.3 mm. The quartz grains are generally monocrystalline with straight or slightly undulose extinction and very rare inclusions. The feldspars are relatively fresh and are mostly plagioclase, with some orthoclase and a few grains of microcline. Many of the chert grains were deformed by post-depositional compaction and seem to be part of the matrix. Clayey impurities are very common in the chert along with polycrystalline quartz. Extensively altered and decayed feldspar laths are the main components of the rock fragments, which also include cherty silica. Small, scattered micritic calcite grains are also present. The matrix is patchy and varies from very dark and clayey to much cleaner, cherty, siliceous cement. Portions of the sample are very high in intergranular porosity and appear to be poorly-consolidated. Silty-clayey streaks and irregular laminae present in the sample include fine flakes of hydrated mica, minute fragments of organic material, and a few clusters of microcrystalline pyrite. Several small patches of micritic calcite act as a cementing agent.

Depth 7,444 feet (from a sidewall core)

Medium-grained sandstone: cherty subarkose

This sample consists of poorly-sorted, well-packed, medium-grained sandstone composed of 35 percent chert, 30 percent quartz, 15 percent feldspar, and 15 percent rock fragments. A portion of the sample consists of silty-clayey laminae. The grains are rounded, equant, and vary in size from fine silt to 0.4 mm. The chert grains often include clayey impurities and chalcedony. A few grains are crosscut by fractures healed with polycrystalline secondary quartz. The quartz grains are mostly monocrystalline and inclusion free, with straight or slightly undulose extinction. Plagioclase is slightly more common than orthoclase. Traces of biotite and glauconite are scattered throughout. The rock fragments are generally composed of fine feldspar laths often masked by clay minerals. The most important cementing agent is secondary silica. Intergranular porosity is very prominent.

Depth 7,450 feet (from a sidewall core)

Medium-grained sandstone: cherty subarkose

This sample consists of moderately well-sorted, poorly consolidated, medium-grained sandstone composed of 40 percent quartz, 25 percent

chert, 15 percent feldspar, and 10 percent rock fragments. The grains are subrounded, equant, and vary in size from silt to 0.35 mm. The quartz grains are generally monocrystalline and inclusion-free with straight extinction. The chert grains are often deformed by post-depositional compaction and contain clayey impurities and specks of chalcedony. The feldspars appear fresh, with plagioclase more common than orthoclase; a few grains of microcline are also present. Fine laths of feldspar and clay minerals are the most common constituents of rock fragments. Secondary chert is the most important cementing agent. Intergranular porosity is locally very high.

Depth 7,604 feet (from conventional core 2)

Medium-grained sandstone: feldspathic graywacke

This sample is a poorly-sorted, medium-grained sandstone composed of 40 percent quartz, 20 percent feldspar, 15 percent chert, lesser amounts of rock fragments, 15 percent clay and chert matrix, and traces of glauconite, opaque organics, epidote, and pyrite. The grains are subrounded and equant and range in size from silt to 0.45 mm. The quartz grains are generally monocrystalline and inclusion-free with lightly undulose extinction. The feldspars are about equally divided between plagioclase and orthoclase. The chert contains variable amounts of clayey impurities. Grains with fractures healed with polycrystalline quartz are also common. The rock fragments contain small, altered feldspar laths. Fossil fragments are rare and poorly preserved.

Depth 7,615 feet (from conventional core 2)

Coarse-grained sandstone: cherty, arkosic arenite

This sample is a poorly-sorted, well-cemented, coarse-grained sandstone composed of 45 percent quartz, chloritized biotite, epidote, and micritic calcite of uncertain origin. The grains are subrounded, equant, and generally range in size from fine sand to 0.7 mm, with a few grains up to 0.9 mm. The quartz grains are generally monocrystalline with slightly undulose extinction and are inclusion-free. The chert grains are often the largest grains in the sample. Chalcedony is common in the chert along with fractures healed with polycrystalline quartz. There is more plagioclase than orthoclase. Volcanic rock fragments rich in randomly-oriented, fine laths of feldspar are the most common. Clayey chert is the most important cementing agent. Some intergranular porosity is present.

Depth 7,681 feet (from a sidewall core)

Silty, fine-grained sandstone: feldspathic graywacke

This sample is a well-sorted, fine-grained sandstone composed of quartz, feldspar, and chert, with minor amounts of chloritized

biotite, glauconite, epidote, organic fragments, and pyrite. The percentages are difficult to estimate because of the fine texture of the sample. The grains are subrounded to subangular, equant, and range in size from 0.15 mm down to very fine silt. The matrix is a mixture of clays and silica and appears to be very soft. Some pyrite is present in large (up to 0.35 mm) clumps.

Depth 8,178 feet (from conventional core 3)

Coarse-grained sandstone: feldspathic graywacke

The sample is a poorly-sorted, coarse-grained sandstone that consists of 40 percent quartz, 20 percent feldspar, 15 percent rock fragments, and lesser amounts of chert, biotite, and traces of epidote. The grains are subangular, equant, and range in size from silt to 0.7 mm. The quartz grains are generally monocrystalline with slightly undulose extinction and no inclusions. The feldspars appear fairly fresh and plagioclase is slightly more common than orthoclase. The rock fragments are of two varieties: one rich in randomly-oriented feldspar laths which are in very advanced stages of alteration into clays, the other consisting of well-oriented, silty, clayey, fine quartz containing fragments of metamorphic origin. About 15 percent of the sample is matrix composed of silt, clays, and cherty silica. The sample is well-cemented and homogeneous. Calcite is also a common cementing agent representing a later diagenetic stage of cementation that often infills fractures in crushed grains. Minute clusters of microcrystalline pyrite are scattered throughout in trace amounts.

Depth 8,181 feet (from conventional core 3)

Coarse-grained siltstone: arkosic arenite

This sample is a well-sorted siltstone that consists primarily of quartz, feldspar, rock fragments, and chert. The percentages are very difficult to estimate due to the fine-grained texture. The grains are well-packed and many show signs of pressure solution and possible secondary overgrowths. The grain boundaries are often interlocking. Clay-stained silica is the most important cementing agent. The clays seem to be a product of local disintegration of feldspars and biotite. Neomorphic sparry calcite is present in an elongated streak along the top margin of the section. Zircon, epidote, microcrystalline pyrite, chloritized biotite, and organic fragments are well-dispersed through the sample in trace amounts. The sample is very homogeneous with the exception of poorly-defined, faint streaks of finer grained pyrite, and organic fragments.

Depth 8,199 feet (from conventional core 3)

Coarse-grained siltstone: arkosic arenite

This sample is similar to the one described above at 8,181 feet.

Depth 9,051 feet (from conventional core 4)*

Clayey fine silt

This sample is a streaky mudstone rich in very fine organic fragments. Macroscopically, the section shows a definite orientation, yet under the microscope, it appears as very irregular with randomly oriented streaks, accumulations, and lenses. The sample shows longitudinal separations lined with dark, clay-organic material and fine lenses which are usually very poorly-defined. The content of these lenses varies from fine-grained, rather clean sandstones, to very dark, fine, organic-rich claystones. Short veinlets with chalcedonic silica show infrequently in the sample. Superficially, this sample, and the one beneath it, resemble algal boundstones, although such an interpretation is not borne out by X-ray diffraction data.

Depth 9,060 feet (from conventional core 4)*

Clayey fine silt

This sample is a streaky mudstone with large deformed lenses. The clotted texture, along with the high clay-organic content and the short irregular (desiccation?) fractures, suggest a possible algal origin with frequent subaerial exposure. Large (up to 10 mm) lenses of silt and micritic calcite are often deformed or fragmented. The main part of the section is made up of streaks of randomly-oriented clays. Short, irregular fractures are present.

*(see discussion in Lithologic Summary chapter)

KSST No. 1 well

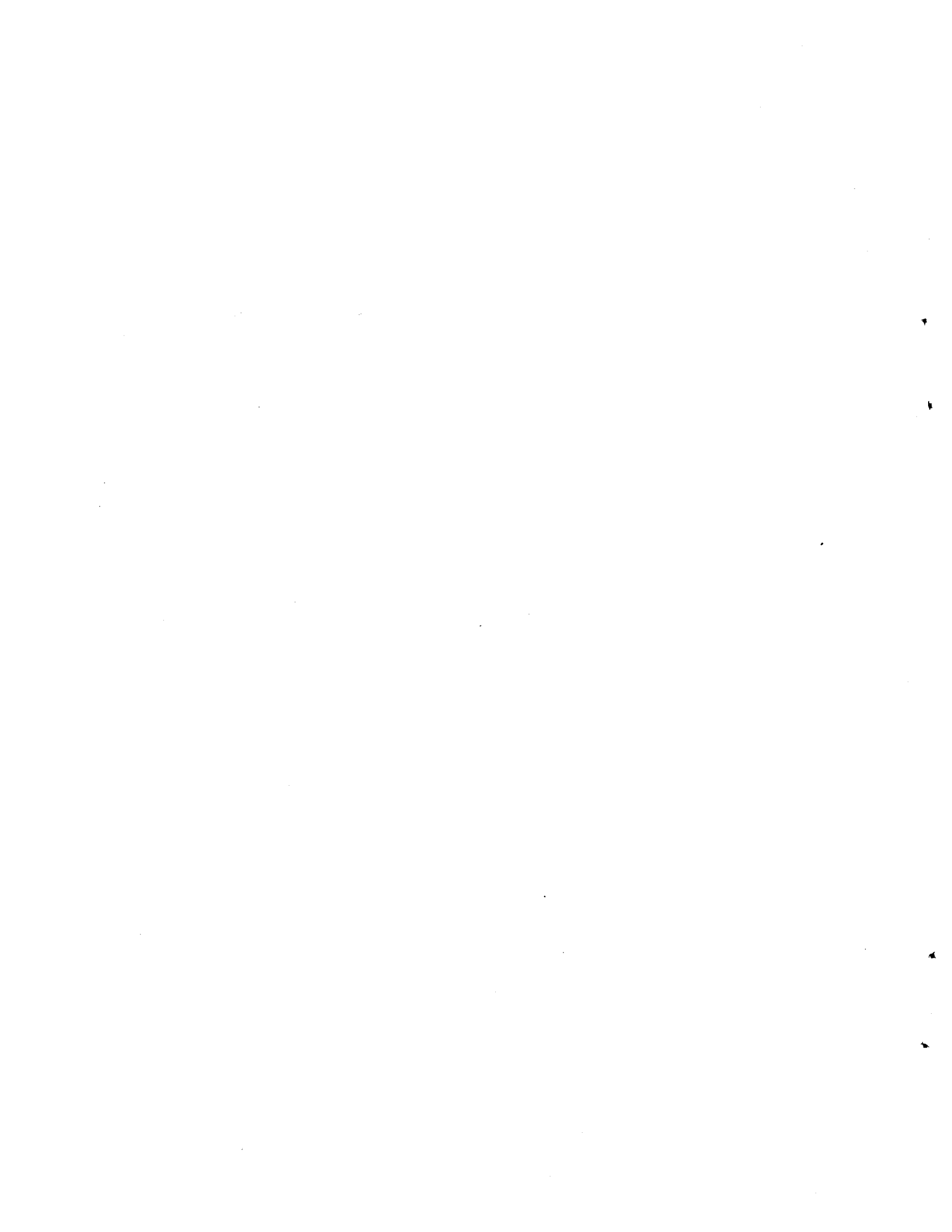
Permeabilities, porosities, and grain densities of sidewall core samples (from Core Laboratories data).

<u>Sample number</u>	<u>Depth (feet)</u>	<u>Permeability (millidarcies)</u>	<u>Porosity (percent)</u>	<u>Grain Density (gm/cc)</u>
1	365	170	30.8	2.63
2	384	62	28.8	2.63
3	396	93	29.1	2.64
4	1,417	41	23.7	2.64
5	1,508	31	20.1	2.65
6	1,773	20	18.6	2.67
7	2,847	27	23.2	2.64
8	3,508	23	19.5	2.66
9	4,029	11	23.8	2.66
10	4,036	30	24.8	2.65
11	4,064	17	22.2	2.65
12	4,075	20	22.7	2.65

KSST No. 2 well

Permeabilities, porosities and grain densities of sidewall core samples (from Core Laboratories data).

<u>Sample number</u>	<u>Depth (feet)</u>	<u>Permeability (millidarcies)</u>	<u>Porosity (percent)</u>	<u>Grain Density (gm/cc)</u>
1	940	8.7	28.9	2.69
2	1,235	61.0	18.0	2.71
3	1,515	5.5	29.3	2.66
4	1,630	78.0	23.8	2.68
5	1,705	73.0	22.6	2.66
6	1,873	21.0	31.8	2.71
7	1,880	fractured	33.8	2.66
8	1,885	fractured	20.1	2.67
9	1,904	1.3	22.9	2.68
10	1,920	1.4	23.1	2.67
11	2,023	1.8	19.4	2.69
12	2,391	126.0	27.8	2.66
13	2,403	157.0	29.1	2.70
14	2,425	15.0	25.2	2.67
15	2,585	81.0	28.1	2.65
16	2,593	32.0	28.9	2.65
17	2,600	42.0	28.3	2.65
18	2,679	2.6	22.1	2.68
19	2,906	13.0	18.9	2.65
20	2,916	37.0	23.9	2.69
21	2,970	28.0	23.8	2.66
22	3,038	17.0	22.0	2.67
23	4,218	86.0	21.0	2.68



APPENDIX 2

Bujak Davies Group
Kerogen Types, TAI, and R_o
Values from the KSSD No. 1 Well

Depth (feet)	<u>KEROGEN TYPES</u>										TAI	R _o
	AM	AT	AG	SA	M	BT	ST	I	R			
2,180	0	0	0	0	5	35	40	20	0	0	2 ⁻ to 2	
2,690	0	0	0	0	5	30	40	25	0	0	2 ⁻ to 2	
2,990	0	0	0	0	5	35	35	25	0	0	2	
3,410	0	0	0	0	5	20	45	30	0	0	2	
3,800	0	0	0	0	5	20	40	30	5	0	2	
4,220	0	0	0	0	10	20	40	25	5	0	2	
4,610	0	0	0	0	10	25	40	25	0	0	2	
5,000	0	0	0	0	5	30	40	25	0	0	2+	
5,420	0	0	0	0	5	35	35	25	0	0	2+	
5,720	0	0	0	0	5	30	45	20	0	0	2+	
5,900	0	0	0	0	5	30	40	25	0	0	2+	
6,020	0	0	0	0	5	20	45	30	0	0	2+	0.39
6,170	0	0	0	0	5	20	45	30	0	0	2+	
6,230												0.48
6,410	0	0	0	0	10	35	30	25	0	0	2+	
6,770	0	0	0	0	10	30	35	25	0	0	3-	
7,010	0	0	0	0	10	30	40	20	0	0	3-	
7,340	0	0	0	0	5	45	30	20	0	0	3-	0.54
7,640	0	0	0	0	10	40	35	15	0	0	3-	
7,820	0	0	0	0	15	35	30	20	0	0	3-	
7,970	0	0	0	0	10	35	35	20	0	0	3-	
8,300	0	0	0	0	10	35	30	25	0	0	3 ⁻ to 3	
8,450	0	0	0	0	5	25	40	30	0	0	3 ⁻ to 3	0.56

Cuttings samples generally represent 30-foot intervals. The given depths indicate the top of each sample interval.

AM: Marine amorphous (remains of unicellular phytoplankton)

AT: Terrestrial amorphous (remains of biodegraded tissues from land plants)

AG: Grey amorphous (same general origin as AM but deposited in anoxic, reducing environments)

SA: Structural aqueous (remains of multicellular marine algae)

M: Miospores (highly resistant walls of spores and pollen of land plants, fungal spores, and dinoflagellate cysts)

- BT: Biodegraded terrestrial (various parts of land plants that have undergone some biodegradation but original structures are still clearly visible)
- ST: Structured terrestrial (plant remains that still retain their cellular structure, have been mechanically broken, but are not significantly biodegraded)
- I: Inertinitic kerogen ("coaly kerogen" or "charcoal," darkened due to various causes including high thermal alteration and/or oxidation)
- R: Resinous material
- TAI: See Appendix 5
- R₀: Mean random vitrinite reflectance (the values given reflect the statistically dominant population from histograms believed to represent the autochthonous kerogen)

APPENDIX 3

Bujak Davies Group
Kerogen Types, TAI, and R_o
Values from the KSSD No. 2 Well

Depth (feet)	<u>KEROGEN TYPES</u>										R _o
	AM	AT	AG	SA	M	BT	ST	I	R	TAI	
1,620	0	0	0	0	0	15	50	30	0	2- to 2	
1,950	0	0	0	0	5	15	50	30	0	2- to 2	
2,130	0	0	0	0	5	25	50	20	0	2- to 2	
2,400	0	0	0	0	0	25	50	25	0	2- to 2	
2,700	0	0	0	0	5	25	45	20	5	2- to 2	
3,090	0	0	0	0	5	30	40	25	0	2- to 2	
3,420	0	0	0	0	0	30	40	25	5	2- to 2	
3,600	0	0	0	0	0	35	35	25	5	2- to 2	
3,900	0	0	0	0	0	35	40	25	0	2- to 2	
4,380	0	5	0	0	0	30	30	35	0	2- to 2	
4,770	0	0	0	0	5	30	35	30	0	2	
5,370	0	0	0	0	5	35	30	30	0	2	
5,760	0	0	0	0	5	30	30	35	0	2	
6,060	0	0	0	0	5	30	35	30	0	2	
6,240	0	0	0	0	5	30	40	25	0	1	
6,510	0	0	0	0	5	30	30	35	0	2	
6,720	0	0	0	0	5	25	35	35	0	2+	
7,020	0	0	0	0	5	20	40	35	0	2+	
7,440	0	0	0	0	5	25	45	25	0	2+	
7,710	0	0	0	5	5	25	45	20	0	2+	
7,980	0	0	0	0	5	25	45	25	0	2+	
8,130											0.47
8,400	0	0	0	5	5	20	50	20	0	2+	
8,640											0.41
8,700	0	0	0	0	5	25	50	20	0	2+	
9,060	0	0	0	0	5	25	45	25	0	2+	
9,330	0	0	0	0	5	30	40	25	0	2+	
9,420											0.41
9,600	0	0	0	0	5	30	40	25	0	2+	
9,960	0	0	0	5	5	25	45	20	0	2+	
10,230	0	0	0	5	5	25	40	25	0	3-	
10,440	0	0	0	0	5	25	40	30	0	3-	0.50

See Appendix 2 for explanation of kerogen types.

APPENDIX 4

Bujak Davies Group
Kerogen Types, TAI, and R_o
Values from the KSSD No. 3 Well

Depth (feet)	<u>KEROGEN TYPES</u>										R _o
	AM	AT	AG	SA	M	BT	ST	I	R	TAI	
1,520	0	0	0	5	10	20	40	25	0	2- to 2	
1,820	0	0	0	0	5	20	45	30	0	2- to 2	
2,300	0	0	0	0	10	25	40	25	0	2- to 2	
2,660	0	0	0	0	10	20	40	25	5	2- to 2	
3,170	0	0	0	0	10	15	40	30	5	2- to 2	
3,620	0	0	0	0	5	25	45	25	0	2	
4,040	0	0	0	0	5	30	40	25	0	2	
4,460	0	0	0	0	5	25	40	30	0	2	
4,850	0	5	0	0	5	20	35	30	5	2	
5,300	0	0	0	0	5	35	30	30	0	2+	
5,630	0	0	0	0	5	30	30	35	0	2+	
6,080	0	0	0	0	5	25	35	35	0	2+	
6,440	0	0	0	0	5	30	35	30	0	2+	
6,860	0	0	0	0	0	35	35	30	0	2+	
7,220	0	0	0	0	5	35	30	30	0	2+	
7,370	0	0	0	0	5	30	45	20	0	2+	
7,520	0	0	0	0	5	30	40	25	0	2+	
7,760	0	0	0	0	10	20	50	20	0	3-	0.39
8,030	0	0	0	0	5	35	35	25	0	3-	
8,180											0.44
8,840	0	0	0	0	10	40	25	25	0	3-	0.48
9,080	0	0	0	0	5	35	30	30	0	3-	
9,320	0	0	0	0	5	40	30	25	0	3- to 3	0.50

See Appendix 2 for explanation of kerogen types.

APPENDIX 5

Correlative Thermal Alteration
Index (TAI) and Random Mean Vitrinite
Reflectance (R_o) Values

<u>TAI</u> ¹	<u>Numerical Scale</u> ²	<u>Approx. R_o Equivalent G.C.L.</u> ³	<u>Approx. R_o Equivalent B.D.G.</u> ⁴
1	1.00	---	---
1+	1.40	---	0.35
1+ to 2-	1.60	0.4	---
2-	1.80	---	0.45
2- to 2	2.00	0.5	0.50
2	2.20	0.6	0.60
2 to 2+	2.40	---	0.70
2+	2.60	0.9	0.90
2+ to 3-	2.80	---	1.0
3-	3.00	1.0	1.1
3	3.40	1.5	1.5
3+	3.80	2.0	2.0
4-	4.20	2.5	2.5
4	4.60	4.0	4.0

1. TAI values are assigned on the basis of the color of plant particles that range from pale yellow through orange and brown to opaque black in transmitted light.
2. GeoChem Labs scale of decimal equivalencies of TAI values.
3. GeoChem Labs (G.C.L.) R_o equivalencies of TAI values.
4. Bujak Davies Group (B.D.G.) R_o equivalencies of TAI values.

APPENDIX 6

Bujak Davies Group
Kerogen Types and TAI Values for the
KSST No. 1, KSST No. 2, and KSST No. 4A Wells

KSST NO. 1

Depth (feet)	<u>KEROGEN TYPES</u>									TAI
	AM	AT	AG	SA	M	BT	ST	I	R	
450	0	0	0	0	10	15	55	20	0	2 ⁻ to 2
840	0	0	0	0	10	15	60	15	0	2 ⁻ to 2
1,330	0	0	0	0	5	20	50	25	0	2 ⁻ to 2
1,710	0	0	0	0	10	25	40	25	0	2 ⁻ to 2
2,100	0	0	0	0	10	15	45	30	0	2
2,970	0	0	0	0	10	15	45	30	0	2
3,120	0	0	0	0	10	25	40	25	0	2
3,540	0	0	0	5	10	35	30	20	0	2
3,900	0	0	0	0	10	35	35	20	0	2

KSST NO. 2

Depth (feet)	<u>KEROGEN TYPES</u>									TAI
	AM	AT	AG	SA	M	BT	ST	I	R	
600	0	0	0	0	5	15	50	30	0	2 ⁻ to 2
960	0	0	0	0	5	15	45	30	5	2 ⁻ to 2
1,830	0	0	0	0	5	15	50	25	5	2 ⁻ to 2
2,280	0	0	0	5	10	20	40	25	0	2
2,520	0	0	0	0	10	20	55	15	0	2
2,910	0	0	0	0	5	15	50	30	0	2
3,300	0	0	0	0	5	15	45	35	0	2

KSST NO. 4A

Depth (feet)	<u>KEROGEN TYPES</u>									TAI
	AM	AT	AG	SA	M	BT	ST	I	R	
530	0	0	0	0	5	15	50	30	0	2 ⁻ to 2
1,000	0	0	0	0	0	20	45	35	0	2 ⁻ to 2
1,370	0	0	0	0	0	20	45	35	0	2 ⁻ to 2

See Appendix 2 for explanation of kerogen types.

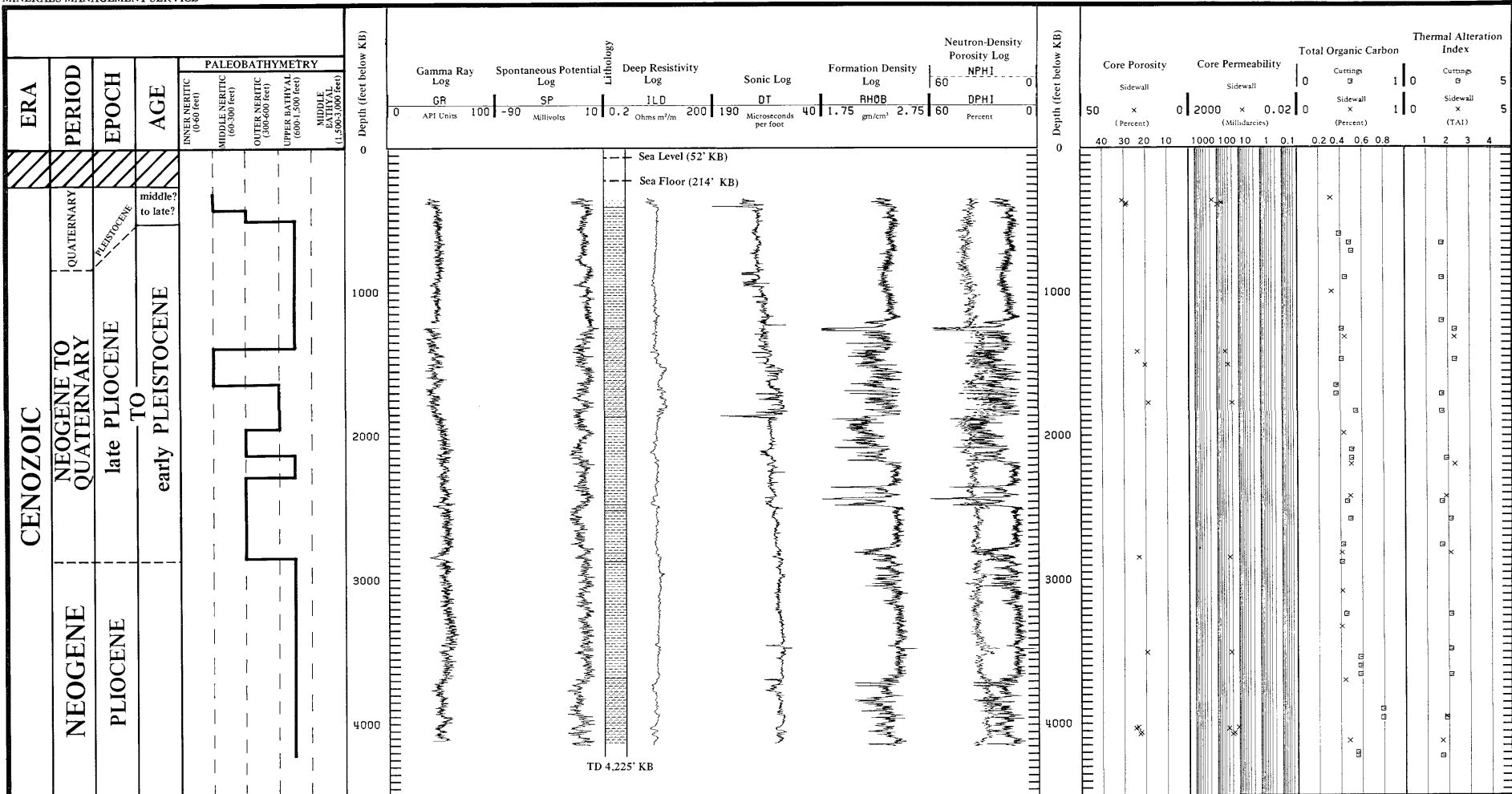


PLATE 1. STRATIGRAPHIC COLUMN AND SUMMARY CHART OF GEOLOGIC DATA, KSST NO. 1 WELL, KODIAK SHELF, ALASKA.

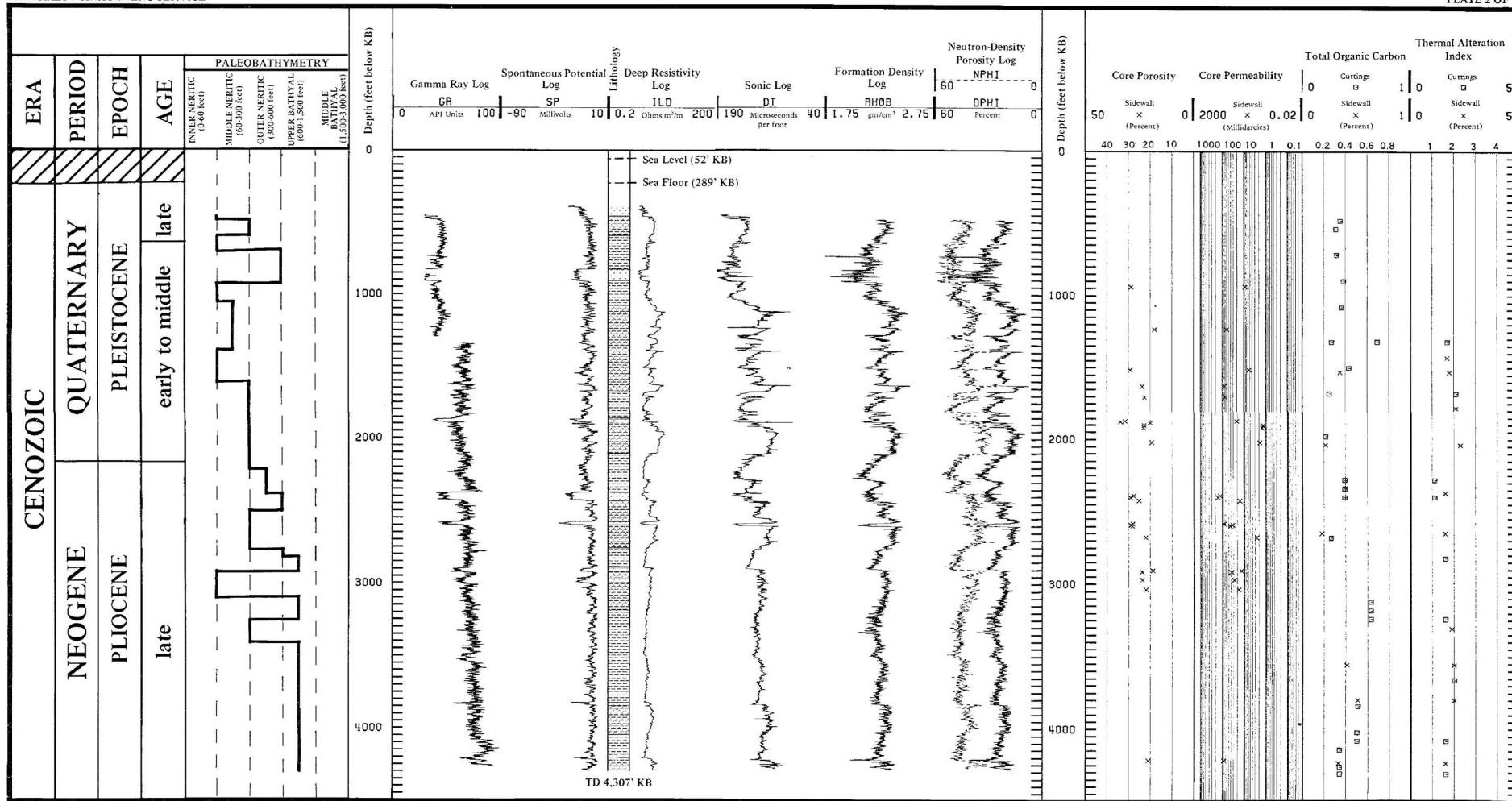


PLATE 2. STRATIGRAPHIC COLUMN AND SUMMARY CHART OF GEOLOGIC DATA, KSST NO. 2 WELL, KODIAK SHELF, ALASKA.

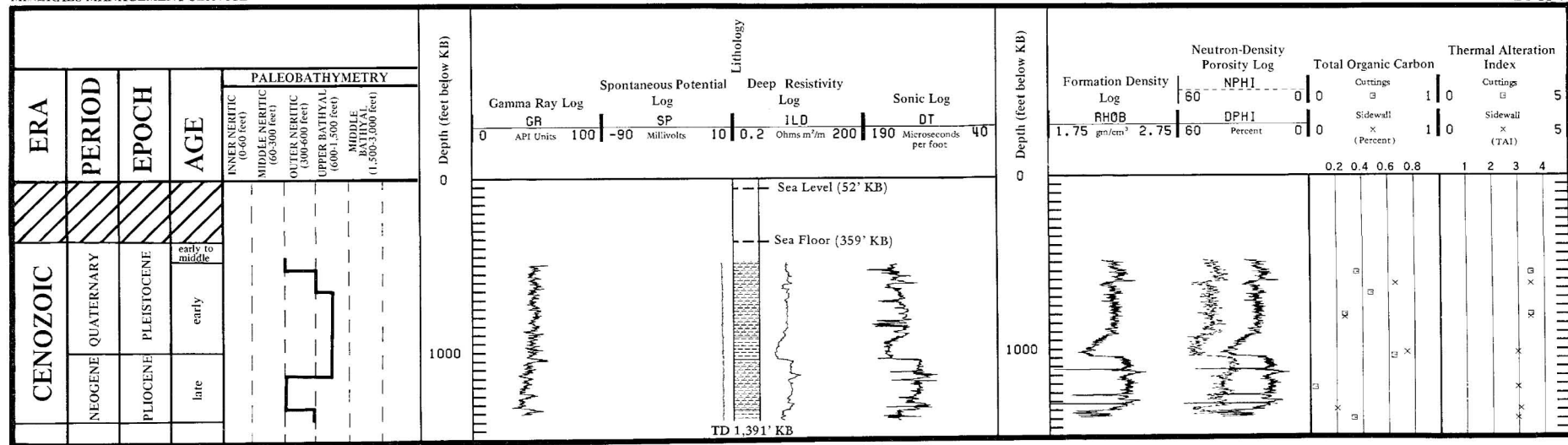


PLATE 3. STRATIGRAPHIC COLUMN AND SUMMARY CHART OF GEOLOGIC DATA, KSST NO. 4A WELL, KODIAK SHELF, ALASKA.

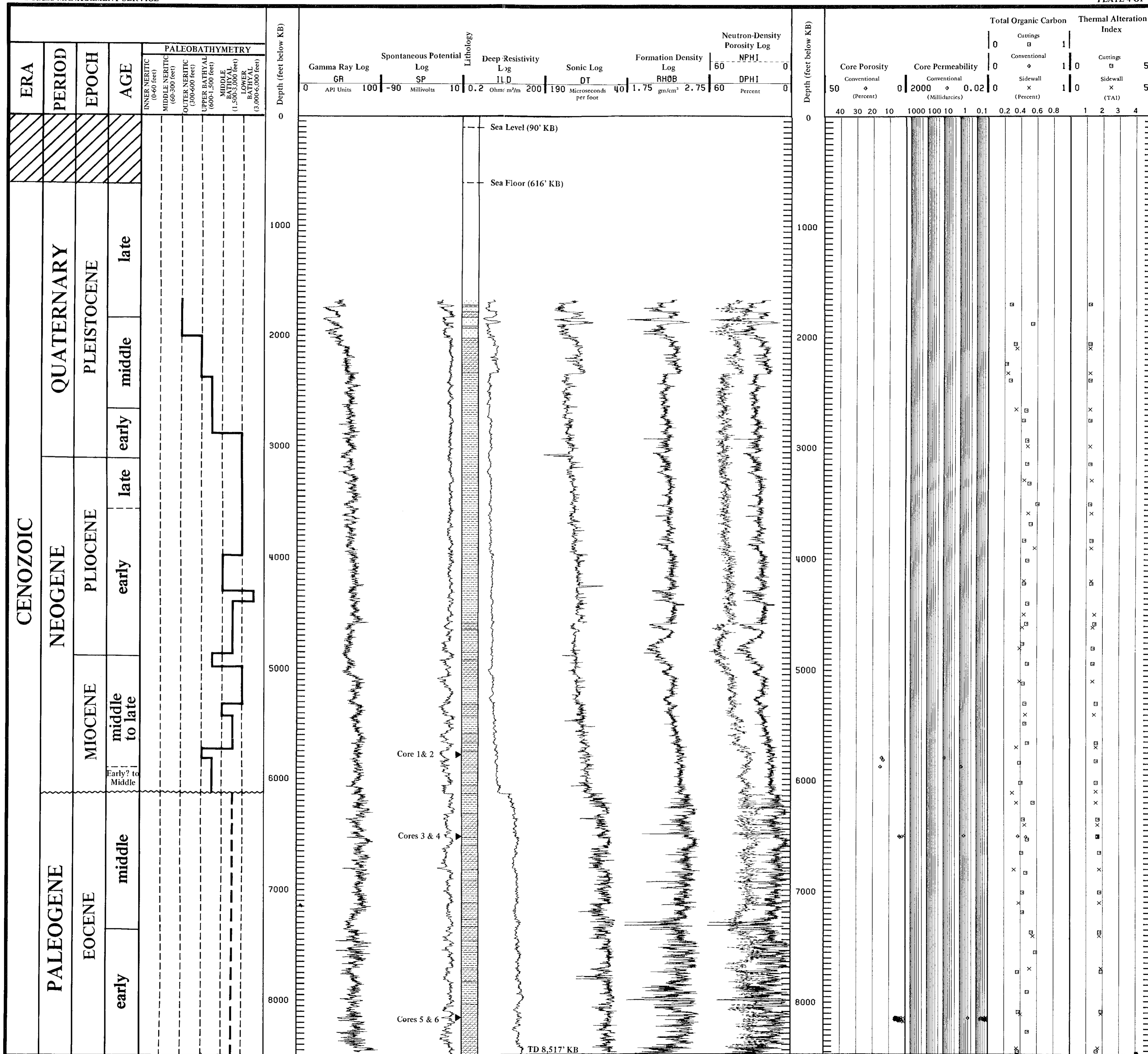


PLATE 4. STRATIGRAPHIC COLUMN AND SUMMARY CHART OF GEOLOGIC DATA, KSSD NO. 1 WELL, KODIAK SHELF, ALASKA.

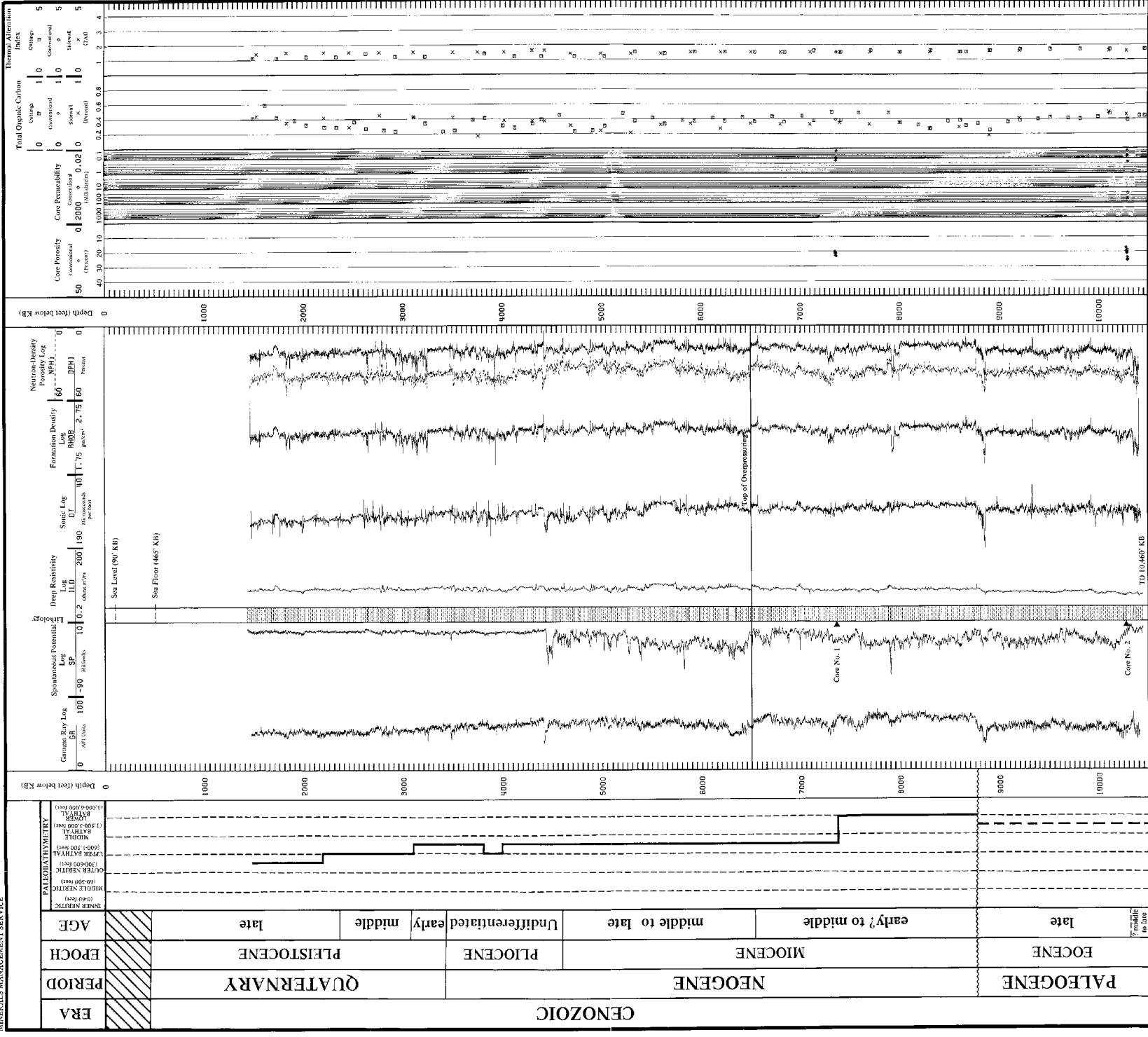


PLATE 5. STRATIGRAPHIC COLUMN AND SUMMARY CHART OF GEOLOGIC DATA, KSSD NO. 2 WELL, KODIAK SHELF, ALASKA.

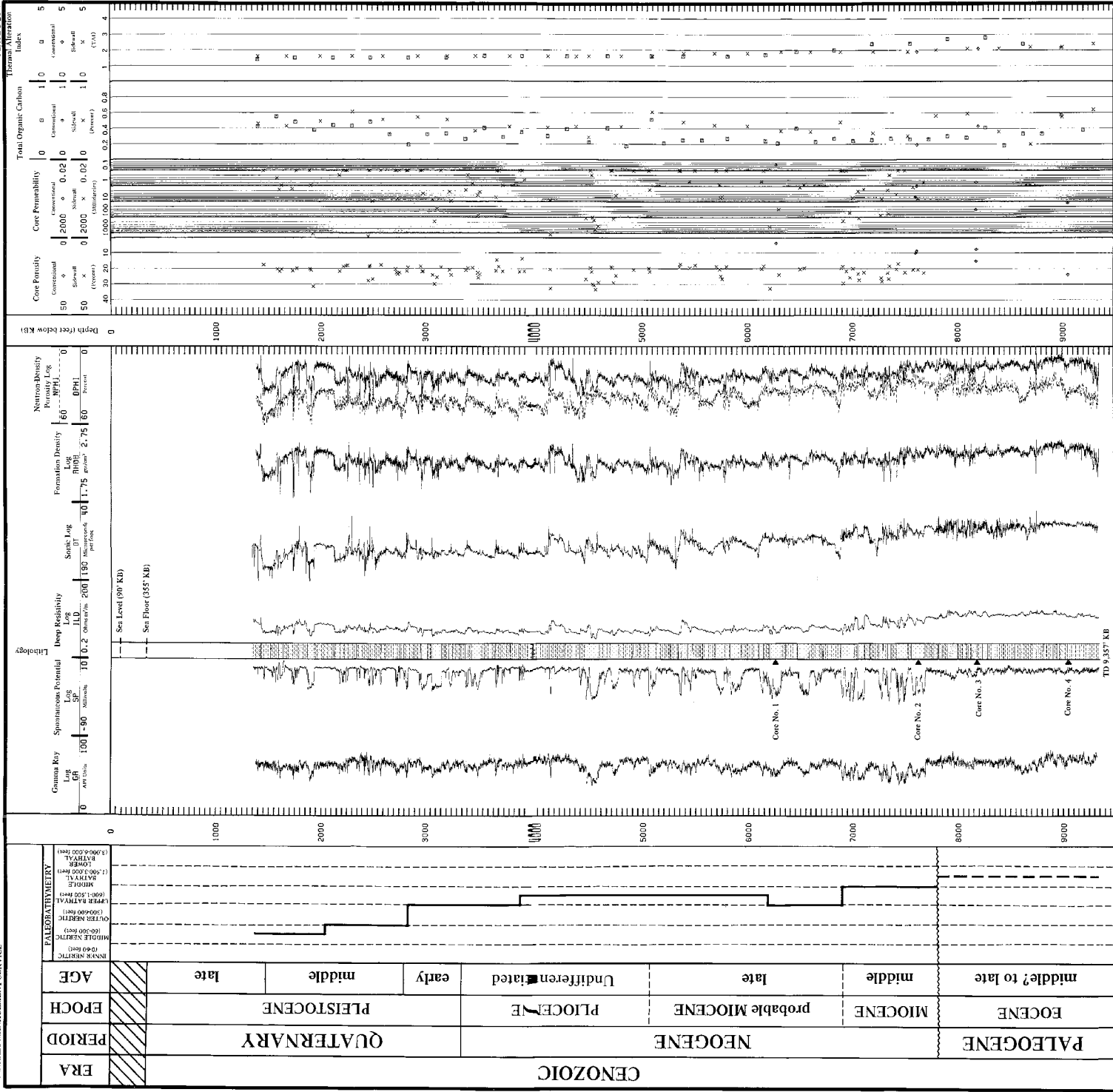


PLATE 6. STRATIGRAPHIC COLUMN AND SUMMARY CHART OF GEOLOGIC DATA, KSSD NO. 3 WELL, KODIAK SHELF, ALASKA.

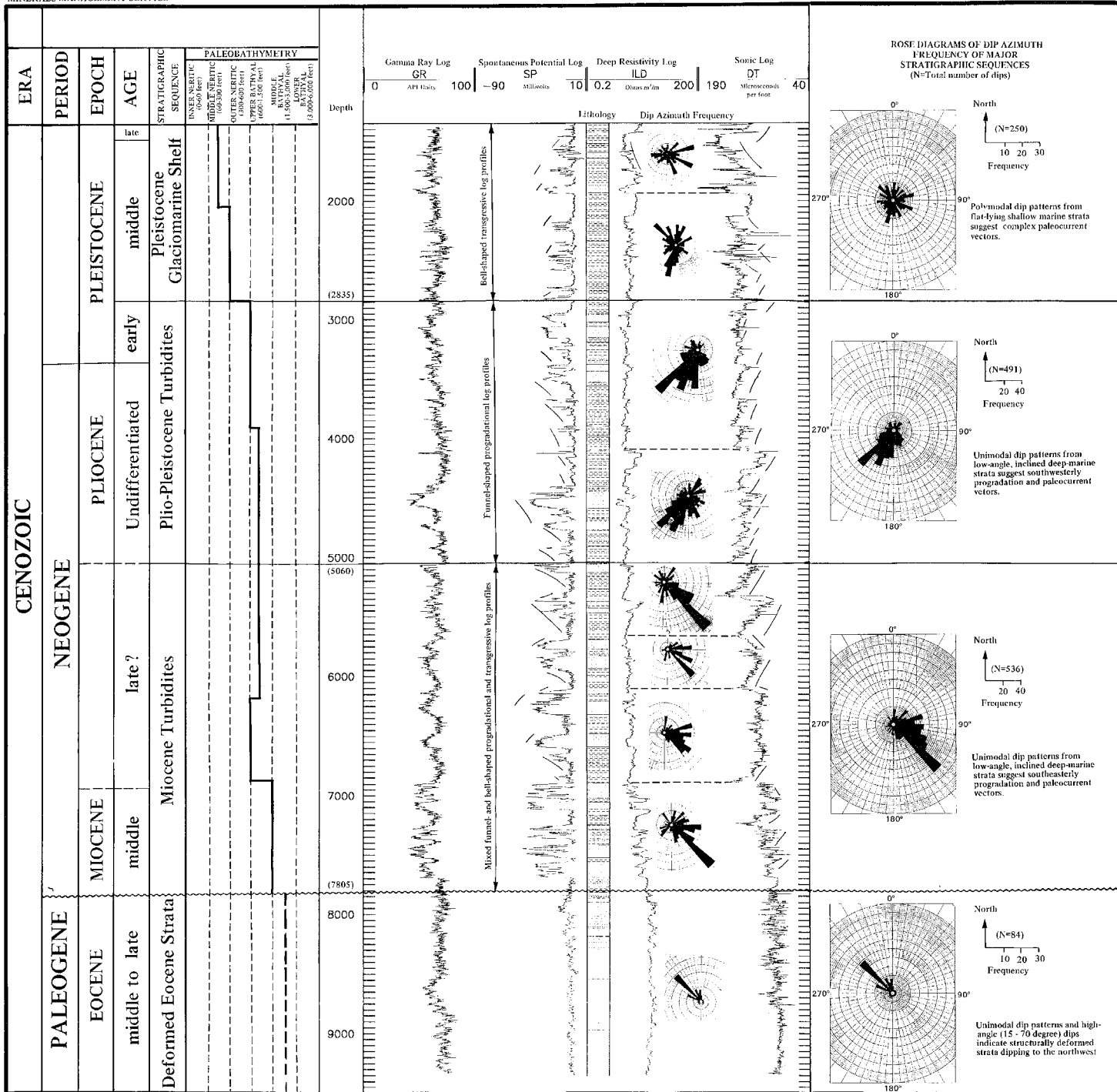


PLATE 7. LOG AND DIPMETER PATTERNS OF MAJOR STRATIGRAPHIC SEQUENCES IN THE KSSD NO. 3 WELL. Three major stratigraphic sequences are represented in the Quaternary and Neogene basin-fill at the well site. Each sequence contains distinct styles of log and dipmeter patterns. Log profiles reflect vertical grain-size and stratification sequences: funnel-shaped profiles indicate upward-coarsening sequences; bell-shaped profiles indicate upward-fining sequences. Dip azimuth patterns from the flat-lying to gently dipping strata of the basin-fill probably reflect paleocurrent transport and direction of sedimentary progradation. The Pleistocene glaciomarine shelf sequence contains transgressive, upward-fining log profiles and random to polymodal dip patterns that reflect complex paleocurrent patterns. The Plio-Pleistocene turbidite contains upward-coarsening log profiles and unimodal dip patterns that indicate a submarine-fan depositional complex that prograded from the northeast. The Miocene turbidite sequence contains both fining- and coarsening-upward log profiles and unimodal dip patterns that indicate a submarine-fan complex that prograded intermittently from the northwest.

As the Nation's principal conservation agency, the Department of the Interior has responsibility for most of our nationally owned public lands and natural resources. This includes fostering the wisest use of our land and water resources, protecting our fish and wildlife, preserving the environmental and cultural values of our national parks and historical places, and providing for the enjoyment of life through outdoor recreation. The Department assesses our energy and mineral resources and works to assure that their development is in the best interest of all our people. The Department also has a major responsibility for American Indian reservation communities and for people who live in Island Territories under U.S. Administration.

